Ultraviolet-induced conduction in liquid dielectrics

David Roger Pugh

ULTRAVIOLET-INDUCED CONDUCTION

IN LIQUID DIELECTRICS

being a Thesis submitted for the Degree of

DOCTOR OF PHILOSOPHY

in the University of Durham

by

DAVID ROGER PUGH, B.Sc.

July 1968.

ACKNOWLEDGMENTS

I wish to express my deep appreciation to Dr. M. J. Morant for his constant attention and for stimulating discussions on the work contained in this thesis. I wish also to thank Professor D. A. Wright for providing the facilities for the research and the Science Research Council who awarded the research grant.

CONTENTS.

CHAPTER I

INTRODUCTION TO, AND SCOPE OF, THIS THESIS

1.1. Introduction

The nature of electrical conduction in liquids is of fundamental importance in physics and engineering. Unlike conduction in gases and solids, which are well understood experimentally and theoretically, no really satisfactory explanation has yet emerged for the corresponding processes in pure liquids. The lack of progress is reflected by two main difficulties, involving; (a) the production of reliable experimental evidence without significantly changing the liquid, (b) the intractibility of the theory of the liquid phase. Nevertheless, non-ionic liquids have extensive engineering applications, including their use as electrical insulators and as the ionisable media in nuclear particle detectors. Whilst it is generally accepted that the conduction in the 'dielectric liquids' is often due to traces of ionic impurities, there are indications that the 'intrinsic conduction' may be electronic in nature. It is, therefore, of considerable interest to find out more about the charge carriers which exist in very pure liquids.

The saturated hydrocarbons, liquefied inert gases, and some aromatic compounds are relatively stable chemically, can be prepared with a high degree of purity and have good insulating

properties. Paraffins have the simplest structure of the hydrocarbons and, being the least polar, are least susceptible to ionic contamination. Hexane is liquid at room temperature and has thus received the greatest attention. Accordingly, this thesis is concerned with the electrical conduction in liquid hexane.

When a sufficiently high field (of the order of 1.0 MV cm^{-1}) is applied to liquid hexane a fast, probably electronic, process known as 'intrinsic' or 'spark' breakdown occurs. There is reason to suppose that the pre-breakdown currents control the breakdown process to some extent, and that these currents may also be electronic in nature. Since the currents are small, and except when breakdown is imminent difficult to observe, some effort has been made to increase the conduction at lower fields by 'artificial' means in the hope of obtaining definite evidence of the nature of the charge carriers. Such conduction may be induced by irradiating the liquid with nuclear particles or X-rays, but since the liquid is then ionised the current is unlikely to be purely electronic. The latter methods have the additional disadvantage of chemically degrading the liquid. A less disruptive way of inducing conduction is to irradiate the electrodes or the liquid with ultraviolet light.

Early work showed that ultraviolet irradiation stimulated very small currents, $\sim 10^{-12}$A., but only if dissolved air had been removed from the liquid. Nevertheless, the method was used (by pulsing the light) to determine the mobility of the generated charges.

The generally accepted model was that the currents were initiated by the photoelectric emission of electrons from the cathode, and that their low magnitude was due to some sort of space charge limitation. Mobilities were found which were similar to those of ions known to be generated in the liquid, e.g. by X-rays. This cast doubts on the validity of the assumption that the charges originated by photoemission from the cathode; the photocurrents could have been generated in the liquid, for the following reasons;

(i) In most cases the cathode was illuminated through the liquid, photostimulation of the hexane was, therefore, not necessarily precluded.

(ii) Commercially available hexane usually absorbs ultraviolet light because of trace quantities of dissolved (organic) impurities. Most of the light would be absorbed before reaching an immersed electrode surface.

(iii) The currents were much smaller than would be expected from a space charge limited process and, anyway, did not exhibit the usual SCL voltage dependence.

(iv) Photoconduction associated with the stimulation of the bulk liquid, even when spectroscopically pure, has been reported.

1.2. Scope of this thesis

In the circumstances, photostimulated currents in the liquid required further investigation. The scope of this thesis is, therefore, to distinguish the nature of the photoconduction processes.

Some advances have been made on four experimental fronts;

(i) The purification of liquid hexane, in order to remove the optically absorbing impurities.

(ii) The distinction of photoconduction in the liquid from photoinjection by the cathode, and the conditions for each process.

(iii) The preparation of active photocathodes (by vacuum evaporation) and their use to photoinject charges into highly degassed n-hexane with low applied fields.

(iv) The detection of photochemical reactions in air saturated n-hexane.

In particular, the factors leading to the apparent disparities between some of the previously published results have been distinguished, and that, with certain precautions, the measurement of the mobility of the photoinjected charge carriers becomes meaningful and precise.

The results indicate that the injection of electrons from a photocathode does occur, provided that some crucial requirements are fulfilled. Finally, a semi-quantitative analysis of the photoconduction processes in liquid dielectrics is presented.

CHAPTER II

REVIEW OF THE LITERATURE ON 'NATURAL' AND 'INDUCED' CONDUCTION IN LIQUID HEXANE

2.1. 'Natural' conduction in liquid hexane

Liquid hexane is reported to have a resistivity of greater than 10^{19} ohm cm. for low applied fields (< 10 KV. cm^{-1}). The 'natural' conduction is thought to be mainly due to ions produced by cosmic rays and radioactive contamination[1]. The conduction, in general, is very sensitive to the effects of minute traces of impurities and spurious ions[2]. Only part of the current-voltage characteristic is ohmic; a space charge limited region is encountered at higher fields, leading to a regime of incipient breakdown[2]. Finally, spark breakdown[3] occurs at fields of between 0.5 and 1.2 MV cm^{-1}. The collection and evaluation of the data has been undertaken in the reviews[4,5,6,7,8]. Some features have emerged which are of paramount importance experimentally but there is not, as yet, a really satisfactory account of the charged species which carries the current in the bulk of the liquid.

Observations and experimental techniques seem to fall into three groups, according to the magnitude of the applied field. The usual nomenclature is 'high field' (> 100 KV. cm^{-1}), 'intermediate field' (between 10 KV. cm^{-1} and 100 KV. cm^{-1}), and 'low field'. Owing to the difficulties involved in measuring the current in the low field

Fig. 2.1

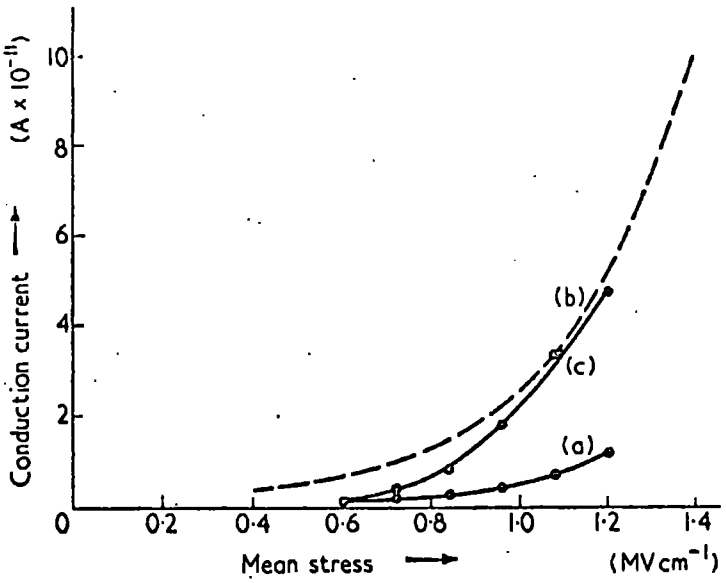

The conduction current of liquid hexane as a function of the mean stress. (a) Purified hexane saturated with air; (b) Purified and degassed hexane; (c) Commercial hexane saturated with air.

region, the processes occurring at intermediate and high field strengths are best known. Probably the most significant outcome of the work at high fields (for the purposes of this thesis, which is concerned with field strengths of < 3 KV. cm^{-1}) is the emergence of dissolved oxygen as an active contaminant in controlling the natural conduction[3,9,10].

A typical set of measurements, at high fields, is shown in Fig 2.1 Curve (a) gives the current (measured by House[11]) after 'conditioning' the electrodes in degassed hexane. Measurements (b) and (c) were for purified and commercial hexane respectively, both being saturated with air (after Sletten[9]). The 'conditioning' process[11,12, 13] was necessary to reduce fluctuations in the current for fields above 100 KV. cm^{-1} in the degassed liquid. Sletten[9,10], by comparing the effects of O_2, N_2, H_2 and CO_2 was able to deduce that the oxygen is the most active constituent of the dissolved air in hexane, and that its presence reduces the fluctuations to make conditioning unnecessary for air saturated liquid. The actual magnitude of the current is determined by both the electrode material (and the nature of its surface) and the liquid sample[2,14]. The activity of the oxygen is not fully understood, but its presence inhibits some processes[3,15], and a specification of the air content (as well as the chemical purity of the liquid) is now usually included with the results.

2.2. The charge carriers

Various suggestions have been made as to the nature of the charge carriers in hexane. Three distinct possibilities have been proposed so far[5], namely that the carriers are (i) hexane ions, (ii) impurity ions (or such molecules with attached charges), or (iii) trapped electrons or holes.

A test for conduction by ions in a liquid is to measure the mobility over a range of temperature and, from a knowledge of the viscosity, to see if Walden's rule[16] is operative. If alternative forms of conduction are available[17] the effective radius of the ion will be reduced and the mobility increased, according to the activation energy 'E' of the charge transfer mechanism.

Measured values of the mobility[8,18,19] were found to be rather too high for simple ionic transport, but not high enough for 'free' electrons or holes. In addition, the product of the mobility and viscosity was found to be temperature dependent, and thus at variance with Walden's rule. It has been pointed out, however, that when the current is unipolar (which is generally the case for mobility measurements) the momentum exchange during collisions between the charge carriers and the neutral molecules will cause the liquid to move as a whole[20,21]. In these circumstances the observed mobilities will be larger than the actual mobility of the charges in the liquid at rest. By taking liquid motion into account the mobility of negative charges injected into liquid hexane by X-rays[19] and

field emission[21] has been shown to be $\sim 5 \times 10^{-4}$ $cm^2.V^{-1}sec^{-1}$. The latter value indicates that ions were the charge carriers, these might have been formed by the method of injection or by the attachment of electrons to hexane or dissolved oxygen molecules.

The alternative possibility that an electron or hole becomes trapped in its own polarisation field to form a 'polaron' has been proposed[15] to explain the role of an activation energy (higher than that due to viscous effects) in controlling the conduction. This is the nearest approximation to 'intrinsic' conduction and is based on solid state concepts.

2.3. The application of solid-state theories to the 'natural' conduction in liquid dielectrics

The transition from a solid to a liquid is characterised by the loss of any long range order. The only type of order left in a liquid (at least above the immediate vicinity of the melting point) is short range and is best described by a radial distribution function[22]. In many organic molecular solids, however, the change from solid to liquid is a less drastic event than for, say, a covalent solid in which the order extending over 10^2 - 10^3 interatomic spacings is lost[23,24]. It has been suggested, moreover, that the long range order is not the only source of a band structure[25-27]. Energy bands have been proposed to arise from certain features of the short range order existing within an amorphous solid or even a liquid.

The mechanism of charge transfer in solids (where the carriers travel as waves, with relatively high mobility and interacting infrequently with the lattice) is supposed to exist within the short range order of a liquid, the carriers moving in an essentially random manner from molecule to molecule[28]. This is frequently referred to as 'hopping'. In liquids the mean free path of the carriers would be very short, and the mobility low. It may well be that the carrier moves as an ion in the applied field, and also by an activated hopping process from one molecule to the next[15].

Le Blanc[16] notes that the fusion of a crystal, by causing the mean free path of a charge carrier to be reduced to molecular dimensions, makes the average time that a charge spends in the vicinity of any one molecule comparable to the period of an intermolecular vibration. The carrier might then cause polarisation of the molecules in the immediate neighbourhood, and become trapped in its own polarisation field. The transfer of the carrier by hopping to an adjacent site would thus require an activation energy 'E' supplied by a strong phonon interaction, which is necessarily a low probability event. In this case the mobility μ would vary with temperature according to the equation

$$\mu = \mu_o \exp - E/KT$$

where E is an energy, and μ need not be much larger than for an ion.

If the charge transport involves two parallel and simultaneous mechanisms, the process can be considered as a kind of electrochemical

reaction and is governed by the theory of reaction rates. Forster[23], for example, has proposed that the conductivity of at least some hydrocarbons is due to both a thermally activated hopping process and charge transport of electrons via an excited state. The conduction would then be proportional to a reaction constant 'K' given by

$$K = \sum_n K_n (KT/N_n) \exp(-E_n/KT)$$

where K_n is the transmission coefficient and E_n the activation energy of the nth partial reaction. For the two processes considered by Forster the conductivity is given by

$$\sigma = A \exp(-E_1/KT) + B \exp(-E_2/KT).$$

The carrier generation process is assumed to take place within the liquid and is independent of any charge injection from the electrodes. Forster notes that the conductivity of liquid aromatics is much greater than for the paraffins, and has ascribed E_1 in benzene to the energy of the triplet state. The insulating properties of the paraffins could be due to the absence of a similar energy level. Similarly, E_2 is supposed to be lower for the charge transfer between molecules in the excited state. Thus benzene, which has a conductivity 10^3 times higher[23] than n-hexane, may reasonably be considered an organic semiconductor.

Since the excited state of the molecule has been invoked to explain the conduction, despite the fact that it is unlikely to be

thermally activated, it has been suggested that excitation may result from the application of an electric field[30]. Although this would seem to be possible for very high fields (near breakdown) it is difficult to reconcile with the conduction at very low fields.

The equilibrium 'contact' potential between an electrode and the liquid is important when considering the injection of charges. Morant[42] has applied the theory of metal/semi-conductor contacts[43] to the metal/liquid case, and has measured a small change in potential of a stainless steel electrode on immersion in air-saturated hexane. His results showed that the interfacial double layer always had the negative side towards the liquid, as required for an electron space charge. His assumption that this voltage corresponded to the diffusion potential of free electrons in the liquid has, however, been questioned[44].

It is seen (from Sections 2.1 - 2.3) that the nature of the conduction in hexane is still largely unknown. The low 'natural' conductivity makes the experimental investigation of the charge carriers difficult, if not impossible. An alternative approach is to induce currents, in some way, and to observe the behaviour of the injected charges. The rest of this Chapter is concerned with the various methods of introducing charges (not necessarily electrons) into the liquid with low applied fields.

2.4. Currents induced in liquid hexane by nuclear radiation and X-rays.

An abbreviated account of the currents induced by ionising radiation (X- and γ-rays, α- and β- particles etc.) will be included in this Section. A comprehensive survey of the (extensive)) literature on this subject has recently been published by Adamczewski[8], to which the reader is referr ed for greater detail. Some aspects of the theory of this type of induced conduction are dealt with more fully in Section 3.1.

When high energy radiation (e.g. α - particles) is passed into a hexane-filled ionisation chamber, a current, typically of the order of 10^{-9}A, flows for applied fields of a few KV.cm^{-1}. The induced current, which is several orders of magnitude greater than the 'dark' current, decreases very rapidly (at a rate which depends on the transit time of the ions between the electrodes) when the radiation is stopped. The form of current-voltage or current-stress characteristic[31], as shown in Fig. 2.2, is exhibited by the conduction induced by a wide range of type (and energy) of radiation. It is seen that the current 'I' for a given field 'E' can be expressed as

$$I(E) = I_1(E) + I_2(E)$$

so that above a certain field 'E_s' (generally 2-10 KV.cm^{-1}) the first term assumes a constant value 'I_o', and the second component 'I_2E' is a linear function of the applied field. Thus, the total current for $E \gg E_s$ can be written in the form

$$I_s = I_o + CE$$

where 'C' is a constant depending on the type of incident radiation,

Fig. 2.2

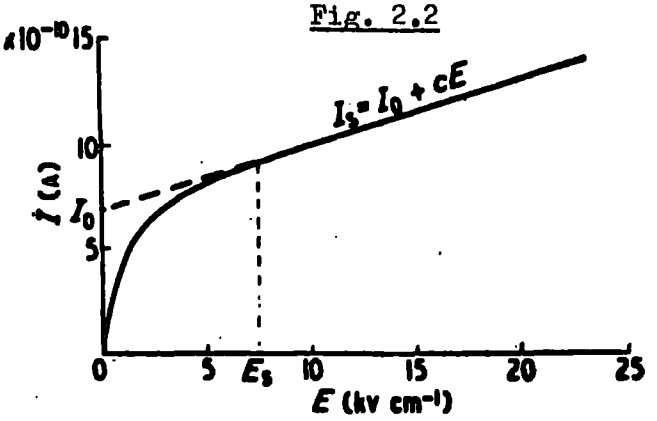

Current–voltage characteristic of induced conduction in a dielectric liquid.[9]

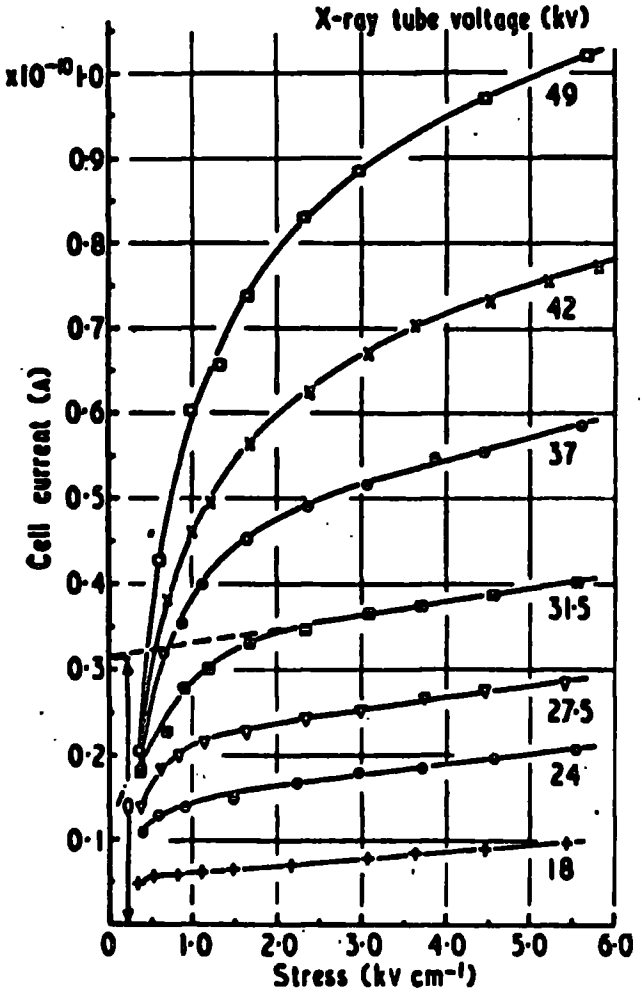

Conduction characteristics of *n*-hexane filled test cell. Molybdenum target in x-ray tube through which electron current of 2·4 mA flowed. Foil electrode negative.[19]

and which increased linearly with the radiation intensity[36,37]. The straight part of the current-voltage characteristic has been shown to continue[32] to very high stresses ($\sim$ 300 KV.cm^{-1}).

A considerable amount of data on the effect of molecular structure, temperature, and electric field on the mobility of the ions produced in the liquid has been amassed[8], generally using pulsed X-ray irradiation and 'time of flight' measurements[33,34]. There are indications that high energy irradiation produces several types of positive ion[34] but only one kind of negative carrier; the latter most probably being an electron which is trapped, or attached to hexane or impurity molecules[32]. Measured values of the ion mobilities in hexane range from 10^{-3} to 10^{-4}cm.^{2}V^{-1}sec.$^{-1}$; the negative carriers usually exhibiting a slight, but consistent, high mobility compared to the positive ions[8]. A similar trend is found for the activation energies ($\sim$ 0.1eV), the value for the negative ions being lower than the positive ions, so that

$$\mu_- \propto \eta^{-1} \quad \text{and} \quad \mu_+ \propto \eta^{-3/2}$$

('η' being the viscosity[35], and 'μ_+' and 'μ_-' being, respectively, the positive and negative ion mobilities).

It is not known for sure, at present, how important the neglect of liquid movement in earlier measurements has been[19,20]. In addition, traces of some impurities in the liquid[38] (notably oxygen[39,40], ethyl alcohol[32,34], carbon tetrachloride[39] and tetrahydrofuran[39])

have been shown to reduce the ion mobilities. In general, relatively little attention has been paid to purifying the liquid samples, or to the accumulation of impurities which are produced by the radiation[41].

2.5. Currents induced in liquid hexane by ultraviolet irradiation

The conduction of hexane is increased by ultraviolet irradiation of the liquid or an immersed electrode. The nature of the conduction is now better known, and so the literature will be re-assessed in Chapter VII with regard to the present results. Pulsed photoconduction has been used as a method of measuring the mobility of the charge carriers in the liquid, and is described in Section 2.6.

The fact that saturated solutions of anthracene in hexane are photoconducting was reported as long ago as 1910[45]. Volmer[46] found that radiation of wavelengths shorter than about 4000Å were effective in this system, but for dilute solutions the threshold shifted to about 2250Å. In the latter case, the slightest trace of anthracene in the hexane produced a 100 to 300 fold increase in current. The maximum effect of the anthracene was found for 2×10^{-4}N. solutions; greater concentrations absorbed the light in a layer close to the window of the cell and away from the electrodes. The current tended towards a saturation value when the applied field was increased above 300-700 $V.cm.^{-1}$. Wavelengths of light between 4000 and 3000Å caused the dilute solution to fluoresce, but not to photoconduct.

Eller[47] associated the photoconduction of 'pure' paraffins

with the ultraviolet absorption edge. His measurements indicated that both the u.v. absorption and the threshold for photoconduction shifted to longer wavelengths with increase in chain length of the molecules. (He also found that benzene did not photoconduct, in spite of its strong absorption in the u.v.)

Jaffé[48], in 1913, observed photoconduction in purified hexane; but did not investigate further, save to report it in the context of his work on columnar ionisation by α-particles in the liquid.

Dornte was the first to purify and degas the liquid[49] for a careful study of the high field conduction[50] of heptane and benzene. Only one measurement of the currents induced by the irradiation of degassed heptane (with a mercury vapour lamp) is recorded. The photocurrent was easily distinguished from the 'natural' conduction at the lower fields, its magnitude being roughly proportional to the intensity of illumination. Dornte noted that these currents were relatively insensitive to the magnitude of the applied field. Above $\sim$ 70 KV.cm^{-1} the 'dark' currents rapidly increased to completely obscure the contribution of the induced current. Dornte deduced that (since the sudden increase of the conduction above 70. KV.cm^{-1} did not depend at all on the presence of photocurrents) this indicated the absence of collisional ionisation at high fields. The sudden transition from low to high currents was probably because of the onset of field emission of electrons from

roughness on the electrodes, the current then behaving according to the Fowler-Nordheim equation for cold-cathode field emission[51].

Morant[52] irradiated polished aluminium electrodes in degassed (to 10^{-5}torr) hexane, steady currents not being obtainable in the air-saturated liquid. The shape of the current-voltage characteristic was found to depend on the wavelength of the radiation; nearly ohmic behaviour was exhibited for wavelengths near the threshold ($\sim$ 3000Å) but there was a tendency towards saturation (see Fig. 2.3a) when using unfiltered radiation from a low pressure mercury vapour lamp. Morant compared the photocurrent in the liquid with the photoemission (from the aluminium) in vacuo, he found that:

(i) The threshold wavelength for photoconduction in the liquid was about the same as for the vacuum photoemission ($\sim$3000Å).

(ii) The maximum photoemission in vacuo was considerably larger than the corresponding liquid photocurrents ($< 10^{-11}$A.).

Later measurements[53], with different electrode surfaces but with the same sample of liquid, indicated a connection between the relative magnitudes of the photoemission (in vacuo) and the photoconduction in the liquid. Polarity reversal tests showever, however, that the photocurrents in the liquid were nearly the same for either direction

Fig. 2.3

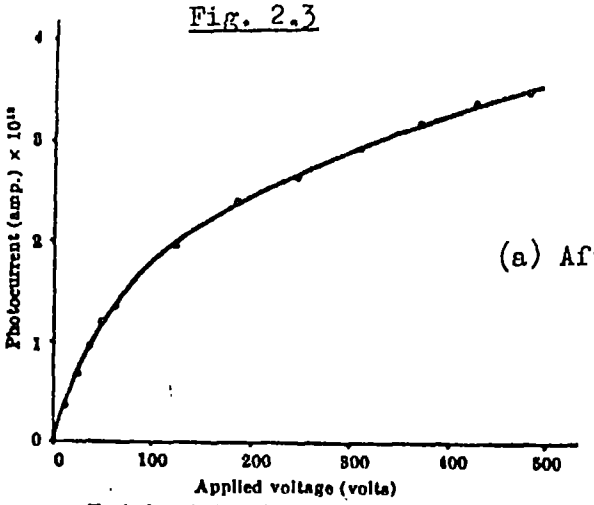

Typical variation of photocurrent with applied voltage (1-cm. diam. electrodes spaced 7 mm. apart)

(a) After Morant[52](1961)

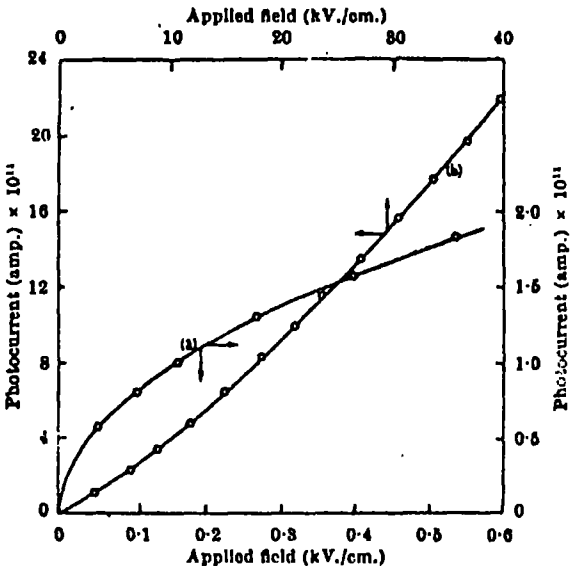

Photocurrent injected into n-hexane for various field strengths with constant ultra-violet illumination

(b) After Swan[54](1961)

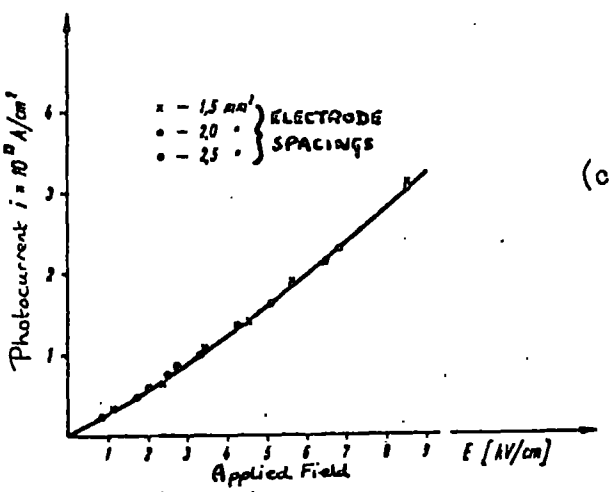

(c) After Gzowski[55](1961)

of current flow, and that radiation of a given intensity was equally effective if directed at the anode, cathode, or the bulk of the liquid.

Swan[54] constructed a test cell in which electrons were emitted (at least in vacuo) from the front surface of a thin metal film when ultraviolet light was directed onto the back surface. An aluminium film which absorbed about 50% of the radiation (the condition for maximum photoemission) was deposited, by vacuum evaporation, on a silica disc. This photocathode was then cemented on to the test cell to face a stainless steel electrode. The aluminium layer was exposed to the atmosphere for some hours and so it must be assumed that its surface would be oxidised.

Irradiation from a medium pressure mercury vapour lamp induced currents of $\sim 10^{-10}$A. in spectroscopically pure hexane (degassed to 10^{-3} torr) at a field strength of 10 KV.cm^{-1} (see Fig. 2.3(b)), the corresponding vacuum photocurrent being $\sim 10^{-8}$A. At fields above 10 KV.cm^{-1} the current was proportional to E^n where n = 1.21, but for lower fields a conductivity similar to Morant's[6] was exhibited. By reversing the polarity it was found that the current injected into the liquid with the metal film as the cathode was about 100 x greater than that injected with the film as an anode. The current when the film was positive indicated that radiation (passing through the film) was either releasing electrons from the stainless steel electrode or photoionising the liquid. The ratio of the 'forward' and 'reverse' currents remained the same when the cell was emptied

and evacuated, and so it appears that the charges originated at the electrodes and not in the bulk of the liquid. Slow variations of the current were observed when the illumination was switched on and off (e.g. the conductivity rose from 10^{-18} to 10^{-15} $ohm^{-1}cm^{-1}$ on initial illumination but decreased, in 20 minutes by a factor of 3, if the radiation was prolonged).

Gzowski and Terlecki[55] investigated the photoemissive properties of technical grade zinc, single crystals of zinc and aluminium, and abraded, etched, or vacuum deposited surfaces of aluminium in air saturated n-hexane and n-decane. They concluded that for irradiation by wavelengths longer than 2600Å the evaporated aluminium layer was the most efficient of the photocathodes examined.

Most of the measurements were made using a cell with an anode consisting of a thin layer of tin oxide on borosilicate glass (the combination being transparent to light of wavelength longer than ~ 2600Å). The cathode was illuminated via the anode/liquid, using a high pressure mercury vapour lamp. Some measurements were made in a cell where the tin oxide layer was replaced by a semi-transparent evaporated coating of aluminium, (c.f. Swan[54]), in which case the layer formed the cathode, emission being obtained by illuminating the layer through the glass backing. The results with both types of cell were essentially the same.

The photocurrents were very dependent on the techniques of evaporation (a rapid evaporation being the best), and they decreased

Fig. 2.4

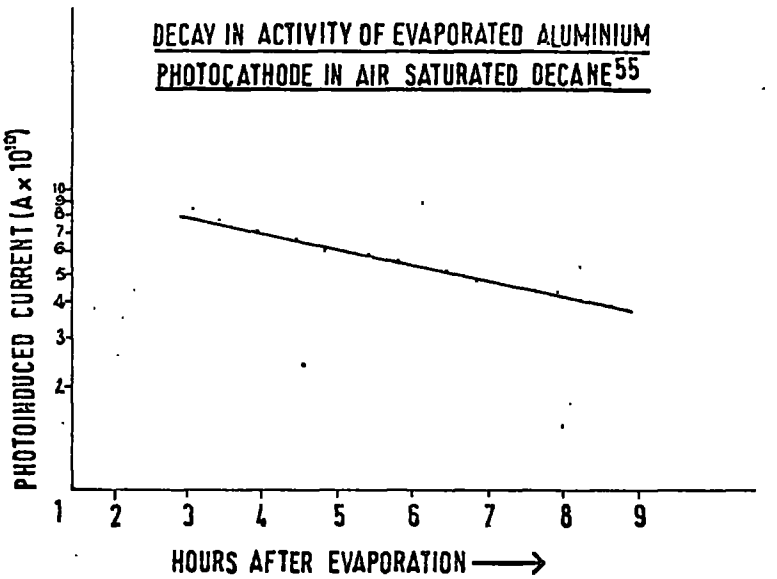
DECAY IN ACTIVITY OF EVAPORATED ALUMINIUM PHOTOCATHODE IN AIR SATURATED DECANE[55]
PHOTOINDUCED CURRENT (A × 10^-9)
8
7
6
5
4
3
2
1 2 3 4 5 6 7 8 9
HOURS AFTER EVAPORATION

(a)

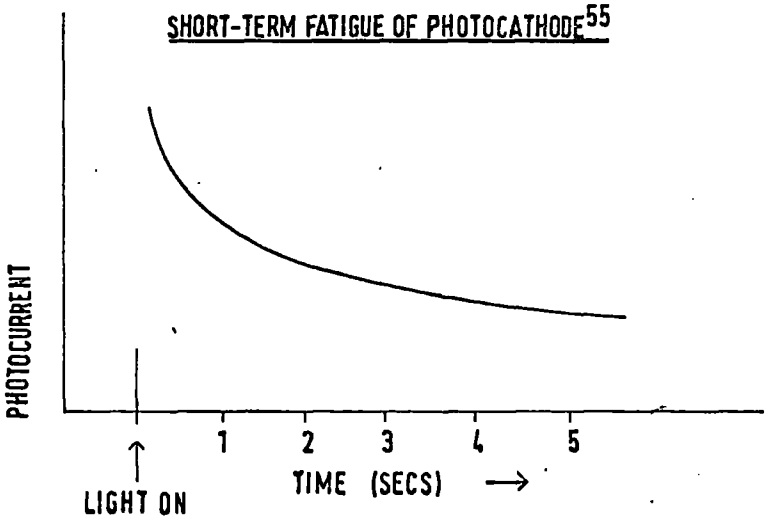
SHORT-TERM FATIGUE OF PHOTOCATHODE[55]
PHOTOCURRENT
1 2 3 4 5
TIME (SECS)
LIGHT ON

(b)

as the electrodes aged in the liquid. A decay of electrode activity over long periods of time was observed (Fig.2.4(a)), but there was also a much more rapid 'fatigue' of the photocathode on sudden illumination (Fig. 2.4(b)). Because of technical difficulties, measurements were not begun until 2 hours had elapsed from the time of evaporation, and the surface had to be immersed in the liquid for a few days before reproducible results were obtained. The current-voltage characteristics shown in Fig. 2.3(c) were measured after both types of fatigue were nearly complete, i.e. with an evaporated layer several days old and after prolonged irradiation. The current was measured for fields up to 200 $KV.cm^{-1}$ for different electrode spacings. The current-stress curves could be represented by

$$I = AE^n$$

where 'A' was a constant depending on the nature of the cathode surface (its age), the type of liquid, the intensity of illumination and the spectral composition of the light, but not the electrode spacing. The value of 'n' was about 1.1 and was nearly the same for hexane and decane, currents being proportional to the light intensity even at low applied fields. There were no measurable photocurrents with the polarity of the cell reversed, i.e. with the tin oxide layer as cathode.

2.6. Mobility Measurements using pulsed ultraviolet irradiation

The discovery of photoconduction in paraffins has led to experiments designed to measure the drift velocity of the injected charges, and thus the mobility; 'μ'.

Le Blanc[56] was the first to use the method. He used a mercury vapour lamp to illuminate an aluminium cathode in spectroscopically pure n-hexane or n-heptane. Pulses of light, of 50 ms. duration, produced currents of about 10^{-12}A. with a transit time of a few seconds at fields less than 2 KV.cm^{-1}. The injected charge was assumed to consist of electrons photoemitted from the cathode; the photoionisation or photoexcitation of the liquid being minimised by the use of suitably filtered irradiation. The effects of space charge were discounted from a consideration of the shape of the current pulse; variations from the expected shape could be accounted for by diffusion of the carriers and internal reflections in the cell. Values of the drift velocity were proportional to the applied field. Measurements were made with vacuum distilled hexane at temperatures between +27°C and -47°C; one in n-heptane at 27°C. The mobility was found to depend on the temperature according to the relationship;

$$\mu = \mu_0 \exp(-E/KT)$$

with $\mu_0 = 0.3 \pm 0.2$ cm^{2}V.$^{-1}$sec

and $E = 0.14 \pm 0.02$ electron volts.

Thus, the mobility of electrons in n-hexane, at 27°C, was found to be $1.4 \pm 0.1 \times 10^{-3}$cm^{2}V.$^{-1}$sec^{-1}, with a similar value for n-heptane.

The activation energy for viscous flow in liquid n-hexane is 0.073 electron volts[35]. Le Blanc concluded that Walden's rule was

not obeyed for these charge carriers, and that for hexane over the temperature range;

$$\mu \propto \eta^{-2}$$

(where 'η' is the shear viscosity).

Le Blanc proposed that the deviation from Walden's rule could be explained if the electrons injected into the liquid neither behave as free particles nor are permanently attached to form negative ions. In this case, the energy 'E' controlling the mobility could be interpreted as the average energy with which an electron is trapped, the injected electrons being trapped and thermally untrapped many times during their drift through the liquid. The traps were calculated to be of molecular size (i.e.$\sim$ 3Å), but their origin remains unknown (see Section 2.3).

Chung and Inuishi[57] used 4μs flashes of light from an unfiltered mercury vapour lamp to inject charges from a magnesium cathode into n-hexane (degassed to 10^{-2} torr). The transit time of the carriers was found from the charging of a capacitance in an integrating circuit at the negative electrode (i.e. CR$\gg$transit time). The mobility was found to be independent of the applied field (up to 500 KV.cm^{-1}) with a value of 1.1 x 10^{-3}cm^{2}V.$^{-1}$sec^{-1} at 27°C and an activation energy of 0.16 electron volts. The addition of small amounts of ethyl alcohol to the hexane reduced the mobility and produced space charge distortion of the current pulses. A similar mobility was observed in benzene.

Terlecki[58] used a vacuum deposited film of aluminium as the photocathode and measured the mobility in air saturated hexane. Light from a mercury vapour lamp reached the cathode via a transparent anode of stannous oxide on glass, (this combination also avoiding the absorption of light by the liquid). Mobilities were found to be 9.8×10^{-4}, 7×10^{-4}, and 3×10^{-4} $cm^2 V.^{-1} sec^{-1}$ for hexane, octane and decane (respectively) at room temperature; and were independent of the field (up to 100 $KV.cm^{-1}$ for hexane, 200 $KV.cm^{-1}$ for octane, and 300 $KV.cm^{-1}$ for decane). Varying the electrode spacing from 0.3 to 2 mm did not affect the mobility.

More recently, Bloor[59] has used the techniques described in this Thesis to carry out precise measurements of the mobility in hexane. The results indicate a value close to those previously obtained, although the experimental conditions are much more clearly defined than earlier.

Mobility values obtained by the photoinjection of charges into hexane correspond fairly well with those obtained by other means (see Sections 2.2 and 2.4).

CHAPTER III

ADDITIONAL MATERIAL RELEVANT TO THE DISCUSSION

This Chapter is in four self-contained Sections. Sections 3.1 and 3.2 deal with processes in the bulk liquid, Sections 3.3 and 3.4 are to do with the injection properties of the electrodes.

3.1. Recombination of ion-pairs in liquid hexane.

Ultraviolet irradiation of the liquid will be assumed to produce carriers which are singly charged (it is much more difficult to remove a second electron from a molecule than the first, and Coulomb forces make the attachment of two similar charges to a neutral molecule unlikely). Thus, ionisation will result in equal numbers of positive and negative carriers. The rate of recombination of ions can now be represented by:[61]

$$\frac{\partial p}{\partial t} = \frac{\partial n}{\partial t} = -\alpha pn$$

where 'p' and 'n' are the concentrations of positive and negative carriers, and 'α' is the recombination coefficient. It should be noted that neither dissociation nor recombination affect the local charge density $\rho = e(p - n)$, and it is thus a general impossibility to observe locally the formation or recombination of ions.[62]

In the steady state, the rate of generation of ion-pairs will be exactly balanced by their neutralisation through recombination and their collection at the electrodes. If the rate of generation is

fixed, the induced current rises with the field to eventually reach a saturation value. The current then corresponds to the rate of production of ion pairs, ~~i.e. eqn approaches zero~~.[62]

In fact, induced currents in hexane do not saturate[64] at ordinary fields. The conduction can generally be represented[8], at moderate fields, (see Fig. 2.2) by:

$$I = I_o + CE$$

To explain this characteristic it will be necessary to define more closely the recombination process. There are three important types of recombination which can occur within the liquid;[61]

(a) Volume

(b) Columnar

(c) Initial.

Volume recombination[61] takes place between positive and negative ions from unrelated ionisation events (i.e. between 'free' ions).

Columnar recombination[48] involves all the ions in the track produced by a single ionising particle (e.g. an -particle).

Initial recombination[63] is the only true re-recombination between each (individual) ion-pair.

It may at once be observed that ionisation in columns does not result from ultraviolet irradiation, and so any special aspects of the theory of columnar recombination cannot be applied here. If only two types of ion are produced by the irradiation, then 'volume' and 'initial' recombination become indistinguishable on a local scale.

The absorption of a photon (in the ultraviolet range of energy) by the liquid may be assumed to eject an electron from a single molecule. Thus, if 'M' is such a molecule:

$$M \rightsquigarrow M^+ + e^-$$

The result is the same as for irradiation of much higher energy[64] (e.g. by γ-rays); but in our case the ejected electron will have insufficient kinetic energy to cause further ionisation, but greater than thermal energy. The positive ion may also move through the liquid, or shift in position by charge exchange with neighbouring molecules, but there will be no loss in generality of the argument if the positive ion is taken as stationary.

The kinetic energy of the electron is diminished by collisions with the molecules of the liquid, and because of its outward motion against the Coulomb field of the parent ion. It stands to reason that the electron, if not removed too far before it becomes attached to another molecule or is otherwise slowed down to thermal energies, may recombine with the parent ion, i.e.,

$$M^+ + e^- \longrightarrow M^*$$

and 'initial recombination'[63] will have occurred.

[Some of the energy of the electron is, in general, lost to frictional forces (in between the ejection and recombination) and the energy of the excited molecule, M*, can be expected to be less than that of the ionising photon.]

The question now arises as to the separation of the ions which do not recombine. The kinetic energy of a 'free' ion in thermal equilibrium with the neutral liquid molecules is similar to that of the molecules themselves. It follows that an ion pair may be considered ready to participate in the conduction if the separation is greater than a 'critical' value, 'r', so that the thermal energy U_{th}, is comparable to the Coulomb attraction energy;[63]

$$\frac{e^2}{\varepsilon r} \simeq U_{th}$$

The thermal energy of individual ions will be distributed about the mean value, kT, and so an averaged critical separation, r_c, can be calculated for a non-interacting assembly of ion-pairs;

$$r_c = \frac{e^2}{\varepsilon(kT)}$$

[The value of r_c for liquid hexane at room temperature is $\sim 300\text{Å}$, the Coulomb field between the ions is given by;

$$E_c = \left(\frac{kT}{e}\right)^2 \frac{\varepsilon}{e} \simeq 8\text{KV. cm.}^{-1}. \ ]$$

Due to Brownian motion, the probability, P, of an ion having an energy $U_{th} > KT$ is;

$$P = \exp(-U_{th}/kT)$$

It is seen that ions with a separation $r < r_c$ can diffuse apart with the same probability;

$$P = \exp(-r_c/r)$$

This expression can be used, if the initial separation is known, to find the yield of 'free' ions in the absence of an applied field.

Onsager[63] has taken into account the effect of an applied field on the recombination/dissociation of the ion-pairs. He has found that the relative effect of a moderately high field on an assembly of isotropically orientated ion-pairs is independent of their separation if $r \ll r_c$. Thus, if G(0) is the yield of free ions at zero field, the yield G(E) with an applied field E is

$$G(E) = G(0) \left[1 + e^3 E / 2\epsilon k^2 T^2\right]$$

substituting for E_c, the above equation reduces to

$$G(E) = G(0) \left[1 + \frac{E}{2E_c}\right]$$

and will be expected to hold for $E \gg E_c$.

It is seen that this treatment, like the Jaffe theory[48], predicts a linear relationship between the recombination and the field, with the intercept presumably giving the yield at zero field. If G(E) is associated with the induced current, then the above equation can be written as

$$I = I_o + CE$$

$$\text{where } C = I_o / 2E_c$$

In addition, for $E \gg E_c$, the induced current should be proportional to the radiation intensity (through G(0)). Onsagers theory predicts an absolute value of the ratio of the slope to the intercept at zero field (C/I_o in Fig.2.2) of the current-stress characteristic, this value being 6×10^{-5} cm.V^{-1} for hexane at room temperature. Hummel and Allen[65], who found a value of C/I_o of 5.8×10^{-5} cm.V^{-1} for the currents induced by X-rays in hexane at 290°K have also found the required temperature dependence.

It has been shown that initial recombination occurs if the separation of the ion-pair is such as to make the mutual Coulomb energy comparable to, or greater than, the thermal energy KT. In the same way, this criterion can be used to describe the volume recombination between the 'free' ions. Adamczewski[8] has proposed that the currents for $E<E_c$ can be calculated by assuming a separate (and field independent) recombination coefficient for the free ions. It must be remembered, however, that this distinction between volume and initial recombination is artificial if only two types of ion are involved.

3.2. Photochemical reactions in hexane

In this section, some of the interactions of ultraviolet irradiation with hexane are discussed. An extensive search in the published literature was not particularly rewarding in elucidating the mechanisms leading to photoconduction in particular, but some facts emerged which will be used to propose an explanation in Chapter 7 (Discussion).

3.2(i) General

The ionisation potentials of the paraffin series fall with increasing molecular size, until a limit of about 10 eV. is reached for a molecule containing seven or more carbon atoms. A theoretical discussion of this effect, based upon molecular orbital theory, is given by Hall and Lennard-Jones[66]. It appears that the fall in ionisation potential is due to the delocalisation of the electrons in C-H

bonds, so that for long molecules they are no longer confined to any one particular C-H location. Thus, the energies of the highest occupied group orbitals in paraffins increase with the number of methylene groups in the chain, and more particularly, with the degree of chain branching[67]. There is a similar progression of the energies of the lowest unoccupied group orbitals, which govern the excitation potentials of the series.

Gaseous paraffins are transparent to visible and near ultraviolet irradiation, the first electronic absorption band appearing in the vacuum ultraviolet[68]. The band corresponds to the transition of an electron from a σ to σ^* state (bonding to antibonding group orbital); and excitation will result when $\lambda_{irr} < 1750$Å. Liquid paraffins absorb at much longer wavelengths, e.g. carefully purified hexane starts to absorb[69] in the ultraviolet (at around 2400Å) the absorption being intense at 2000Å. The infra-red spectrum of the liquid is similar to the vapour except for slight differences in the band contours[70], fine structure due to rotational modes of vibration being observable in the vapour but not in the liquid.

3.2(ii) Impurity absorption

Hexane itself is transparent to the visible and most of the ultraviolet range of wavelengths (Section 4.6) the liquid will however dissolve most organic compounds and is thus widely used as a solvent for spectroscopy. Some impurities (commonly present in 'pure' hexane) may absorb so strongly that, even in trace quantities, their presence

may obliterate the true hexane continuum (see Section 4.3). The ultraviolet absorption of the liquid is important because (i) The hexane exhibits photoconductivity (if dissolved air is removed[52]). (ii) The irradiation of an immersed electrode may be restricted. The absorption due to impurities will be discussed here, although an account of the absorption edge of degassed and purified hexane must ultimately be involved in a consideration of the photoconduction (Section 7.2).

There are two classes of impurity which, when dissolved in hexane, exert quite different influences on the electronic absorption spectrum. The first group, comprising the vast majority of substances, superimpose their own characteristic absorptions upon that of the hexane[71]. Thus, the solute exhibits absorption bands which retain (in shape and wavelength) the spectrum of the vapour phase. The bands in the liquid are diffuse (because of the loss of fine structure in the infra-red) and there is usually a very slight bathochromic shift, but the spectra are readily recognisable as belonging to the solute (e.g. benzene, Figs. 4.1, 4.7). In general the concentration can be calculated according to Beer's law;

$$I = I_0 10^{-\epsilon cd}$$

where c is the concentration (of solute) in moles per litre (of hexane), d is the thickness of the solution through which a proportion I of the initial light intensity I_0 is transmitted, ϵ is known as the molar absorptivity. The transmission coefficient (I/I_0) for a particular

concentration of, for example, benzene in hexane is about the same as for benzene on its own, taking into account the refractive index of the liquid[77]. Absorption by impurities of this type will certainly complicate the irradiation of an electrode via the liquid. However, impurity absorption does not necessarily lead to photoconduction in hexane[47]. (Even anthracene solutions do not photoconduct[46] unless $\lambda_{irr} \leq 2250$Å, although the anthracene absorbs[72] (and fluoresces) in the liquid when $\lambda_{irr} \geq 3700$Å.

The second group of solutes, of which only a few examples are recorded, are those which form complexes with the hexane molecules. For these substances (e.g.. dissolved O_2, I_2)[73], absorption bands appear at wavelengths which are not directly related to the spectra of either the solute or solvent on their own[74]. Dissolved oxygen not only modifies the absorption edge[79] of the pure liquid (Section 4.6) but also quenches photoconduction[53]. This is an important feature of the present work, and it is necessary to include (in the next few pages) a brief account of charge-transfer complexes.

The absorption spectra of charge-transfer complexes have been explained on a quantum-mechanical basis, by Mulliken[75]. Essentially, a photon is absorbed by two adjacent molecules, one of which is an electron donor 'D' and the other an electron acceptor 'A'. The ground state is often partially ionic, in which case a definite complex is formed[76]. A 'contact' charge transfer complex[74] can, however, absorb in a liquid <u>without the formation of a stable ground state</u>; a suitable configuration of the molecules being obtained by little more

than the process of statistical collision pairing. Molecular oxygen or iodine[74] dissolve to form the latter type of complex with the hexane.

The ground state of a charge-transfer complex may be described[77] by a wave function φ_{DA};

$$\varphi_{DA}(D,A) = a\,\varphi_o(D,A) + b\,\varphi_1(D^+A^-) \qquad (1)$$

where φ_o represents a nonbonding, and φ_1 a charge-transfer wave function, involving the transfer of an electron from D to A. If the coupling is weak, $a \gg b$; $a \to 1$, and $b \to 0$. The ground state is essentially non-polar.

For the excited state, a wave function φ_E is given by;

$$\varphi_E(D,A) = a^*\varphi_1(D^+A^-) - b^*\varphi_o(D,A) \qquad (2)$$

The transition to this state is responsible for the characteristic absorption of the complex. For $a^* \gg b^*$ the excited state is ionic; there is at least a partial transfer of an electron from D to A, the electron (on the average) spending more time in the vicinity of A than in the proximity of D.

Murrell[78] has pointed out that even if b in (1) is essentially zero, and there is no ionic stabilisation of the ground state, a charge transfer band could still be observed through the excited state of the donor. Thus, if the isolated donor has a transition $\phi_D \to \phi_D^*$ which gives rise to an intense absorption band, and if the charge-transfer state interacts with ϕ_D^* to give an eigenfunction for the DA complex of the form

$$\varphi(D^+A^-) = a\varphi^*(D^+A^-) + \lambda_{D^*A}\phi_D^* \qquad (3)$$

the effect will be that the charge-transfer band arising from the transition $\phi_D \rightarrow (D^+A^-)^*$ will have borrowed some intensity from the donor absorption band. Since ϕ_D^* is an excited state orbital it can be expected that it will be physically larger than ϕ_D. Even if the donor and accepter do not approach close enough for ϕ_D and ϕ_A to overlap appreciably there may still be sufficient overlapping of ϕ_D^* and ϕ_A.

For this simple one-electron model, the energy[75] of the transition $(D,A) \rightarrow (D^+A^-)$ is given in the first (zero ground-state overlap) approximation by

$$h\nu_{C.T.} = I_D - E_A - C$$

where 'I_D' is the ionisation potential of the donor, 'E_A' the electron affinity of the accepter, and 'C' is the mutual electrostatic (Coulomb) energy of D^+ and A^- relative to that of D and A. The separation of the charges is only a few Ångstroms and so the Coulomb energy can be a large fraction of I_D.

It is generally accepted[77] that the above mechanism accounts for the absorption of I_2-heptane mixtures (at around 2600Å), and that ... due to O_2 (starting at around 2500Å in hexane). In addition, since the ionisation potential of cyclohexane is about 0.2 eV. lower than the other hexane isomers, the oxygen absorption is correspondingly shifted to slightly longer wavelengths[79].

3.2(iii) Photochemical reactions in liquid hexane

The heats of combustion of isomeric organic compounds are nearly the same, and in a homologous series the increase per CH_2 (methylene)

group is almost constant at about 160 K.cal. Thus, the energies associated with particular bonds in a paraffin molecule are, to a large extent, additive[80]. For hexane the C-C bond energy is 60 K.cal (2.6 eV.), the C-H band energy being 87 K.cal (3.8 eV.). The bonds may break if the corresponding energy is supplied to vibrational modes of the molecule, i.e. by a thermal process. However, the absorption of a photon gives the molecule rather more than the bond energy (Sec. 3.2(ii). It is very likely that if the excitation is not deactivated by fluorescence, a bond may be stretched sufficiently to rupture. The bond which is broken generally belongs to the group orbital which absorbed the incident photon but a C-H group excitation in a hexane molecule can be internally converted to break a C-C bond[80]. In either case, two (or more) radicals are produced.

The separation of the radicals is restricted, in a liquid, by the close proximity of the other molecules. This 'solvent cage' is very effective in protecting the excited molecules from total rupture but is not so efficient in preventing rearrangement decomposition (isomerisation etc.). [It must be remarked that there are similarities between the 'cage effect' for radicals[90] and the recombination of ion-pairs in the liquid (cf. Section 3.1). Free radicals do not, however, carry an excess charge.] Some (especially small) radicals can always be expected to escape with subsequent reactions among themselves and with impurity molecules (notably oxygen).

Excitations, and subsequently radicals, are known to result from

high energy irradiation of the liquid[41]; it is to be expected that a comparable (and wide) range of substances will result from photo-excitation. The products will probably include unsaturated hydrocarbons (e.g. olefins), which are likely to be photochemically active themselves. It is seen that if light is absorbed by the liquid there can be an accumulation of diverse impurities.

Impurities are already dissolved in some specimens of hexane and will probably be present in greater quantities than those resulting from short periods of exposure to ultraviolet irradiation. Common impurities (Section 4.3) are dissolved oxygen and benzene; both absorb in preference to, or in conjunction with, the hexane (Section 3.2(ii)). However, photoconduction seems to result from the use of rather more energetic radiation than is absorbed by some impurities (Section 7.1), and the primary process may be excitation of the hexane. The reactions of excited hexane molecules with benzene or oxygen are important.

Burton[82] has proposed that benzene can remove the energy from an excited hexane molecule by energy transfer. The benzene molecule (in solution) has an excited singlet state at 4.7 eV. and a triplet state at 3.65 eV.[83] It is seen that the excitation potentials of hexane (M) and benzene (B) are such that

$$E_M^* > E_B^*$$

and it is possible that

$$M^* + B \rightarrow M + B^* + \text{kinetic energy}.$$

The benzene will probably be excited to a triplet state. This state is relatively stable (it has the same shape and is symmetrically related to the ground state), and the molecule will eventually dissipate its energy by internal conversions rather then decomposing into radicals[87].

Oxygen complexes with hexane on the absorption of the radiation (Section 3.2(ii)). Each molecule in the resultant species will be partially an ion (because of the charge it will have acquired) and partially a radical (by virtue of the unpaired spin of the electron)[84]. In view of the highly exothermic reactions between oxygen and hexane, it is likely that the molecules will chemically combine[85]. This might proceed (or be followed) by the dissociation of either molecule

i.e. $[R - H + O_2]^* \longrightarrow ROOH^* \longrightarrow$ oxidation products

or $[R - H + O_2]^* \longrightarrow R^{I} + R^{II} + O_2 \longrightarrow$ oxidation products

etc.[86] (See also Appendix I)

3.3 Injection of charges from the cathode

The distribution of potential V when a current of density J is flowing between two plane parallel electrodes of spacing L is given by

$$\frac{d^2V}{dx^2} = \frac{dE}{dx} = -\frac{\rho}{\varepsilon} \qquad \ldots\ldots\ldots\ldots (1)$$

and

$$J = -\rho\mu E \qquad \ldots\ldots\ldots\ldots (2)$$

in which ρ is the charge density and μ the mobility (both being negative), ε is the permittivity of the liquid, and 'x' is the distance from

the cathode at which the field is E.

The elimination of ρ in (1) from (2) and integration gives

$$E^2 = \frac{2Jx}{\varepsilon\mu} + \text{const.} \qquad \ldots\ldots\ldots\ldots (3)$$

The constant of integration describes the field exerted at the cathode by the anode; taking this field as E_o, (3) becomes

$$E^2 = \frac{2Jx}{\varepsilon\mu} + E_o^2 \qquad \ldots\ldots\ldots\ldots (4)$$

A further integration for 'U', the potential difference between the electrodes, results in[87]

$$U = \frac{\mu\varepsilon}{3J}\left[\left\{\left(\frac{2JL}{\mu\varepsilon} + E_o^2\right)\right\}^{3/2} - E_o^3\right] \qquad \ldots\ldots\ldots\ldots (5)$$

Equation (5) does not allow for movement of the liquid as a whole; if this velocity is 'v' relative to the electrode system, equation (2) must be modified[20] to

$$J = -\rho(\mu E + v) \qquad \ldots\ldots\ldots\ldots (6)$$

where u remains the mobility of the charges (relative to the liquid).

Substitution of (6) in (1) etc. results in [20]

$$U = \frac{\mu\varepsilon}{3J}\left[\left\{\left(\frac{2JL}{\mu\varepsilon} + \left(E_o + \frac{v}{\mu}\right)^2\right)\right\}^{3/2} - \left(E_o + \frac{v}{\mu}\right)^3\right] - \frac{vL}{\mu} \quad \ldots\ldots (7)$$

The velocity v will, in general, depend in a complicated way on the restrictions imposed by the electrode arrangement and the walls of the cell[44].

Two limiting cases will now be considered.

(i) $\frac{2JL}{\mu\varepsilon} \gg \left(E_o + \frac{v}{\mu}\right)^2$

Equation (7) reduces to

$$J = \frac{9}{8}\frac{\mu\varepsilon}{L^3}\left(U + \frac{vL}{\mu}\right)^2 \qquad \ldots\ldots\ldots\ldots\ldots (8)$$

and for $\frac{v}{\mu} \ll \frac{U}{L}$

(which, taking $\mu \sim 10^{-4}$ cm.^{2} V.$^{-1}$ sec.$^{-1}$ and $v = 1$ cm.sec.$^{-1}$, is when $\frac{U}{L} \gg 10$ KV.. cm.$^{-1}$)

$$J_{S.C.L.} = \frac{9}{8}\varepsilon\mu\frac{U^2}{L^3}$$

(ii) $\frac{2JL}{\mu\varepsilon} \ll \left(E_o + \frac{v}{\mu}\right)^2$

Equation (7) reduces to

$$U = E_o L$$

The effect of space charge on the potential distribution between the electrodes is negligible, the current is controlled by the conditions at the cathode, i.e.. is emission limited. Bulk liquid movement will, however, influence the value of the applied field at which the transition from space charge limitation occurs, through the $\frac{vL}{u}$ term in (8). When $E_o = \frac{U}{L}$ the current is given by

$$J_{E.L.C.} = n_o(U)e$$

where $n_o(U)$ is the rate of emission of carriers from the cathode (a function of U).

Thus, if $n_o(0)e \gg J_{S.C.L.}$, i.e. $E_o \leq 0$, the current is space charge limited.

If $n_o(0)e \ll J_{S.C.L.}$, i.e. $E_o \to \frac{U}{L}$, the current is, by definition, emission limited.

N.B. The value of n_o may be controlled, for photoinjection, by the intensity of illumination.

In condition (i) the current will not be increased by raising the intensity of illumination. When $(E_o + \frac{v}{\mu})^2 \simeq \frac{JL}{\mu\varepsilon}$ the current is controlled partly by space charge and partly by the rate of production of carriers. Finally, when $(E_o + \frac{v}{\mu})^2 \gg \frac{JL}{\mu\varepsilon}$ (condition (ii)) the current will depend directly on the intensity of the illumination, through n_o, and will increase according to $J = n_o(U)e$. For low intensities of illumination, the transition to emission limited conditions will be for low values of U.

3.4. Photoemissive properties of electrode materials

In the present work, films of aluminium, magnesium or gold were deposited (by vacuum evaporation) on clean, but oxidised metal substrates. These layers were used to photoinject charges (probably electrons) into liquid hexane. Some similarities were found between the photoemission in vacuo and the currents in the liquid. This section outlines the properties of such surfaces with regard to the vacuum photoemission. Some of these features are represented in Fig. 3.1.

(i) Aluminium[89]

The work function of clean aluminium[95] is about 4.2 eV, corresponding to a photoelectric threshold at 2900Å. Unless maintained in an ultra-high vacuum the surface can be expected to oxidise[88]. The thickness of the oxide layer will, to a large extent, determine the work function and quantum efficiency of photoemission[89].

Key to Fig. 3.1

(A) Gaviola and Strong;[95] evaporated Al. film

1. Surface with adsorbed gas (10^{-5} torr).
2. Clean surface.

(B) Edlinger and Muller;[96] decay of photoemission from abraded aluminium (10^{-4} torr).

(C) Cashman and Huxford;[94] evaporated Mg. film

1. At 10^{-7} torr O_2 (partial pressure) after stabilisation for 3 hours.
4. After initial sensitisation (O_2 at 10^{-7}torr).
5.)
6.) O_2 pressure slowly raised.
7.)

(D) Cashman and Huxford;[94] evaporated Mg. film ('gas-free').

(E) Ramsey and Garlick;[91] Decay of photoemission after abrasion of Al. in vacuum of 10^{-5} torr.

All photocurrents are in arbitrary units (identical units for C and D).

Fig. 3.1

PHOTOEMISSION FROM AL. & MG.

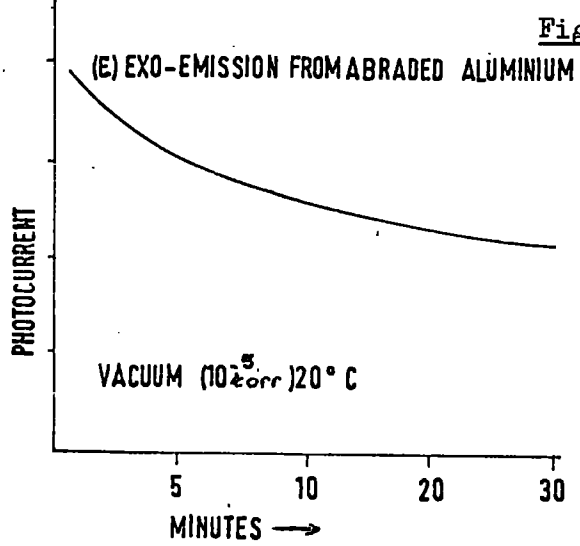

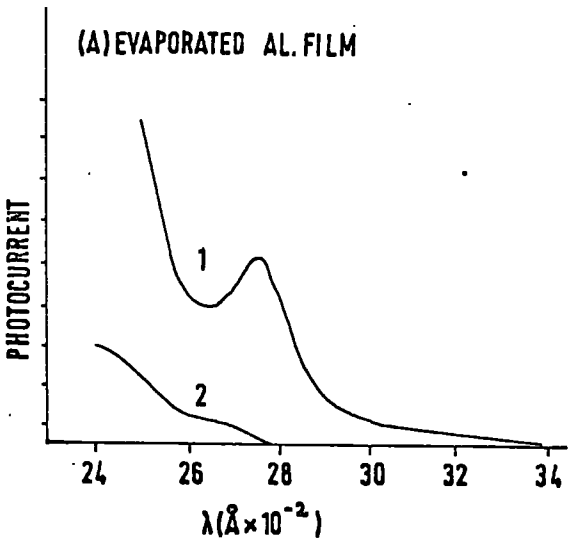

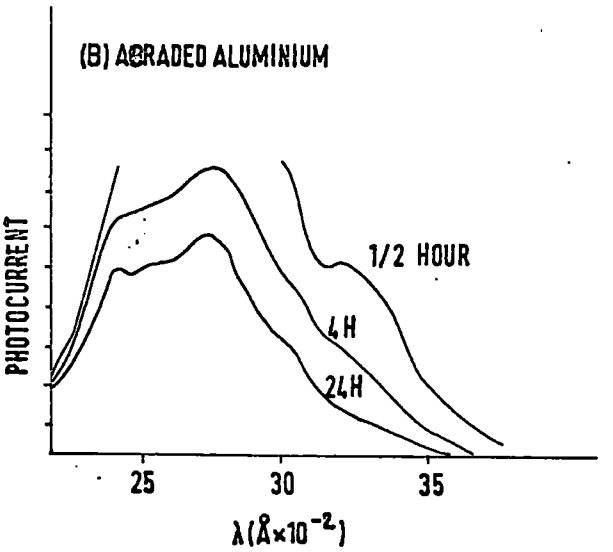

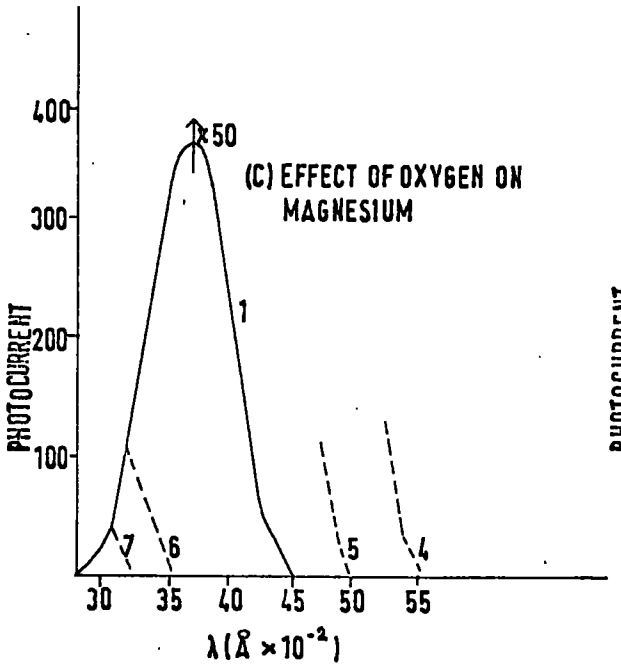

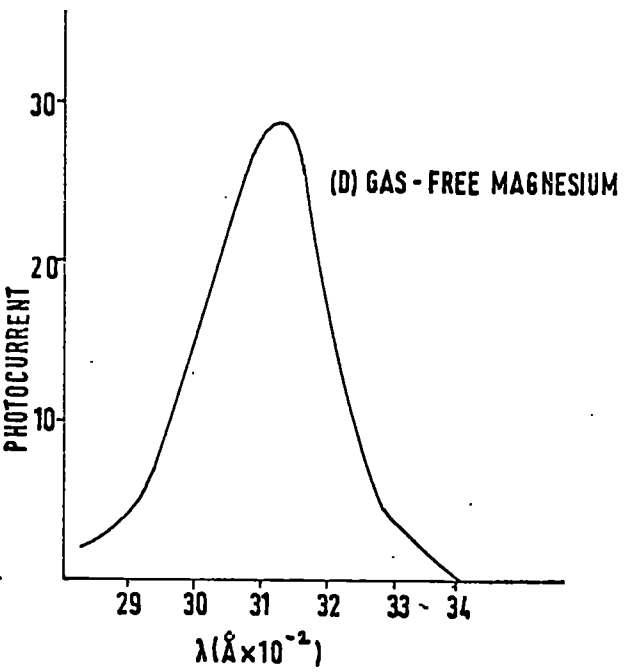

Aluminium films were prepared in a vacuum of $\simeq 10^{-6}$ torr. At this pressure, the chemisorption of oxygen at the metal surface will be complete in about 1 second. The immediate effect of chemisorption is to raise the work function by an amount equal to the electron affinity of oxygen. [A rough estimate, based on the ion size, dipole, and coverage oxygen, indicates the appearance of a negative contact potential of between 1 and 2 eV.] The oxygen is then incorporated in the metal to form an amorphous oxide, i.e. containing large numbers of cation and anion vacancies. As a result of the movement of these vacancies a relatively slow diffusion of metal ions will occur, to promote the growth of the oxide layer[91]. According to Bloomer[92], electrons from the metal may be trapped at the cation vacancies which Grunberg and Wright[93] assume to be at about 1 eV. below the oxide conduction band. These electrons may be photoemitted at energies less than the clean metal threshold since, if the electron affinity of the oxide is 1 eV., the effective work function of the complex will be about 3 eV. Because of the amorphous nature of the oxide layer the trapping levels will be indeterminate and the work function will be much less well defined in value than that for the clean surface[91]. Electrons trapped on the outer surface will be in much deeper levels and will not contribute directly to the photoemission, but will continue to be active in promoting oxide growth.

The photosensitivity will decay[96,97] with further growth of the oxide, until a physical adsorption equilibrium is reached between the impinging gas molecules and those leaving by thermal activation.

Thus, when exposed to air (at N.T.P.) a compact oxide layer, some tens of Ångstroms thick, will eventually cover the surface. This layer (after recrystallisation) protects the metal from further oxidation, and the photosensitivity will be relatively low[91] (being more characteristic of the oxide than the metal).

(ii) Magnesium[94]

The work function of gas-free surfaces of magnesium is about 3.5 eV., corresponding to a photoelectric threshold at 3430Å. The exposure of the clean surface to oxygen at a partial pressure of 10^{-7} torr causes a very great increase in overall sensitivity and a shift of the threshold to about 5700Å. The response to unfiltered light from a mercury vapour lamp may thus be as high as 10^6 times that of the pure layer. (If the clean surface becomes covered with a monolayer of hydroxyl groups the response can extend as far as 7000Å.) Exposure to oxygen at a higher pressure causes a recession of the threshold towards the ultraviolet. The oxidation of magnesium (on exposure to air at N.T.P.) eventually makes the surface insensitive to light of $\lambda > 2000$Å, with a corresponding decay in photosensitivity, (the layer being characteristic of MgO).

Magnesium, unlike aluminium, forms an oxide which has smaller volume than the metal. Thus, magnesium oxide, being porous, has little protective effect; and so oxidation does not limit (like aluminium), but proceeds linearly with time. The oxides of both metals are, to begin with, ~~amphous~~ amorphous and they will exhibit similar changes in photoemission. However, since aluminium produces an n-type, and magnesium

a p-type, oxide the latter (according to Grimley and Trapnell[98]) should have a pressure-dependent growth rate. Oxidation might be arrested and, possibly, even reversed by pumping on a magnesium surface.

(iii) Gold[99]

Gold does not oxidise appreciably[100], but sites for preferential photoemission may exist during the process of recrystallisation and rearrangement of the surface atoms[101]. Once this stabilisation is complete, i.e. within a few minutes from deposition, the photoemission should remain constant, with a work function of ~ 4.7 eV. (Adsorbed atomic layers can change the work function slightly, e.g. it is increased by H^+ ions, and reduced by air; but the changes are small compared to those encountered in true oxidation[99]). The overall sensitivity to irradiation from a mercury vapour lamp will be low, as the quantum efficiency is small even for light well above the threshold.

Experimental considerations

The photoemission from layers of aluminium or magnesium is seen to be very dependent on the state of oxidation. This, in turn, will be controlled by the partial pressure of oxygen (and other gases) over the surface, the rate of deposition, the thickness of the film, etc. It is best to employ as high a vacuum as possible during evaporation to avoid excessive contamination of the layers, and to deposit a fairly thick coating in a short time[102]. (Gases are less likely to be occluded in the film for a high rate of deposition, a thick layer reduces the risk of contamination from the substrate). However, the photoemission may be enhanced by slight oxidation of the surface; exposure of the

film to a partial pressure of oxygen of $\sim 10^{-7}$ torr should sufficiently sensitise aluminium[95] or magnesium surfaces[94] to produce useful photocathodes. In addition, the effective area of the film will be determined by the contours of the substrate; deposition on to a rough surface may substantially increase the photoemission (but there may be a more rapid decay with time because of the greater facility of oxidation).

CHAPTER IV

ANALYSIS AND PURIFICATION OF HEXANE

This chapter describes the analysis of hexane samples, and the purification of n-hexane to 'spectroscopic standards'. Two methods of analysis have been used; vapour phase chromatography (V.P.C.), and ultraviolet spectrophotometry. These methods have been found to be complementary; V.P.C. will detect all compounds within a small boiling range (including the isomers of n-hexane), and the u.v. spectrum is sensitive to unsaturated compounds.

4.1. Analysis of Hexane by Vapour Phase Chromatography

Two sets of chromatography apparatus were used; a Perkin-Elmer model 451 fractometer (used by courtesy of the Chemistry Department, Durham), and an apparatus constructed by E. Kahan[3,103]. Most measurements were taken with the Perkin-Elmer instrument, as this was somewhat more sensitive and convenient in use.

The Perkin-Elmer model 451 is a general purpose machine for the analysis of hydrocarbons. A wide range of columns is available from the manufacturers, three types of detector are supplied and there is a choice of carrier gas. Good results were obtained with a silicone grease packed column, a hot-wire detector, and hydrogen as carrier gas. Sensitivity to sample content was reasonably uniform, and for molecules of similar size was practically constant. The absolute sensitivity depended on the temperature of the column, detector voltage, and (to

a lesser extent) on the flow rate of the carrier gas. The column was kept at 60°C, so that a flow rate of 50 ml/min gave a retention time of about 2½ minutes for n-hexane with sufficient resolution to separate the isomers (which emerged in relation to their respective boiling points). Samples were injected into the carrier gas stream through a self-sealing rubber septum with a 40 microlitre hypodermic syringe. The sample injection block was kept at 80°C to ensure complete vaporisation of the hexane.

The apparatus gave an output on a potentiometric recorder, each (time resolved) peak corresponding to an individual hydrocarbon. Areas under the peaks were proportional to the quantities of each constituent, the concentration being obtained by summing the total area and taking this as 100% (i.e. assuming no large undetected components). Compounds were identified by their retention times and, where possible, were checked by the effect of adding small quantities of each to the sample under test. No arrangements were made, or needed, to inject precise quantities of liquid into the column.

Attenuation of the detector output was provided, in successive multiples of 2 to 512:1, this allowed peaks to be kept on the scale of the recorder. A component comprising 50% of an injected 5 µl. sample produced a full scale deflection of 12" with an attenuation of 64 x. Concentrations greater than about 0.1% were readily measured by reducing the attenuation. An increase in the sample volume gave a larger output and, with an injection of 30 ul., concentrations less than .01% could be detected. For maximum resolution the smallest reasonable

quantity of hexane was injected. Only when detecting minor or trace quantities, having well separated retention times, was it desirable to use the larger quantities; overload of the column or detector being avoided for accurate quantitative measurements.

4.2. Analysis of Hexane by Spectrophotometry

Pure liquid alkanes are transparent over the visible and most of the ultraviolet range of the spectrum[69]. Absorption by hexane begins at about 2400Å and is intense at 2000Å. Unsaturated hydrocarbons absorb strongly in the wavelength range 2000-4000Å and so very small quantities of these substances can be detected as impurities in hexane[71]. In the present work, it was desirable that radiation should reach the electrodes without complications due to absorption in the bulk of the liquid. The ultraviolet absorption of the liquid was, therefore, investigated in considerable detail.

An Optica CF4DR double beam spectrophotometer was used for the absorption measurements. Most of the spectra were taken over the wavelength range 2000 to 3500Å. The recorder trace gave transmission on a scale of 0-100% with an accuracy of $\pm$ 0.2% and $\pm$ 5Å.

The liquid samples were contained in stoppered silica cells with optically polished end windows. Cells with light paths of 1 and 10 cm. were chosen, matched pairs of cells being purchased to compare the hexane against a water blank in double beam operation. Unfortunately, sufficiently transparent water was not obtainable and so the hexane was measured, in each case, against an air blank; internal reflections

in an empty cell prohibiting its use as a compensator. The absorption of the cells themselves was about 8% over most of the range. Cells were cleaned according to the manufacturer's recommendations, and were rinsed with clean hexane before each test. Care was taken not to contaminate the cells and, in particular, the windows were not touched except in polishing them with a clean Selvyt cloth.

4.3. Grades of Hexane and their Purity

During the course of this work the following grades were analysed

(i) British Drug Houses (B.D.H.) 'Fraction from Petroleum' hexane

(ii) Hopkin and Williams 'General Purpose Reagent' hexane

(iii) B.D.H. 'Special for Spectroscopy' hexane fraction

(iv) B.D.H. 'n-hexane'

(v) Koch-Light Ltd '99% n-hexane', 'puriss grade'.

These are described in turn.

(i) B.D.H. 'Fraction from Petroleum'

An analysis of this grade was obtained (informally) from the manufacturers. This is compared with the results obtained by V.P.C.;

	B.D.H. Analysis w/w	Present Work	
2 Methyl pentane	5.9%	2-methyl pentane or 2-3 methyl butane or both	6.0%
3 Methyl pentane	11.5%	3-methyl pentane	10.7%
n-hexane	67.7%	n-hexane	67%
methyl cyclopentane	14.2%	methyl cyclopentane	14.0%
cyclohexane	0.7%	cyclohexane + benzene	1.3%
benzene	0.5% (v, by i.r.)		

+ other traces amounting to about 1% (n-pentane, and tarry compounds)

Fig. 4.1

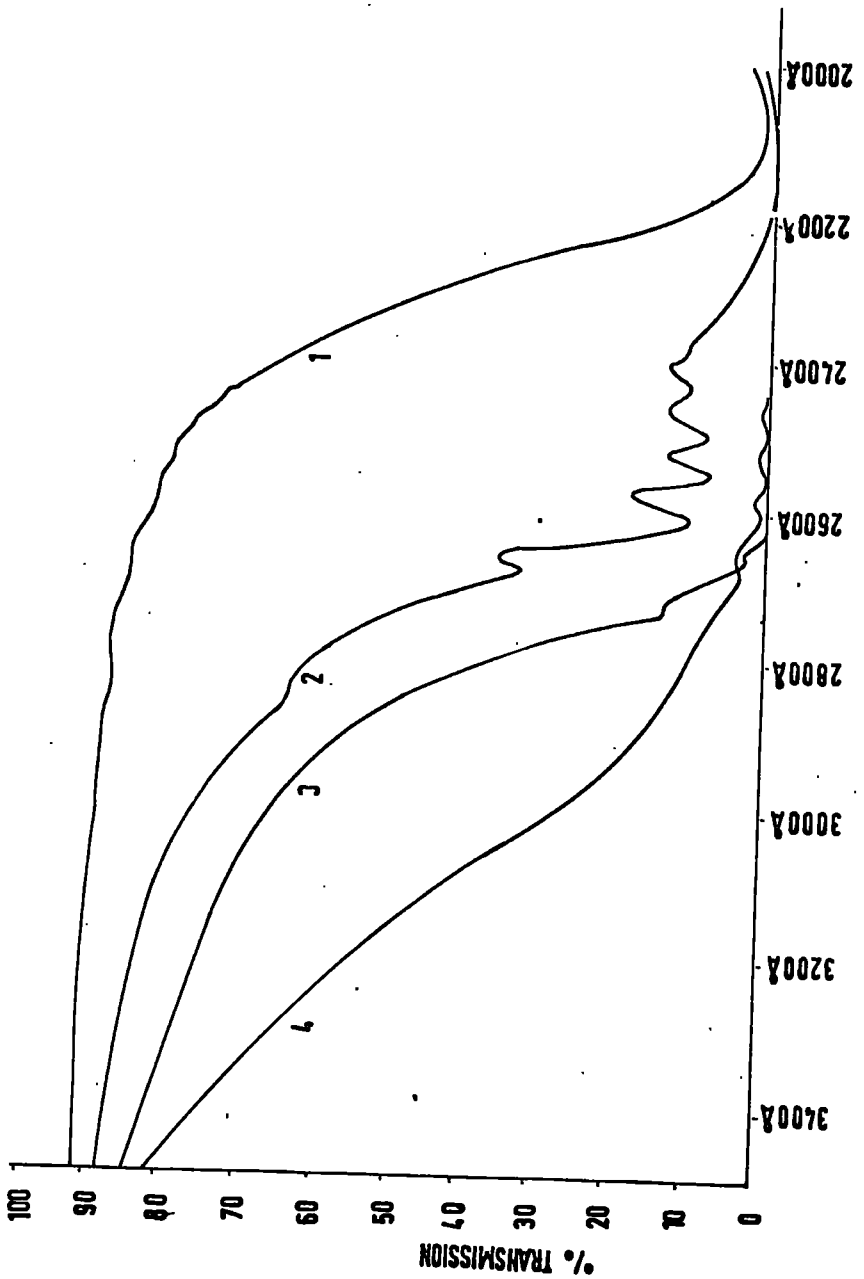

1 SPECTROSCOPIC HEXANE

2 HOPKIN & WILLIAMS G.P.R.

3 LIGHTS N-HEXANE

4 B.D.H. N-HEXANE

In view of the expected variation of composition between bottles the results seem to be in reasonable agreement.

(ii) Hopkin and Williams 'General Purpose Reagent' grade hexane

This is described as having a specific gravity of about 0.68 and a boiling range of 95% (minimum) between 68° and 70°C.

The composition by V.P.C. was found to be similar to the foregoing B.D.H. grade. The u/v transmission is shown in Fig. 4.1.

(iii) B.D.H. 'Special for Spectroscopy' hexane fraction

This grade of hexane is in general use as a photometric solvent, and is specified as having a minimum transmission, in a 1 cm. cell against a water blank, of 70% at 2200Å and 95% at 2500Å.

The 'Spectroscopic' hexane appeared to be substantially the same as the B.D.H. 'Fraction from Petroleum' when analysed by V.P.C. (see Fig. 4.2). However, the Spectroscopic grade contains practically no benzene, as is shown in Fig. 4.1 by the high u/v transmission. (This difference in benzene content was found to be obscured in the analysis by V.P.C. because of the coincidence of the retention times of benzene and cyclohexane). Apart from the isomer content, there were traces of other substances in this grade. Some of these were identified, the analysis being as follows;

Peak	Substance	Quantity
1	n-butane	trace (V. small)
2	iso-pentane	trace (V. small)
3	n-pentane	0.05%
4	2-2 dimethyl butane	trace (V. small)

Fig. 4.2

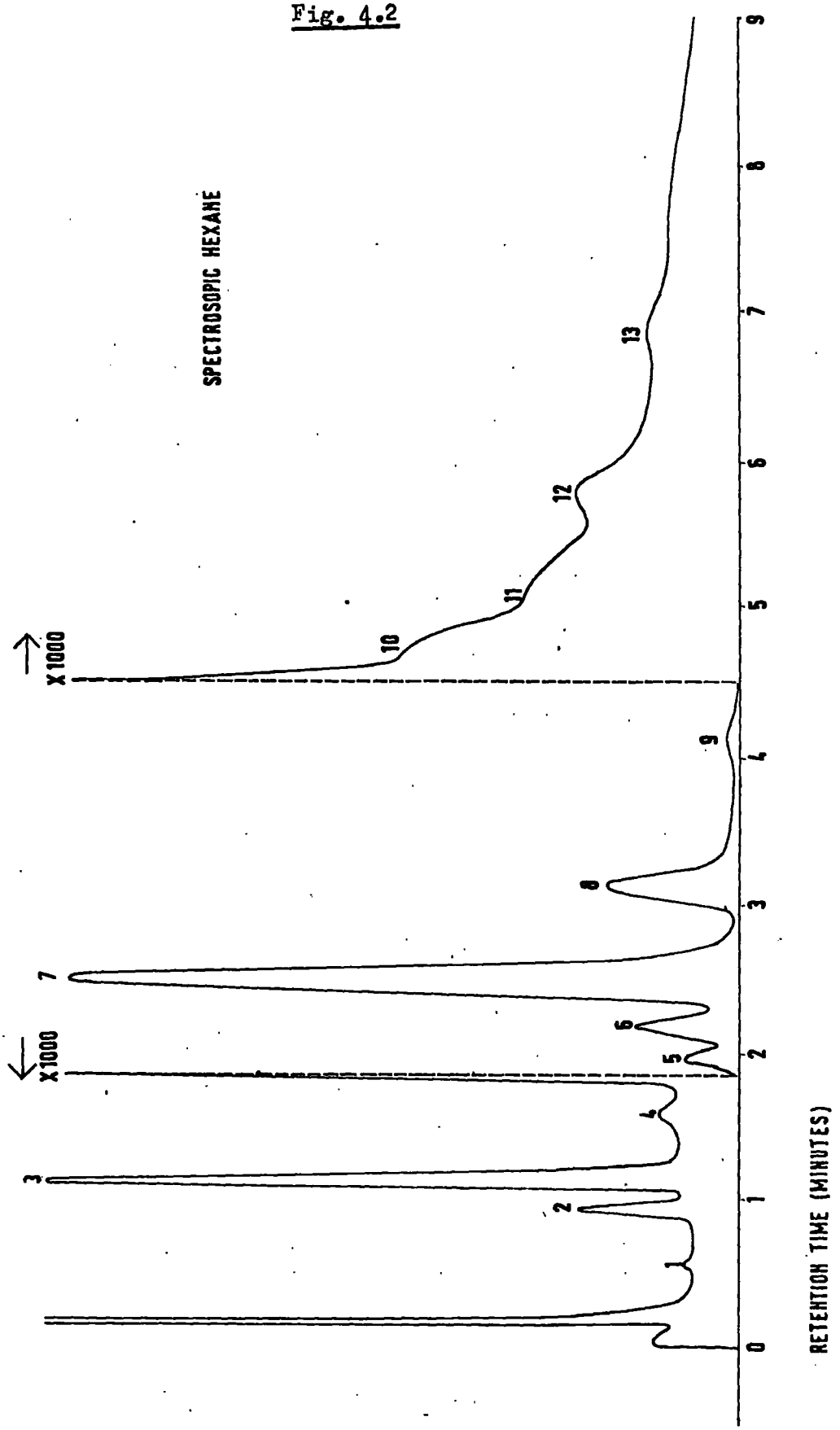
SPECTROSOPIC HEXANE
X1000
X1000
2
3
4
5
6
7
8
9
10
11
12
13
0
1
2
3
4
5
6
7
8
9
RETENTION TIME (MINUTES)

Peak	Substance	Quantity
5	2-3 methyl butane or 2 methyl pentane or both	5.8%
6	3 methyl pentane	10.9%
7	n-hexane	68.0%
8	methyl cyclopentane	13.5%
9	cyclohexane	0.8%
10,11,12,13	unidentified	traces

Measurements made by Kahan[103] on this grade are very similar except in the interpretation of peaks 8 and 9, which he ascribed to 2,4 dimethyl pentane and methyl cyclopentane respectively, using a squalane capillary column. With the silicone grease column these peaks are well separated, and peak 9 has now been positively identified as cyclohexane.

This analysis can only be taken as typical, isomer and trace content can be expected to vary with the nature of the crude and its subsequent fractionation.

(iv) B.D.H. n-hexane

The manufacturer's limits include a boiling range of not more than 1°C, a specific gravity of about 0.66 at 20°C, and 99% n-hexane.

The analysis by V.P.C. is shown in Fig. 4.3. The peaks were identified as follows; (see Table overleaf)

The u.v. transmission (shown in Fig. 4.1) indicated the presence of benzene and unsaturates in trace quantities.

Fig. 4.3

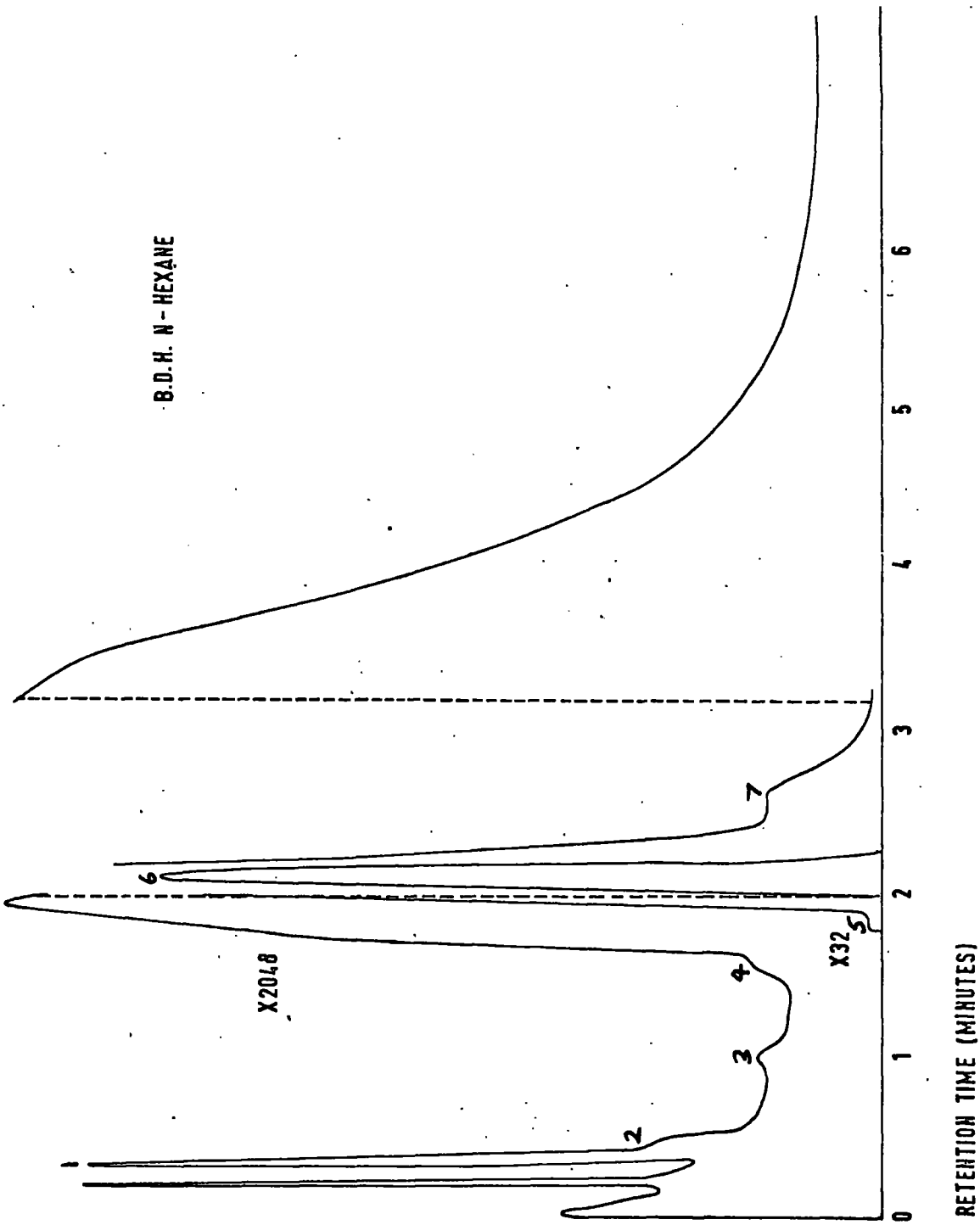
B.D.H. N-HEXANE
X2048
X32
1
2
3
4
5
6
7
0
1
2
3
4
5
6
RETENTION TIME (MINUTES)

Fig. 4.4

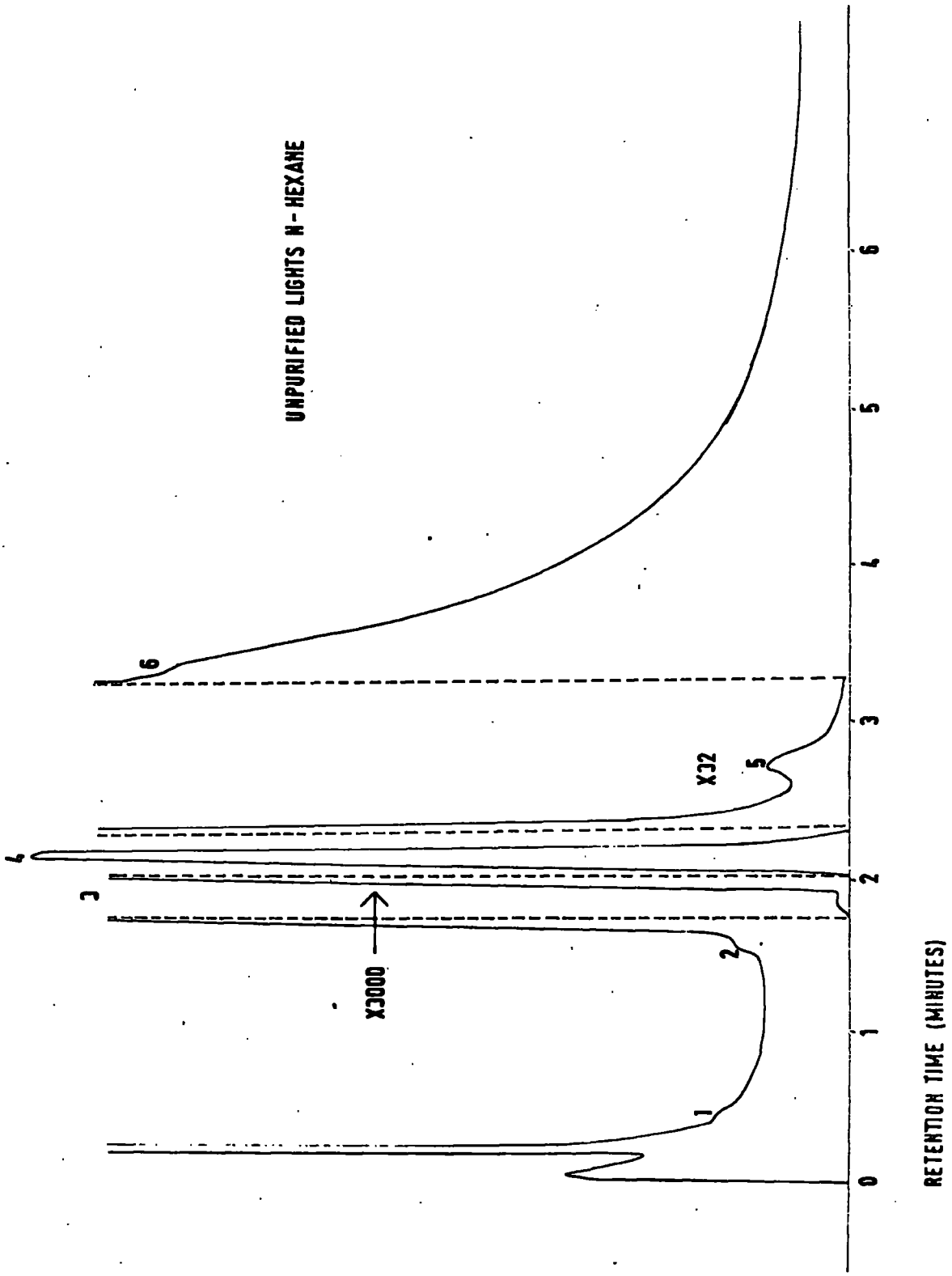
UNPURIFIED LIGHTS N-HEXANE
X3000
X32
1
2
3
4
5
6
0
1
2
3
4
5
6
RETENTION TIME (MINUTES)

Peak	Substance	Quantity
1	n-butane	0.02%
2	unidentified	trace
3	n-pentane	trace
4	2,2 dimethyl butane	trace
5	3 methyl pentane	0.03%
6	n-hexane	99.5%
7	2,4 dimethyl pentane	0.4%

(v) Koch-Light 'Puriss Grade' n-hexane

The 'Puriss' grade is guaranteed to consist of at least 99% n-hexane. A typical analysis (of Batch no. 8249) by V.P.C. is shown in Fig. 4.4, the peaks are identified as follows;

Peak	Substance	Quantity
1	probably n-butane	trace
2	2,2 dimethyl butane	trace
3	3 methyl pentane	0.03%
4	n-hexane	major constituent
5	2,4 dimethyl pentane	0.3%
6	benzene	trace

This grade was thus about 99.7% n-hexane with only small quantities of other compounds (mainly isomers). One sample (batch no. 14151) contained very little 2,4 dimethyl pentane and was consequently more pure. The u.v. absorption of this liquid is shown in Fig. 4.1.

Some samples of this grade were slightly yellow in colour. After pumping off 100 gm. of hexane in a closed container, a residue of approximately 10 m.g. of yellow plate-like crystals, soluble in hexane and smelling strongly of moth-balls was obtained. This was examined in the infra-red with a Grubb-Parsons 'Spectromaster' spectrophotometer. The impurity was identified as a disubstituted napthylamine.

Light's 'Puriss' grade hexane is probably the most pure and reliable source of n-hexane available in this country. The level of impurity was within the manufacturers specification on all specimens tested (and subsequently used) for the purpose of this thesis.

4.4 Further purification of n-hexane

The analyses, described in Section 4.3, showed that most of the available grades of hexane were not suitable for the present work because of their high u.v. absorption. The only sample which was sufficiently transparent was the 'Special for Spectroscopy' grade, but its high isomer content made it useful only for general exploratory work. The best source of n-hexane was that from the Koch-Light laboratories, the analysis of which showed only a small isomer content, but traces of unsaturated compounds were invariably present. Apart from the general undesirability of impurities, their presence could lead to photochemical activity of an uncertain nature. Accordingly, a purification technique was developed to remove the unsaturates; and very clean, almost completely transparent, n-hexane was obtained from the Koch-Light grade.

Three methods of purification were considered;

(i) Catalytic hydrogenation[104], this is best carried out at high pressure with a Raney nickel catalyst at 120°C.

(ii) Percolation through silica gel[69], to remove unsaturates by adsorption. (See also Appendix II)

(iii) Emulsification with concentrated sulphuric acid[104], which precipitates unsaturates after neutralisation with sodium hydroxide.

All three methods introduce contamination by particles while(i) and (iii) produce chemical residues which can only be removed by fractional distillation. For this reason, method (ii) was chosen, and steps taken to remove particles (of gel) by filtration.

The u.v. spectrophotometer was used to measure the extent of purification in each stage. In practice, benzene was the most obvious and optically damaging impurity;; its characteristic absorption (Figs. 4.6 and 4.7), being distinguished even for concentrations of less than one part per million in the hexane. The liquid after purification showed no trace of benzene and was thus more pure than any commercially available hexane. In addition, the remaining impurities consisted only of small quantities of the less harmful hexane isomers, not removeable by silica gel.

4.5. Experimental Details of the Purification Process

The liquid was percolated down a long narrow column of gel contained in a clean Pyrex tube. The gel/hexane slurry was supported in the column by a sintered glass disc (1μ max.. pore diameter), below

Plate I

A. Silica gel column for preliminary purification of hexane, and water cooled column for final percolation.

B. Yellow impurity removed from each specimen of Koch-Light n-hexane by first percolation (indicated by arrow in A).


A

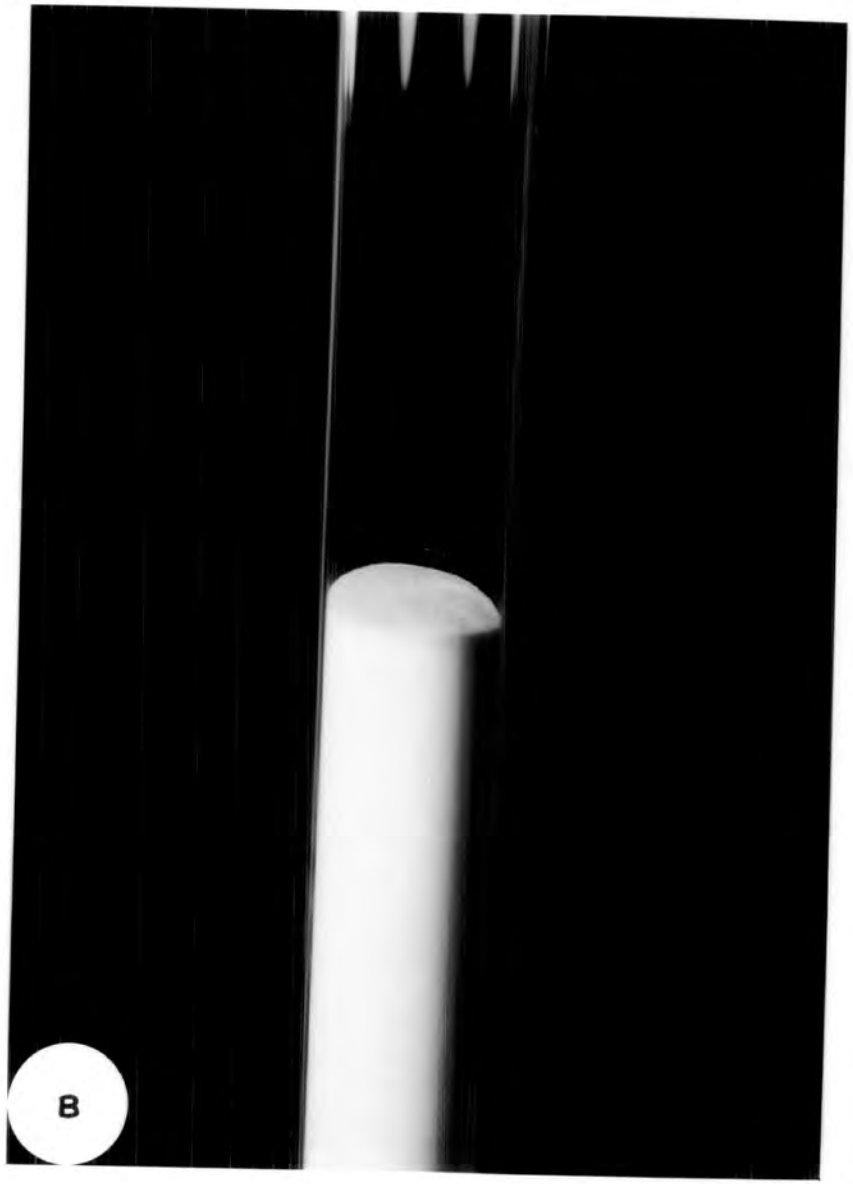
B

Fig. 4.5

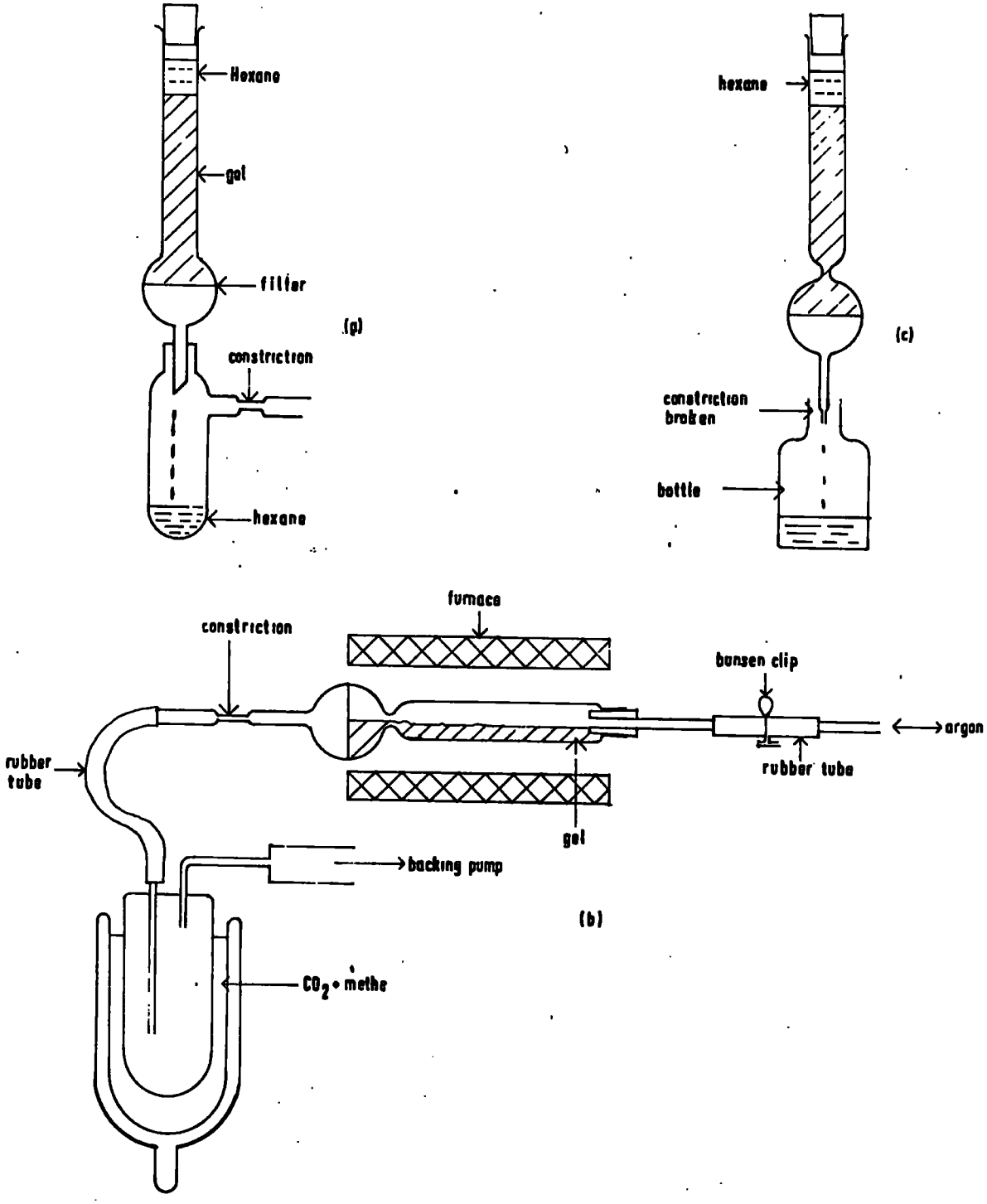
Hexane
gel
filter
constriction
hexane
(a)
hexane
constriction broken
bottle
(c)
furnace
constriction
bunsen clip
argon
rubber tube
rubber tube
gel
backing pump
(b)
CO_2 + methe

which was a taper to direct the flow of hexane (see Fig. 4.5(a)). All glass parts were cleaned by rinsing with 'Special for Spectroscopy' grade hexane and were dried, by evacuation, before filling with gel.

For maximum efficiency, the gel surfaces needed to be dry and freshly cleaved. Crushing the crystals of gel to a fine powder was generally satisfactory, but subsequent heating to 250°C under vacuum produced the best results, (see Appendix II). The capacity to absorb unsaturates was reduced considerably by the presence of moisture in the hexane, and at least two percolations (with fresh gel each time) were usually necessary. A distinct yellow discoloration of the top of the column was observed (see plate (i)) after the first percolation of every batch of Koch-Light n-hexane; presumably being due to the separating out of the napthylamine compound which had been already detected in this grade (see Section 4.3(v)).

The initial percolation was always accomplished with freshly crushed gel without further treatment. For each percolation 300-500 gm. of gel, from a newly opened bottle, were required. The crystals were wrapped in several thicknesses of 12" dia. filter paper and crushed in a hydraulic press to a fine powder. (The wrapping eliminated the risk of contamination from the press and helped to avoid the adsorption of water vapour from the air). The filled column was then shaken, to pack down the gel, and the hexane introduced as soon as possible. The leeching of impurities down the column was avoided by not allowing the level of the hexane to fall below the top surface

of the gel. With a tightly packed column of fine powder, and not more than 4" head of hexane over the gel, the flow rate was satisfactorily slow; 300 gm. of hexane taking about 3 hours to percolate through. The liquid was gathered in a clean glass container as it emerged from the filter, a narrow breather hole restricting the intake of moisture from the atmosphere (see Fig. 4.5(a)). Liquid left in the column was drained into a separate bottle for use again; the clean hexane being kept for further purification.

The remaining impurities were removed by another percolation. For the best results, the freshly crushed gel was heated at 250°C in a partial vacuum (10^{-2} torr) for six hours in the column itself (see Fig. 4.5(b)). A stream of pure argon was passed over the gel as it cooled to room temperature. The constriction in the outlet of the column was sealed, with a gas blowtorch, and the vacuum pump and trap removed. (This latter procedure was advisable to avoid the blow-back of wet air into the column, but it also had the advantage of providing a clean outlet for the hexane). The column was removed from the furnace and the gel was shaken down. Hexane was poured in and the constriction broken (Fig. 4.5(c)). A little hexane was allowed to run from the outlet (to rinse the inside of the tube) and then a carefully cleaned and dried bottle, or preferably a container as shown in Fig. 4.5(a), was placed to catch the hexane.

With a very dry column some of the hexane is adsorbed, and local heating in the gel may result. This was undesirable, as high boiling point impurities could vaporise and pass freely down the tube. The

Fig. 4.6

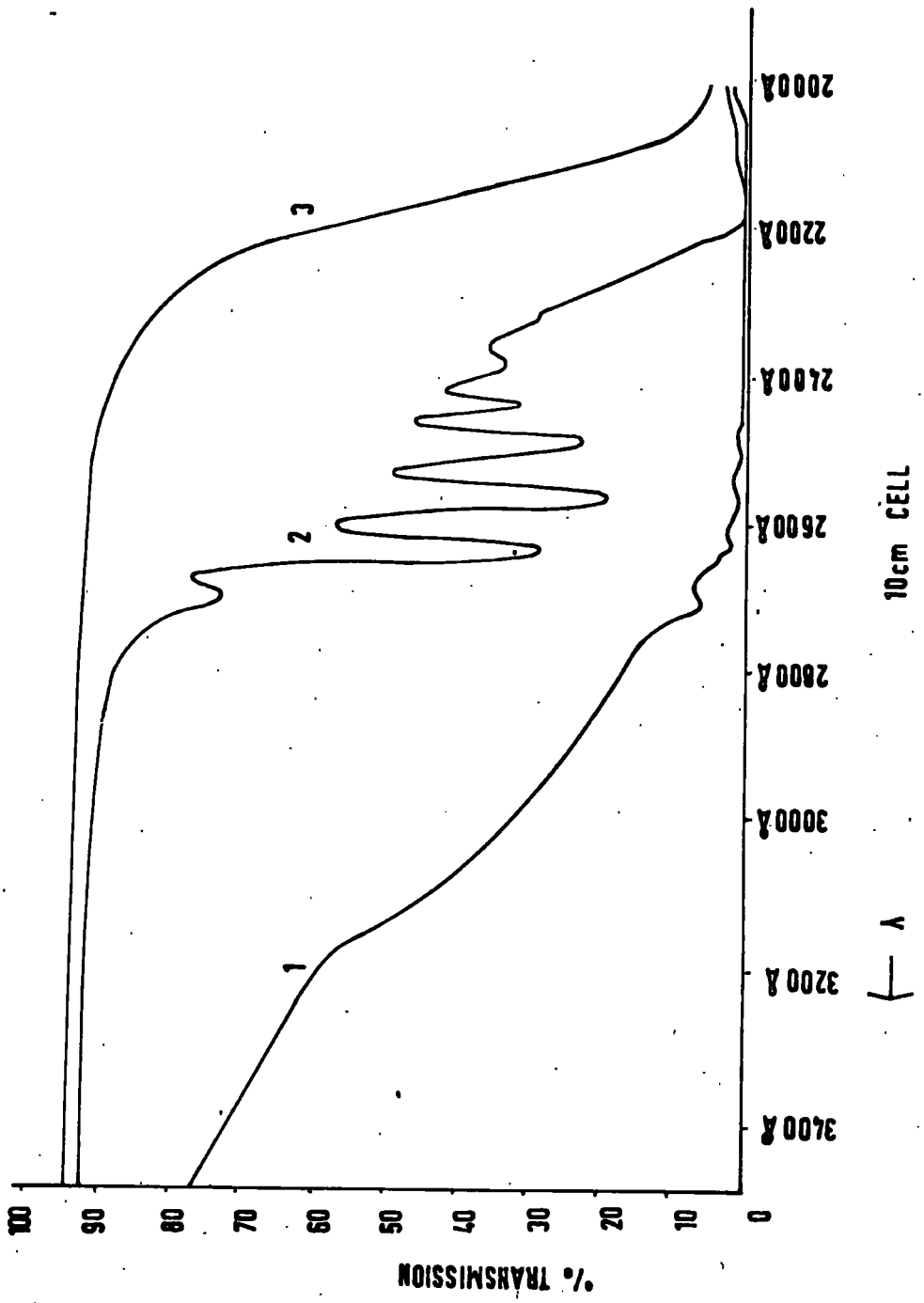
% TRANSMISSION
100
90
80
70
60
50
40
30
20
10
0
3400 Å
3200 Å
3000 Å
2800 Å
2600 Å
2400 Å
2200 Å
2000 Å
A
10cm CELL
1
2
3
1 UNPURIFIED LIGHTS N-HEXANE
2 AFTER FIRST PURIFICATION
3 AFTER SECOND PURIFICATION

Fig. 4.7

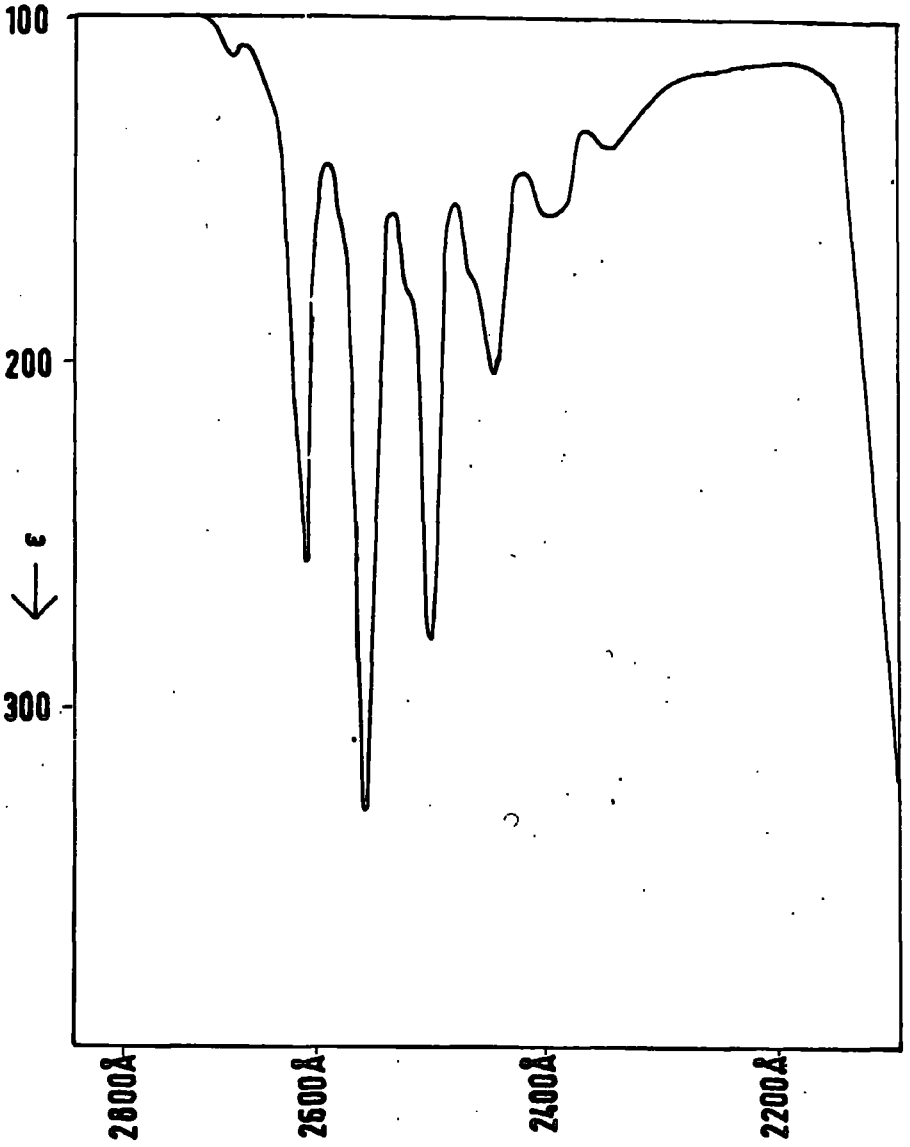

BENZENE IN HEXANE

$(I = I_0 10^{-\varepsilon c d})$

ε - MOLAR ABSORPTIVITY

c - MOLES / LITRE

d - cm LIGHT PATH

FROM MOLECULAR SPECTROSCOPICS

G.H. BEAVEN & E.A. JOHNSON

HEYWOOD & CO. LTD. 1961.

heating was minimised by using a tightly packed column to restrict the flow of hexane. Water cooling was desirable with a fully activated column.

Freshly crushed gel could sometimes be used without further activation, thus reducing the time taken to prepare the column. In any case, at least two percolations were necessary to obtain good results (see Fig. 4.6).

The clean hexane was stored under argon and in coloured bottles to avoid any photochemical reactions. Dust protection was provided for the stoppers, and the bottles were opened as infrequently as possible; since all liquids tend to collect dust and fibrous particles.

Each sample used in the electrical measurements was subjected to u.v. examination a few hours before the degassing process. The sample was discarded if found to be unsatisfactory.

4.6 Ultraviolet absorption of pure n-hexane

The purified n-hexane (Fig. 4.9), contained no unsaturated compounds which could be detected by V.P.C. or by optical means, and the benzene content was certainly less than 1 part in 4×10^6. (This was confirmed by the addition of known quantities of benzene to the hexane (Fig. 4.8).) The absorption of the pure liquid is, however, increased by dissolved air (see Fig. 4.9). Evans[73], and others, have shown that dissolved oxygen in a variety of organic solvents gives rise to absorption bands (most probably of charge-transfer origin[74]). Thus,

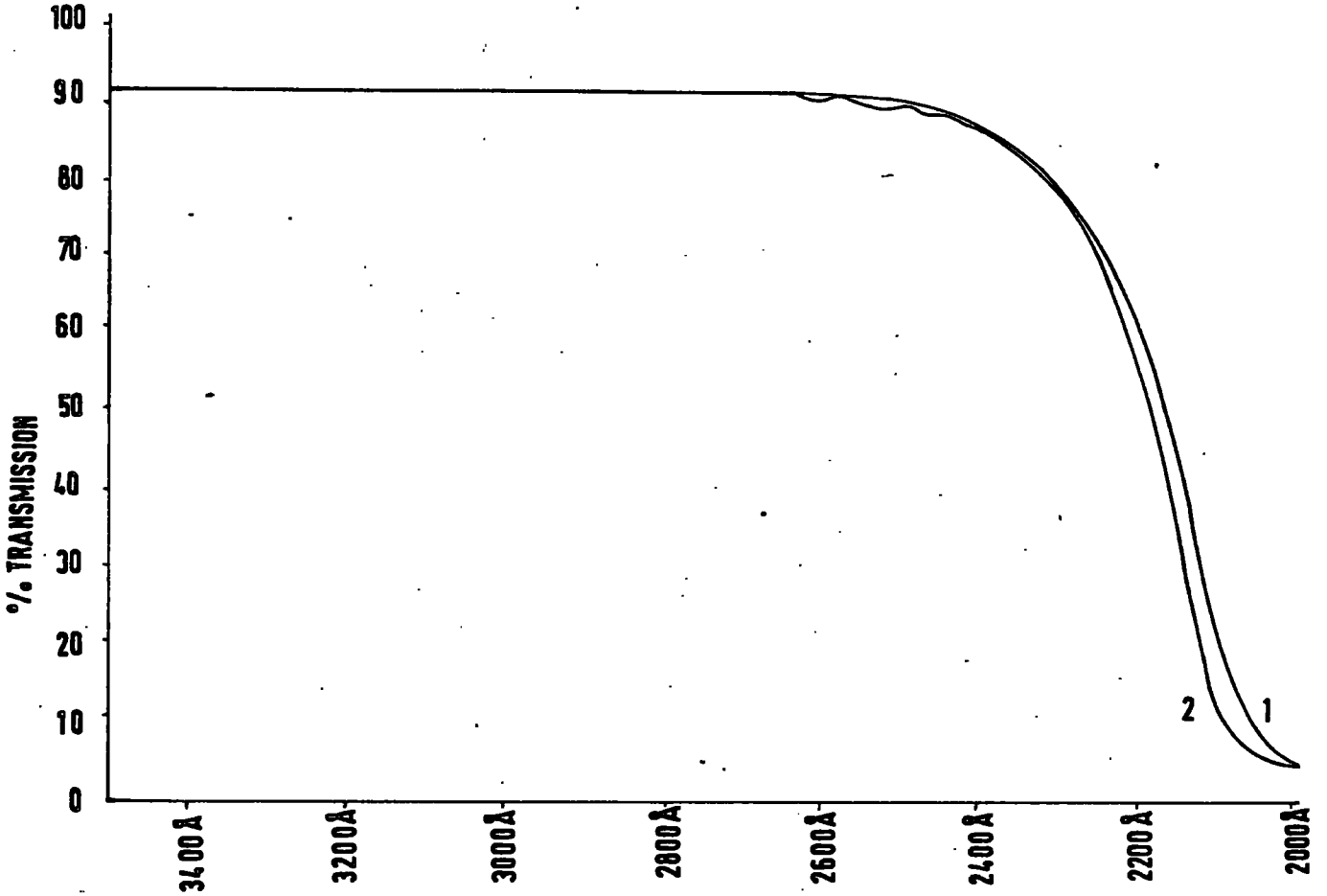

Fig. 4.8

1 PURE N-HEXANE

2 PURE N-HEXANE + 1 PART IN 4×10^6 BENZENE

Fig. 4.9

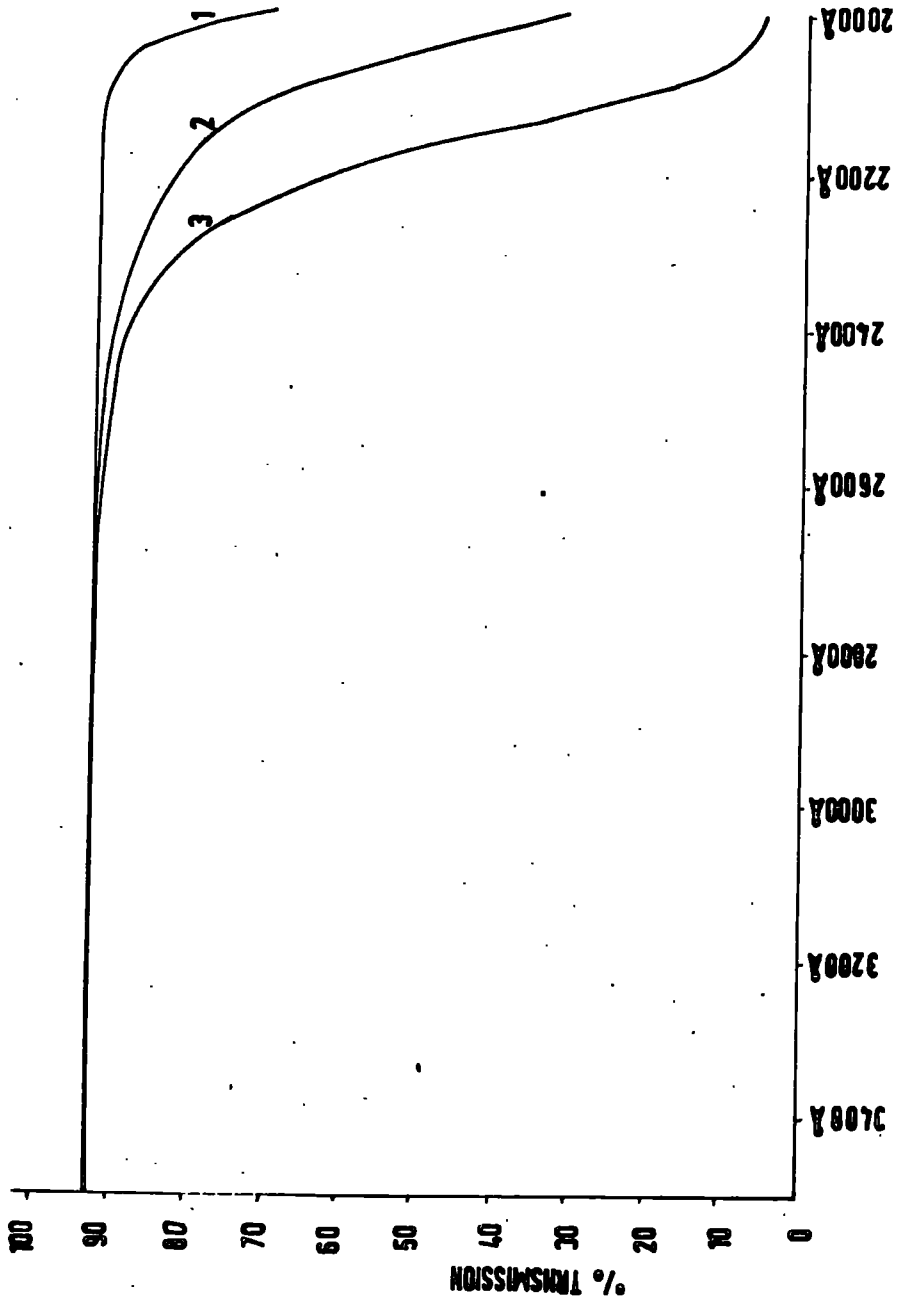

1 1cm PURIFIED N-HEXANE DEGASSED

2 1cm PURIFIED N-HEXANE GASSY

3 10cm PURIFIED N-HEXANE GASSY

the removal of oxygen from air saturated hexane will reduce the absorption in the 2000-2200Å region to about a quarter of its previous level. The effect of oxygen is considerably greater in cyclohexane than for the other hexane isomers, and is least for n-hexane (Munck and Scott[79]).

In the present work, specimens of purified n-hexane have been degassed to 10^{-6} torr. Although the absorption was considerably reduced (as is shown in Fig. 4.9) and is increased again as soon as air is let in, it is not known if the remaining absorption in the highly degassed liquid is due to the last traces of oxygen, unsaturates, or is the true hexane limit. An extensive search in the literature failed to clarify this. (In general, absorption edges are quoted only for gassy specimens or for hexane vapour, which does not absorb irradiation of wavelengths longer than about 1750Å.)

Nevertheless, the purification process does provide very clean n-hexane. The analysis by V.P.C. and ultraviolet spectrophotometry allows much more rigorous control of samples for electrical measurements than has previously been evident.

CHAPTER V

APPARATUS AND TECHNIQUES

5.1 Test cells

This Section describes the test cells used for the conduction measurements. Cells are listed in chronological order of their manufacture and use. Their design is discussed with regard to their general functions only; modifications for a specific experiment are stated in the context of the results obtained.

Each cell contained two flat electrodes. These were spaced approximately 1 cm. apart in a parallel plate configuration. The circumference of each electrode was contoured to avoid excessive field distortion, but no attempt was made to approach the 'ideal profile' for very uniform field distribution. Cells were constructed mainly from Pyrex glass; a silica window (cemented on with hot-setting Araldite) admitted ultraviolet irradiation to the electrode system.

Measurements involving the use of degassed hexane were made with cells 1-4. Each of these cells was evacuated by, and subsequently received hexane from, the degassing system. A narrow bore (2 mm.) constriction in the (Pyrex) pumping port could be sealed off to enable the cell to be removed for the electrical measurements. Hexane was frozen into the cell reservoir ($\sim$ 80 cc. capacity) at liquid nitrogen temperature during this procedure (see Sec. 5.2), and when it was desired to take measurements in vacuum. Consequently,

each cell was required to maintain a high vacuum (approx. 10^{-6}torr) for long periods of time after sealing off.

Experience in the use of cells 1-3 led to the development of cell 4, which had provision for the repetition of 'crucial measurements.

Cell 1.

For the first measurements, which were essentially exploratory, a cell constructed by Morant was used (see Fig. 5.1).

Both electrodes (1.5 cm. dia.) were constructed from solid aluminium. The cell had been kept in dry air for some time and the electrodes, though otherwise quite clean, had lost their original polish. For later experiments the cell was opened, to remove the electrodes for repolishing, but it was otherwise undisturbed.

Detail of Cell 1.

Electrical contacts to the electrodes was made through 1 mm. diameter tungsten leads, which were sealed into the envelope of the cell. The electrodes were supported on these leads by tight fits into aluminium bosses, secured by recessed 10 B.A. grub screws. At each seal, a long leakage path provided the necessary insulation for the measurement of the low photocurrents ($\sim 10^{-13}$A.) in the hexane. A length of fine wire, wound around the neck of each insulator and around the circumference of the cell, served as a guard ring when connected to earth. The electrodes were obliquely illuminated through a 2 mm. thick silica window.

Fig. 5.1

CELL 1

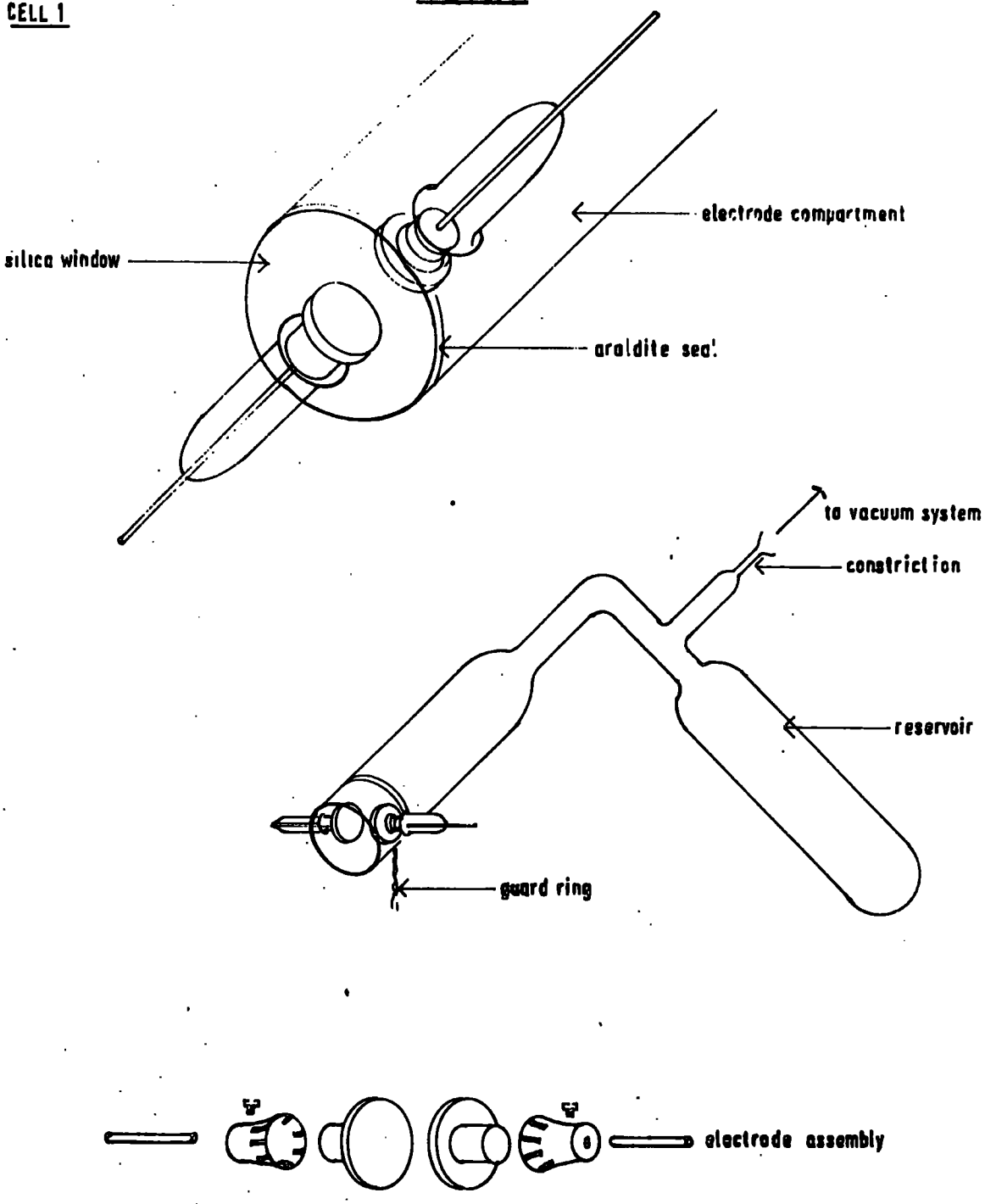
electrode compartment
silica window
araldite seal
to vacuum system
constriction
reservoir
guard ring
electrode assembly

Cell 2

Cell 2 was manufactured to see if charges could be injected into degassed hexane from a photocathode of evaporated aluminium. This cell (see Figs. 5.2 and 5.3) incorporated a tungsten filament, from which aluminium was evaporated in the high vacuum provided by the degassing system. Degassed hexane was admitted to the cell, shortly after coating the electrode, and was frozen into the reservoir. The cell was then isolated by sealing off the constriction, so that the vacuum was maintained. The coated electrode was rotated through 180° to face the other fixed electrode (a semitransparent layer of tin oxide on silica) for the electrical measurements.

Detail of Cell 2

The rotatable electrode was made, from solid aluminium, in the form of two 1 cm. discs which were linked by a shaft 1 cm. long. The discs were polished to provide two similar flat electrode surfaces. A 0.5 mm. tungsten wire, passing through a central hole in the shaft, allowed the electrode assembly to rotate. (This wire had been previously sealed into the Pyrex envelope of the cell, so that it protruded 20 mm. across the 30 mm. diameter of the tubular electrode compartment. Bearings on either side of the electrode shaft limited the rotation to a plane normal to the wire in the centre of the tube). The balanced system could be revolved, to the desired position, by the external application of a bar magnet to a tool steel rod attached to the electrode shaft.

The second electrode was a thin conducting layer of tin oxide

Fig. 5.2

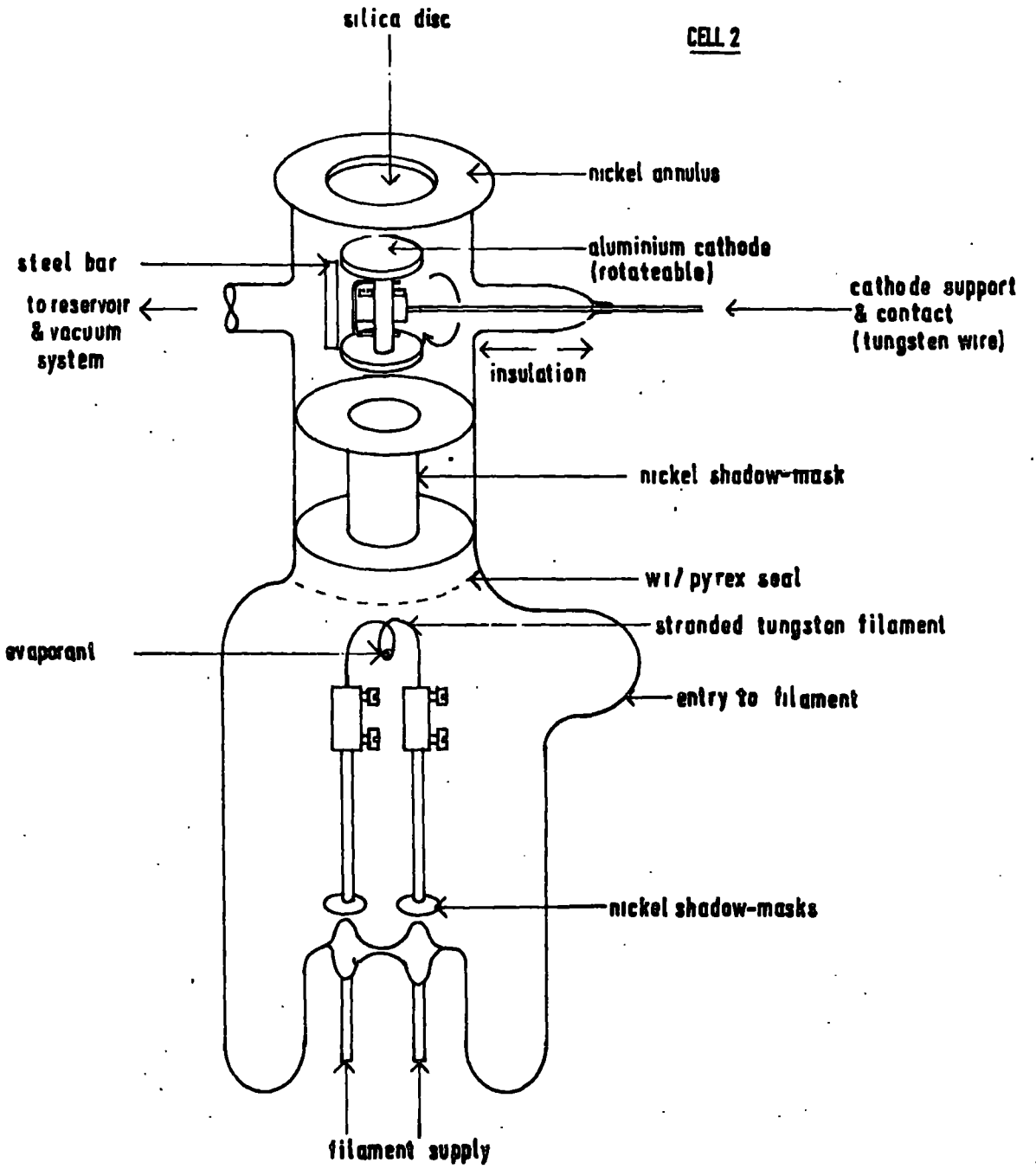
silica disc
CELL 2
nickel annulus
steel bar
aluminium cathode
(rotateable)
to reservoir
& vacuum
system
cathode support
& contact
(tungsten wire)
insulation
nickel shadow-mask
W/pyrex seal
stranded tungsten filament
evaporant
entry to filament
nickel shadow-masks
filament supply

Fig. 5.3

Detail of Cell 2

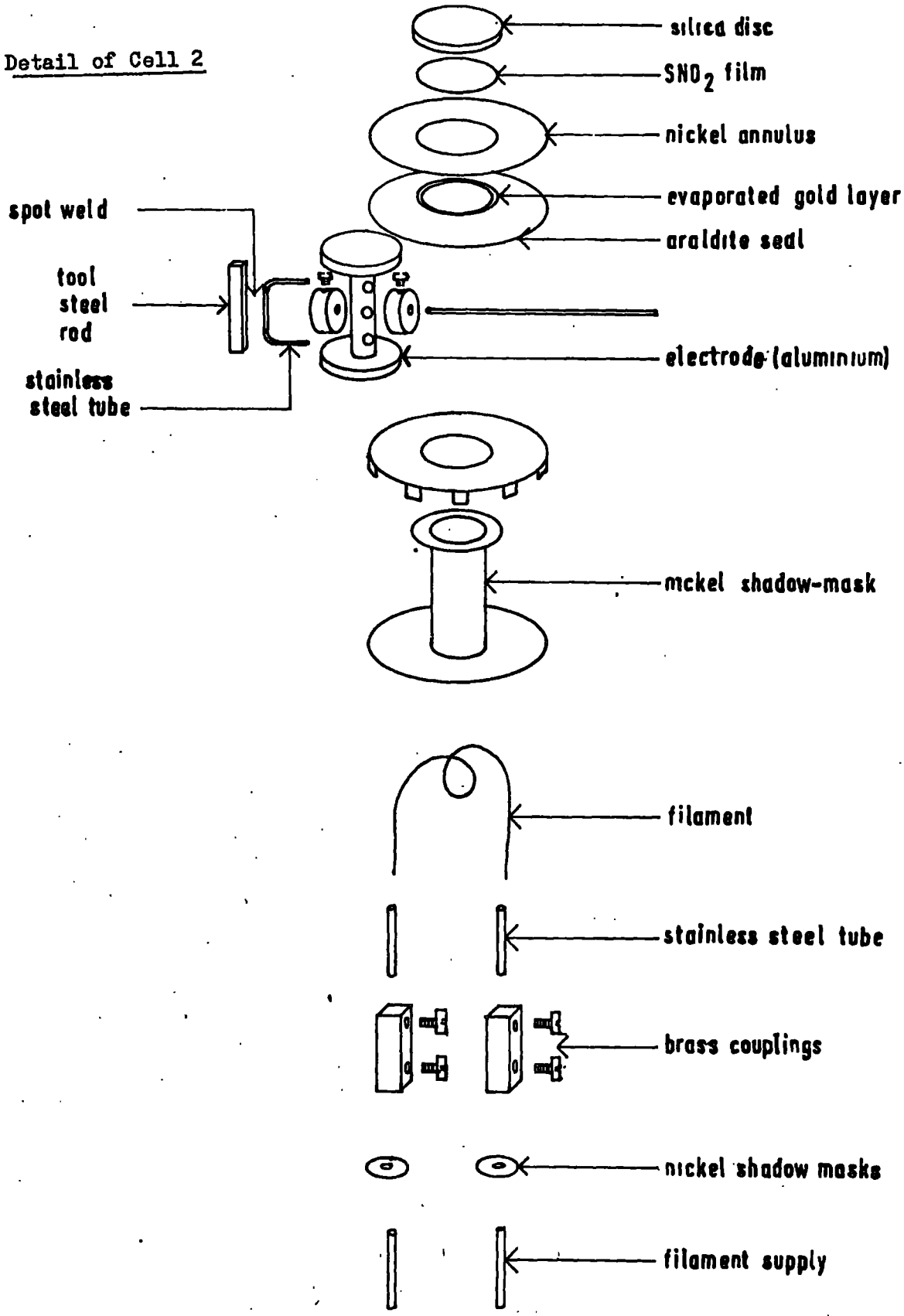

on one face of a 1.5 cm. diameter silica disc. The silica/tin oxide combination, being transparent to the light of $\lambda > 2300$Å, was used as the window for the photoconduction measurements. [A transparent tin oxide layer of low electrical resistance (2K$\Omega\,\square$ cm.) was prepared by passing a stream of $SnCl_2$ vapour over the surface of the silica disc, heated to about 500°C in air. A very brief exposure to the vapour, ~1 sec., was sufficient to produce a film of the required thickness. The layer was very hard, strongly adherent to the silica surface, and was continuous (though variable in thickness) judging from the interference colours seen.]

The coated silica disc was cemented (with hot-setting Araldite) into a nickel annulus. (This annulus was shaped to reduce field inhomogenities at the edges of the silica disc). A gold layer was deposited over this seal (after 'curing') to make good electrical contact from the nickel to the tin oxide layer. A nickel screen was inserted into the cell, between the filament and the electrode system, to avoid the deposition of evaporant on the walls of the electrode compartment. With the rotatable electrode and screen in position, the tin oxide electrode was cemented on to the end of the cell with Araldite. The curing process was repeated and the cell washed out with clean hexane.

The evaporant (aluminium) was heated on a four-stranded tungsten filament. This was supported by a pair of 2 mm. tungsten rods in a W.1 glass pinch (of G.E.C. manufacture), sealed into a 4.5 cm. bore W.1. tube. The electrode compartment was sealed coaxially to the end of the tube so that the source was about 5 cm. from the electrode

surface. The replacement of spent filaments was effected through a 2 cm. bore side arm, which was then sealed off.

Major disadvantages with this cell were -

(i) The replacement of the filament was very difficult; the W1/Pyrex side arm seal became increasingly fragile, as it could not be properly annealed without excessive heating of the rest of the cell.

(ii) The aluminium evaporant was contaminated with the glass-blower's flame when sealing off the side arm.

(iii) There were mechanical problems in keeping the nickel screen in place.

Cell 3

The photocurrents observed with cell 2, using coated electrode surfaces, were quite different to those using the simple polished electrodes in cell 1. To allow a fair comparison to be made, it was necessary to be able to photostimulate one electrode at a time, and not to use a tin oxide anode. Cell 3, see Fig. 5.4, was constructed so that metallic layers could be (simultaneously) evaporated on to both electrode surfaces. A diagram of this cell is shown in Fig. 5.4.

Each electrode (aluminium 1 cm. diameter) was unbalanced and free to move, under gravity, to either of two positions which were determined by the angle of tilt of the cell to the horizontal. Thus, with the cell sealed on the vacuum system, the tilt was arranged so that both electrodes faced the evaporant source. With the cell removed from the main system, the electrodes were pivoted through

Fig. 5.4

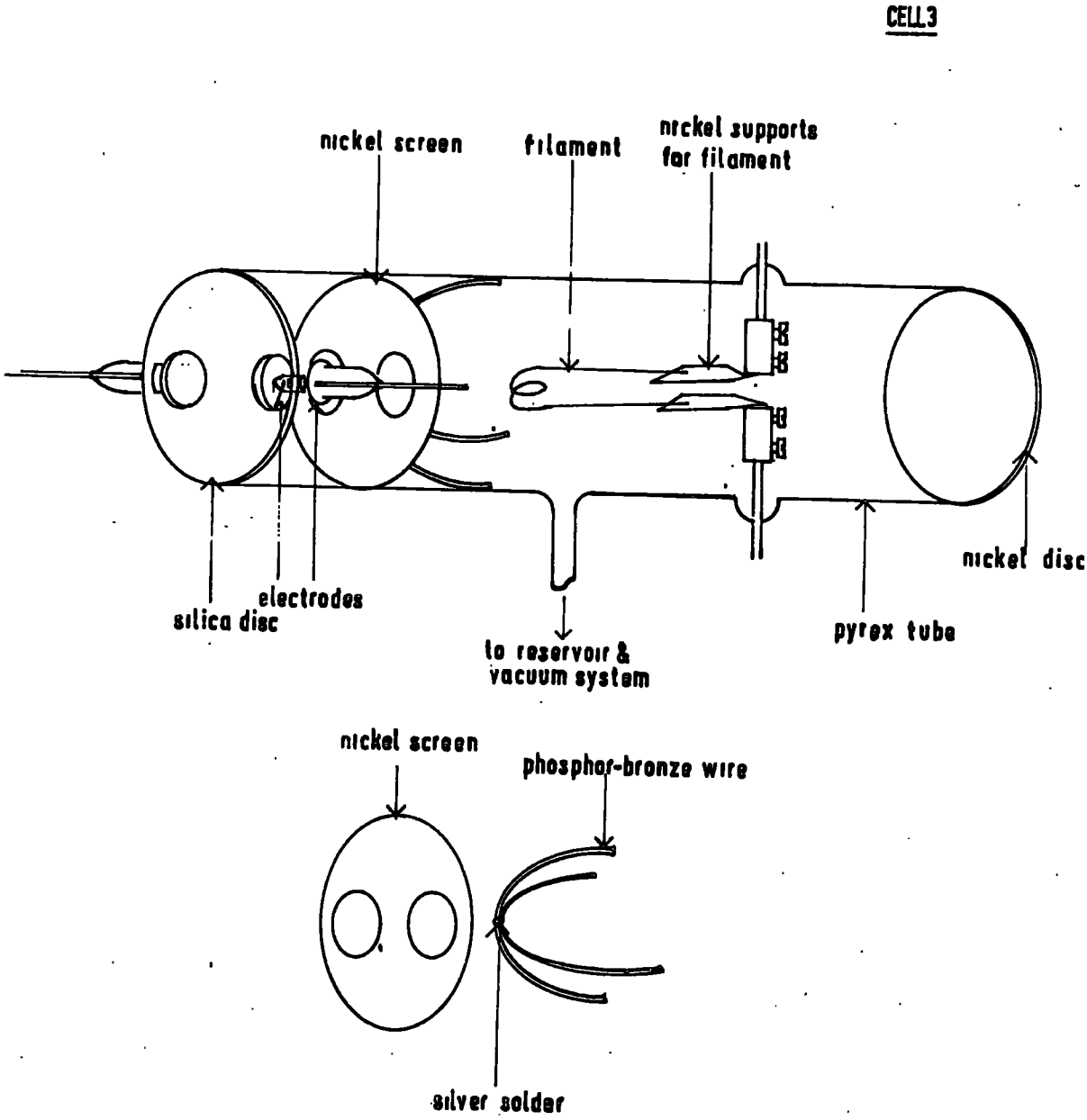
CELL 3
nickel screen
filament
nickel supports for filament
silica disc
electrodes
to reservoir & vacuum system
pyrex tube
nickel disc
nickel screen
phosphor-bronze wire
silver solder

Fig. 5.5

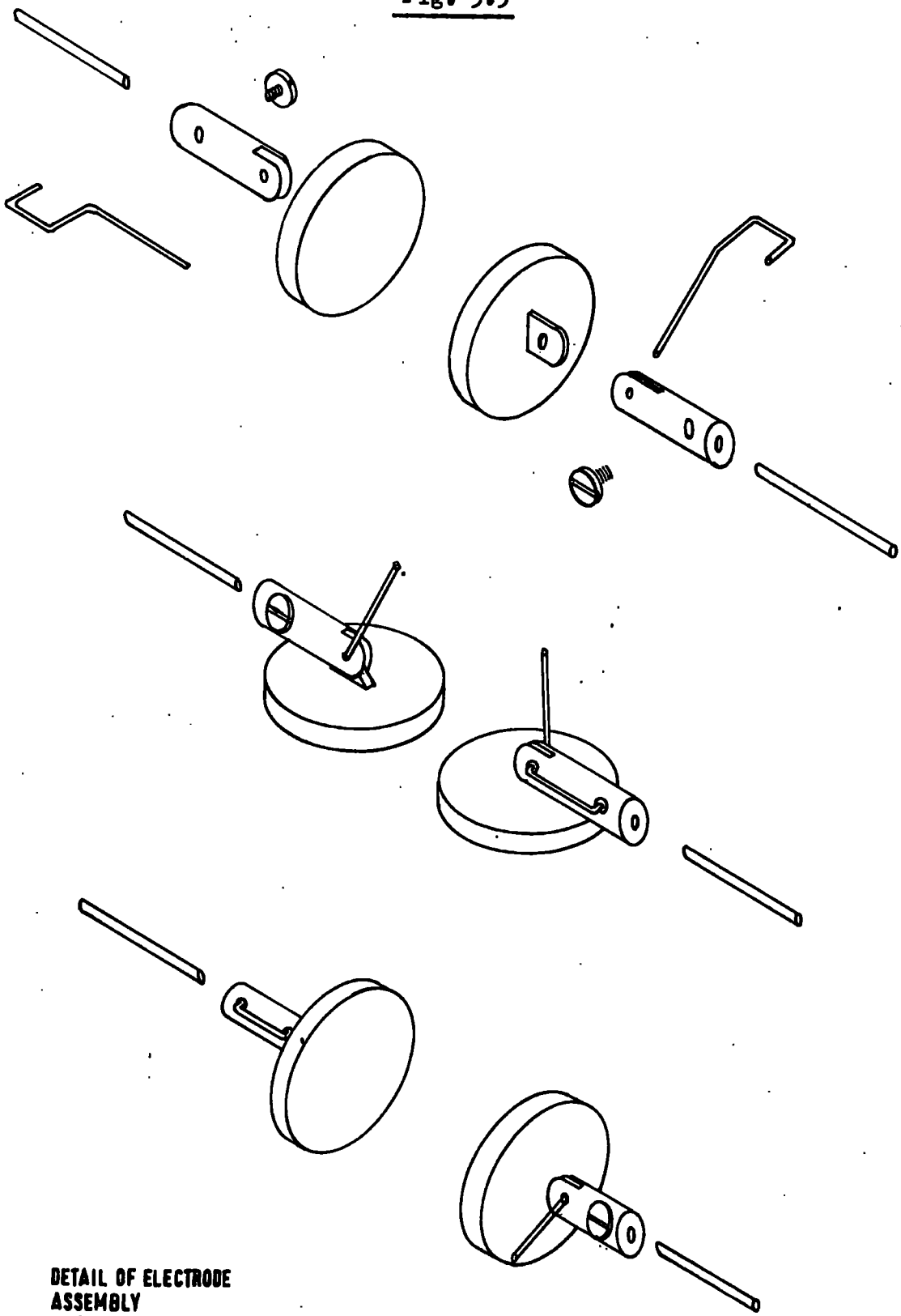

DETAIL OF ELECTRODE
ASSEMBLY
CELLS 3 & 4

90° by tilting the electrode compartment downwards. The electrodes then faced each other for the electrical measurements (see Fig. 5.5).

Detail of Cell 3

The vacuum envelope of the cell was constructed from a Pyrex tube, 25 mm. internal diameter and 22 cm. long, with both ends ground flat. Tungsten wire (1 mm. diameter) seals were made to support the electrodes about 1 cm. from one end of the tube. The electrode assemblies were secured to the leads with 10 B.A. screws. A nickel screen (with two apertures corresponding to the electrodes in the position for evaporation) was kept in place by two phosphor-bronze spring clips. A 30 mm. diameter, 1.5 mm. thick, silica window was then sealed to the end of the electrode compartment with hot-setting Araldite.

Current was supplied to the filament by a pair of (2 mm. diameter) tungsten rods. These were sealed into the Pyrex tube so that the filament was about 5 cm. from the electrodes. The filament, with its metallic charge, was inserted through the open end of the tube. The cell was then closed by cementing on a nickel foil disc. (To replace the spent filaments the nickel disc was removed, and the seal re-made).

A disadvantage with this cell was that the electrode surfaces were contaminated when the glass-blower sealed the cell to the de-gassing system.

Cell 4

Most of the measurements were obtained using cells of a fourth

Fig. 5.6

Cell 4.

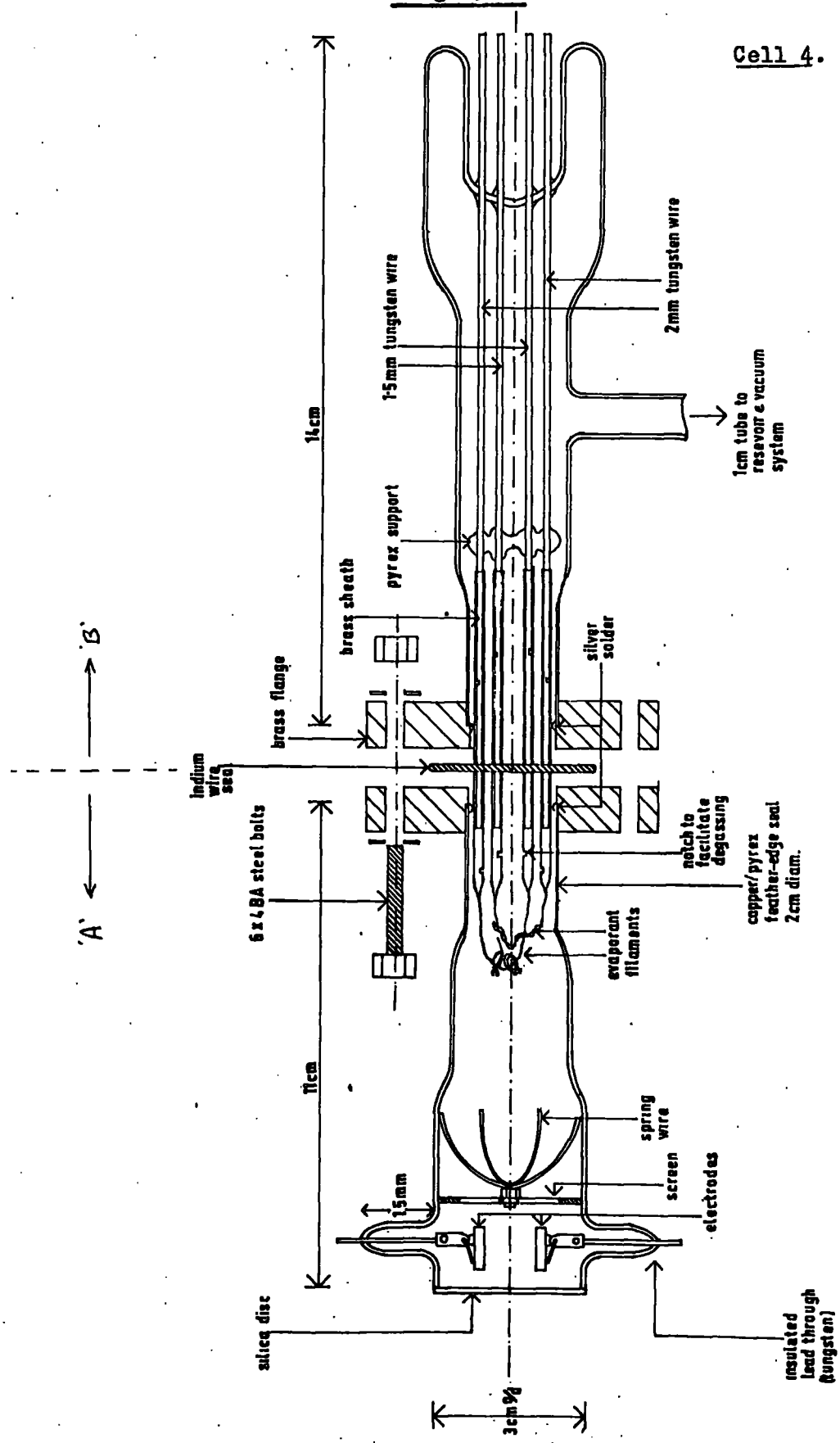
'A'
'B'
14cm
11cm
1·5mm tungsten wire
2mm tungsten wire
1cm tube to reservoir & vacuum system
pyrex support
brass sheath
brass flange
silver solder
indium wire seal
6 x 4BA steel bolts
notch to facilitate degassing
copper/pyrex feather-edge seal 2cm diam.
evaporant filaments
spring wire
screen
electrodes
1·5mm
silica disc
insulated lead through (tungsten)
3cm ⌀

type (Fig. 5.6). The electrode arrangement was identical to that in cell 3, but with this cell the electrode compartment could be removed by breaking an indium wire between the brass flanges. In this way the glassblowing, required to replace the constriction, was confined to the other half of the cell. Two separate filaments were incorporated; these enabled two (or more) layers to be deposited for subsequent measurements with the same sample of liquid. The Pyrex envelope (including the electrical leads and the copper/Pyrex seals) of the cells were constructed, to order, by the General Electric Co. Ltd. Their adherence to the design specification, with regard to the accurate positioning of the electrode supports, allowed close parallelism of the electrodes.

Detail of Cell 4

The two parts of the cell were fitted into brass flanges, so that the minimum area of the joint (made with silver solder) was exposed to the liquid. The mating surfaces of the flanges were then polished on an optical flat. The reservoir and pumping port were sealed to part 'B'. This part of the cell, after being thoroughly washed with hexane and dried, was joined on to the degassing system.

The two pivoting electrodes were contained in part 'A' of the cell. The screen was constructed from 1 mm. thick stainless steel sheet, two slots allowing for its insertion into the cell past the protruding electrode leads, and was kept in position by two phosphor-bronze spring clips. (These were silver soldered to a 6 B.A. brass nut and bolt screwed into the centre of the disc). With the electrodes

and screen in position, a silica window ($1\frac{1}{2}$ mm. thick) was cemented to the end of the electrode compartment.

Each filament was mounted on two thin-walled tubes, and was inserted in the cell by slipping the tubes over the tungsten supply rods. This arrangement allowed both the filaments and their supports to be outgassed in an auxiliary coating unit (vacuum approx. 10^{-4} torr) before insertion in the test cell. The supports were made long enough to project into the electrode compartment of the assembled cell so that the evaporant source on the filament was about 4 cm. from the electrode surfaces. Slots cut at intervals along the tubes facilitated outgassing.

Vacuum joints between the two parts of the cell were made by compressing 1 mm. diameter indium wire to a thickness of about 0.1 mm. between the brass flanges. Both the indium wire and the flanges were degreased with trichlorethylene and dried thoroughly before making the seal. The total force required to make a good seal was comparatively small, but for even compression (and rigidity of the cell as a whole) it was decided to use six 4 B.A. steel bolts to compress the seal. The joint tended to 'settle' after a few hours, and so the bolts were tightened up again to compensate.

This type of cell was employed with solid magnesium or aluminium electrodes and Al, Mg and Au were evaporated. In a final experiment, a screen with a single aperture was used so that only one electrode was coated.

Cell 5

A simpler cell, cell 5, was used for the measurements with coated electrodes in gassy hexane. The electrode assembly and the screen were identical to those in cell 4, but the evaporating system was omitted, the end of the cell being left open. This allowed the electrode surfaces to be coated in an Edwards vacuum evaporation unit.

5.2. High Vacuum System and Techniques

Dissolved gases are known to have a marked influence on the electrical properties of hexane. For the present work an apparatus, built by Morant, was used to degas the liquid and test cell.. Previously purified hexane was initially degassed at a vacuum of approx. 10^{-2} torr, followed by a slow distillation at 10^{-6} torr.

Degassing Apparatus

The two stage vacuum distillation system is shown in Fig. 5.7. All parts were constructed of Pyrex (borosilicate) glass.

Rough vacuum was provided by an Edwards High Vacuum Ltd. model 15C50B oil-filled rotary pump, said to be capable of providing an ultimate pressure of approx. 5×10^{-3} torr. A phosphorus pentoxide trap and air ballast valve were incorporated in the pump.. A 20 lite/sec mercury diffusion pump, of G.E.C. manufacture, in conjunction with a liquid nitrogen trap, enabled a pressure of approx. 10^{-6} torr. to be reached in the entire system. Vacua of this order were reached without much difficulty, providing there were no large leaks:

Fig. 5.7

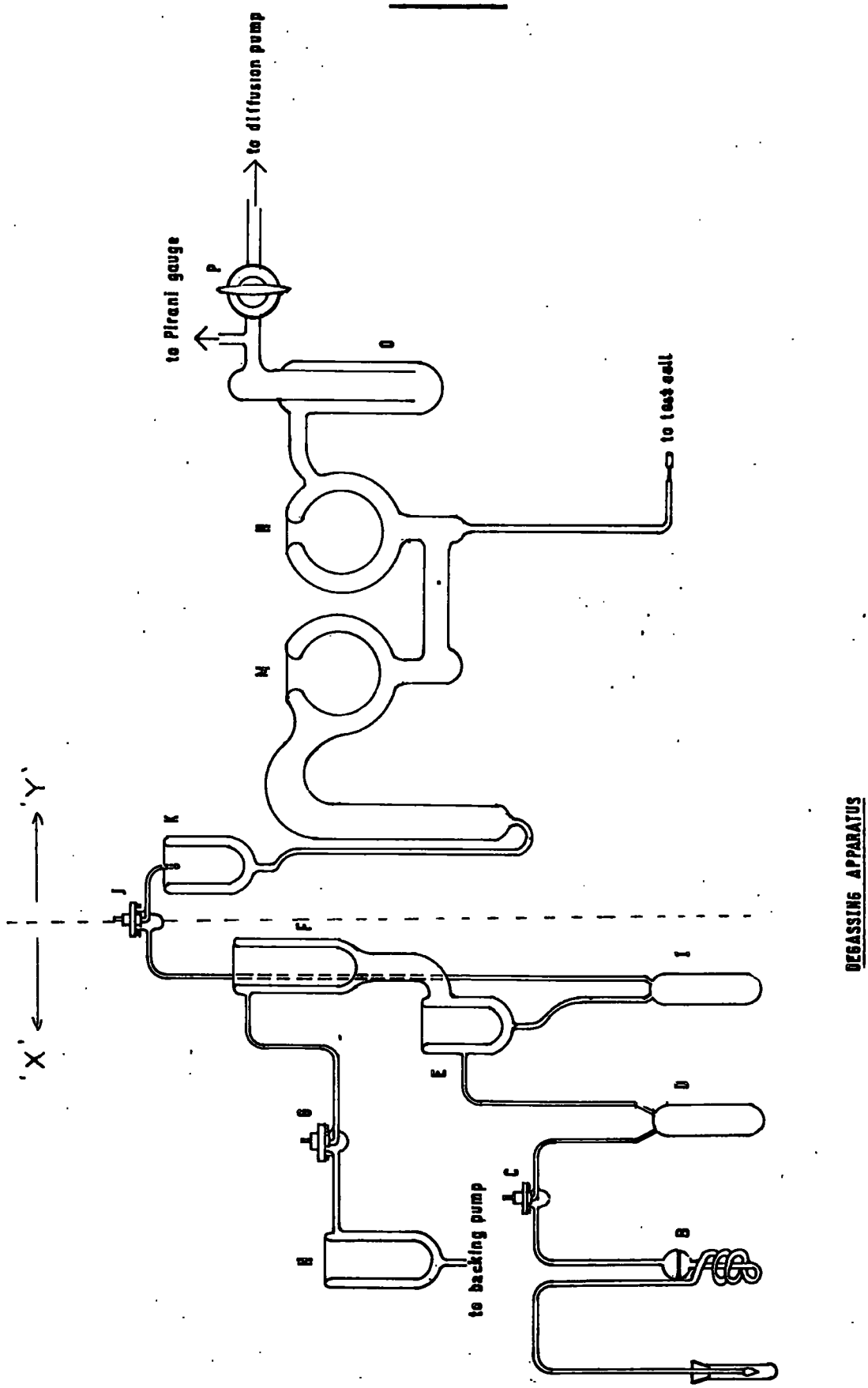

DEGASSING APPARATUS

and the apparatus was thoroughly outgassed.

Contamination of the hexane by the system was carefully avoided at each stage. The elaborate arrangement of traps avoided back-streaming from the pumps, and greaseless taps manufactured by G. Springham and Co., with 'Viton A' inserts as the sealing material, afforded the minimum contamination of the liquid. One large (2.5 cm. bore) greased tap, between the diffusion pump and the system, could not be avoided but this was isolated by a further liquid nitrogen trap.

Preparation of the Vacuum System

The system was not let down to air except when absolutely necessary and then only for the shortest possible time, e.g. when sealing on the test cell. The apparatus was pumped (before introducing the liquid) until the total leak and degassing rate was less than 10^{-7} lusecs, as measured on a sensitive Pirani gauge. (This measure of the degassing rate was obtained by determining the rise of pressure in the system over a period of time with the pumps isolated). The greater proportion of the residual gases was usually hexane vapour remaining from the previous distillation; this was easily distinguished by condensing the vapour in a trap at liquid nitrogen temperature, the gauge then indicating only the remaining (incondensible) gases. It was desirable to bake the test cell, at a moderate temperature, before sealing it on to the system.

In later experiments the inlet, including the sintered disc B, was also evacuated; a constriction seal enabling tap C to be left open. This constriction was broken to introduce hexane into the

system. It was also advantageous to enclose the inlet tube (when not in use) to avoid contamination of its outer surface from the atmosphere.

Rough Degassing (see Fig. 2.7)

When all parts of the system were thoroughly degassed (including the cell and its filaments), tap J was closed; section Y of the system remaining open to the diffusion pump. Rough degassing of the hexane was then commenced in section X at backing pressure (approx. 10^{-3} torr).

Backstreaming of oil, from the rotary pump into the hexane, was prevented by filling trap H with cooling mixture (a slurry of CO_2 and methylated spirits, at -79°C). The inlet spiral A, sintered glass filter B, and reservoir D were then surrounded by cooling mixture. The inlet was immersed in hexane and the capillary seal broken. Taps C and G were opened and hexane flowed slowly into D. (The cooled sintered disc, pore size approx. 1μ, removed any large particles, and possibly water in the form of ice crystals).

With about 80 cc of liquid collected in D, tap C was closed. (The closure of this tap was not complete immediately due to the brittleness of the 'Viton A' insert at the low temperature of the hexane. It was necessary to progressively tighten the seal as it warmed up to room temperature). Traps E and F were filled with cooling mixture, and the Dewar removed from D. Hexane evaporated from D, condensed on the cold surfaces of E and F and percolated towards reservoir I. Within a few minutes the evaporation of hexane from I produced a low enough temperature for the drops of liquid to settle.

A slow transfer of liquid from D to I was then completed in about 90 minutes, the vapour being pumped continuously. The hexane in I was then assumed to be well degassed to an estimated air pressure of approx. 10^{-2} torr.

Degassing at High Vacuum

Degassing of hexane at approx. 10^{-6} torr was completed in section Y of the apparatus.

Cooling mixture was placed around L, and liquid nitrogen around trap O (to prevent any residue from the greased tap P from reaching the hexane). A little liquid nitrogen was placed in trap K and, with the taps J and P opened, hexane evaporated slowly from reservoir I to solidify on the surface of K. Liquid nitrogen was added to gradually raise the level of hexane in K and to form as uniform a layer of hexane as possible (consistent with the maintenance of high vacuum in the system). When only a few drops of liquid remained in I, the taps J and P were closed, and traps K and O were allowed to warm to room temperature. The hexane in K then melted to fall into L where it was kept, at cooling mixture temperature, until the final slow distillation was commenced. As the previous manipulations required most of the day to complete, it was usual to postpone the final stage until the next morning; sufficient cooling mixture being added to keep trap L cool overnight.

The slow distillation of hexane from L (at $-79^{\circ}C$) to M (at $-182^{\circ}C$) was initiated by placing a little liquid nitrogen in M. A small quantity of the cooling mixture was placed in N and tap P was

opened. The pressure in section Y fell to about 10^{-6} torr in a few seconds, indicating that little or no air had entered the system overnight. Pumping was continued on the shell of solid hexane in M, and the slow evaporation of hexane from L in this high vacuum ensured thorough degassing; incondensible gases being exhausted by the pumps. Transfer of hexane from L to M took about 5 hours, the level of liquid nitrogen being raised gradually to form a uniform shell of solid hexane in M. When this was complete, the system was prepared for the evaporation process.

Evaporation of metallic layers, filling the cell with hexane and sealing off

Current to the filament in the test cell was increased until the evaporation of metal was sufficiently rapid to form an opaque film in about five seconds. The current was then switched off. The liquid nitrogen was then removed from M, liquid nitrogen applied to the cell reservoir, and the tap P closed. The hexane in M melted and flowed into the cell reservoir. When all the hexane had solidified in the reservoir, traps O and N were filled again with liquid nitrogen and tap P reopened to the pumps. The constriction was then closed, with an oxy coal-gas flame, and the cell removed for the electrical measurements.

5.3. Evaporation Techniques

Milligramme quantities of aluminium and gold were evaporated from electrically heated tungsten filaments. Attempts were made to

evaporate magnesium in the same way, but a method of self-evaporation from magnesium ribbon was found to be more reliable.

(i) Aluminium

Aluminium forms an alloy with most refractory metals, and a high temperature ($\sim$ 1100°C) must be exceeded before appreciable evaporation takes place. Tungsten is the best available metal from which to evaporate aluminium, but it becomes brittle, due to phase change, at approx. 1000°C. To reduce the likelihood of filament failure, due to alloying, the amount of aluminium to be evaporated was kept small compared to the thickness of the wire. The tungsten was still very fragile, both during and after the evaporation, and it was advantageous to use a multistranded filament. The best results were obtained by taking care not to overheat the filament, and so a manual control of the electricity supply was used.

(ii) Gold

There was little difficulty in evaporating gold. Unlike aluminium films, however, the gold was not strongly adherent to the metal substrate. If too thick a layer was deposited, it was found that flakes of gold were likely to fall off the electrodes when an electric field was applied. The best (i.e. most adherent) layers were thin, with a greenish tint, and the evaporation was controlled accordingly.

(iii) Magnesium

Magnesium sublimes rapidly in a small temperature range before melting. Because of this, the magnesium will not 'wet' a tungsten

filament. Thus, the porous oxides (formed during the evaporation) are easily removed. In addition, the oxides were ejected on to the electrode surface as a result of the large temperature difference between the filament and the magnesium suspended on it. Such poor layers (coupled with the risk of contamination of the liquid by the oxide) were undesirable. It was found that the use of an electrically heated magnesium ribbon, from which the magnesium was sublimed, gave better results. With this method, highly reflecting surfaces were obtained and, if care was taken not to overheat the ribbon, the problem of oxide contamination was minimal.

Experimental

Preparatory clean-up of the filament was usually completed in an Edwards vacuum coating unit before mounting in the cell. For degassing in the cell, and for the evaporation itself, the current was supplied by a heavy duty low voltage transformer (5V. 10A), which was controlled by a Variac in the primary circuit.

5.4 Electrical Equipment

A Dynatron, Type N103, high stability D.C. powerback was used to supply calibrated voltages from 300 to 3,300 V. (of either polarity) to the test cell. Some voltages (less than 300 V.) were taken from high tension batteries or from a potential divider across the output of the Dynatron. Special low noise coaxial cable was used to connect the test cell to the voltage source.

Fig. 5.8

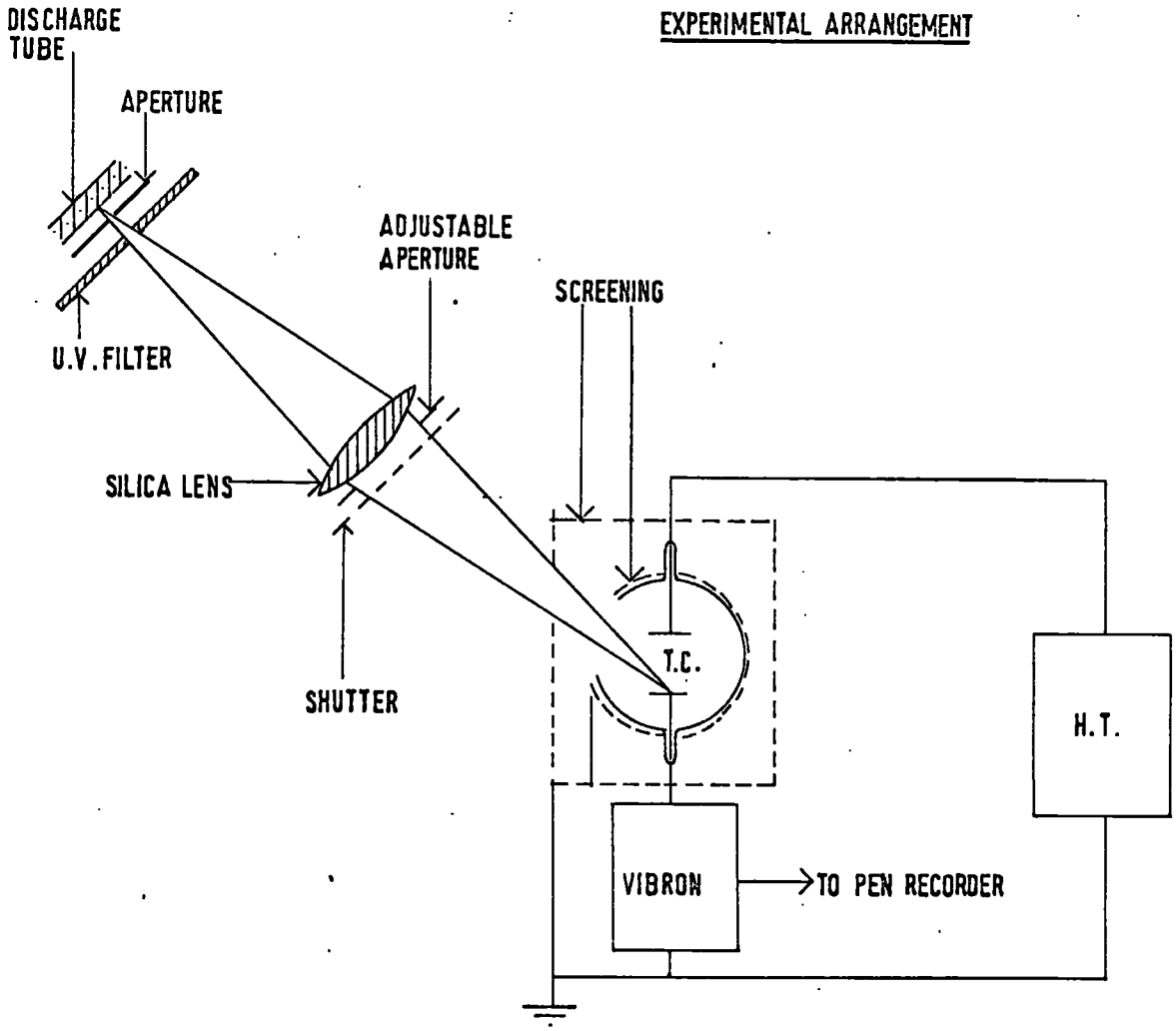
EXPERIMENTAL ARRANGEMENT
DISCHARGE TUBE
APERTURE
ADJUSTABLE APERTURE
SCREENING
U.V. FILTER
SILICA LENS
SHUTTER
T.C.
H.T.
VIBRON
TO PEN RECORDER

Currents were measured by finding the P.D. across a switched range of resistors (10^9 - 10^{12} ohm) between the low voltage electrode of the test cell and earth (Fig. 5.8). The P.D. was measured with a vibrating reed electrometer ('Vibron' Model 33C, manufactured by Electronic Instruments Ltd.), switched voltage ranges (10^{-2} to 1 V F.S.D.) allowed currents larger than 10^{-15}A to be measured. In the absence of feedback to the test cell, the transient response was determined by the time constant of the input circuit. Measurements were made for times much longer than instrumental transients after (for example) making a change of voltage.

A pen recorder, supplied from the 'Vibron', was found to be useful in registering the currents.

Screening

A large aluminium box, with apertures corresponding to the test cell window and the electrode terminals, was assembled around the test cell to form a 'Faraday cage' when connected to earth. The electrometer head was mounted within two inches of the low voltage terminal of the cell.

5.5. Lamp and Filters

All the photocurrents were stimulated with a 125 watt (A.C.) medium pressure mercury vapour lamp, type 6721 A/T, manufactured by Hanovia Ltd. The discharge tube was enclosed in an air-cooled holder (supplied by the manufacturers) so that an aperture, of 0.5 cm. diameter, gave an approximation to a point source. A silica lens

Fig. 5.9(a)

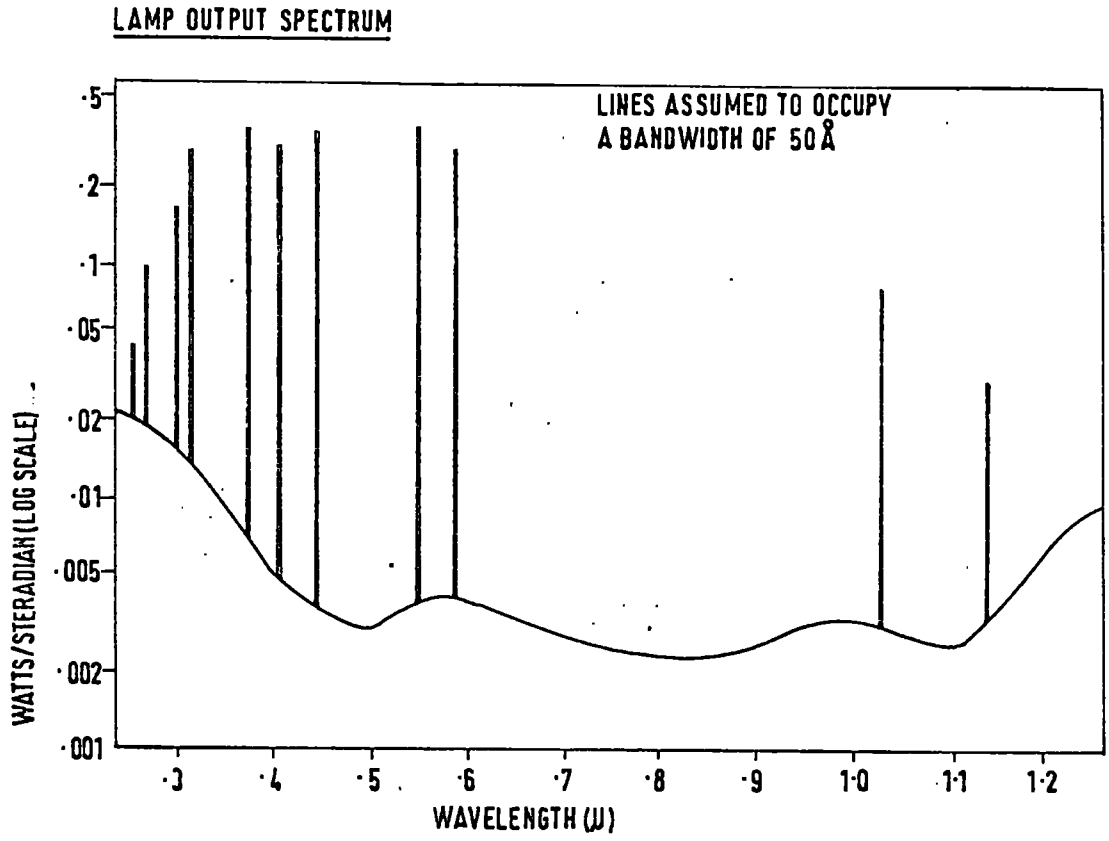

Fig. 5.9(b)

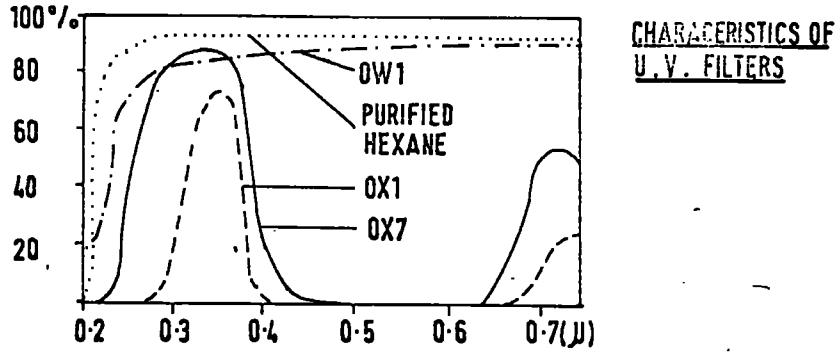

focussed this spot in the test cell, generally to illuminate one of the electrodes. The intensity of illumination could be controlled to some extent, by adjusting an iris diaphragm in the lens holder, the light being interrupted when necessary with a camera-type shutter. The test cell and lamp were mounted on a rigid framework in a fixed geometry for the duration of each experiment.

After a 'warming up' period of about 15 minutes, the intensity of the lamp remained constant (within $\sim$ 10%) over a period of days. Most of this variation was due to changes in the position of the discharge. The latter fluctuations were reduced in frequency, but not entirely removed, by using a constant-voltage transformer in the supply circuit. Even so, it was often necessary to wait for the arc to settle to one position or another before taking measurements. The 100 c.p.s. mains ripple, being much too fast to be recorded by the Vibron, did not involve any difficulties.

The output spectrum, for a typical lamp, is shown in Fig. 5.9(a). Band-pass filters (Chance-Pilkington OX1, OX7 etc.) were used to separate the spectrum; the characteristics of the more important ones being shown in Fig. 5.9(b).

CHAPTER VI

RESULTS

Preliminary

The results are presented in chronological order, with the main divisions by the cell number (see Chapter V for details). The most important observations are included in Sections 6.7, 6.8, 6.14 and in Sections 6.15, 6.16.

All experiments were conducted at room temperature ($\sim 20^{\circ}C.$). The hexane was usually 'highly degassed' i.e. to 10^{-6} torr, and (unless otherwise stated) was better than 99.5% n-hexane (Koch-Light 'Puriss' grade). An account of the purification of this grade of hexane, together with an analysis of other samples, will be found in Chapter IV.

Applied voltages, rather than field strengths, are given in the diagrams (the latter term implies the absence of space charges, for which there is no guarantee). Parallel-plate electrodes, with a spacing of 1 cm. were used in each cell. Similarly, 'cell currents' rather than 'current densities' are quoted because the coverage by an evaporated metal layer was always slightly less than the overall electrode area. Graphs are thus presented as '$\frac{I}{V}$ characteristics', the 'I' referring to the photocurrent.

'Times elapsed' were recorded from the deposition (by evaporation) of a metallic layer on the electrodes. There were two further manipulations, taking about half an hour (with variations due to the

circumstances), before starting measurements. These were the removal ('sealing off') of the cell from the degassing system, and the introduction of liquid hexane to the electrode compartment.

Errors in the measurement of photocurrents were minimised by the extensive use of pen-recorder traces, and are typically of the order of 5 - 10%. Other details, including the output spectrum of the lamp, and the characteristics of the filters, are to be found in Chapter V.

Some abbreviations are used in the text;

(i) 'Highly degassed (to 10^{-6} torr) and purified n-hexane' is referred to as H.D.P. n-hexane. (The measurements described in Sections 6.5 to 6.14 were made with such samples).

(ii) 'The radiation from the high pressure, mercury vapour lamp, as filtered by (e.g. OX7) glass' is truncated to 'filtered (OX7) radiation'.

N.B. The radiation was always directed at one of the electrodes when using Cells 4 and 5, (Sections 6.9 to 6.15).

6.1. Exploratory, (Cell 1)

The 1.5 cm. diameter aluminium electrodes in cell 1 had been subjected to a previous polishing and degreasing treatment and had retained an oxide coating. Various grades of hexane were used, but their (optical) purity was not initially considered.

6.1.1. 'Spectroscopic' grade hexane (degassed to 10^{-3} torr)

Currents of $\sim 10^{-12}$A. were induced by unfiltered irradiation of

Fig. 6.1

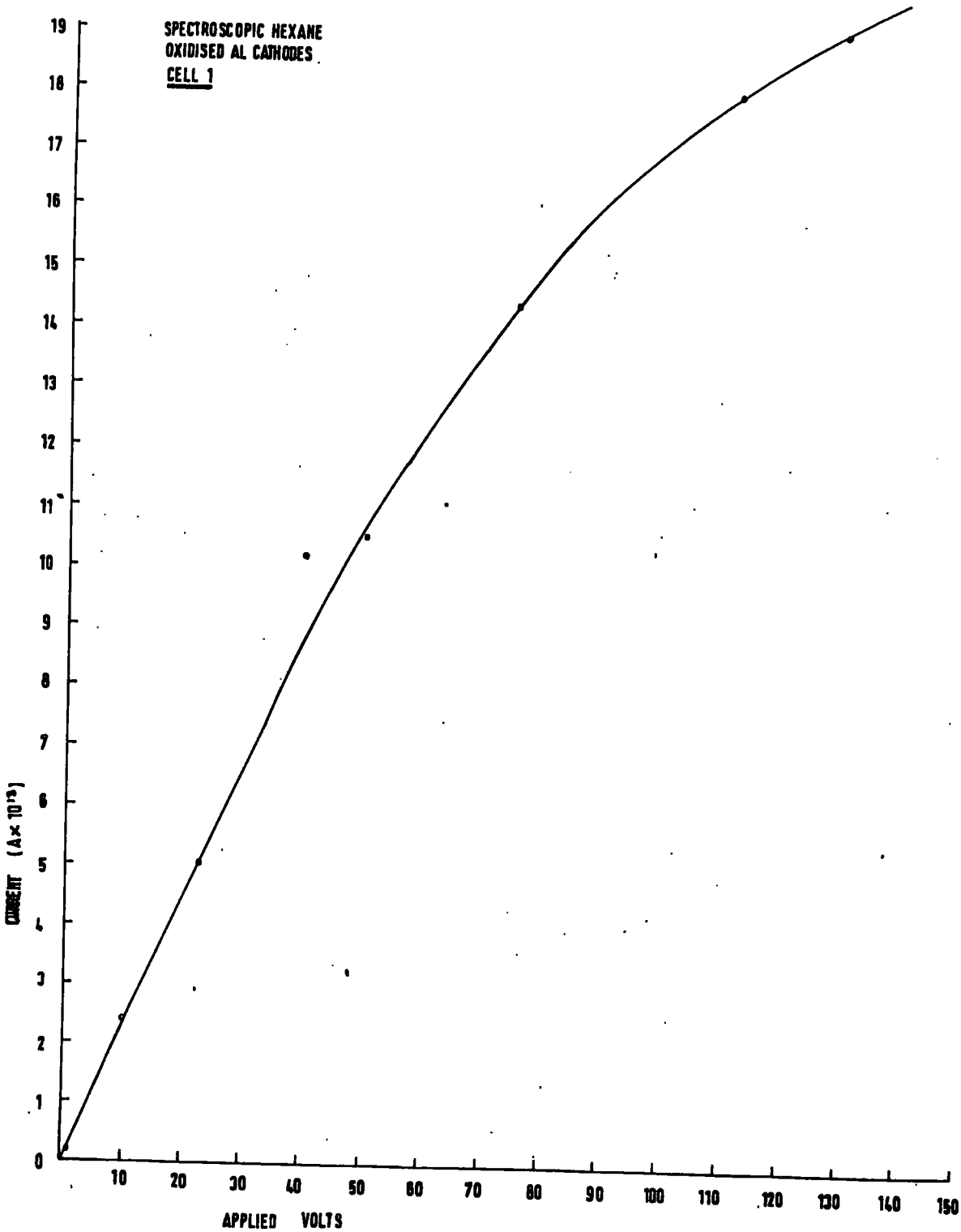
SPECTROSCOPIC HEXANE
OXIDISED AL CATHODES
CELL 1
CURRENT (A × 10¹³)
APPLIED VOLTS
0
1
2
3
4
5
6
7
8
9
10
11
12
13
14
15
16
17
18
19
10
20
30
40
50
60
70
80
90
100
110
120
130
140
150

Fig. 6.2

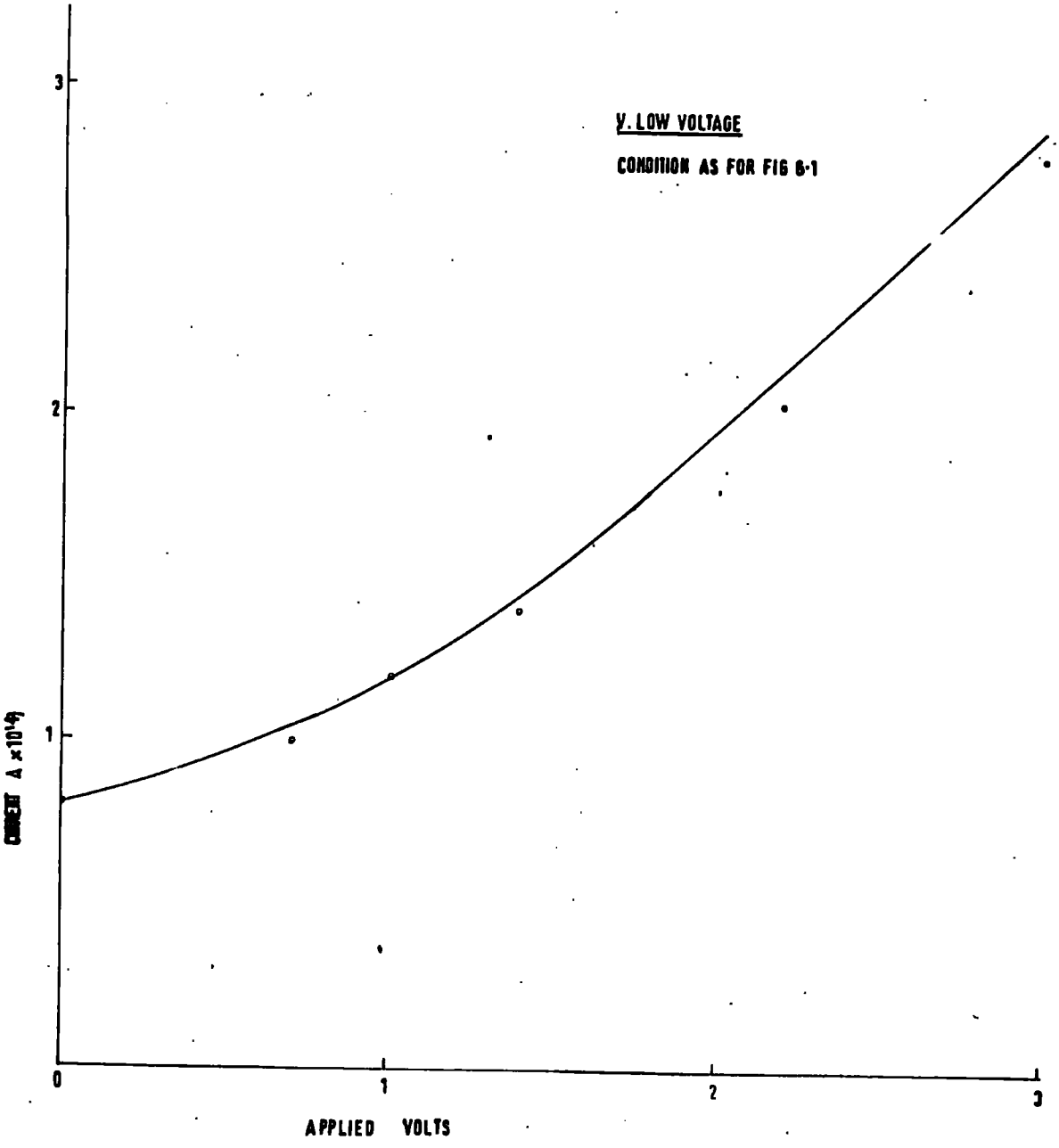

the cathode, the 'dark' current being less than 10^{-14}A. Some $\frac{I}{V}$ curves were obtained with long ($\sim$ 2 minute) pulses of unfiltered radiation, the voltage being continuously applied to the cell (see Fig. 6.1). There were no measurable ($> 10^{-14}$A.) photocurrents using (0X7) or 0X1) radiation, even with 150 V. applied to the cell.

There was an 'overshoot' at the onset of photoconduction (Fig. 6.44(a)); and, after stopping the radiation, the currents decayed very slowly. (These transients were considerably longer than the time constant of the Vibron which, with the measuring resistance of 10" ohms, was about 10 seconds).

For very low applied voltages, the measurements were complicated by 'standing currents'; these were partially attributable to the microphony of the cell and 'static' in the surroundings. Thus, measurements of $< 10^{-14}$A. (Fig. 6.2) may have been unreliable.

The photocurrents remained about the same after leaving the cell for long periods of time (days) with a voltage applied or not.

Finally, when air was let into the cell, the photocurrents rapidly decayed to zero ($<10^{-14}$A.).

6.1.2. Unpurified n-hexane, degassed to 10^{-6} torr.

Photocurrents slightly lower in magnitude to those with the 'Spectroscopic' grade (Section 6.1.1) were induced by directing pulses of unfiltered radiation at the cathode. There were (again) no measurable photocurrents for (0X7) or 0X1) radiation.

It was found that the magnitude of the photocurrents remained

Fig. 6.3

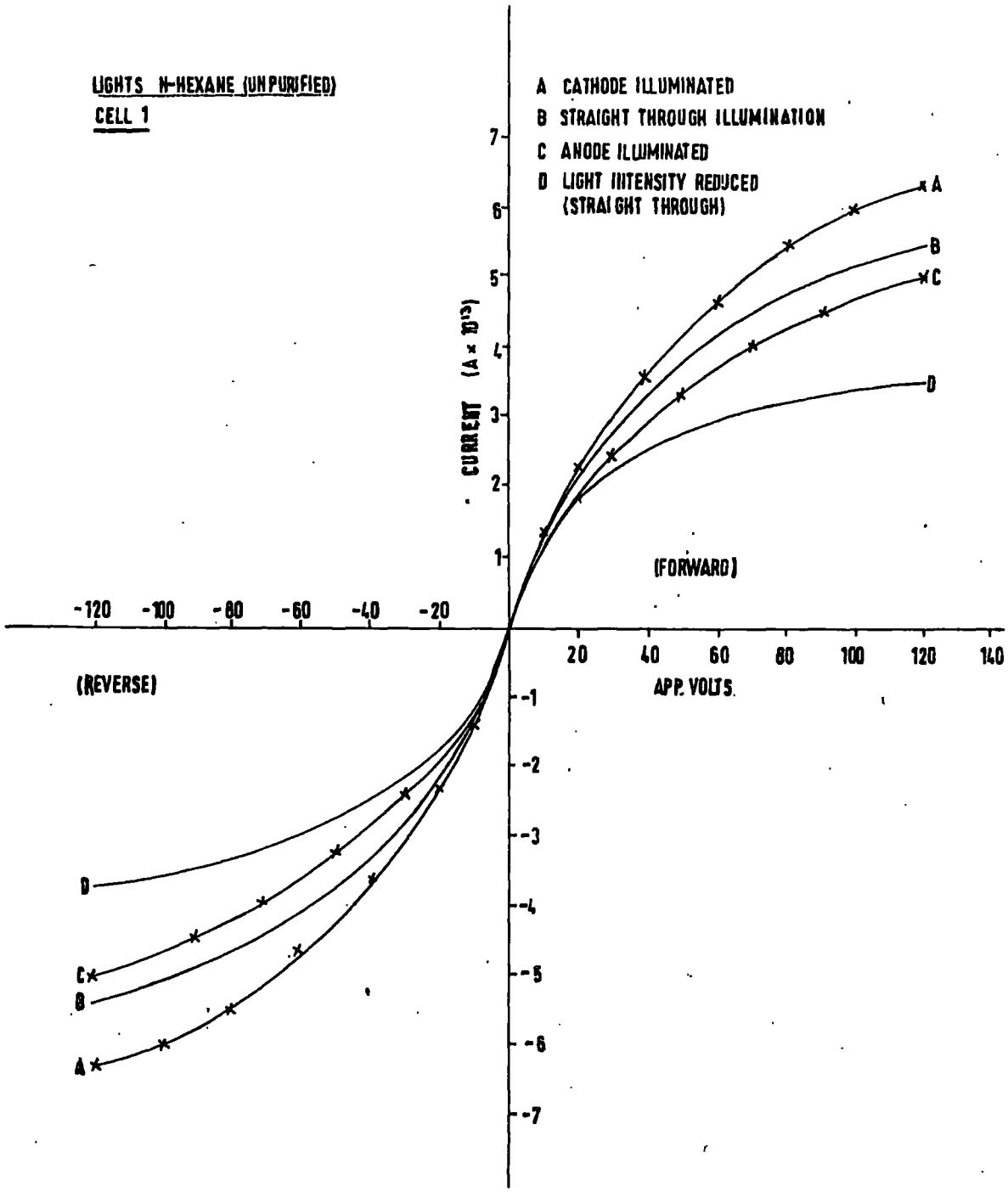
LIGHTS N-HEXANE (UNPURIFIED)
CELL 1
A CATHODE ILLUMINATED
B STRAIGHT THROUGH ILLUMINATION
C ANODE ILLUMINATED
D LIGHT INTENSITY REDUCED (STRAIGHT THROUGH)
CURRENT (A × 10¹³)
(FORWARD)
(REVERSE)
APP. VOLTS.
A
B
C
D
-120
-100
-80
-60
-40
-20
20
40
60
80
100
120
140
1
2
3
4
5
6
7
-1
-2
-3
-4
-5
-6
-7

Fig. 6.4

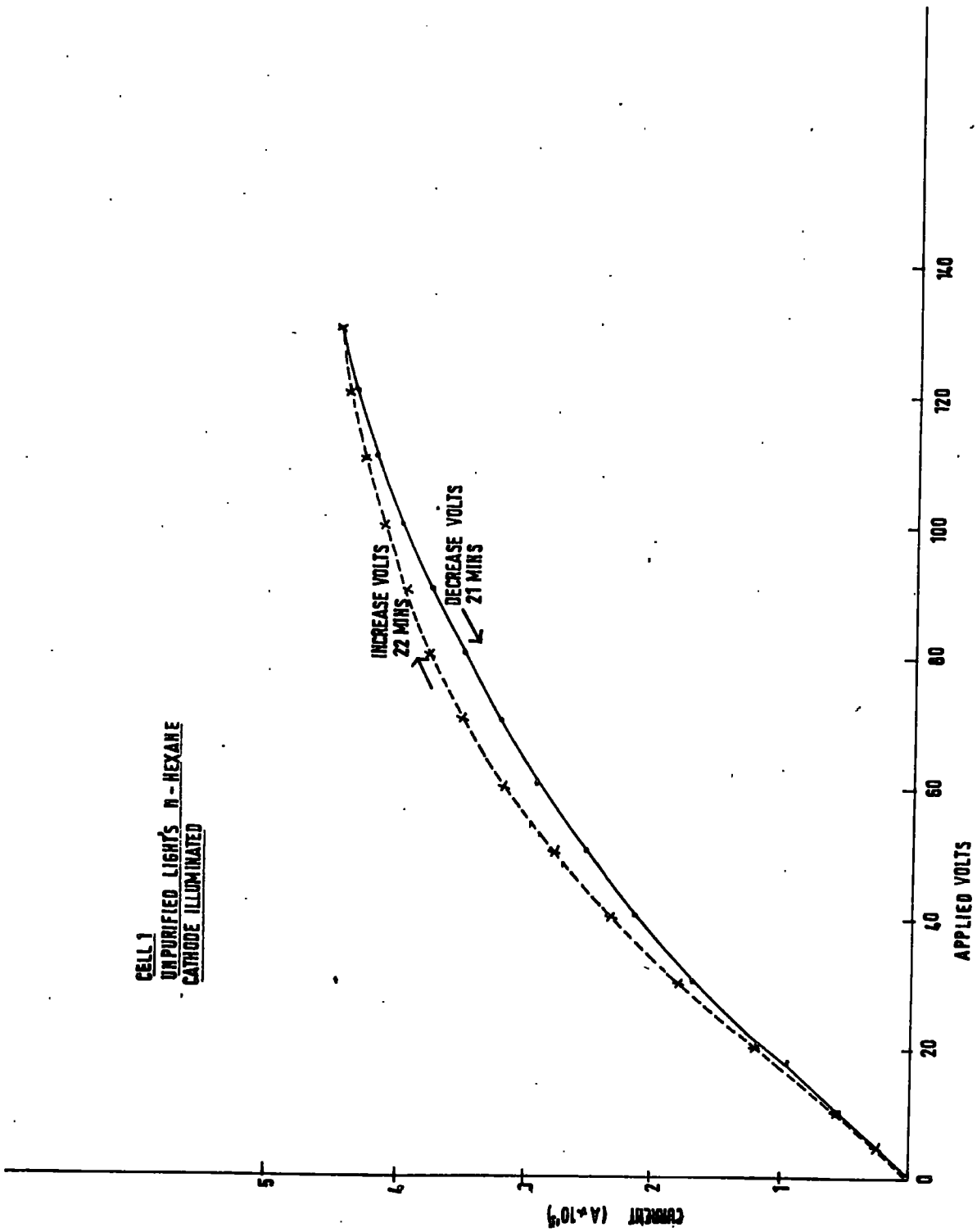
CELL 1
UNPURIFIED LIGHT'S N-HEXANE
CATHODE ILLUMINATED
INCREASE VOLTS
22 MINS
DECREASE VOLTS
21 MINS
CURRENT (A x 10⁻⁹)
APPLIED VOLTS
0
20
40
60
80
100
120
140
1
2
3
4
5

Fig. 6.5

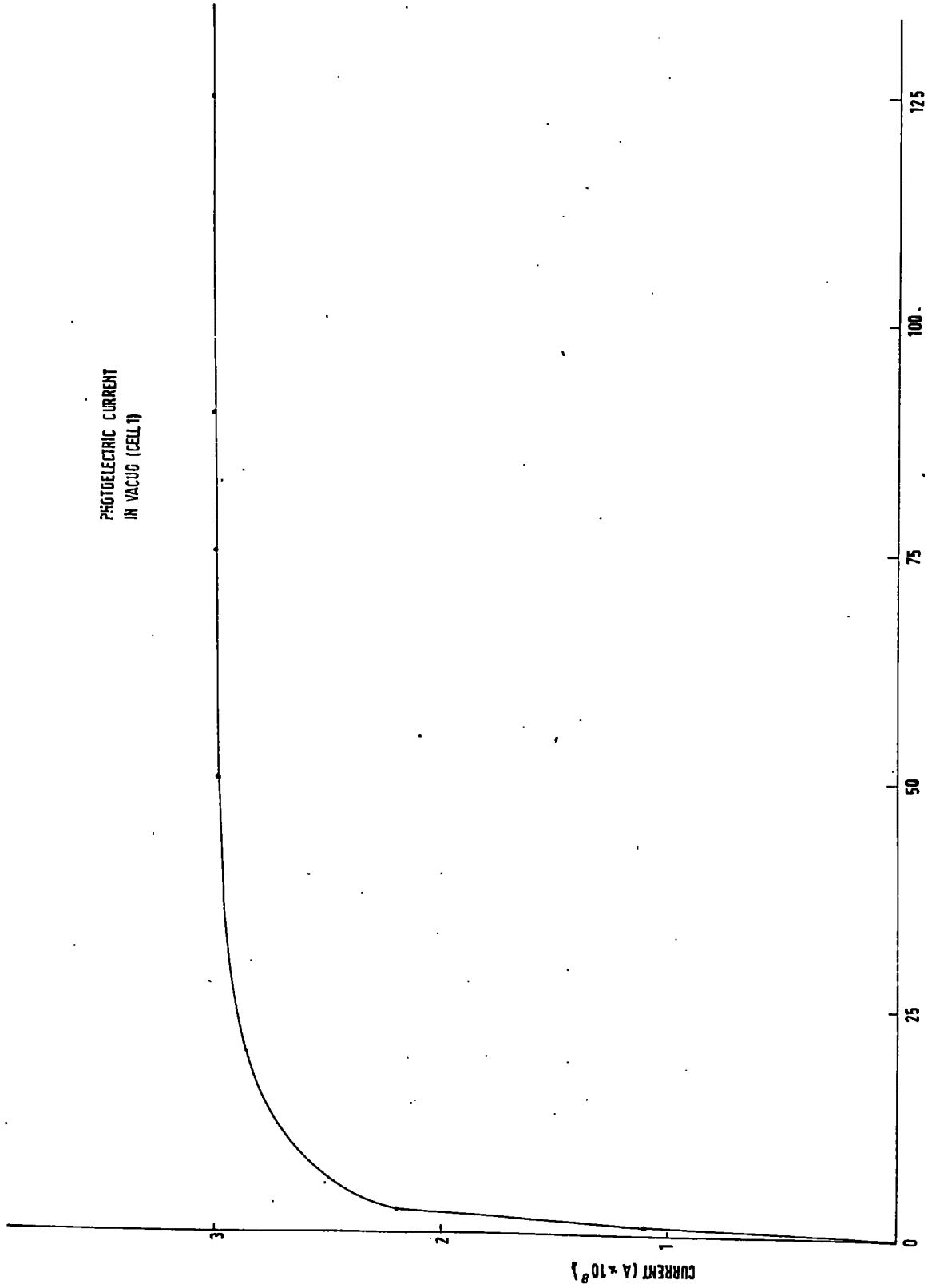
PHOTOELECTRIC CURRENT
IN VACUO (CELL 1)
CURRENT (A x 10⁸)
APPLIED VOLTS (POSITIVE)
0
1
2
3
25
50
75
100
125

the same for either polarity of the applied voltage. Moreover, the shape of the transients was unchanged for either direction of current flow.

The $\frac{I}{V}$ characteristics, resulting from the (unfiltered) irradiation of the anode, cathode, or the liquid in the electrode interspace are shown in Fig. 6.3. (The photocurrents were slightly different because of the intensity variations involved in moving the cell, rather than the changes in the configuration of irradiation).

Some other measurements were made with continuous radiation. It was found that rapid increments of the applied voltage were to be avoided for accurate measurements because of the slow response of the photocurrents. Fig. 6.4 shows a typical 'hysteresis effect'; the photocurrents being measured ~ 2 minutes after making a change of voltage (in steps of 10 V.). Subsequent measurements were made for longer times after the application of voltage to the cell, this reduced the latter effect to negligible proportions.

Fig. 6.5 shows the vacuum photoemission, for unfiltered irradiation of the cathode. (Vacua were obtained by freezing the hexane, at liquid nitrogen temperature, into the reservoir of the cell.)

6.1.3 Repolishing the electrodes (Cell 1) and some modifications to the degassing apparatus

The previous measurements indicated that the photocurrents originated in the liquid, rather than at the electrode surface. An attempt to obtain cathodic photoinjection was made by:

(i) Repolishing the electrodes (to improve the photosensitivity).

(ii) Using samples of hexane which were more transparent to the radiation (see Section 4.3).

The most practicable way to gain access to the electrodes in cell 1 was to sever the neck of the electrode compartment near the reservoir. Both electrodes were then withdrawn and polished on a mop with diamond paste; finishing off with very light pressure to minimise oxidation. They were then returned, after being washed in hexane, to the cell. Glassblowing was required to assemble the two parts of the cell; the (unavoidable) residues being subsequently removed by rinsing with hexane. The cell was then dried and evacuated.

Some attention was paid to improving the optical purity of the liquid. It was considered that the absorption due to dissolved impurities could;

(i) Result in 'impurity photoconduction'.

(ii) Attenuate the intensity of radiation reaching the electrodes.

It was found (Section 4.3) that the Koch-Light n-hexane was practically opaque to the ultraviolet, but that the 'Spectroscopic' grade was comparatively transparent. The latter samples contained a high proportion of isomers, but it was decided to use them for subsequent tests until the n-hexane could be successfully purified.

Purifying the liquid would not be very useful if impurities were returned to the hexane by the degassing apparatus. Considerable care had been taken in the design of this system to avoid contamination, but a closer examination revealed that the neoprene inserts of the Springham taps made the hexane fluorescent. 'Viton A' inserts were

available and, as this substance caused no fluorescence, they were substituted for the neoprene ones. The reservoirs 'D' and 'I' being the most likely places in the system to accumulate residues, were also replaced. The whole apparatus was then flushed out, and subjected to a specially prolonged pumping.

6.1.4 Further measurements, and summary of observations with Cell 1

There were no indications of any electrode activity in subsequent measurements with Cell 1, the results being very similar to those in Section 6.1.1. It was considered that the electrode surfaces had probably oxidised again in the time interval (a few hours) between polishing and evacuation. The vacuum photoemission also indicated that repolishing had not greatly affected the aluminium surfaces, since its magnitude remained at $\sim 10^{-8}$A. (for unfiltered radiation).

The electrodes were repolished again, and this time the cell was evacuated within an hour. Some $\frac{I}{V}$ curves were obtained but, again, the results were no different. The liquid removed from the test cell, judging from the ultraviolet absorption edge, had not been contaminated in its passage through the degassing system.

Summary

Unfiltered radiation induced currents of $\sim 10^{-12}$A. in both degassed n-hexane and in the 'Spectroscopic' grade. These currents were suppressed completely if the liquid was saturated with air; degassing to 10^{-3} torr being sufficient to allow photoconduction, but further degassing (to 10^{-6} torr) made little (if any) difference. The photocurrents depended on the intensity of the radiation, and on

the magnitude (but not the polarity) of the applied voltage. There was a tendency for the photocurrents to 'saturate' as the applied voltage was increased (to a maximum of 150 V.). Filtered (OX7) or (OX1) radiation did not induce conduction even if absorbed by unpurified n-hexane. Charges appeared to be generated in the bulk of the liquid; there was no indication of photoinjection from either electrode (cathode or anode), even after repolishing their surfaces.

6.2. Photoinjection of charges from 'activated' electrodes

The inactivity of polished aluminium electrodes in photoinjecting charges into liquid hexane has been demonstrated. Such surfaces were not very efficient photocathodes (in vacuo) either. It seemed likely that if the vacuum photoemission could be increased, photoinjection into the liquid would result. It was not desirable to increase the intensity of the radiation (because of the 'bulk' photoconduction), and so a search was made for better photocathode materials. In general, however, metal surfaces were convenient and (if known catalysts are avoided) should not react with the liquid.

The most active photocathodes, for use in vacuo, are the 'composite' type. These consist of an alkali metal layer (e.g. caesium) on an oxide substrate (usually silver oxide). Unfortunately, these surfaces are highly reactive and were not very suitable for immersion in liquid hexane. Of other metals, the best emitters are also the most susceptible to surface oxidation; this causes a reduction in sensitivity and usually an increase in the photoelectric work function.

Relatively oxide-free metal layers can, however, be prepared by vacuum evaporation. If these layers are maintained in an ordinary vacuum ($\sim 10^{-6}$ torr) there will still be some oxidation, but this can increase the photosensitivity of some metals (see Section 3.4). Al, Mg, and Au were chosen for further investigation since Al and Mg have the lowest work functions of the stable metals and Au, having a high work function but a very inert surface for the sake of comparisons. A method of vacuum evaporation of these metals in the test cell itself was evolved, so that these surfaces were maintained in vacuo for subsequent photostimulation in highly degassed hexane. This technique is described in Chapter V, together with the design of the test cells. The results to be described in the following Sections were obtained using test cells (no 2 et seq.) in which at least one of the electrode surfaces was coated with an evaporated metal layer.

6.3. Photocurrents with an evaporated layer of aluminium on one electrode surface (Cell 2)

Aluminium metal was evaporated on to one (polished aluminium) electrode in the test cell itself. The other electrode (SnO_2/silica combination) admitted the radiation, which was directed at the surface of the aluminium layer. Photoconduction measurements, in highly degassed 'Spectroscopic' hexane, were commenced within half an hour of the deposition of the metal.

It is seen (Fig. 6.6) that the induced current for the 'forward' direction (the coated electrode negative) was up to 30 times greater

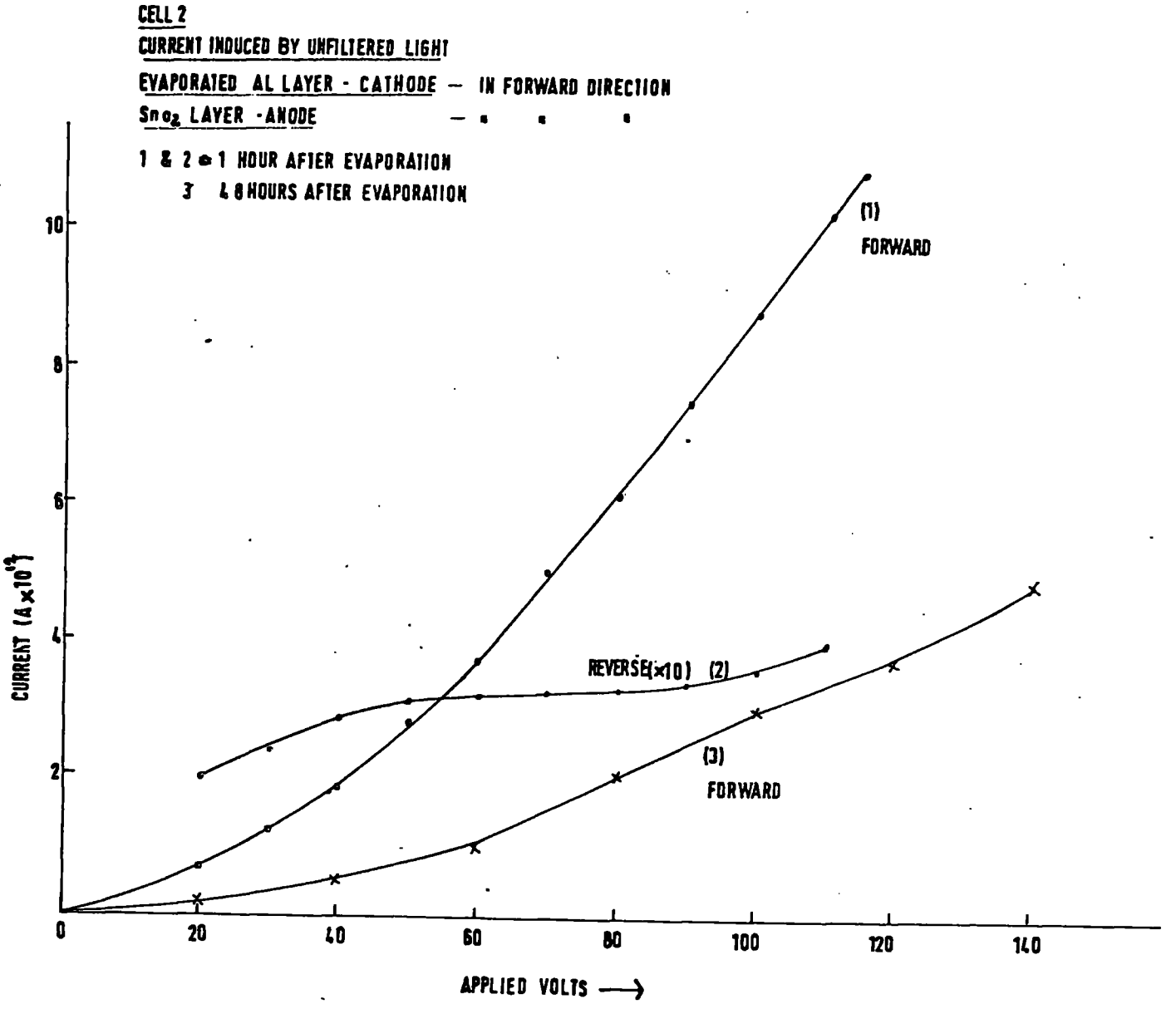
CELL 2
CURRENT INDUCED BY UNFILTERED LIGHT
EVAPORATED AL LAYER - CATHODE — IN FORWARD DIRECTION
SnO_2 LAYER - ANODE — . . .
1 & 2 ≈ 1 HOUR AFTER EVAPORATION
3 & 4 HOURS AFTER EVAPORATION
(1)
FORWARD
REVERSE(×10) (2)
(3)
FORWARD
CURRENT (A ×10⁻⁹)
APPLIED VOLTS ⟶
0
20
40
60
80
100
120
140
2
4
6
8
10

Fig. 6.6

Fig. 6.7

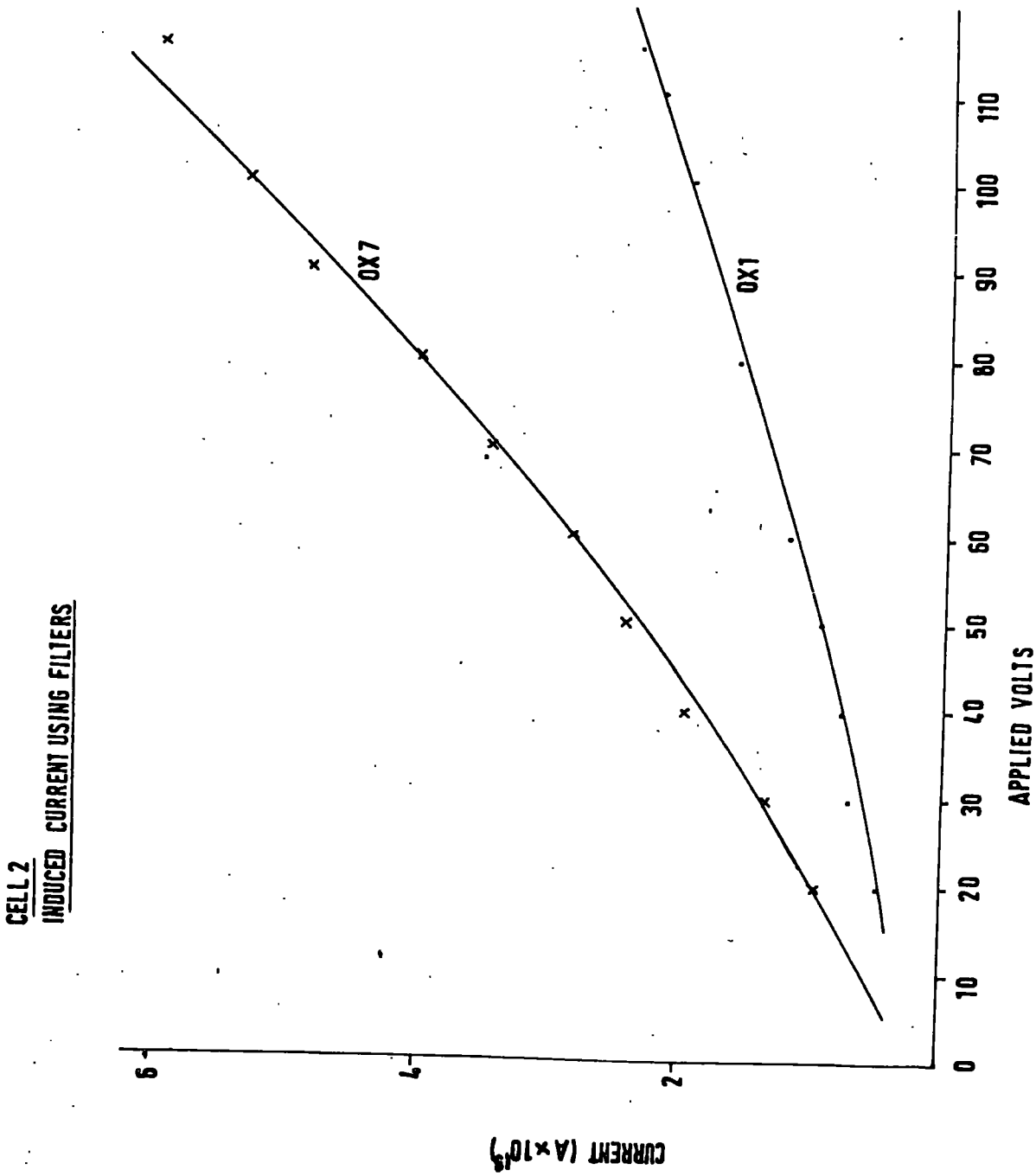
CELL 2
INDUCED CURRENT USING FILIERS
0X7
0X1
CURRENT (A×10⁻⁹)
APPLIED VOLTS
0
10
20
30
40
50
60
70
80
90
100
110
2
4
6

than that for the opposite polarity ('reverse'). Furthermore, the forward current showed no signs of saturation as the applied voltage was increased, in marked contrast to the previous measurements with polished electrodes (Section 6.1). It became evident that the forward currents were decaying with time; curve 3 in Fig. 6.6 shows the conduction 48 hours after the evaporation. The reverse photocurrents, however, remained essentially constant throughout the duration of the tests (2 days).

Filtered (OX7, OX1) radiation also induced currents in the forward direction, although their magnitude (Fig. 6.7) was substantially smaller than for unfiltered radiation. Filtered (OX7) radiation did not induce reverse photocurrents (i.e.. over and above the 'dark' currents of $\sim 10^{-15}$A.).

An attempt was made, using a monochromator, to find the photoelectric threshold of the aluminium layer in the liquid, but the currents were too small to be measured with any accuracy because of the low aperture of this instrument. The photoelectric threshold of the coated surface in vacuo was found to be about 3400Å, i.e.. roughly the same as that estimated from the photocurrents in the liquid for filtered radiation.

There was no measurable activity of the polished aluminium surface, made available by rotating the electrode assembly by 180°, in the hexane even when unfiltered radiation was used. (The photocurrents were comparable to those previously observed for reverse bias, but their magnitude remained the same for either polarity of

the applied voltage). The uncoated surface in vacuo was much less photosensitive than the evaporated layer, the threshold being at about 2400Å.

The photocurrents disappeared almost immediately after letting air into the cell.

Of four separate 'runs' with this cell, including the evaporation of an aluminium layer and with fresh samples of highly degassed 'Spectroscopic' hexane each time, only two were successful because of the failure of the filament during the evaporation, or mechanical difficulties associated with the positioning of the screen (see Section 5.1). The results which have been outlined are a composite of those obtained during the two sucessful attempts.

Summary

(i) Charges could be injected (with unfiltered radiation) into highly degassed hexane from evaporated aluminium cathodes. The electrode activity decreased with time, probably because of slow oxidation of the aluminium.

(ii) Filtered (OX7, OX1) radiation was also effective in injecting (reduced) quantities of charge from the evaporated layer. This radiation did not induce significant conduction in the bulk of the liquid.

(iii) Polarity reversal tests indicated that both SnO_2 layers and polished aluminium surfaces are non-injecting. This could, to some extent, be linked to their low photosensitivities in vacuo.

6.4. Cell 3

The photocathode has been irradiated obliquely (in cell 1), and directly (through a SnO_2 anode) in cell 2. Both configurations require the radiation to pass through the liquid, and the separation of 'liquid' and 'electrode' photostimulation is consequently difficult.

A third method, initiated by Swan[54], is to irradiate the back surface of the photocathode. If the metal (e.g. aluminium) is deposited as a thin film on silica the vacuum photoemission may be substantial if about 50% of the radiation is absorbed.[105] Very careful control of the thickness of the film is necessary (and this is relatively easy with vacuum deposition methods) but technical difficulties prevented Swan (and later Gzowski[55]) from maintaining their photocathodes free from oxidation. In any case half the radiation passes into the liquid.

Swan's method was rejected in favour of oblique irradiation of the electrodes since, in the latter arrangement;

(i) Either electrode may be irradiated, by suitably positioning the lamp.

(ii) It was a simple matter to design a test cell in which one, or both, of the electrodes could be coated.

(iii) The photoinjected currents may be distinguished from bulk liquid photostimulation by the use of suitable ultraviolet filters with the lamp. (e.g. Filtered (OX7) radiation would not be absorbed by purified n-hexane, but could still promote electrode activity.)

The largely unknown action of the SnO_2 layer in cell 2 can thus be avoided, and a fairer comparison between the properties of polished and vacuum deposited electrode surfaces could be made.

For effective oblique irradiation of parallel plate electrodes, the electrode spacing must be comparable to the electrode diameter. The lamp emitted a useful intensity of radiation through an aperture of $\sim$ 5 mm. diameter, this could be focussed (with a silica lens) to a spot of about the same size. To allow for the angle of incidence of the beam with the electrode surface (which distorts the spot into an ellipse) it was decided to use 1 cm. dia. electrodes, at a similar separation. This, in turn, set an upper limit of $\sim$ 3KV.cm.$^{-1}$ to the field which could be applied with the existing voltage supply.

6.5. Photocurrents with both electrodes coated with an evaporated layer of aluminium. (Cell 3).

Layers of aluminium were evaporated on to both (polished aluminium) electrodes in cell 3. Photoconduction measurements were made with highly degassed and purified n-hexane. (H.D.P. n-hexane).

Some $\frac{I}{V}$ curves were obtained with continuous unfiltered or (OX7, OX1) filtered irradiation of one of the electrodes. Those for OX7-filtered irradiation are shown in Fig. 6.8, being similar (except in magnitude) to the others. The currents were changing with time (Fig. 6.9 shows these variations, at a fixed voltage). The main observations were;

Fig. 6.8

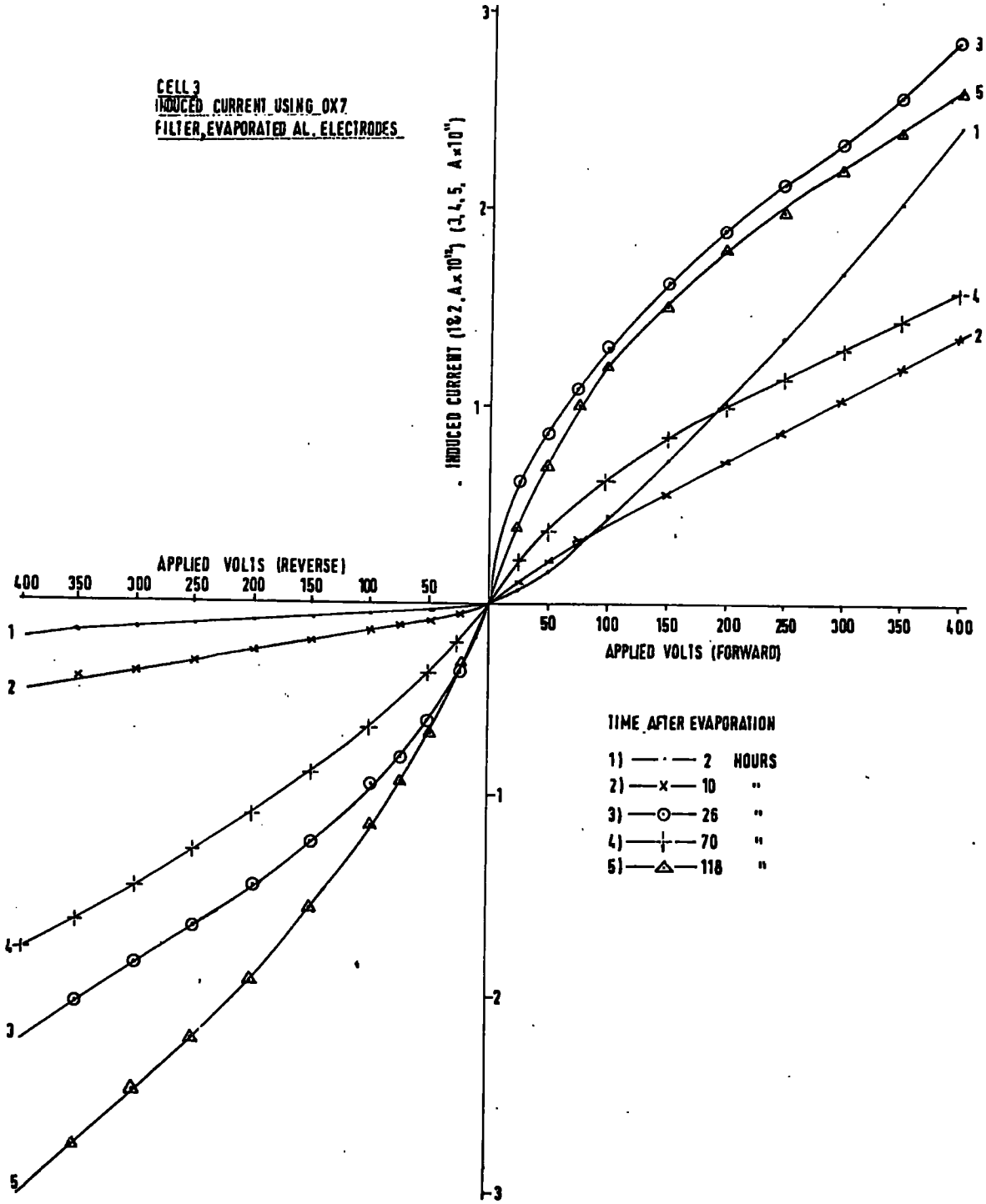
CELL 3
INDUCED CURRENT USING OX7
FILTER, EVAPORATED AL. ELECTRODES
INDUCED CURRENT (1&2, A×10⁻¹²) (3,4,5, A×10⁻⁹)
APPLIED VOLTS (REVERSE)
APPLIED VOLTS (FORWARD)
400 350 300 250 200 150 100 50
50 100 150 200 250 300 350 400
3 2 1 -1 -2 -3
TIME AFTER EVAPORATION
1) — · — 2 HOURS
2) —x— 10 "
3) —⊙— 26 "
4) —┼— 70 "
5) —△— 118 "

Fig. 6.9

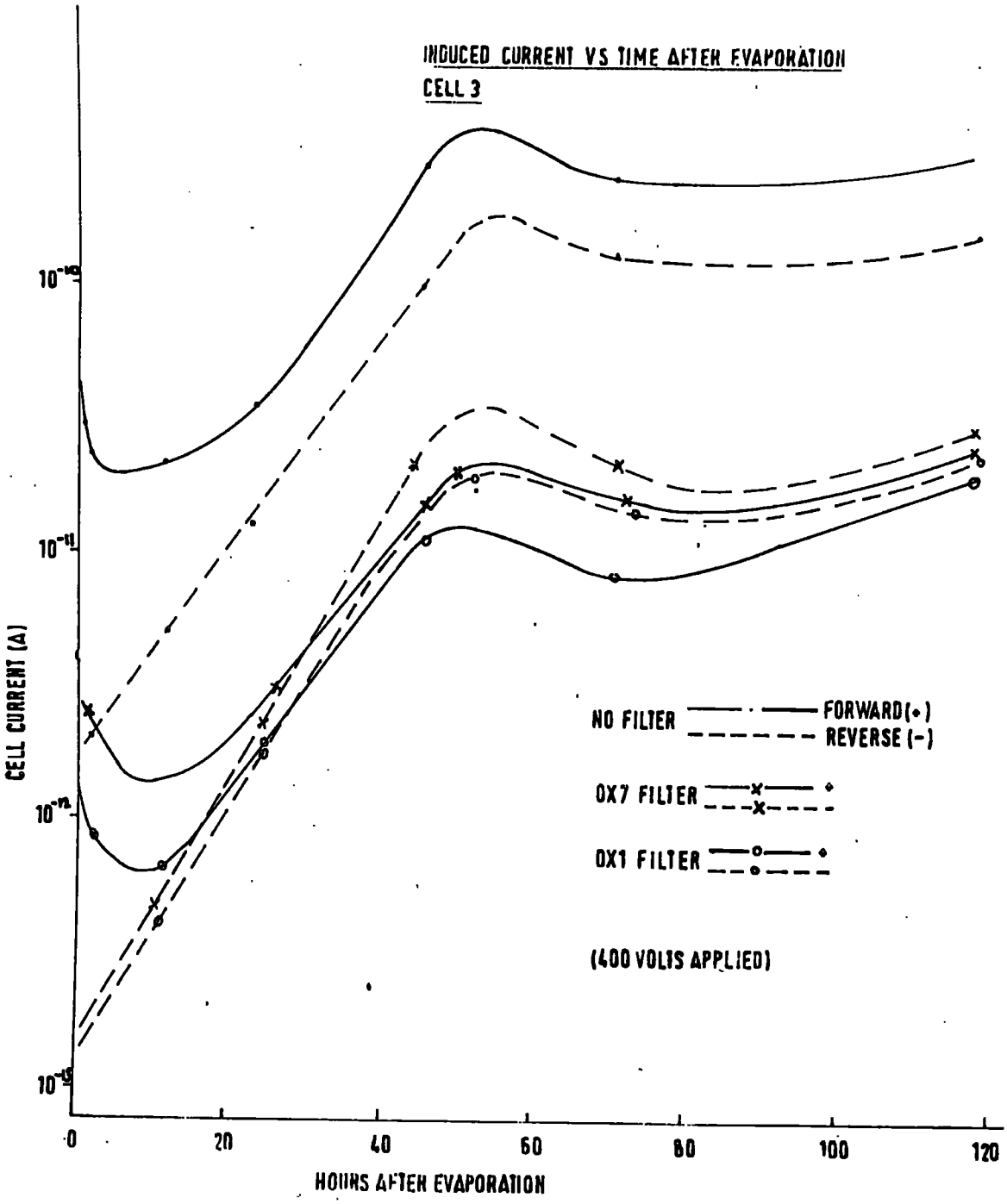
INDUCED CURRENT VS TIME AFTER EVAPORATION
CELL 3
CELL CURRENT (A)
HOURS AFTER EVAPORATION
0
20
40
60
80
100
120
NO FILTER
FORWARD (+)
REVERSE (-)
0X7 FILTER
0X1 FILTER
(400 VOLTS APPLIED)

Fig. 6.10

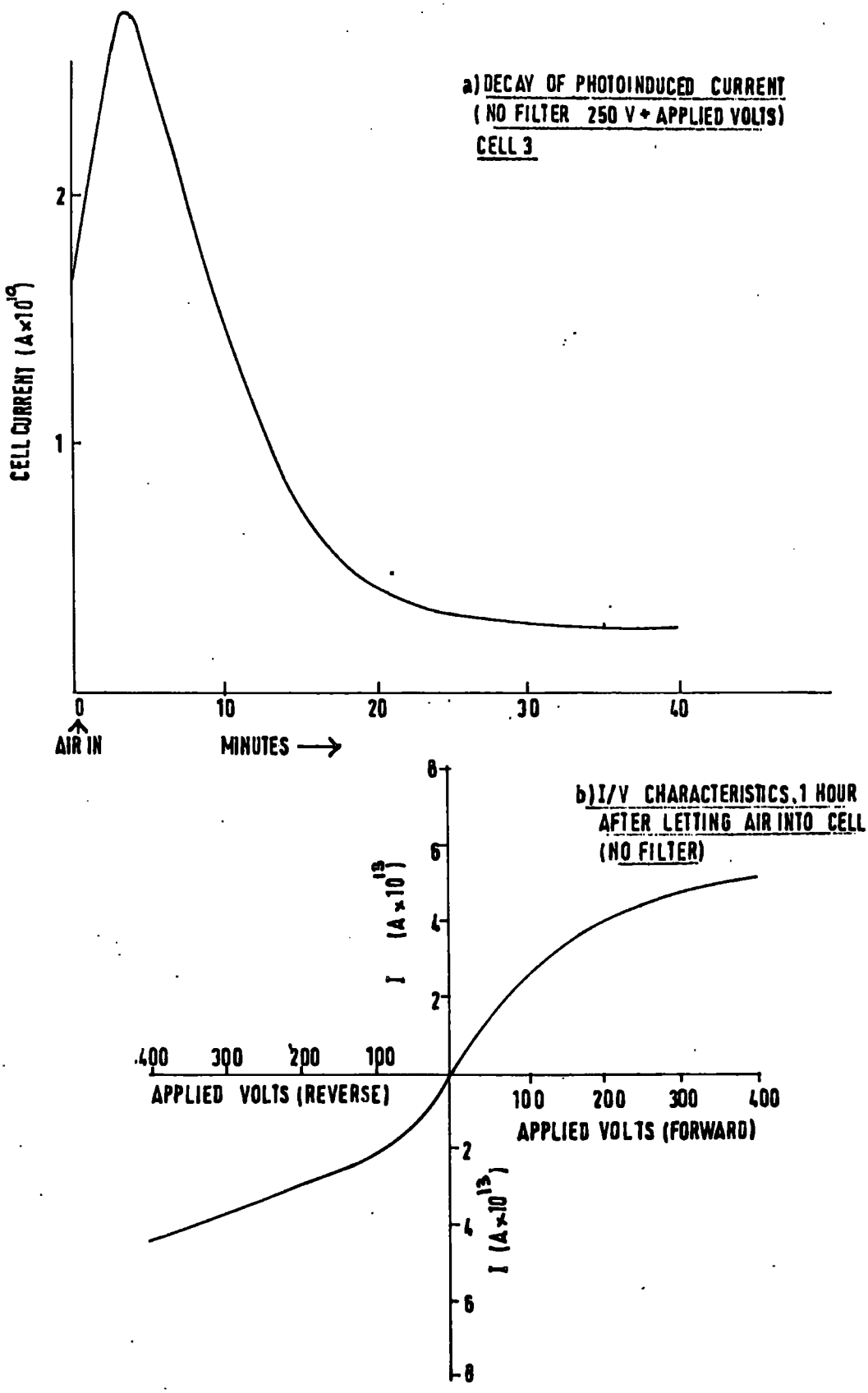
a) DECAY OF PHOTOINDUCED CURRENT
(NO FILTER 250 V + APPLIED VOLTS)
CELL 3
CELL CURRENT (A×10^9)
2
1
0
AIR IN
10
20
30
40
MINUTES
b) I/V CHARACTERISTICS, 1 HOUR AFTER LETTING AIR INTO CELL (NO FILTER)
I (A×10^13)
8
6
4
2
400
300
200
100
APPLIED VOLTS (REVERSE)
100
200
300
400
APPLIED VOLTS (FORWARD)
2
4
6
8

(i) The photocurrents were, at first, about 10 times greater with the irradiated electrode negative ('forward' direction) than with this electrode positive ('reverse'). These $\frac{I}{V}$ curves sloped upwards (i.e. I increased faster than V). Photocurrents in the forward direction were slowly decreasing, but those for reverse polarity were increasing.

(ii) After about 10 hours the photocurrents began to 'saturate' at the higher voltages (400 V. max.).

(iii) At later times the 'saturation' type photocurrents increased, the forward/reverse ratio approaching unity.

Finally, a minute hole was made in the cell and the photocurrents monitored as the hexane saturated with air (Fig. 6.10(a)). The saturation-type $\frac{I}{V}$ characteristic was retained even when the photocurrents had dropped to a very low level (e.g. Fig. 6.10(b)).

6.6. A tentative explanation of the results in Sec. 6.5.

It was plausible that the induced currents resulted from a mixture of;

(i) Injection from the photocathode.

(ii) Photoionisation of the bulk liquid.

The magnitude of the photocurrents shown in the upward sloping $\frac{I}{V}$ curves depended on the polarity of the irradiated electrode, and were thus consistent with the photoinjection of negative charges from the cathode. Photoinjection for reverse polarities could result from reflections in the cell.

The 'saturation-type' photocurrents resembled those measured with cell 1 (Sec. 6.1), and remained the same for either polarity of the applied field. It was not unreasonable to assume that these currents originated from the photoionisation of the bulk liquid.

Both types of conduction were changing with time, the tentative explanation being;

(A) The efficiency of photoinjection was reduced as the aluminium layer oxidised (to bring the conditions in cell 3 more nearly equivalent to cell 1; where polished, and thus oxidised, electrodes were used). Filtered (OX1, OX7) radiation would cause injection as long as the work function of the layer remained low enough.

(B) The 'bulk' photocurrents were increased by the exposure of the liquid to long periods of unfiltered radiation; a proportion of which could be expected to cause photochemical reactions. The additional absorption, of the reaction products, could then result in a 'sensitised' or 'impurity' bulk photoconduction. It will be remembered (from Chapter IV) that most organic compounds, i.e. impurities, absorb radiation of longer wavelengths than the hexane itself.

It is seen that the decreasing contribution of the photoinjected currents will, because of the cumulative degradation of the liquid, be obliterated by the rise in bulk photoconduction.

6.7. (a) Photoinduced currents with both electrodes coated with an evaporated layer of aluminium (ii) cell 3.

In order to test the suppositions in Sec. 6.6, it was decided to avoid the use of unfiltered radiation. Another layer of aluminium

Fig. 6.11

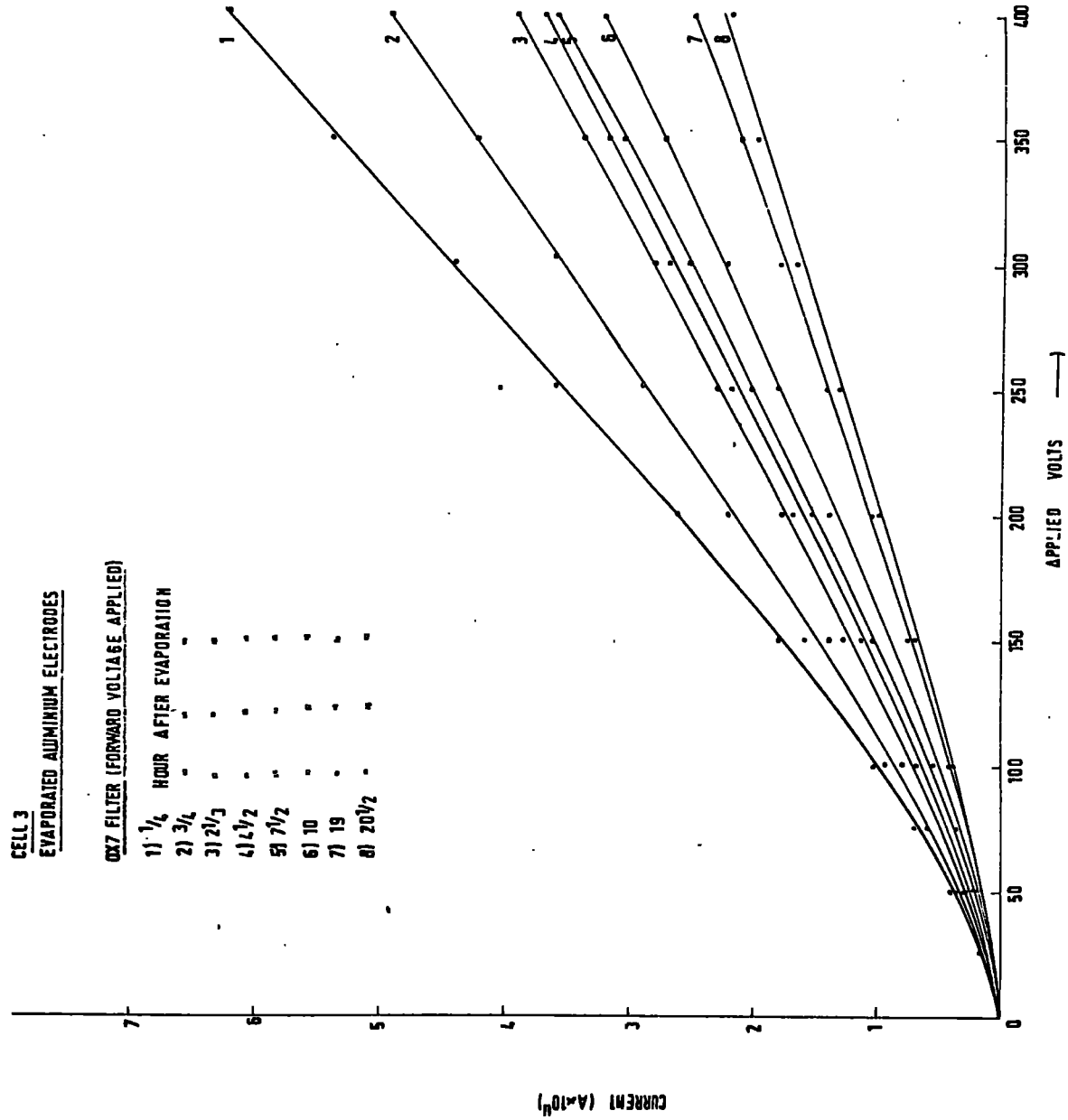
CELL 3
EVAPORATED ALUMINIUM ELECTRODES
OX7 FILTER (FORWARD VOLTAGE APPLIED)
1) 1/4 HOUR AFTER EVAPORATION
2) 3/4 " " "
3) 2 1/3 " " "
4) 4 1/2 " " "
5) 7 1/2 " " "
6) 10 " " "
7) 19 " " "
8) 20 1/2 " " "
CURRENT (A×10^n)
APPLIED VOLTS

Fig. 6.12

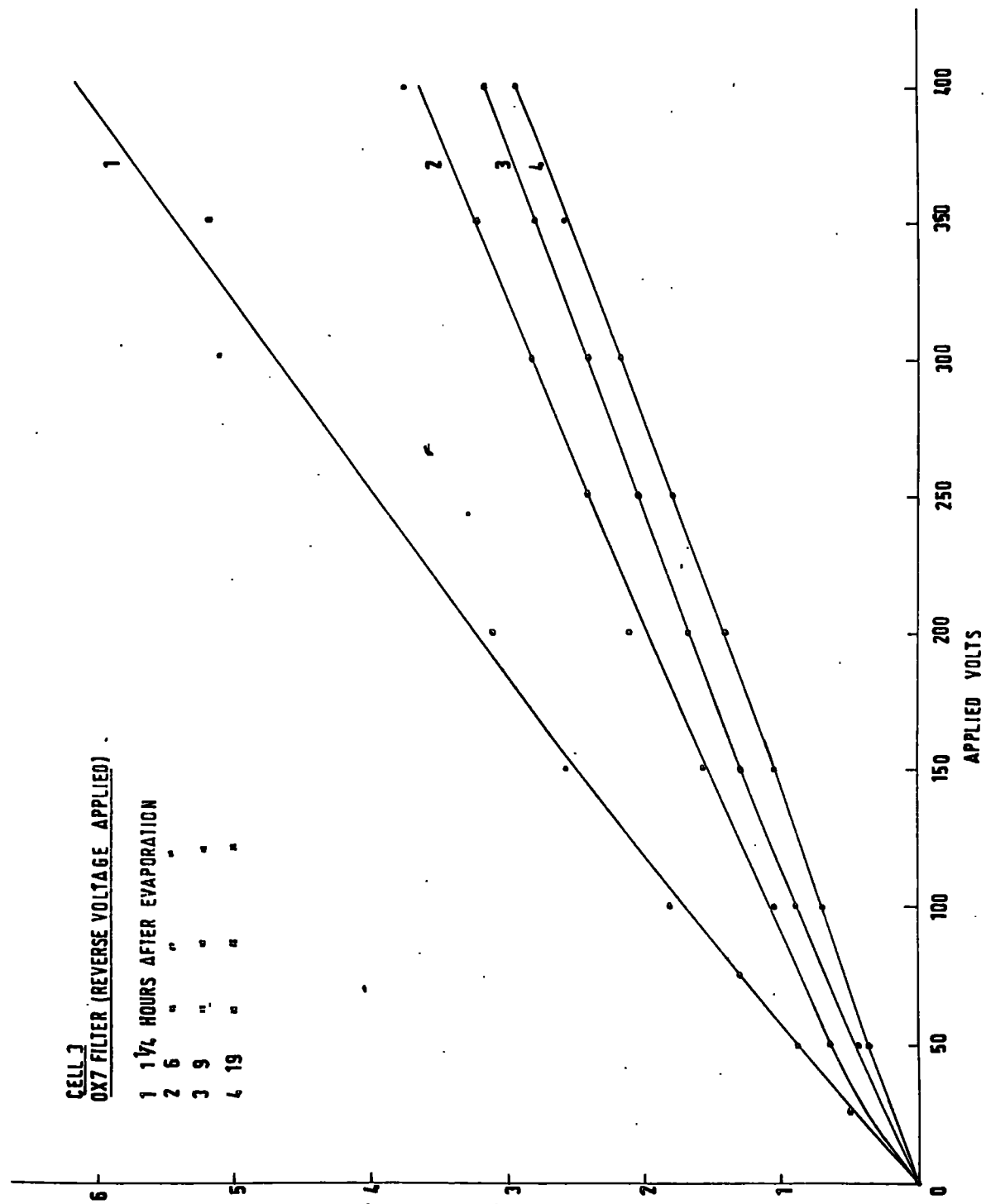
CELL 3
OX7 FILTER (REVERSE VOLTAGE APPLIED)
1 1½ HOURS AFTER EVAPORATION
2 6 " "
3 9 " "
4 19 " "
CURRENT (A×10⁻⁹)
APPLIED VOLTS
0
50
100
150
200
250
300
350
400
1
2
3
4
5
6

Fig. 6.13

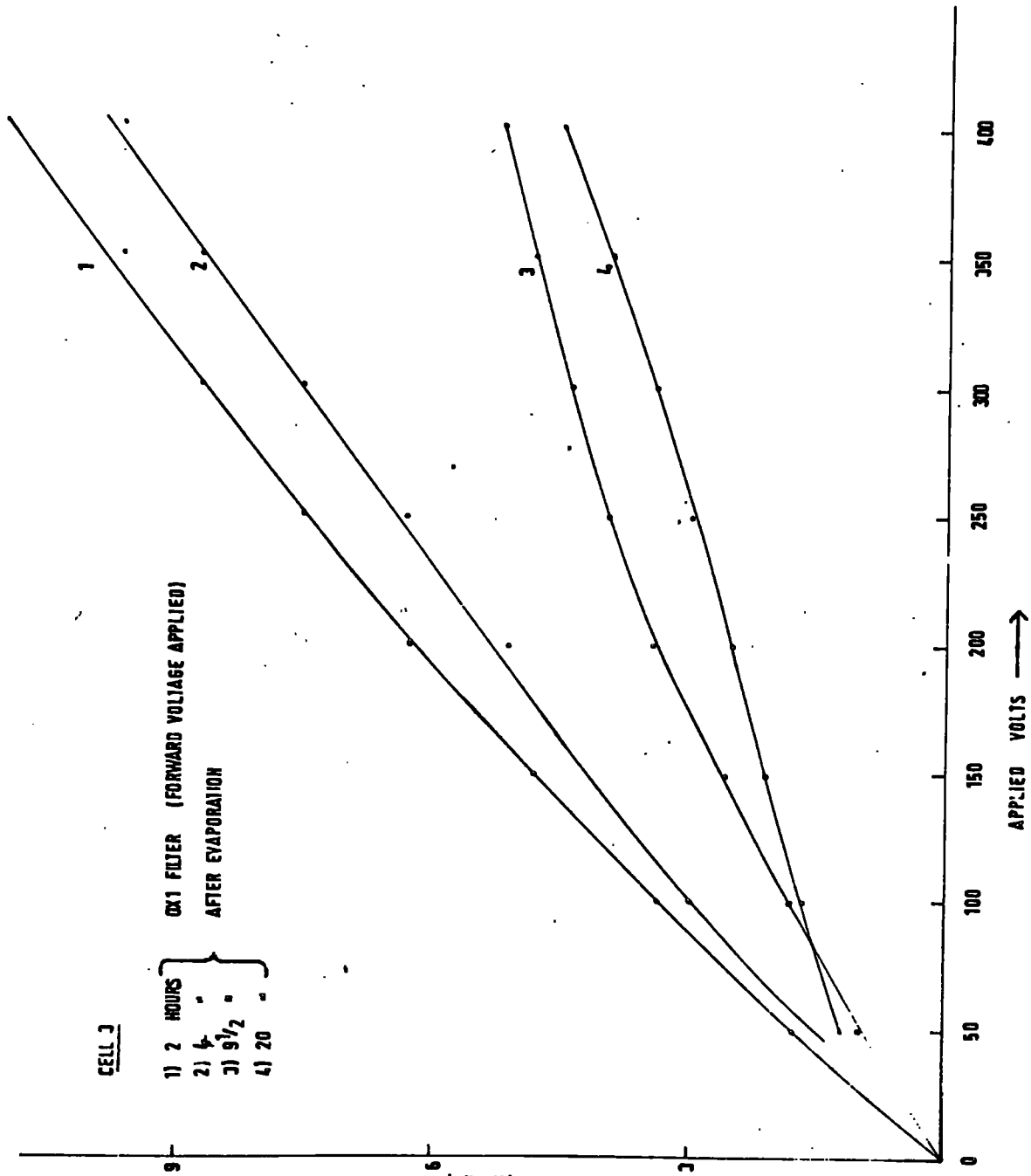
CELL 3
1) 2 HOURS
2) 4 "
3) 9½ "
4) 20 "
OX1 FILTER (FORWARD VOLTAGE APPLIED)
AFTER EVAPORATION
1
2
3
4
0
50
100
150
200
250
300
350
400
APPLIED VOLTS

Fig. 6.14

EVAPORATED ALUMINIUM ELECTRODES
DECAY OF PHOTOINJECTED CURRENT AND RISE OF BULK PHOTOCONDUCTIVITY
400 v APPLIED VOLTAGE

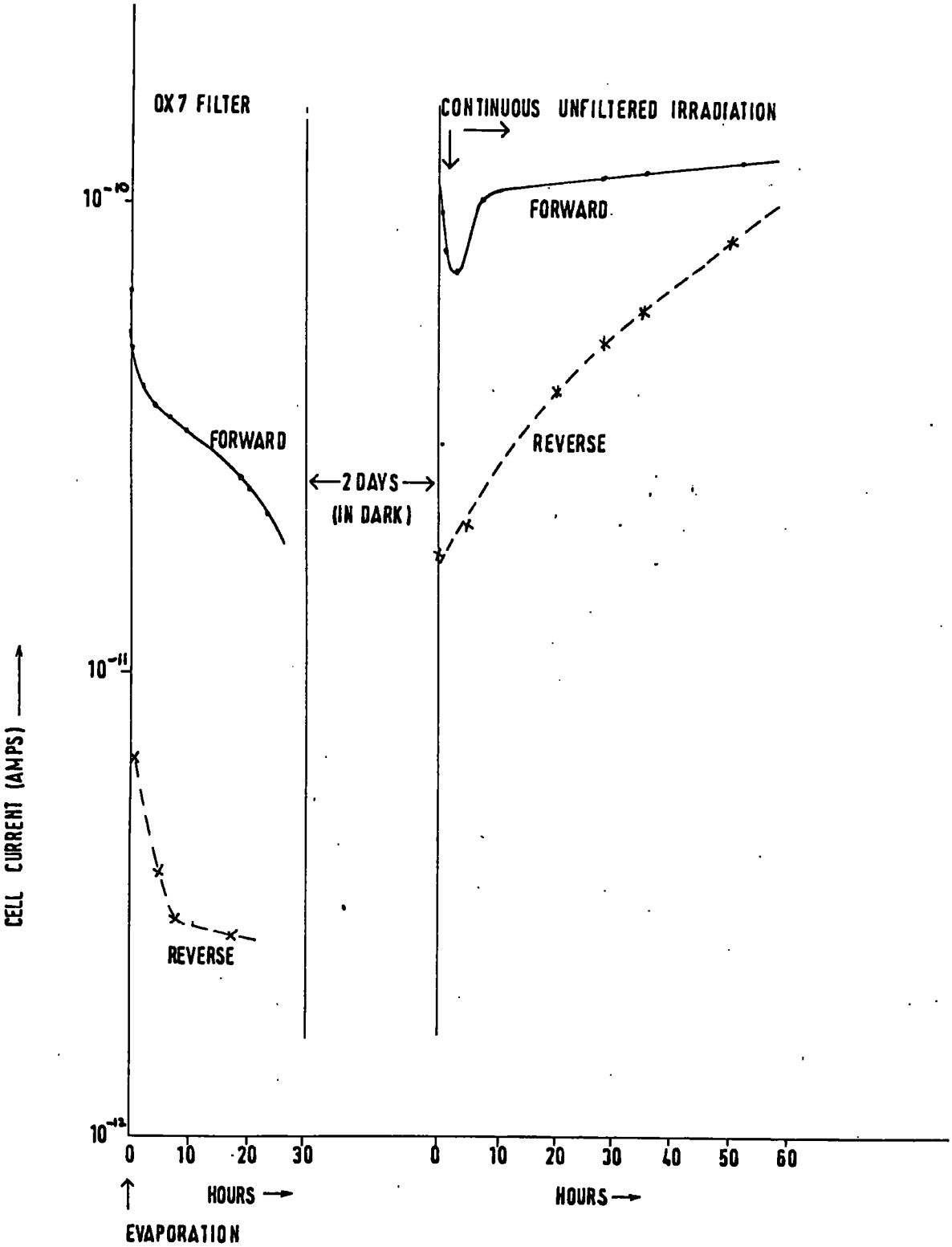

was deposited over both electrodes in cell 3, and H.D.P. n-hexane admitted to the cell.

A series of $\frac{I}{V}$ curves were obtained with OX1- and OX7-filtered irradiation of one of the electrodes. These measurements (Figs. 6.11, 6.12) indicated the absence of appreciable 'bulk' photostimulation. The forward/reverse ratio remained at about 10:1 for the duration of the measurements (20 hours from the evaporation). Except for a slight tendency towards saturation for OX1-filtered radiation (Fig. 6.13) these curves maintained their upward curvature for the whole time. The photocurrents for either polarity exhibited a deceleratory decay with time; so that after 20 hours they were still decreasing, but only very slowly (Fig. 6.14). The cell was then left (in darkness) for 2 days, subsequent measurements showed that the photocurrents had fallen only slightly ($\sim 10\%$) during this time.

At this stage, the vacuum photoemission was measured (neither the lamp nor the cell being moved). The forward photoemission (40 V. applied) was 5×10^{-7}A. for OX7-filtered radiation, the forward/reverse ratio being 12:1. (This latter measurement indicated the proportion of reflected radiation arriving at the 'dark' electrode).

Measurements were then continued with the liquid in the cell but this time using continuous unfiltered radiation. After an initial slight decrease in the forward current, the photocurrents for both polarities rose steadily with the period of exposure. Measurements were continued for 50 hours, during which time the currents were approaching polarity independence (Fig. 6.14). The $\frac{I}{V}$ characteristics,

Fig. 6.15

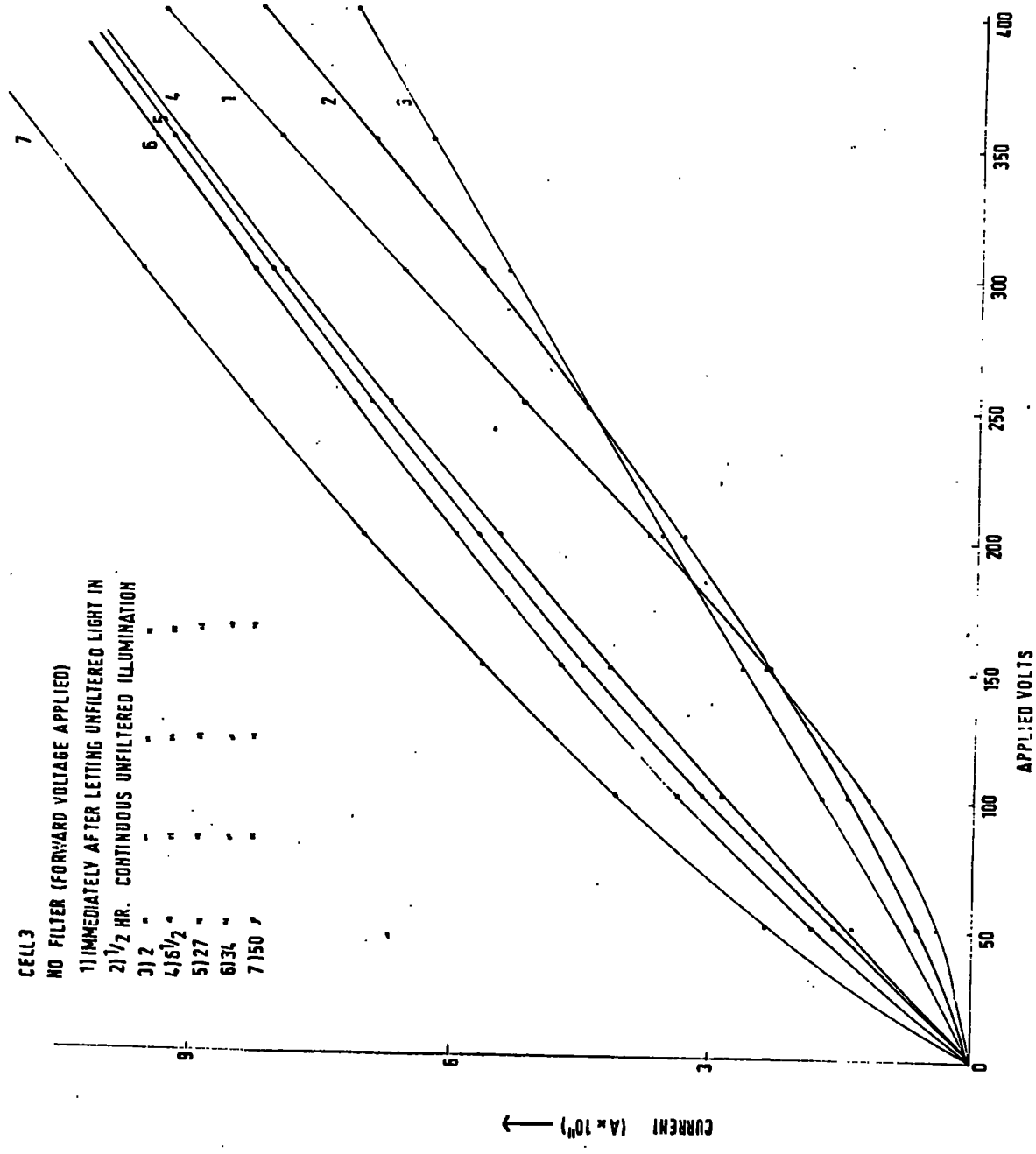
CELL 3
NO FILTER (FORWARD VOLTAGE APPLIED)
1) IMMEDIATELY AFTER LETTING UNFILTERED LIGHT IN
2) 1/2 HR. CONTINUOUS UNFILTERED ILLUMINATION
3) 2 " " "
4) 15 1/2 " " " "
5) 27 " " " "
6) 36 " " " "
7) 150 " " " "
CURRENT (A × 10^-11)
APPLIED VOLTS
0
50
100
150
200
250
300
350
400
3
6
9
1
2
3
4
5
6
7

Fig. 6.16

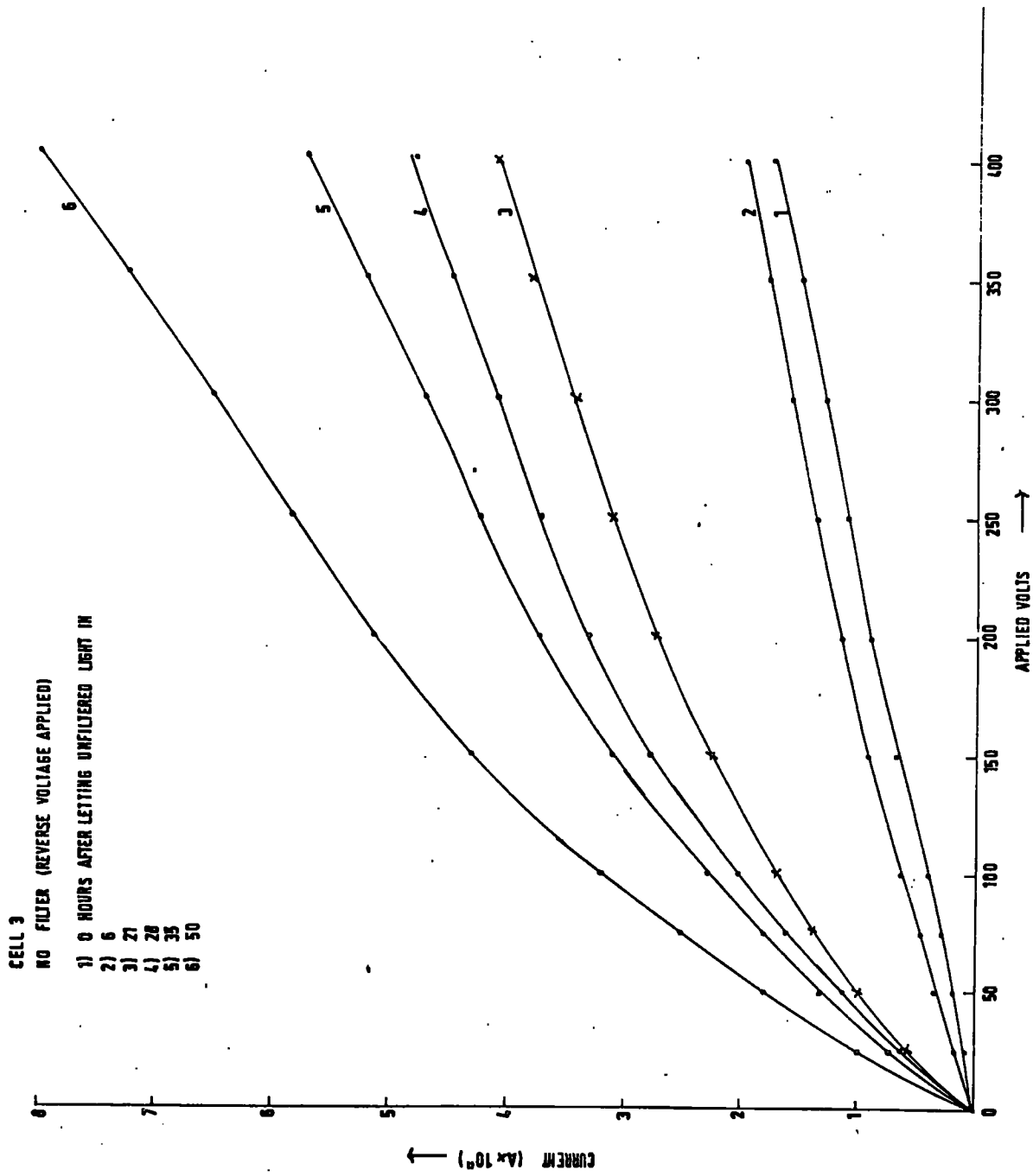
CELL 3
NO FILTER (REVERSE VOLTAGE APPLIED)
1) 0 HOURS AFTER LETTING UNFILTERED LIGHT IN
2) 6
3) 21
4) 28
5) 35
6) 50
CURRENT (A x 10⁻⁶)
APPLIED VOLTS
0
1
2
3
4
5
6
7
8
0
50
100
150
200
250
300
350
400

e.g. Figs. 6.15, 6.16, were comparable to those previously obtained (Sec. 6.5). The vacuum photoemission was measured again (after the 50 hours unfiltered radiation). The forward/reverse ratio had remained at about 10:1, but the 'saturated' photoemission (using the OX7 filter) had fallen to $\sim 2 \times 10^{-7}$A. (forward). For unfiltered radiation the corresponding current was 1.4×10^{-6}A.

Finally, the cell was emptied and the liquid retained for chemical analysis (see Sec. 6.16).

6.7. (b)

The experiments described in 6.7(a) were repeated, but this time using interrupted (filtered) radiation for the first phase of the measurements.

The photocurrents decayed in a manner consistent with that described in Sec. 6.7(a). Furthermore, it was found that the rise in bulk photoconduction (in the second phase of the measurements) was arrested if the unfiltered radiation was stopped.

6.8. Summary of the findings in Secs. 6.7(a) and 6.7(b) in relation to the proposals in Sec. 6.6.

It has been shown that cathodic photoinjection can be distinguished from bulk photoconduction by the proper use of filters. The decay in activity of the aluminium layers could then be observed without complications due to bulk photoconduction (see Fig. 6.14). The photoinjected charges originated at the cathode; reverse currents being attributable to reflections in the cell (of the order of 10%).

Bulk photocurrents have been shown to be initiated by the use of unfiltered radiation and to increase with the period of exposure; i.e. changes are brought about in the liquid which are cumulative. This type of conduction is, apparently, insensitive to the state of oxidation of the aluminium layers on the electrodes. There were, however, indications that unfiltered radiation also accelerated the decay of electrode activity (presumably by promoting oxidation of the aluminium).

Even when the activity of the electrodes had largely decayed there was still a useful photoinjected current (e.g. two days after the evaporation). The use of OX7-filtered radiation to promote these currents did not appreciably affect the decay in the activity of the electrodes. It was decided to use continuously filtered radiation in subsequent investigations of the injection of charges from the electrodes.

6.9. Photocurrents with both electrodes coated with an evaporated layer of magnesium. (Cell 4).

It was decided to ascertain if larger currents could be obtained using magnesium, with its lower photoelectric work function, than aluminium.

Using cell 4, an evaporated layer of magnesium was deposited over both (polished magnesium) electrodes, photoinduced currents being subsequently measured in H.D.P. n-hexane. Unfiltered radiation was not allowed to enter the cell at any time, currents being stimulated with the use of OX1 and OX7 filters.

Fig. 6.17

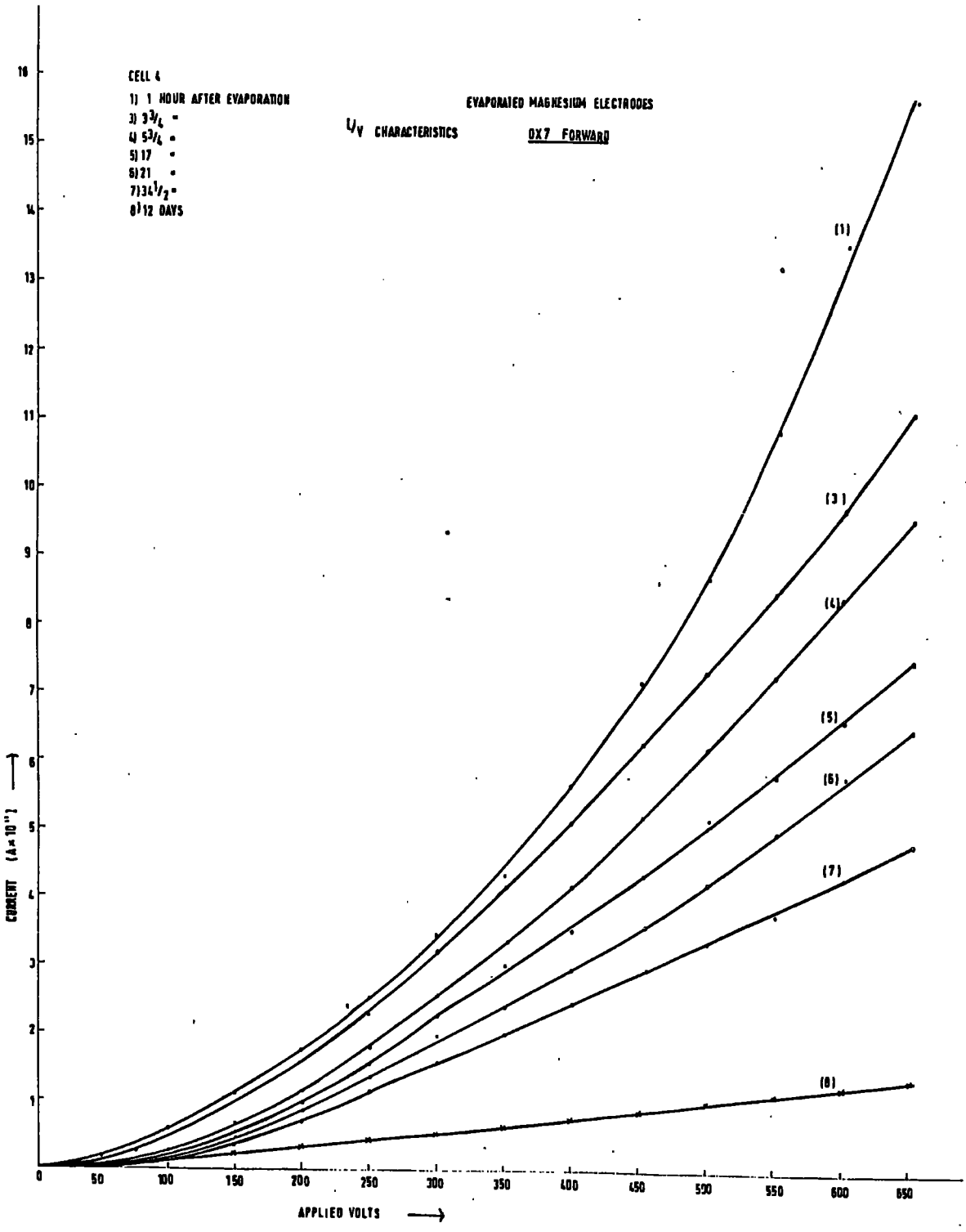
CELL 4
1) 1 HOUR AFTER EVAPORATION
3) 3 3/4 "
4) 5 3/4 "
5) 17 "
6) 21 "
7) 34 1/2 "
8) 12 DAYS
EVAPORATED MAGNESIUM ELECTRODES
I/V CHARACTERISTICS
0X7 FORWARD
(1)
(3)
(4)
(5)
(6)
(7)
(8)
CURRENT (A x 10⁻¹¹) ⟶
APPLIED VOLTS ⟶
0
50
100
150
200
250
300
350
400
450
500
550
600
650
1
2
3
4
5
6
7
8
9
10
11
12
13
14
15
16

Fig. 6.18

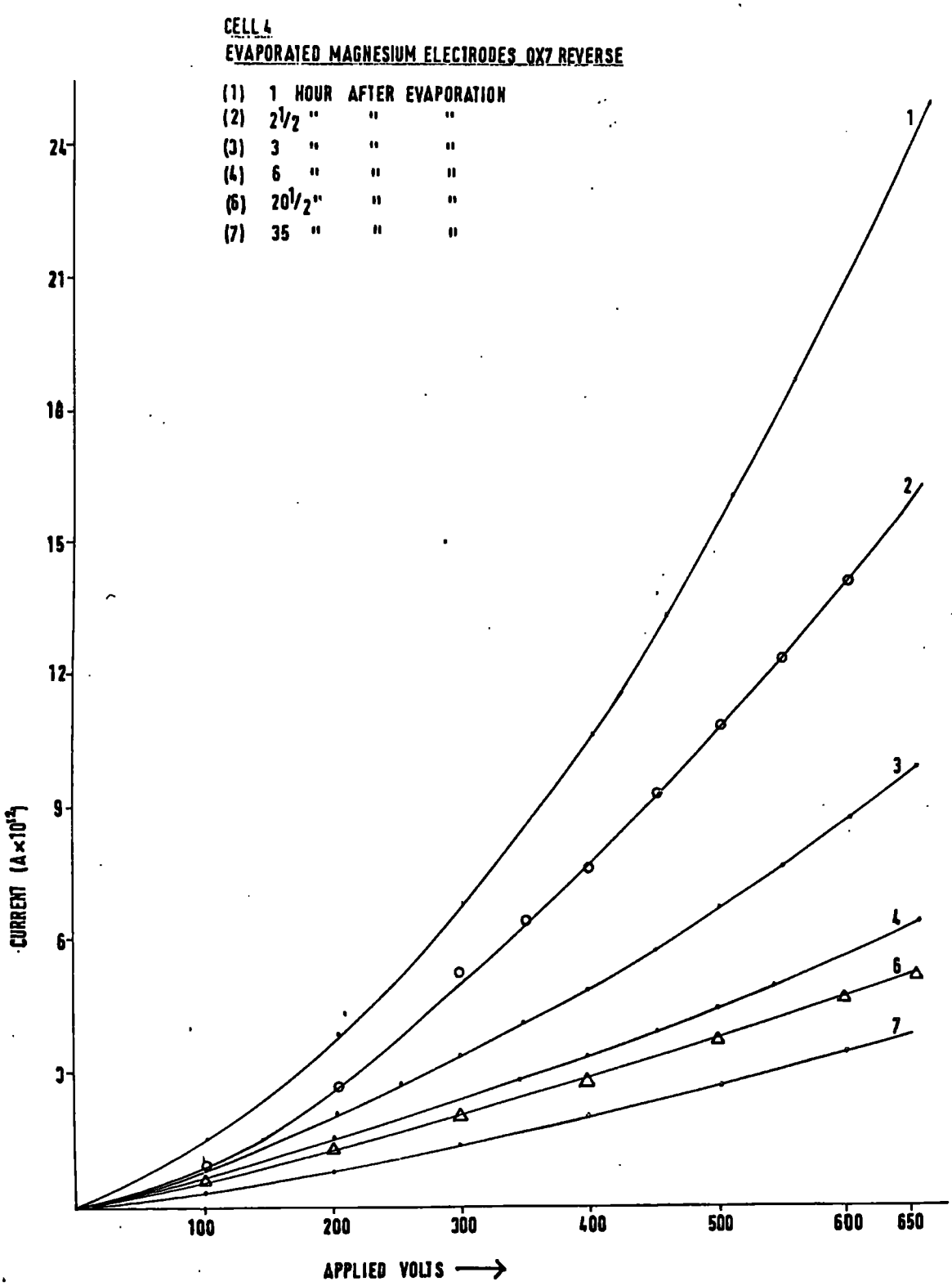
CELL 4
EVAPORATED MAGNESIUM ELECTRODES QX7 REVERSE
(1) 1 HOUR AFTER EVAPORATION
(2) 2 1/2 " " "
(3) 3 " " "
(4) 6 " " "
(6) 20 1/2 " " "
(7) 35 " " "
24
21
18
15
12
9
6
3
CURRENT (A×10¹²)
100
200
300
400
500
600
650
APPLIED VOLTS ⟶
1
2
3
4
6
7

Fig. 6.19

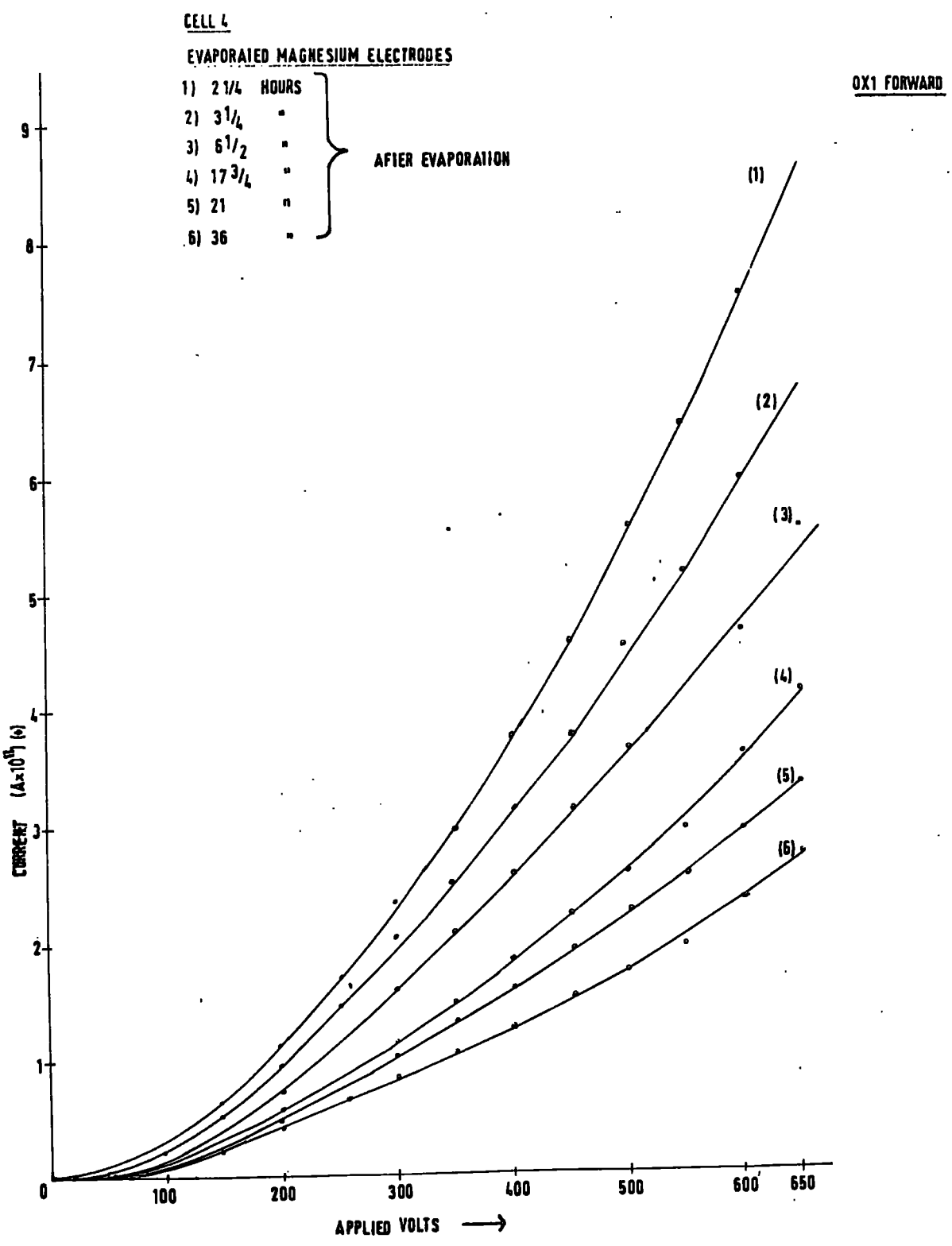
CELL 4
EVAPORATED MAGNESIUM ELECTRODES
1) 2 1/4 HOURS
2) 3 1/4 "
3) 6 1/2 "
4) 17 3/4 "
5) 21 "
6) 36 "
AFTER EVAPORATION
OX1 FORWARD
(1)
(2)
(3)
(4)
(5)
(6)
CURRENT (A x 10^-11) (→)
APPLIED VOLTS →
0
1
2
3
4
5
6
7
8
9
100
200
300
400
500
600
650

Fig. 6.20

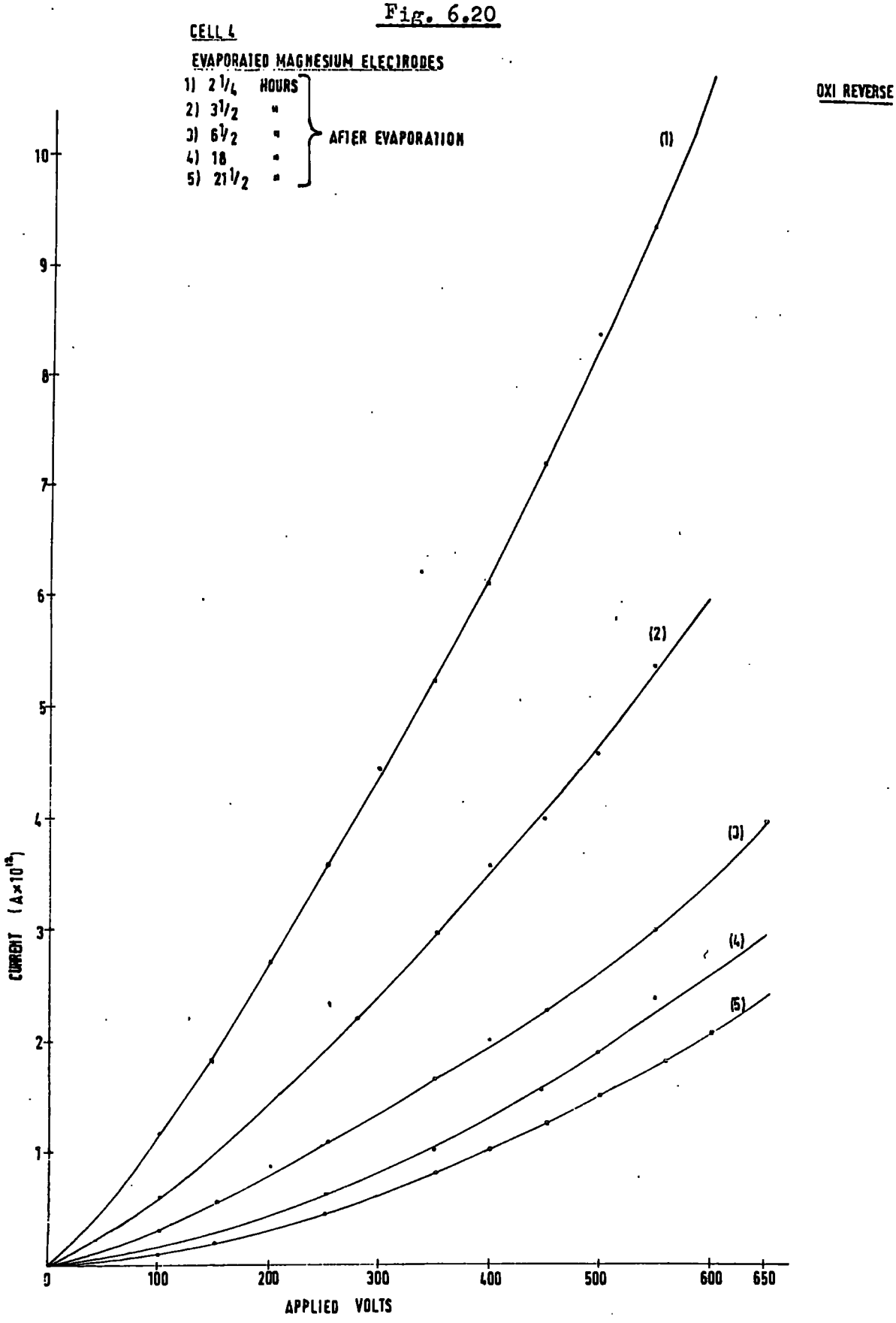
CELL 4
EVAPORATED MAGNESIUM ELECTRODES
1) 2 1/4 HOURS
2) 3 1/2 "
3) 6 1/2 "
4) 18 "
5) 21 1/2 "
AFTER EVAPORATION
OXI REVERSE
(1)
(2)
(3)
(4)
(5)
CURRENT (A×10^-12)
APPLIED VOLTS
0
100
200
300
400
500
600
650
1
2
3
4
5
6
7
8
9
10

Fig. 6.21

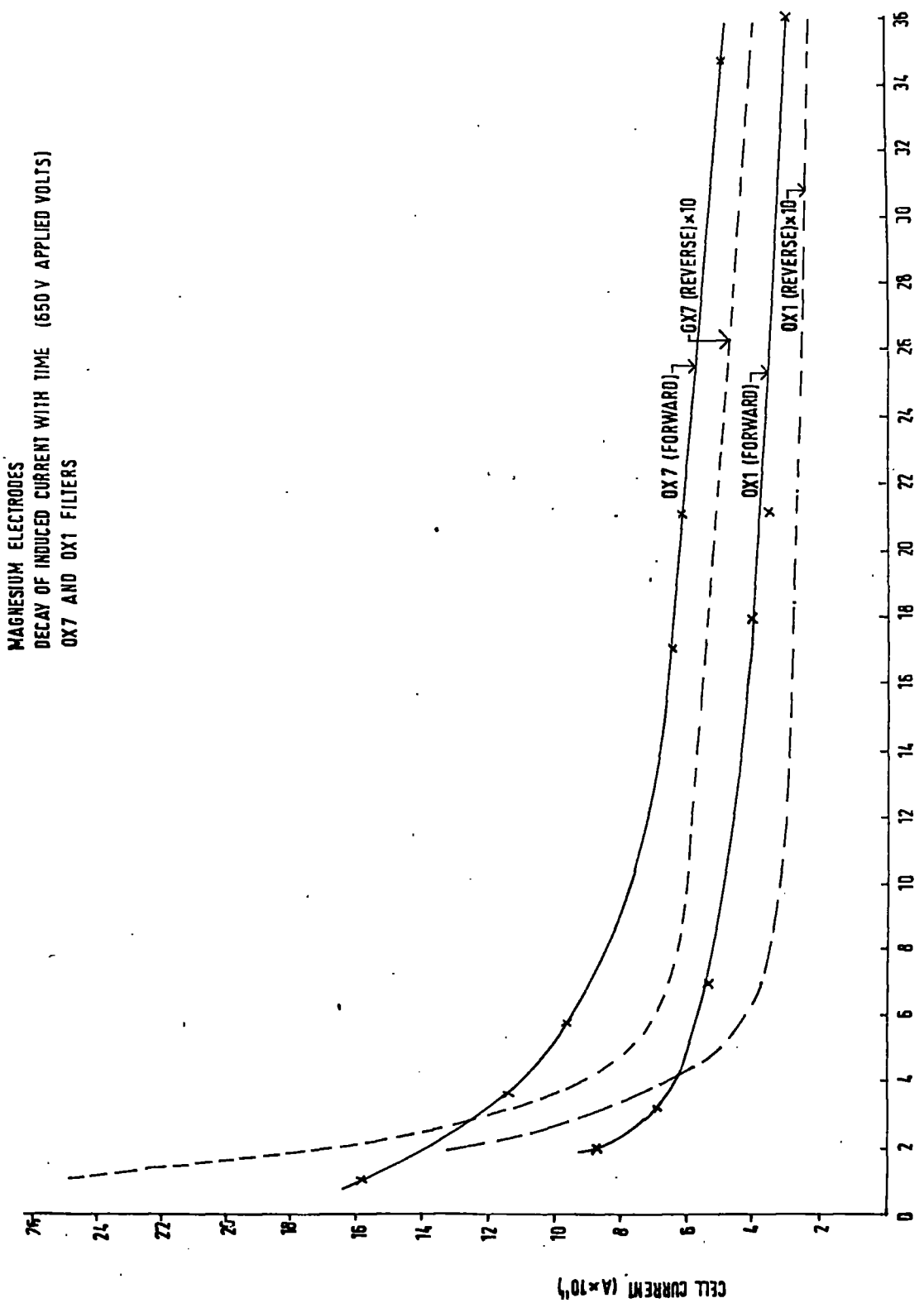
MAGNESIUM ELECTRODES
DECAY OF INDUCED CURRENT WITH TIME (650 V APPLIED VOLTS)
OX7 AND OX1 FILTERS
OX7 (FORWARD)
OX7 (REVERSE)×10
OX1 (FORWARD)
OX1 (REVERSE)×10
CELL CURRENT (A×10¹⁵)
HOURS AFTER EVAPORATION
0
2
4
6
8
10
12
14
16
18
20
22
24
26
28
30
32
34
36
2
4
6
8
10
12
14
16
18
20
22
24
26

Observations were continued for 12 days from the evaporation, a 'family' of $\frac{I}{V}$ curves being obtained for applied voltages up to 650V. using each filter in turn (Figs. 6.17, 6.18, 6.19, 6.20). It is seen that there was a consistent and deceleratory decay in magnitude of the currents with time. There were no signs of any photostimulation of the liquid in these characteristics. In fact, a plot of the decay of current indicated an increasing forward/reverse ratio with time (Fig. 6.21).

It was noted that magnesium did not seem to be much more active than aluminium (Sec. 6.7) so far as injection was concerned. It remained to be seen, however, if other evaporated layers of these metals were the same.

6.10. Photocurrents with evaporated gold electrodes (i). Cell 4.

Gold does not oxidise appreciably, and has a much higher work function (4.2 eV) than Al. or Mg. It was considered that the photo-injected currents with evaporated gold electrodes ought to afford an interesting comparison with Al. and Mg.

Cell 4 was baked in dry air (at 120°C) for about two hours so that the (polished magnesium) electrodes became covered with a thin layer of oxide. Gold was subsequently evaporated over the electrodes (in the test cell itself) so that measurements could be made with H.D.P. n-hexane.

It was found that the photocurrents, for filtered (OX7) radiation, were obscured by noise ($\sim 10^{-13}$A.). These disturbances, which were

Fig. 6.22

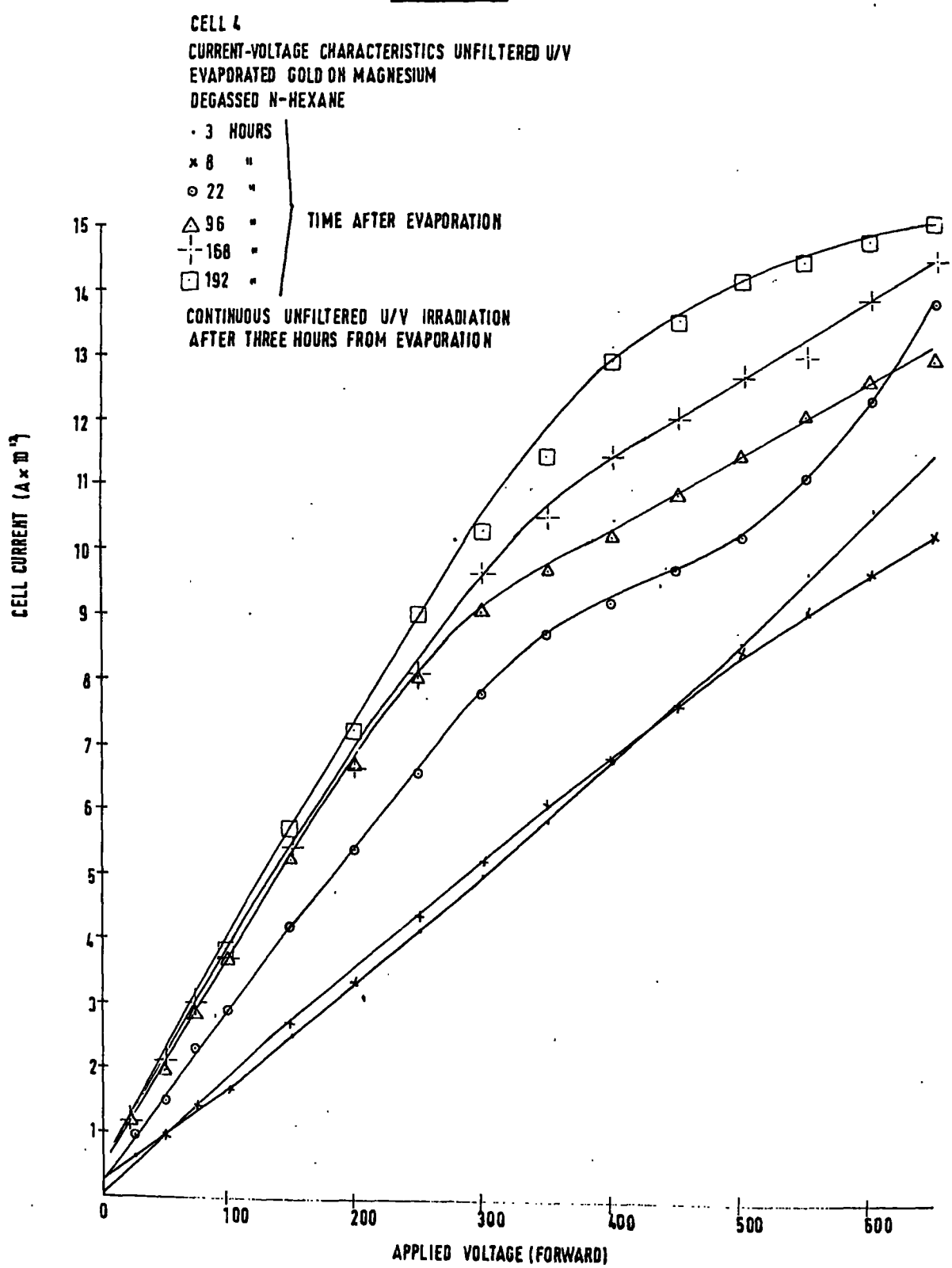
CELL 4
CURRENT-VOLTAGE CHARACTERISTICS UNFILTERED U/V
EVAPORATED GOLD ON MAGNESIUM
DEGASSED N-HEXANE
· 3 HOURS
× 8 "
⊙ 22 "
△ 96 "
⊹ 168 "
⊡ 192 "
TIME AFTER EVAPORATION
CONTINUOUS UNFILTERED U/V IRRADIATION
AFTER THREE HOURS FROM EVAPORATION
CELL CURRENT (A × 10⁻¹³)
APPLIED VOLTAGE (FORWARD)
0
100
200
300
400
500
600
1
2
3
4
5
6
7
8
9
10
11
12
13
14
15

Fig. 6.23

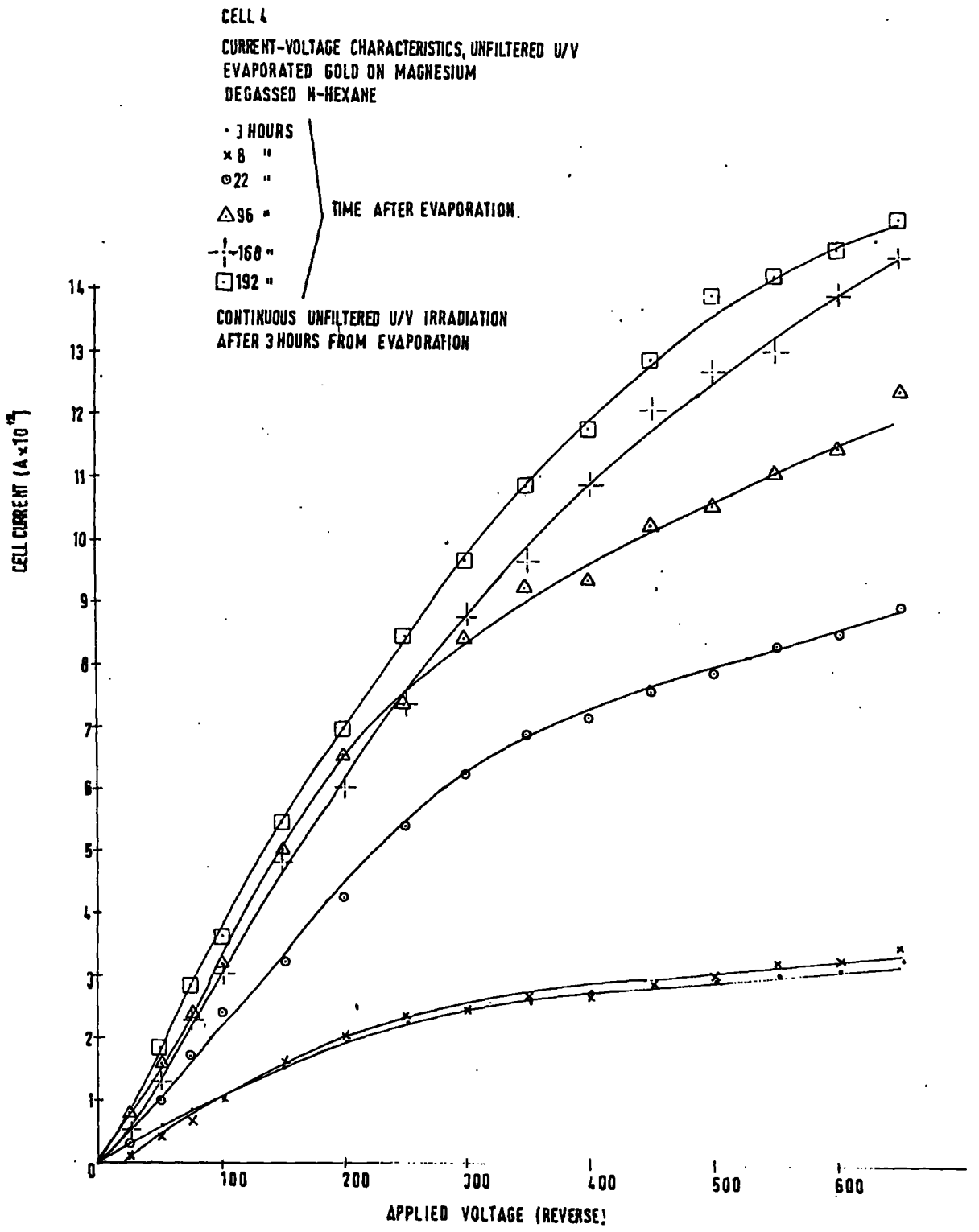
CELL 4
CURRENT-VOLTAGE CHARACTERISTICS, UNFILTERED U/V
EVAPORATED GOLD ON MAGNESIUM
DEGASSED N-HEXANE
· 3 HOURS
× 8 "
⊙ 22 "
△ 96 "
-|- 168 "
⊡ 192 "
TIME AFTER EVAPORATION.
CONTINUOUS UNFILTERED U/V IRRADIATION
AFTER 3 HOURS FROM EVAPORATION
CELL CURRENT (A×10⁻¹³)
APPLIED VOLTAGE (REVERSE)
0
1
2
3
4
5
6
7
8
9
10
11
12
13
14
100
200
300
400
500
600

Fig. 6.24

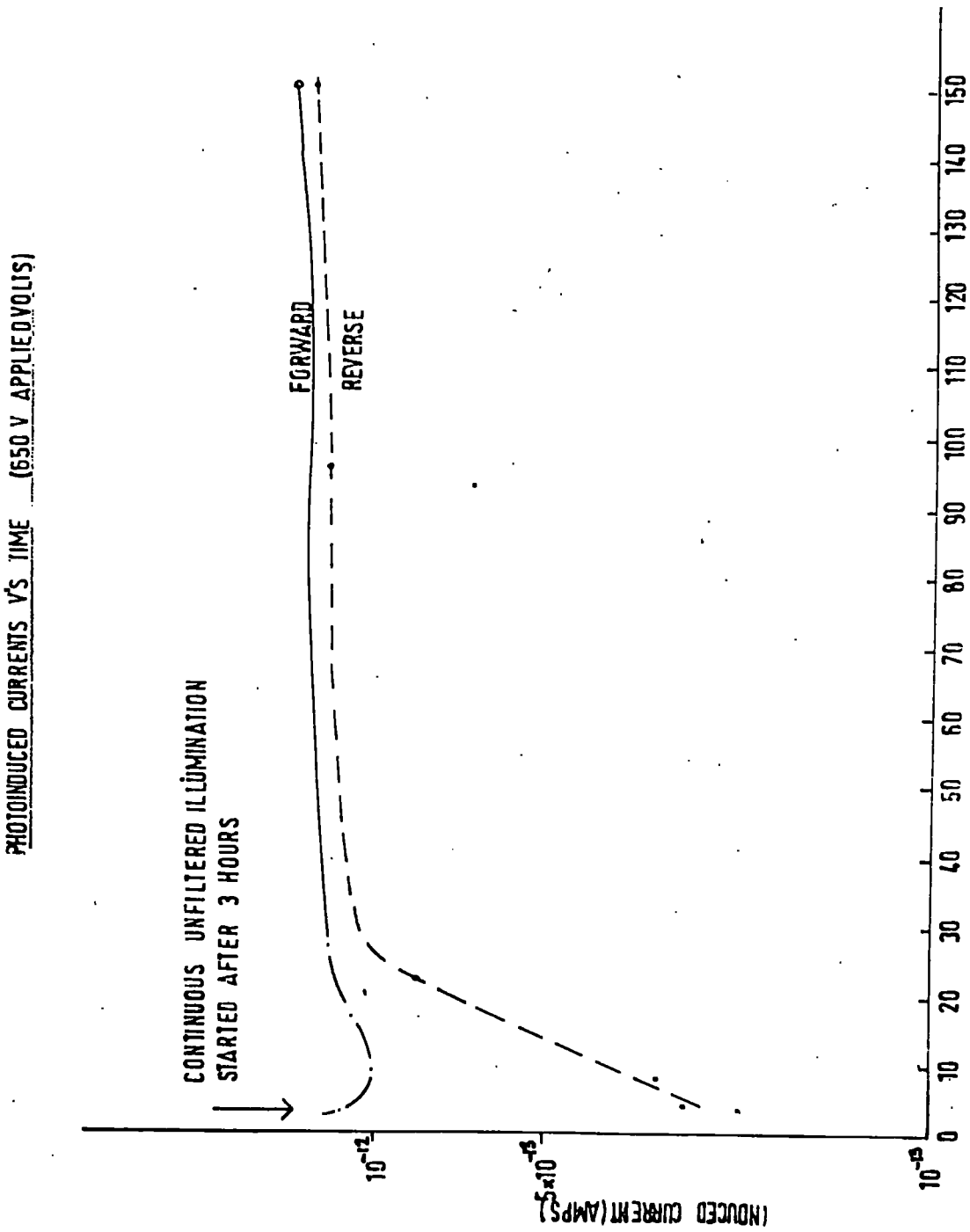
PHOTOINDUCED CURRENTS V'S TIME (650 V APPLIED VOLTS)
CONTINUOUS UNFILTERED ILLUMINATION
STARTED AFTER 3 HOURS
FORWARD
REVERSE
10^{-12}
5×10^{-13}
10^{-13}
0
10
20
30
40
50
60
70
80
90
100
110
120
130
140
150
HOURS AFTER EVAPORATION

not affected by switching the lamp off, could not be traced to any fault in the cell or the electrical circuit. It became apparent, after two or three hours, that the currents were 'settling down' and it was eventually found that the currents for (0X7)-filtered radiation were $\sim 5 \times 10^{-14}$A. at 650V. (forward direction). Since unfiltered radiation induced currents of $\sim 10^{-12}$A. it was decided to proceed without using filters rather than to abandon the experiment altogether. Possibly because of the three hours delay in starting measurements, the electrodes were not very active (the forward/reverse ratio being only 4:1). The 'bulk' photoconduction increased with the period of exposure to the radiation, so that the currents were virtually independent of the polarity of the applied voltage after about 40 hours (Fig. 6.24). The $\frac{I}{V}$ characteristics, during this time, are shown in Figs. 6.22, 6.23. The 'saturated' vacuum photoemission, some 72 hours after the evaporation of the gold layer, was as follows;

unfiltered radiation; 1.3×10^{-8}A.

with 0X7 filter; 1.2×10^{-9}A.

with 0X1 filter; 7.8×10^{-11}A.

It would appear, from a comparison of the photoemission for the different filters, that gold has a work function of ~ 4.1 eV. The threshold for photoinjection in the liquid was about the same as in vacuo. Bulk photocurrents were (initially) stimulated by rather shorter wavelengths, (> 2500Å, corresponding to a threshold of ~ 5 eV.).

6.11. Photocurrents with evaporated gold electrodes (ii). (Cell 4).

The first series of measurements using evaporated gold electrodes (Sec. 6.10) were hampered by the unaccountably high noise level, and the only reliable results were obtained with unfiltered radiation. Some useful information regarding the degradation of the liquid was obtained, but measurements of the photoinjection using filters would have been of interest. Furthermore, although the most likely external sources of the noise had been checked, it seemed doubtful that the fluctuations would originate from such a passive surface as gold. It was suspected that part of the (magnesium) electrode surface which was uncovered by the gold might have been active.

It was decided to deposit the gold over polished aluminium electrodes instead. Measurements were commenced, with cell 4, in which a layer of gold was evaporated, and with a fresh sample of H.D.P. n-hexane. The opportunity was also taken to extend the applied voltage to a maximum of 2.5KV.

It was evident that there was, again, too much noise for the photocurrents to be measured with (OX1 or OX7)-filtered radiation. The measurements were continued, somewhat reluctantly, with unfiltered radiation. The $\frac{I}{V}$ curves (Figs. 6.25 and 6.26) indicate that gold is active in photoinjecting charges into n-hexane (although not as active as Al. or Mg.) and that, after a slight initial decrease (lasting perhaps 3 hours), the photocurrents in the forward direction were stable. The fall in the forward/reverse ratio with time of exposure

Fig. 6.25

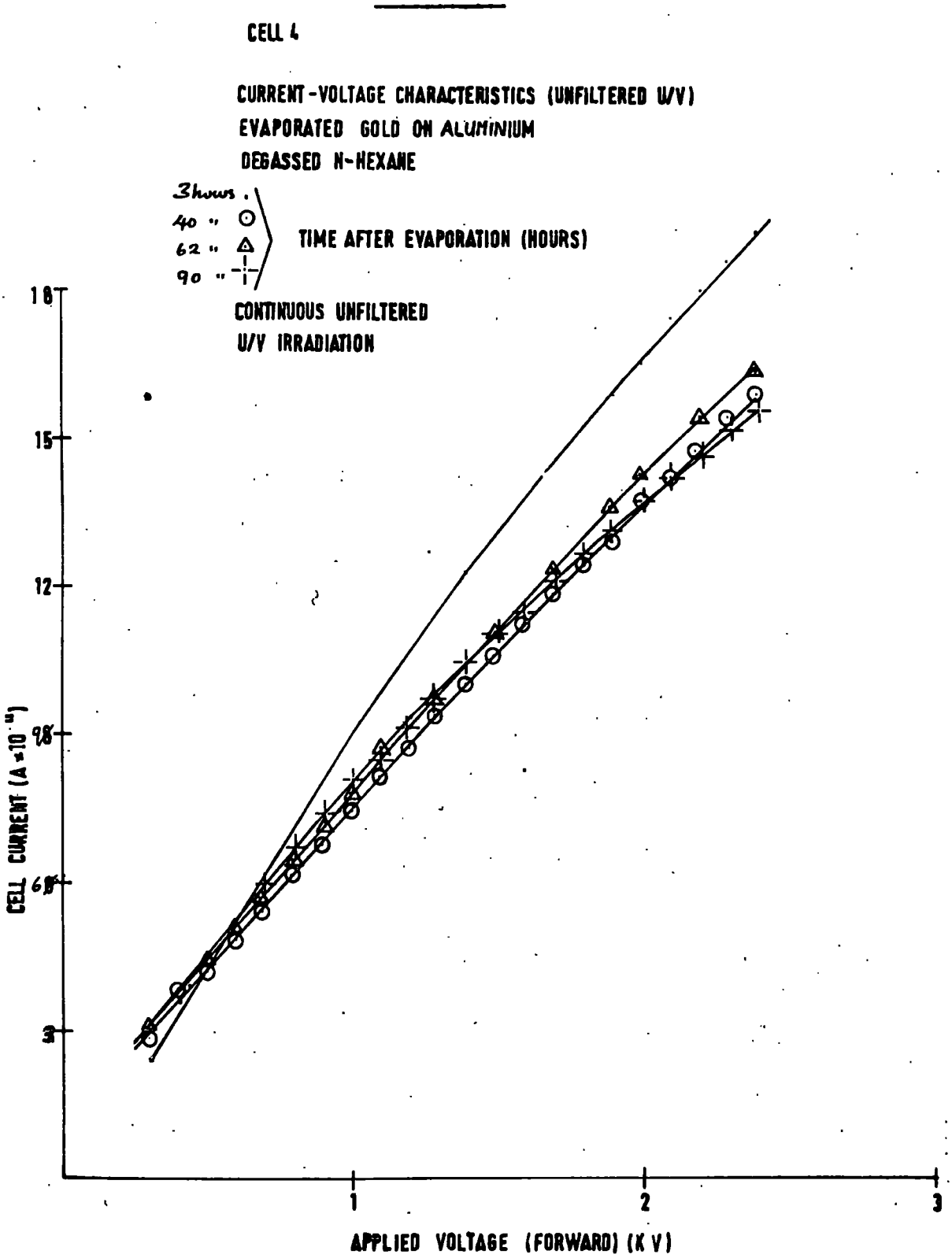
CELL 4
CURRENT-VOLTAGE CHARACTERISTICS (UNFILTERED U/V)
EVAPORATED GOLD ON ALUMINIUM
DEGASSED N-HEXANE
3hours.
40 "
62 "
90 "
TIME AFTER EVAPORATION (HOURS)
CONTINUOUS UNFILTERED
U/V IRRADIATION
CELL CURRENT (A×10⁻¹¹)
APPLIED VOLTAGE (FORWARD) (K V)

Fig. 6.26

CELL 4
CURRENT-VOLTAGE CHARACTERISTICS, UNFILTERED U/V
EVAPORATED GOLD ON ALUMINIUM
DEGASSED N-HEXANE
• 3 HOURS
× 5 "
⊙ 40 "
△ 62 "
-|- 90 "
} TIME AFTER EVAPORATION
CONTINUOUS UNFILTERED U/V IRRADIATION

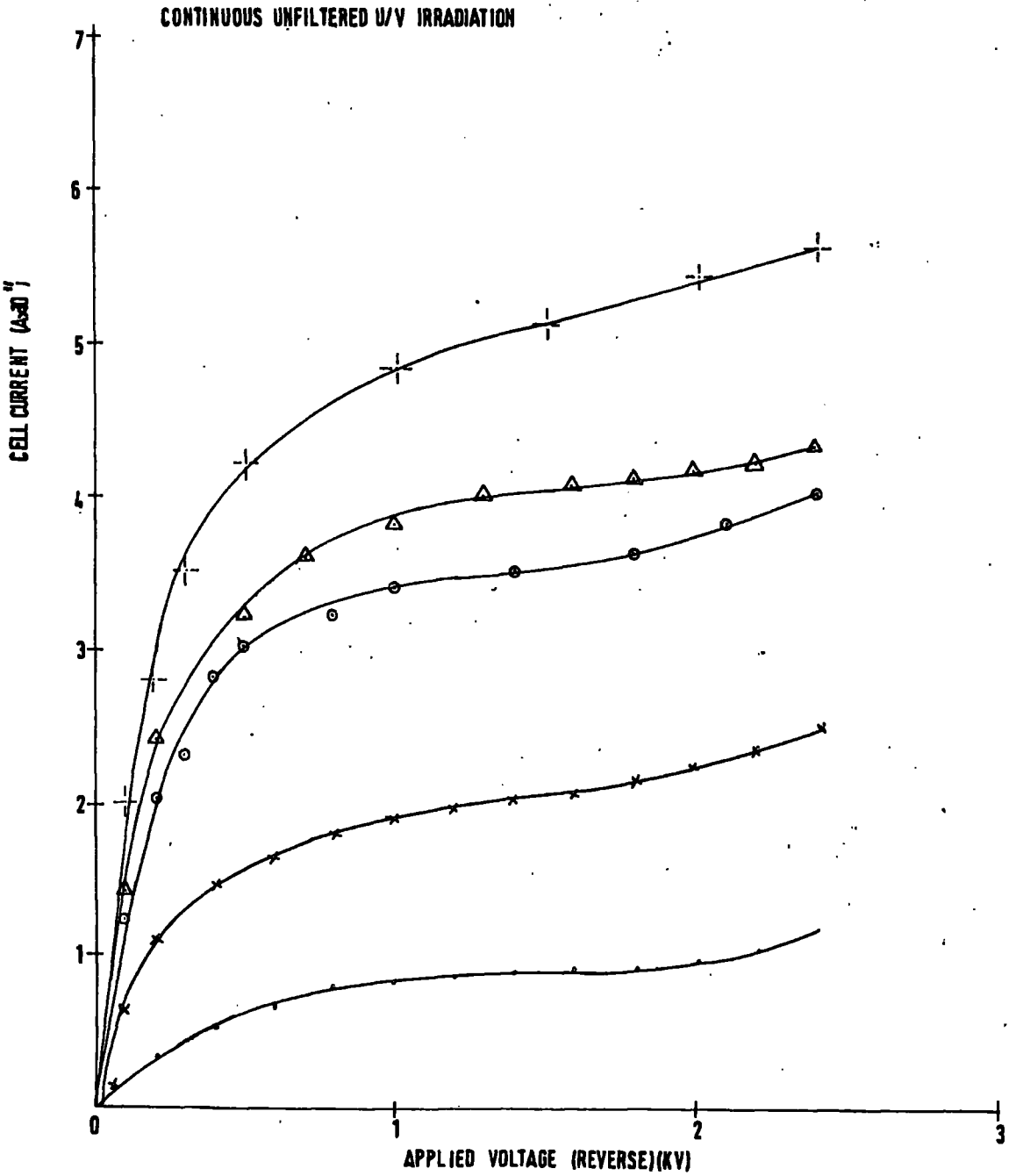

to unfiltered irradiation was similar to that discussed previously (Sec. 6.11).

The vacuum photocurrent (in the forward direction) using OX1 or OX7 filters was very small ($\sim 10^{-11}$A.) but for unfiltered radiation was 1.8×10^{-8}A., the forward/reverse ratio being about 27:1. It must be pointed out, however, that the evaporated layer was nearly a week old and had been subjected to prolonged unfiltered irradiation, this ratio might have been different for a fresh surface of gold.

6.12. Photocurrents with evaporated aluminium electrodes (iv). Cell 4).

Further measurements were made using cell 4, with evaporated aluminium electrodes and H.D.P. n-hexane. The applied voltage was increased to a maximum of 3KV., the currents being stimulated mostly in conjunction with the OX7 filter. (Short pulses of unfiltered radiation were used, to obtain some 'spot' measurements, but the total period of exposure was kept to a minimum.)

With the maximum forward voltage, photocurrents exceeding 2×10^{-10}A. (OX7) and 7×10^{-10}A. (no filter) were observed within the first 20 minutes from the evaporation. A 'family' of $\frac{I}{V}$ curves were obtained for times up to 12 hours after the evaporation (see Fig. 6.27). The forward/reverse ratio remained within 10% of 20:1 at 3KV. applied voltage for this period of time. The decay of photo-injection is shown in Fig. 6.28 under the heading '1st evaporation'.

Fig. 6.27

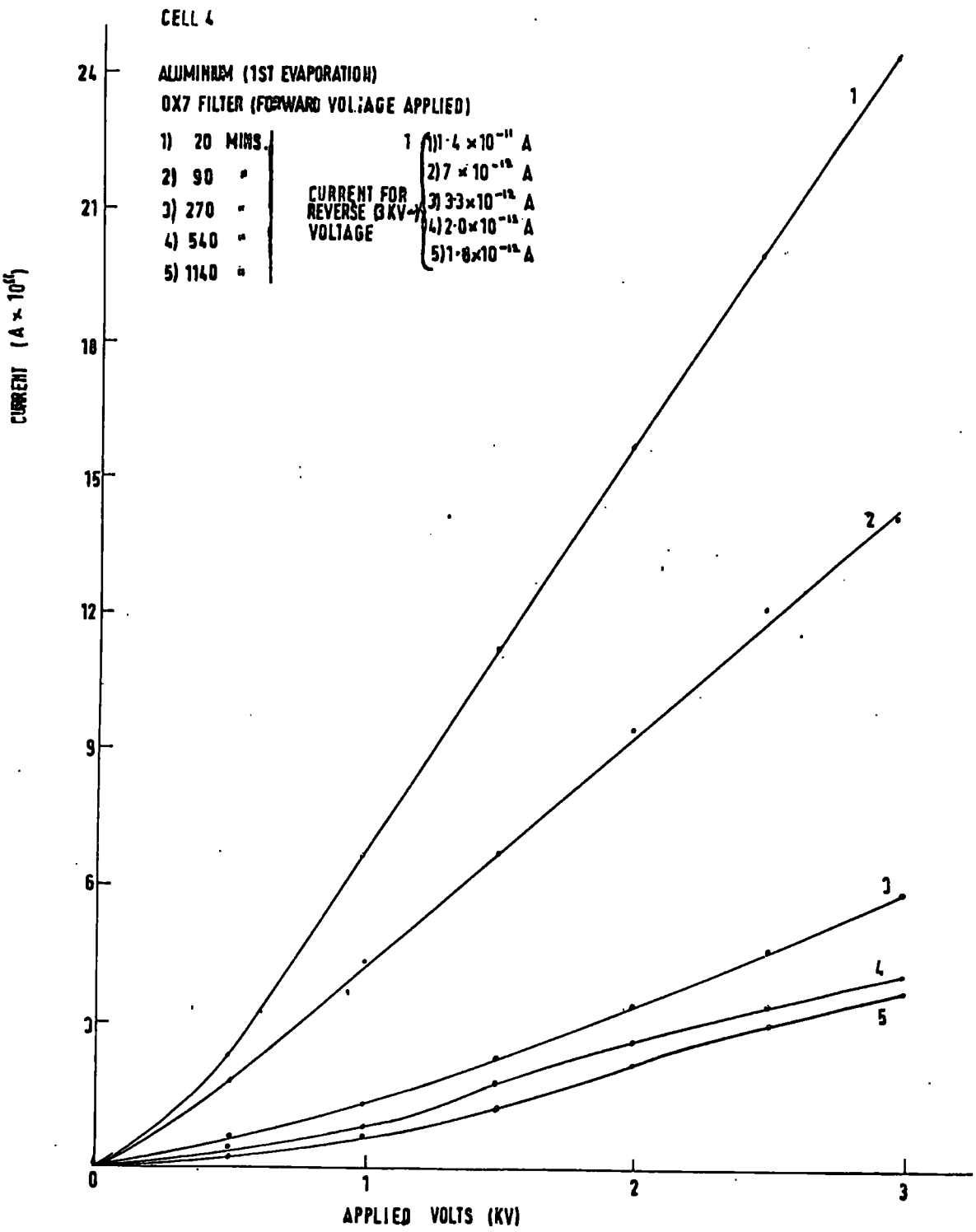
CELL 4
ALUMINIUM (1ST EVAPORATION)
0X7 FILTER (FORWARD VOLTAGE APPLIED)
1) 20 MINS.
2) 90 "
3) 270 "
4) 540 "
5) 1140 "
CURRENT FOR REVERSE (3 KV) VOLTAGE
1
1) 1·4 × 10⁻¹¹ A
2) 7 × 10⁻¹² A
3) 3·3 × 10⁻¹² A
4) 2·0 × 10⁻¹² A
5) 1·8 × 10⁻¹² A
CURRENT (A × 10¹²)
APPLIED VOLTS (KV)
0
1
2
3
6
9
12
15
18
21
24

Fig. 6.28

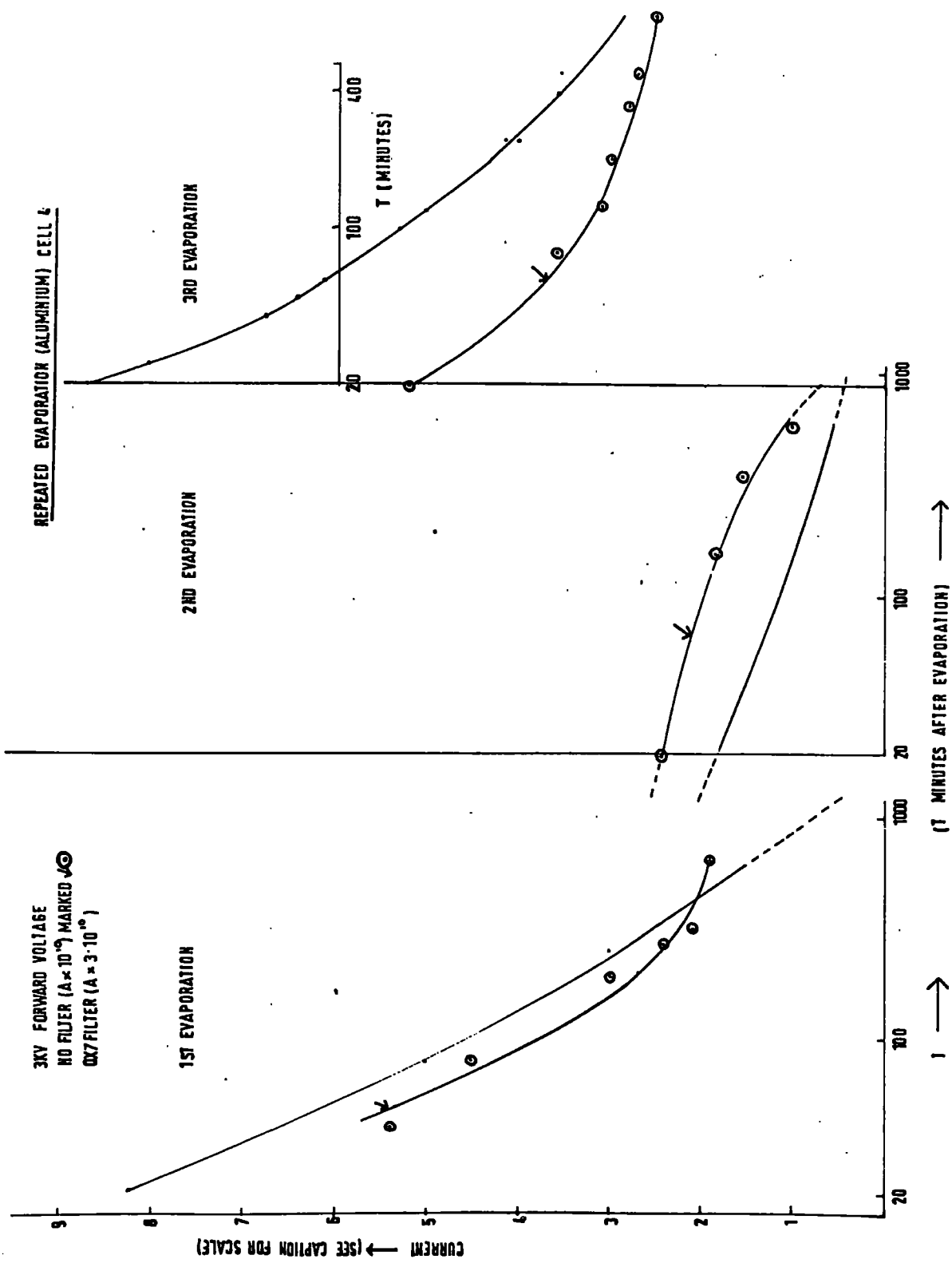
REPEATED EVAPORATION (ALUMINIUM) CELL 4
3KV FORWARD VOLTAGE
NO FILTER (A × 10⁻⁹) MARKED ⊙
QX7 FILTER (A = 3·10⁻¹⁰)
1ST EVAPORATION
2ND EVAPORATION
3RD EVAPORATION
T (MINUTES)
CURRENT ⟵ (SEE CAPTION FOR SCALE)
t ⟵ (T MINUTES AFTER EVAPORATION) ⟵

Table 6(i) lists the photocurrents obtained with different filters, at a forward voltage of 3KV. These measurements were made 24 hours after the evaporation. The second column shows the corresponding 'saturated' photoemission in vacuo (40V. applied).

TABLE 6(i)

Photocurrent in liquid (Amps at 3KV.+)		Vacuum Photoemission (Amps at 40V.+)
No filter	2.3×10^{-11}	7.0×10^{-8}
OX7	2.4×10^{-12}	9.0×10^{-9}
OX1	5.6×10^{-13}	3.4×10^{-10}
OX9A	5.1×10^{-13}	2.0×10^{-10}
OX1A	4.4×10^{-13}	1.6×10^{-10}
OB10	2×10^{-14}	5.4×10^{-12}

There were photocurrents in vacuo for the following filters, but they were too small to be accurately determined in the liquid ($< 10^{-14}$A.).

ON33	2.4×10^{-13}
OB 2	2.4×10^{-14}

Cell 4 was equipped with two separate tungsten filaments each with a charge of aluminium. This made it possible to evaporate more than one layer of aluminium on to the electrodes (in the vacuum obtained by freezing the hexane into the cell reservoir at liquid nitrogen temperature) and to continue measurements with the same sample of liquid.

Fig. 6.29

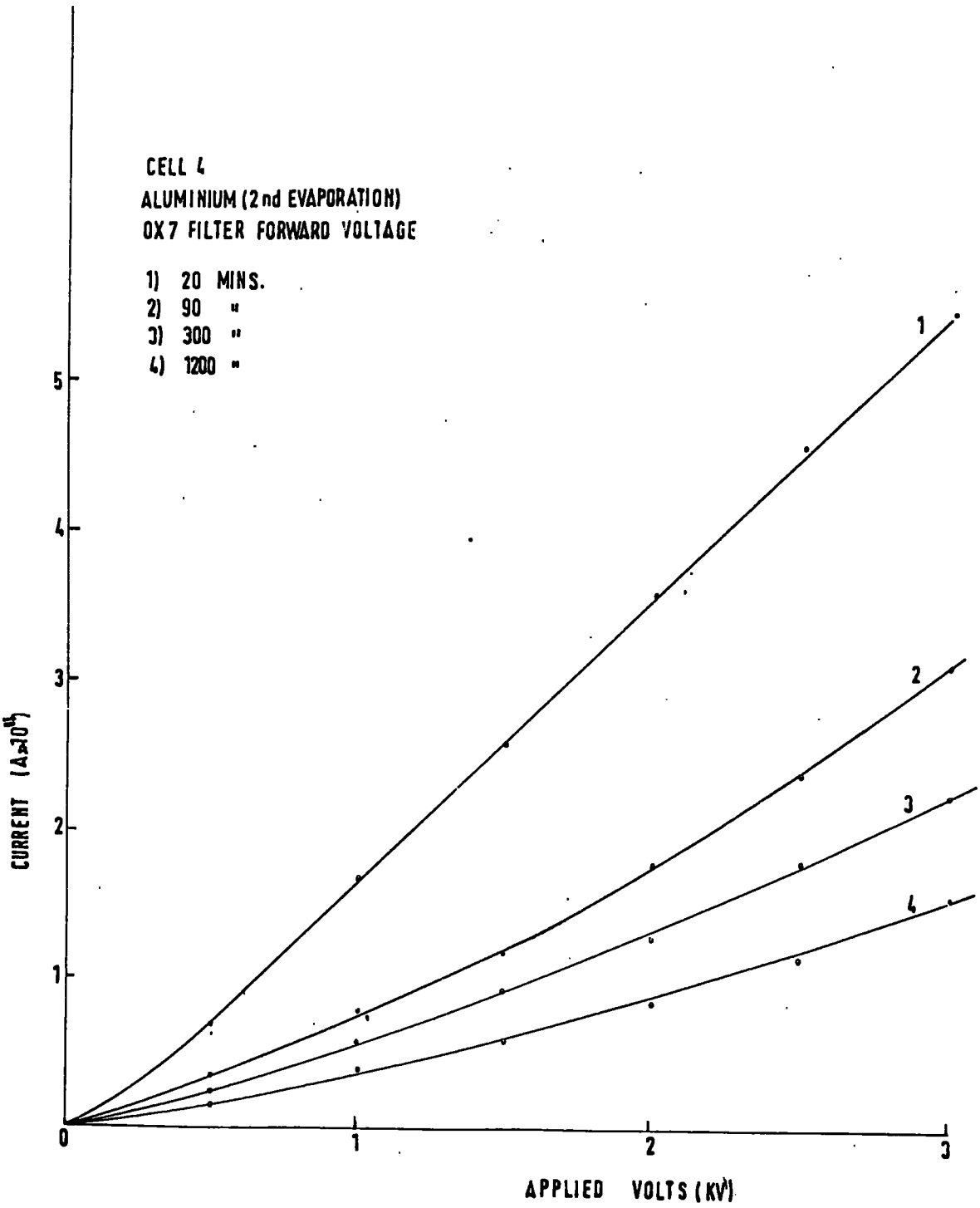
CELL 4
ALUMINIUM (2nd EVAPORATION)
OX7 FILTER FORWARD VOLTAGE
1) 20 MINS.
2) 90 "
3) 300 "
4) 1200 "
CURRENT (A×10⁻⁶)
APPLIED VOLTS (KV)
0
1
2
3
4
5

Fig. 6.30

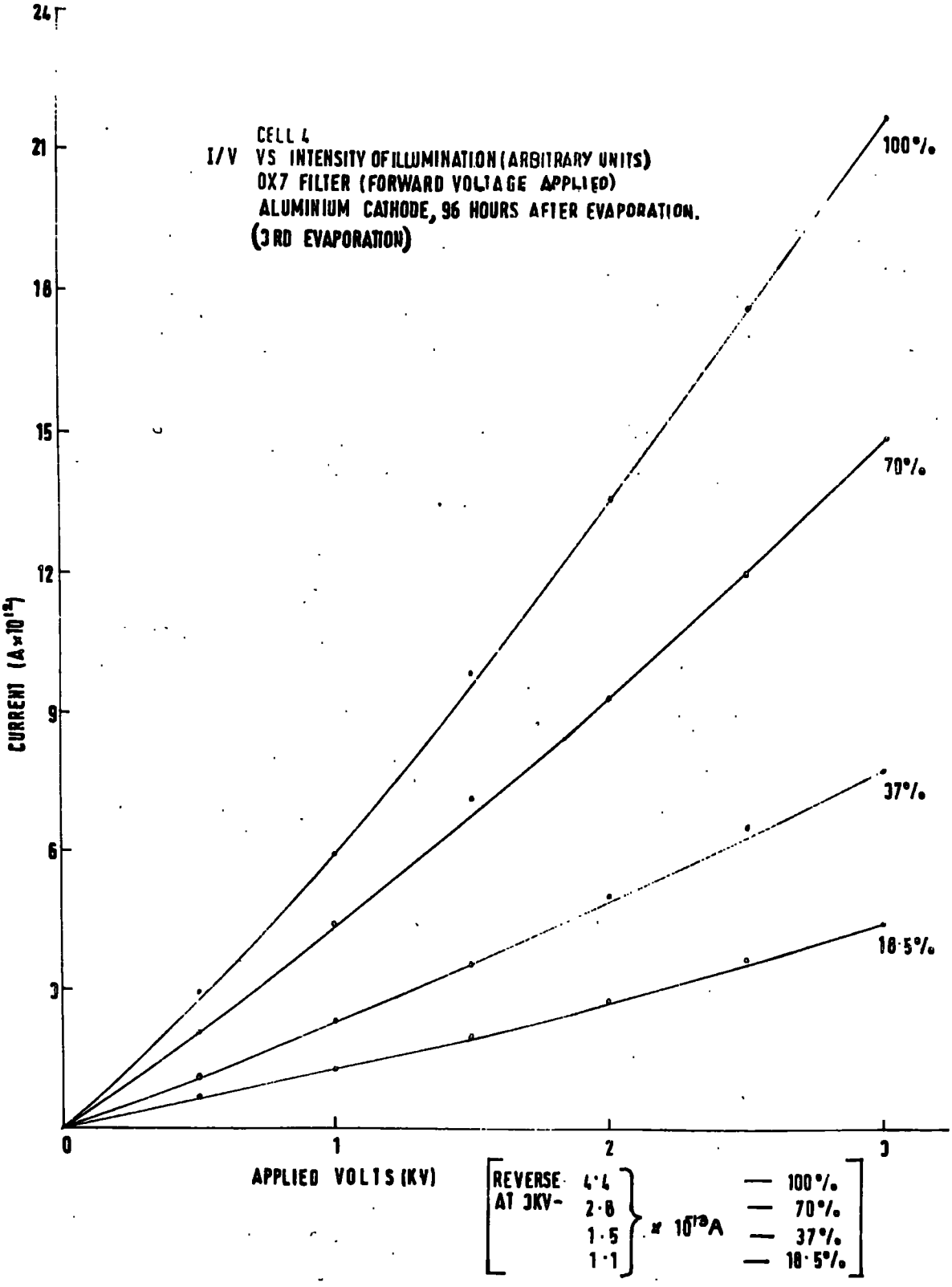
CELL 4
I/V VS INTENSITY OF ILLUMINATION (ARBITRARY UNITS)
0X7 FILTER (FORWARD VOLTAGE APPLIED)
ALUMINIUM CATHODE, 96 HOURS AFTER EVAPORATION.
(3RD EVAPORATION)
100%
70%
37%
18·5%
CURRENT (A×10¹²)
24
21
18
15
12
9
6
3
0
1
2
3
APPLIED VOLTS (KV)
REVERSE AT 3KV-
4·4
2·8
1·5
1·1
× 10¹²A
— 100%
— 70%
— 37%
— 18·5%

Fig. 6.31

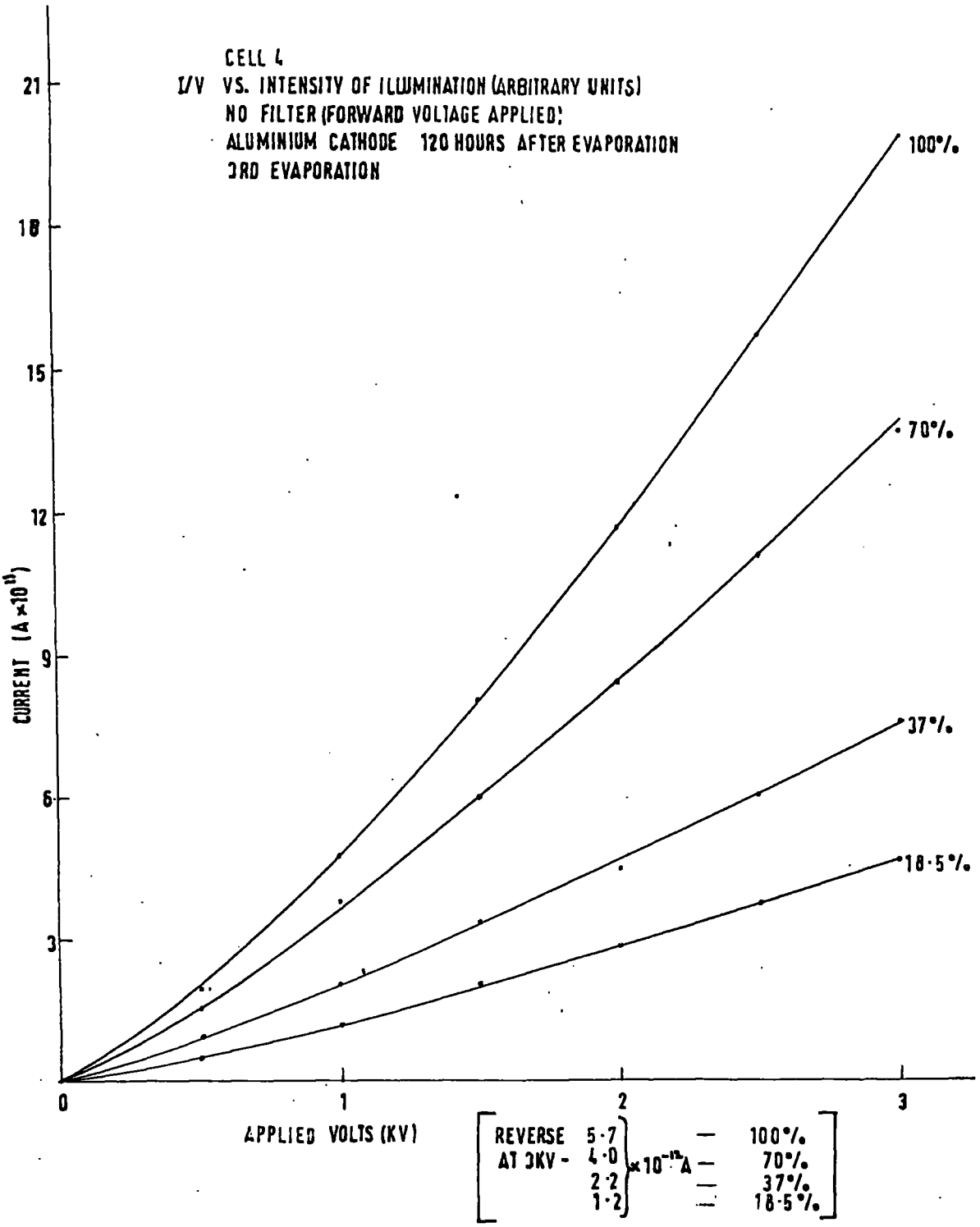
CELL 4
I/V VS. INTENSITY OF ILLUMINATION (ARBITRARY UNITS)
NO FILTER (FORWARD VOLTAGE APPLIED)
ALUMINIUM CATHODE 120 HOURS AFTER EVAPORATION
3RD EVAPORATION
100%
70%
37%
18·5%
CURRENT (A ×10⁻¹²)
21
18
15
12
9
6
3
0
1
2
3
APPLIED VOLTS (KV)
REVERSE AT 3KV - 5·7 4·0 2·2 1·2 ×10⁻¹²A — 100% — 70% — 37% — 18·5%

The second evaporation utilised the small quantity of aluminium remaining on the filament which had already been used. The subsequent measurements indicated only a partial recovery of electrode activity (see Figs. 6.28 and 6.29).

A third evaporation (from the second filament) was more effective; the photocurrents showing a substantial recovery (see Fig. 6.28). This diagram also shows a more detailed plot of the decay of electrode activity with time.

The photoinjected currents were remarkably free from fluctuations, and so it was decided to experiment with different intensities of radiation. (The intensity of radiation was altered by the adjustment of an iris diaphragm in the lens system. Apertures were calibrated, rather crudely, by recording the corresponding vacuum photoemission.) A set of $\frac{I}{V}$ curves were obtained, with OX7-filtered irradiation of the cathode, approximately 90 hours after the (3rd) evaporation (Fig. 6.30). Some similar curves were obtained, with unfiltered irradiation, after 120 hours (Fig. 6.31).

A fourth evaporation (from the second filament) was made with the object of measuring the vacuum photoemission from a fresh surface. The currents obtained with different filters, 45 minutes after the evaporation, are given in Table 6(ii). The corresponding photo-injection into the liquid was measured about 35 minutes later. (These currents could not be measured sooner because the hexane had to be thawed and distilled back into the electrode compartment without disturbing the cell or the lamp). It was noticed that in the

liquid the forward/reverse ratio of the photocurrents was lower for unfiltered radiation (10:1) than when using the OX1 or OX7 filters (~ 30:1). The corresponding ratio in vacuo was, unfortunately, not measured.

Finally, air was let into the cell. The photocurrents rapidly decayed, and an 'overshoot' was observed with interrupted radiation (cf. Section 6.15). This overshoot was not evident at any stage of the experiments with the highly degassed liquid.

TABLE 6(ii)

	Photocurrent in liquid (Amps at 3KV.+)	Vacuum photoemission (Amps at 40V.+)
No filter	3.6×10^{-10}	1.3×10^{-7}
OX7	3.8×10^{-11}	1.1×10^{-8}
OX1	1.2×10^{-11}	7.5×10^{-9}
OX9A	- (not det)	6.0×10^{-11}
OX1A	- (not det)	4.3×10^{-11}

6.13 Photocurrents with evaporated magnesium electrodes (ii). (Cell 4)

The technique of multiple evaporations was used, with magnesium, to obtain some information regarding the changes in the photoelectric threshold (in vacuo, and in the liquid) as the surfaces aged. In addition, it was desired to find the relationship between the photocurrents and the intensity of irradiation (with a view to obtaining space-charge-limited conditions).

Magnesium was evaporated on to both electrodes in cell 4, measurements being made with H.D.P. n-hexane.

The $\frac{I}{V}$ curves, corresponding to (OX7)-filtered irradiation of

Fig. 6.32

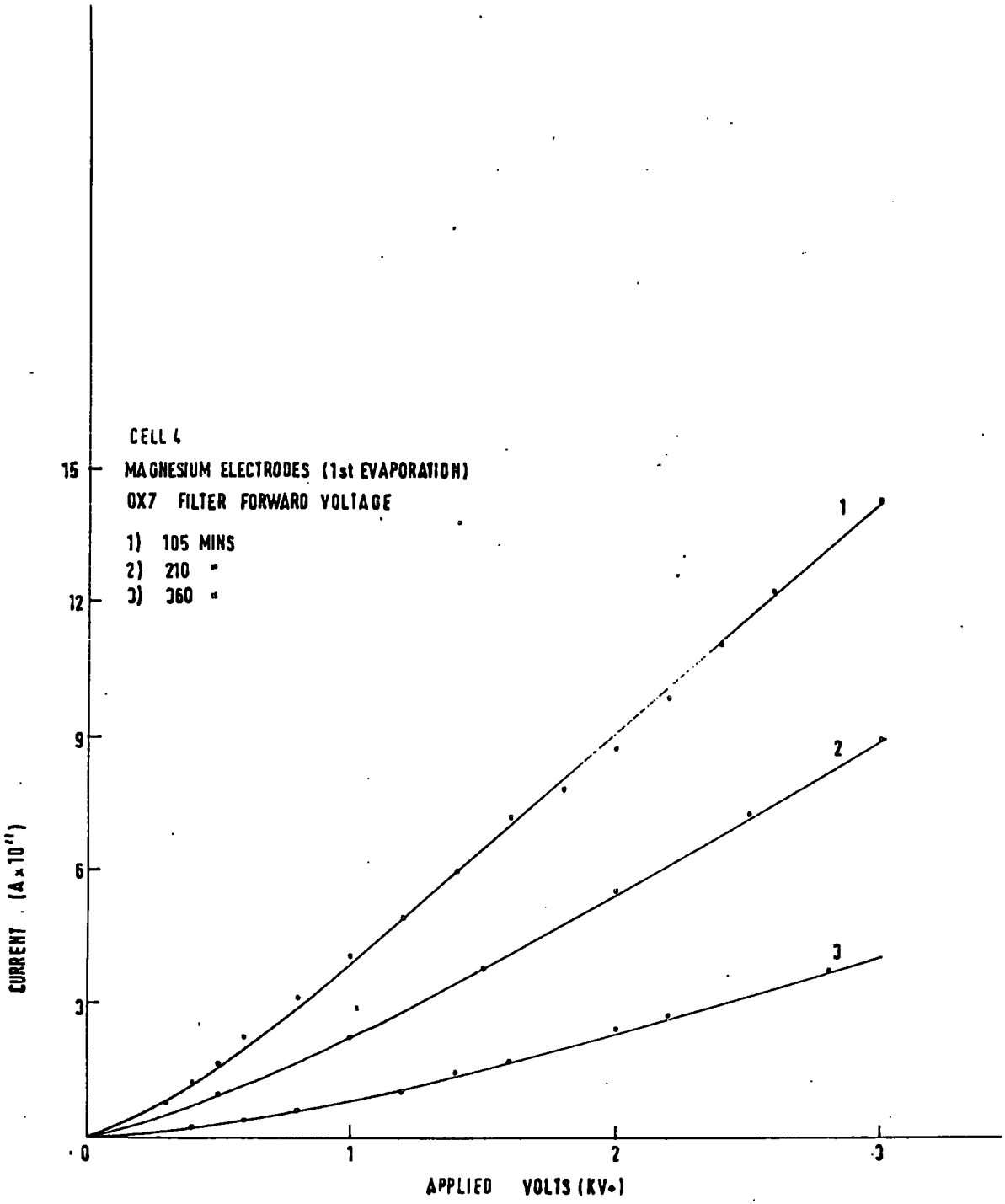
CELL 4
MAGNESIUM ELECTRODES (1st EVAPORATION)
0X7 FILTER FORWARD VOLTAGE
1) 105 MINS
2) 210 "
3) 360 "
15
12
9
6
3
0
1
2
3
1
2
3
CURRENT (A x 10⁻¹¹)
APPLIED VOLTS (KV.)

Fig. 6.33

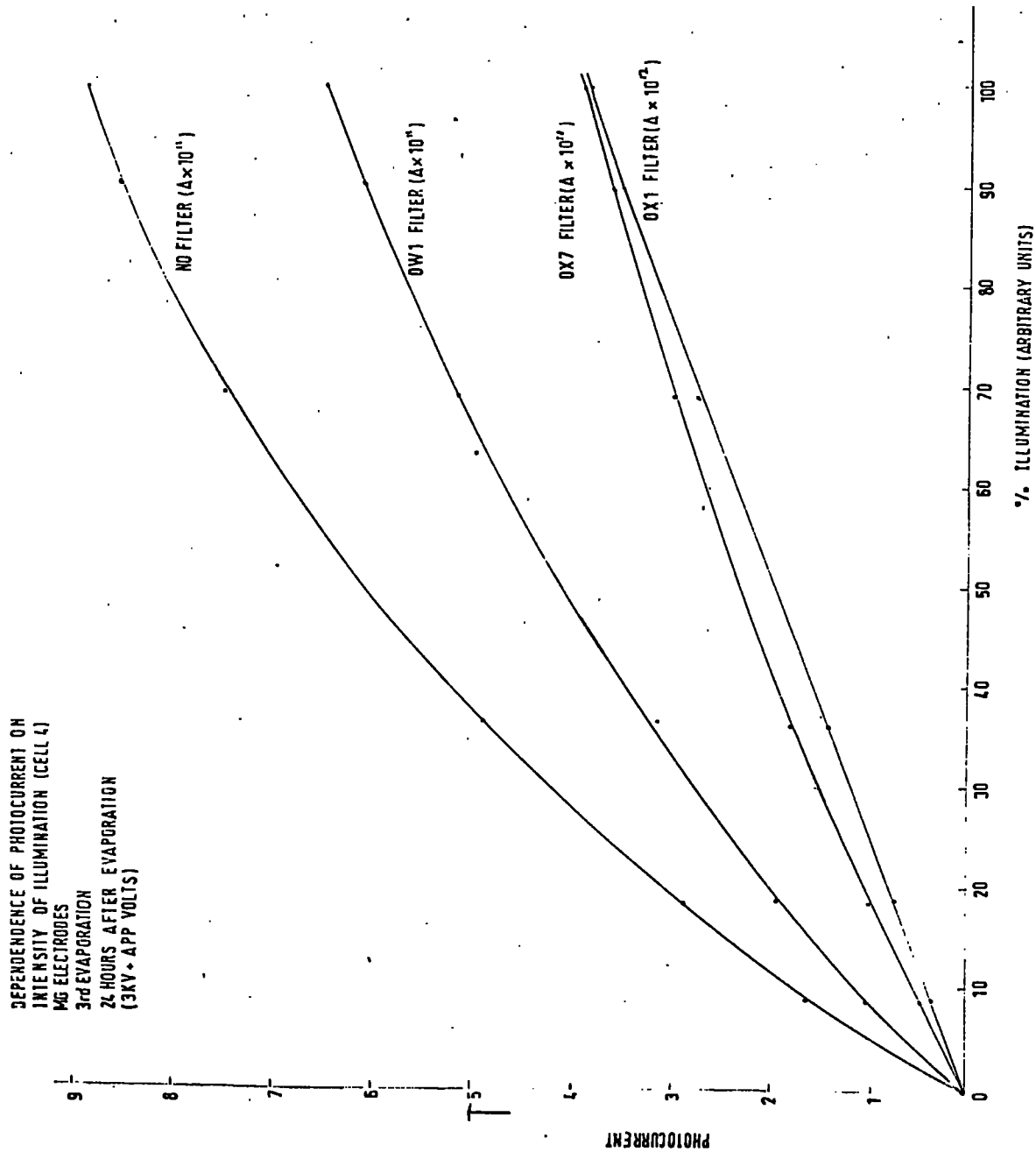
DEPENDENCE OF PHOTOCURRENT ON
INTENSITY OF ILLUMINATION (CELL 4)
MG ELECTRODES
3rd EVAPORATION
24 HOURS AFTER EVAPORATION
(3KV • APP VOLTS)
NO FILTER (A×10⁻¹¹)
0W1 FILTER (A×10⁻¹¹)
0X7 FILTER(A ×10⁻¹¹)
0X1 FILTER(A ×10⁻¹¹)
PHOTOCURRENT
% ILLUMINATION (ARBITRARY UNITS)

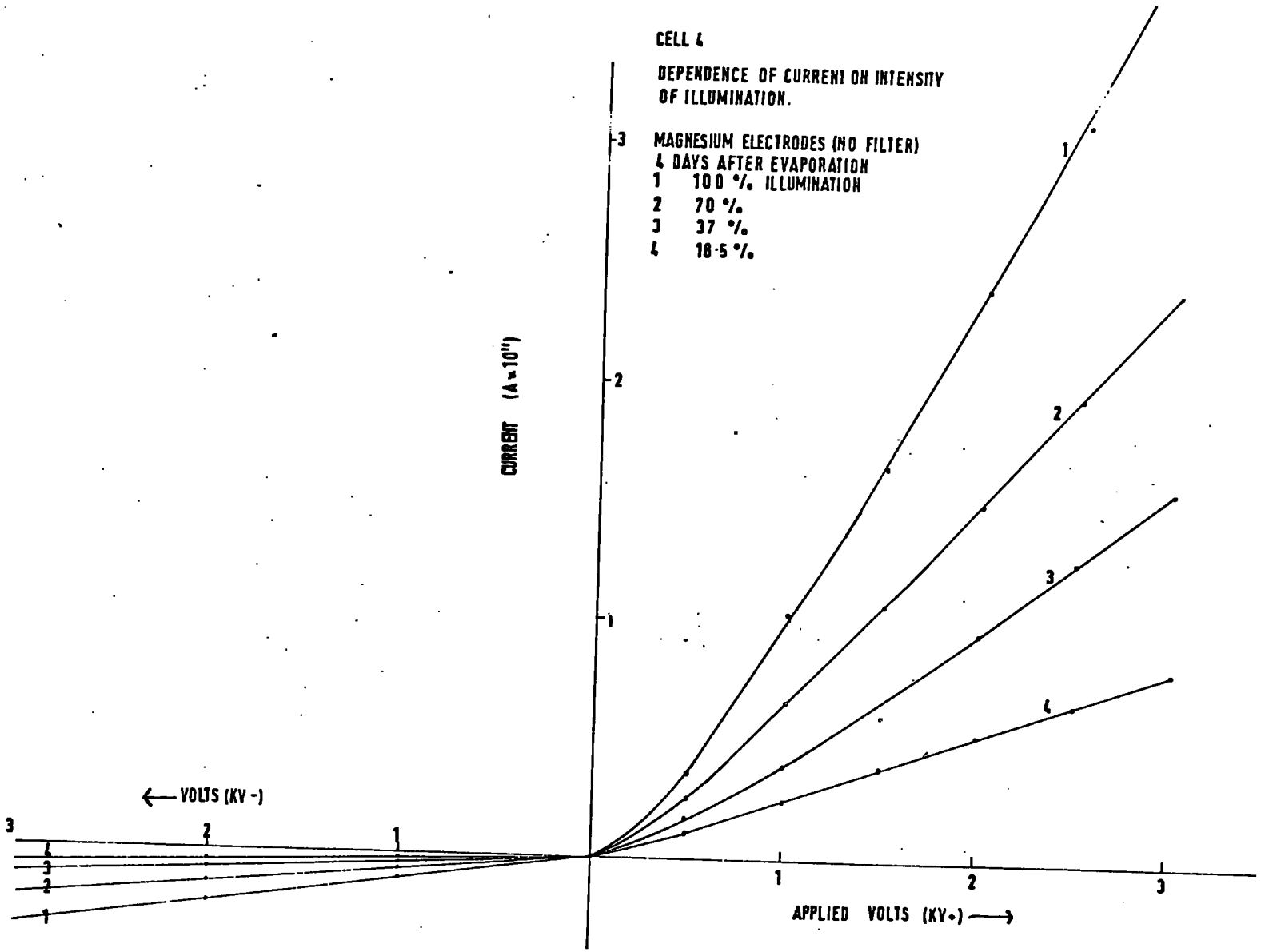
CELL 4
DEPENDENCE OF CURRENT ON INTENSITY OF ILLUMINATION.
MAGNESIUM ELECTRODES (NO FILTER)
4 DAYS AFTER EVAPORATION
1 100 % ILLUMINATION
2 70 %
3 37 %
4 18·5 %
CURRENT (A×10¹¹)
APPLIED VOLTS (KV+)
VOLTS (KV -)

Fig. 6.34

TABLE 6(iii)

FILTER	(i) 2 hours		(ii) 24 hours		(iii) 48 hours		(iv) 72 hours	
	I_{LIQ}	I_{VAC}	I_{LIQ}	I_{VAC}	I_{LIQ}	I_{VAC}	I_{LIQ}	I_{VAC}
NONE	3×10^{-10}	$1{\cdot}9 \times 10^{-7}$	$1{\cdot}5 \times 10^{-10}$	$7{\cdot}4 \times 10^{-8}$	$1{\cdot}1 \times 10^{-10}$	$4{\cdot}8 \times 10^{-8}$	$1{\cdot}0 \times 10^{-10}$	$4{\cdot}8 \times 10^{-8}$
OWI	$1{\cdot}7 \times 10^{-10}$	$8{\cdot}2 \times 10^{-8}$	$7{\cdot}5 \times 10^{-11}$	$3{\cdot}3 \times 10^{-8}$	$5{\cdot}2 \times 10^{-11}$	$2{\cdot}1 \times 10^{-8}$	$5{\cdot}0 \times 10^{-11}$	$2{\cdot}1 \times 10^{-8}$
OX7	$1{\cdot}6 \times 10^{-10}$	$7{\cdot}2 \times 10^{-8}$	$6{\cdot}4 \times 10^{-11}$	$2{\cdot}5 \times 10^{-8}$	$4{\cdot}3 \times 10^{-11}$	$1{\cdot}8 \times 10^{-8}$	$4{\cdot}2 \times 10^{-11}$	$1{\cdot}8 \times 10^{-8}$
OX1	$2{\cdot}9 \times 10^{-11}$	$3{\cdot}8 \times 10^{-9}$	$1{\cdot}2 \times 10^{-11}$	$2{\cdot}4 \times 10^{-9}$	$6{\cdot}0 \times 10^{-12}$	$1{\cdot}6 \times 10^{-9}$	$6{\cdot}0 \times 10^{-12}$	$1{\cdot}6 \times 10^{-9}$
OX9A	$2{\cdot}5 \times 10^{-11}$	$3{\cdot}2 \times 10^{-9}$	$1{\cdot}1 \times 10^{-11}$	$2{\cdot}2 \times 10^{-9}$	$4{\cdot}5 \times 10^{-12}$	$7{\cdot}4 \times 10^{-10}$	$4{\cdot}4 \times 10^{-12}$	$8{\cdot}4 \times 10^{-10}$
OX1A	$2{\cdot}0 \times 10^{-11}$	$2{\cdot}3 \times 10^{-9}$	$7{\cdot}7 \times 10^{-12}$	$1{\cdot}5 \times 10^{-9}$	$4{\cdot}1 \times 10^{-12}$	$7{\cdot}2 \times 10^{-10}$	$4{\cdot}0 \times 10^{-12}$	$7{\cdot}8 \times 10^{-10}$
OB8	$8{\cdot}3 \times 10^{-12}$	$5{\cdot}3 \times 10^{-10}$	$3{\cdot}6 \times 10^{-12}$	$2{\cdot}0 \times 10^{-10}$	$1{\cdot}6 \times 10^{-12}$	$1{\cdot}3 \times 10^{-10}$	$1{\cdot}3 \times 10^{-12}$	$1{\cdot}2 \times 10^{-10}$
OB10	$3{\cdot}4 \times 10^{-12}$	$2{\cdot}1 \times 10^{-10}$	$1{\cdot}4 \times 10^{-12}$	$8{\cdot}5 \times 10^{-11}$	$5{\cdot}8 \times 10^{-13}$	$4{\cdot}4 \times 10^{-11}$	$5{\cdot}5 \times 10^{-13}$	$4{\cdot}8 \times 10^{-11}$
OV1	$3{\cdot}2 \times 10^{-12}$	$2{\cdot}3 \times 10^{-10}$	$1{\cdot}3 \times 10^{-12}$	$8{\cdot}4 \times 10^{-11}$	$6{\cdot}2 \times 10^{-13}$	$3{\cdot}4 \times 10^{-11}$	$5{\cdot}4 \times 10^{-13}$	$3{\cdot}8 \times 10^{-11}$
OB2	$9{\cdot}5 \times 10^{-13}$	$7{\cdot}9 \times 10^{-11}$	$4{\cdot}4 \times 10^{-13}$	$2{\cdot}5 \times 10^{-11}$	$2{\cdot}0 \times 10^{-13}$	$1{\cdot}3 \times 10^{-11}$	$1{\cdot}7 \times 10^{-13}$	$8{\cdot}8 \times 10^{-12}$
ON16	$6{\cdot}5 \times 10^{-13}$	$4{\cdot}5 \times 10^{-11}$	$3{\cdot}0 \times 10^{-13}$	$1{\cdot}9 \times 10^{-11}$	$1{\cdot}5 \times 10^{-13}$	$6{\cdot}0 \times 10^{-12}$	$1{\cdot}4 \times 10^{-13}$	$7{\cdot}6 \times 10^{-12}$
ON11A	$5{\cdot}2 \times 10^{-13}$	$4{\cdot}5 \times 10^{-11}$	$2{\cdot}5 \times 10^{-13}$	$1{\cdot}3 \times 10^{-11}$	$1{\cdot}1 \times 10^{-13}$	$6{\cdot}6 \times 10^{-12}$	$9{\cdot}2 \times 10^{-14}$	$6{\cdot}4 \times 10^{-12}$

the cathode, are shown in Fig. 6.32. The currents were easily measured, with complete freedom from fluctuations. They were also rapidly decaying, and it was obvious that S.C.L. currents were not being obtained. It was decided to complete a second evaporation and to take some 'spot' measurements (with different filters) of the liquid and vacuum photocurrents. The electrode activity was fully restored by the deposition of a fresh layer, as is seen from the first column in Table 6(iii). The corresponding vacuum photo-emission is recorded in the second column of Table 6(iii). These measurements were repeated after the surfaces had been immersed in the hexane for 24 hours, 48 hours and 72 hours.

After a third evaporation, the variation of the photocurrents on the relative intensity of radiation (corresponding to three different filters) was measured (see Fig. 6.33). Some $\frac{I}{V}$ curves for different intensities of unfiltered radiation were obtained nearly a week after the third evaporation (Fig. 6.34).

It was noted that the currents for the same voltage, were higher in previous measurements (Sec. 6.9)than are recorded here. This may have been due to differences in the polish of the electrode surfaces before evaporation, since (i) a further evaporation restored the activity of the cathode to almost exactly the level just after the previous evaporation. (ii) The reflectivity of the latter films was considerably lower than in 6.9.

It is seen (from Table 6(iii) that the photocurrents in the liquid decayed in step with the vacuum photoemission. However, the ratio between the photoinjected current and the vacuum photoemission depended on the filter used with the lamp, as well as the time elapsed after the evaporation.

6.14. Photocurrents with only one electrode coated with an evaporated layer of aluminium. (Cell 4).

When both electrodes were coated with a similar evaporated metal layer there was always some 'reverse' photoinjection. Thus, the reverse photocurrents amounted to 5-10% of those for a similar forward voltage. In the absence of 'bulk' photostimulation, these currents were accounted for by reflections in the cell (since a similar forward/reverse ratio was generally found for the photoemission in vacuo). Consequently, the ratio ought to be greatly increased if one electrode was non-injecting, e.g. if an ordinary polished surface was used. The latter arrangement should show conclusively that only negative charges are injected, as well as accentuating any relationships between the vacuum photoemission and the photoinjection process. It remained to be seen, however, if this sort of anode would be as effective as an evaporated metal layer in discharging the carriers.

Cell 4 was modified, for this experiment, by inserting a screen with a single aperture. Thus, only one electrode was coated (by the evaporation of aluminium), the other electrode (polished, but heavily oxidised aluminium) retaining its 'inactive' surface. Two similar

Fig. 6.35

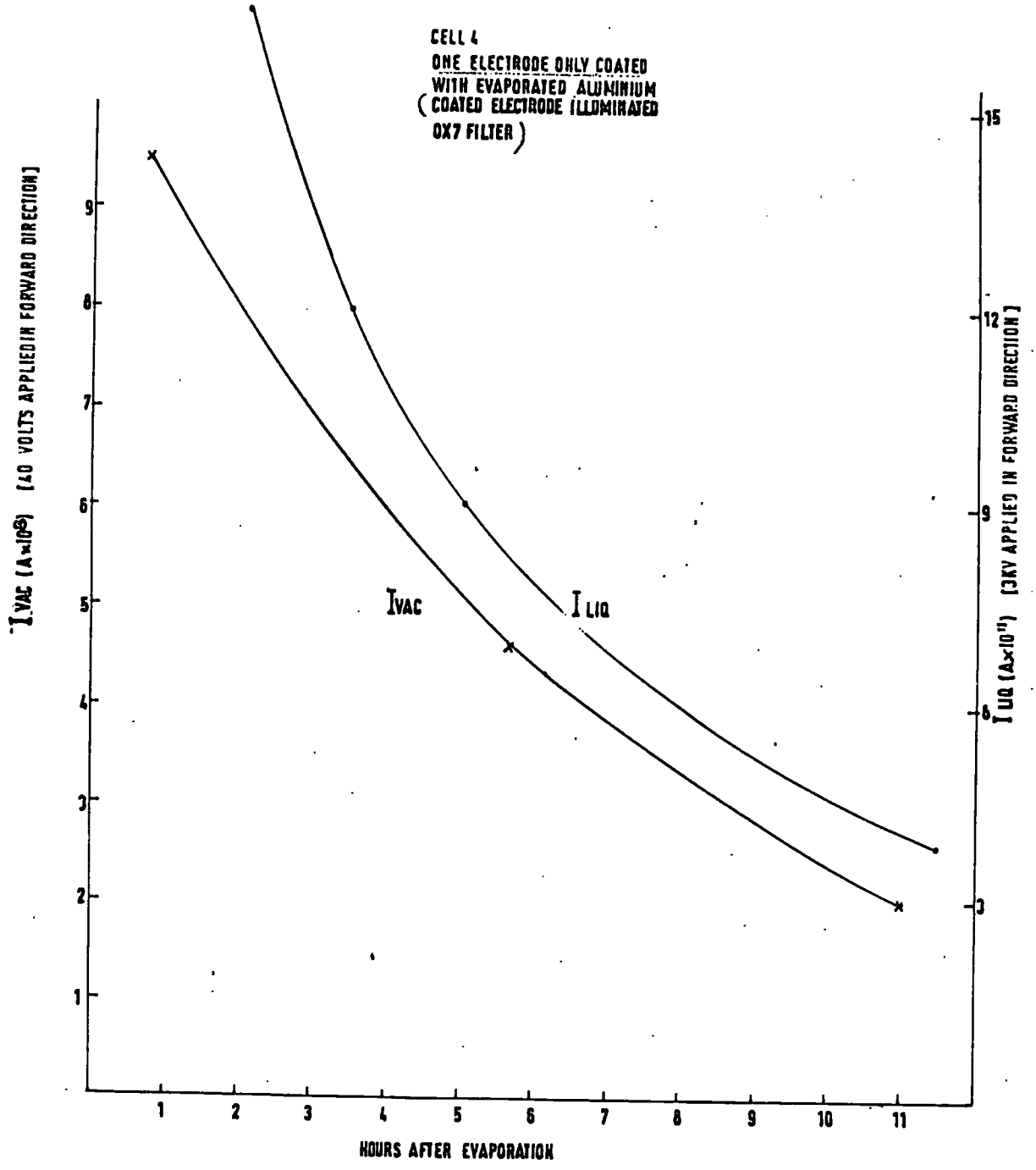
CELL 4
ONE ELECTRODE ONLY COATED
WITH EVAPORATED ALUMINIUM
(COATED ELECTRODE ILLUMINATED
0X7 FILTER)
I VAC (A×10⁹) (40 VOLTS APPLIED IN FORWARD DIRECTION)
I LIQ (A×10¹¹) (3KV APPLIED IN FORWARD DIRECTION)
IVAC
I LIQ
HOURS AFTER EVAPORATION
1
2
3
4
5
6
7
8
9
10
11
3
6
9
12
15

Fig. 6.36

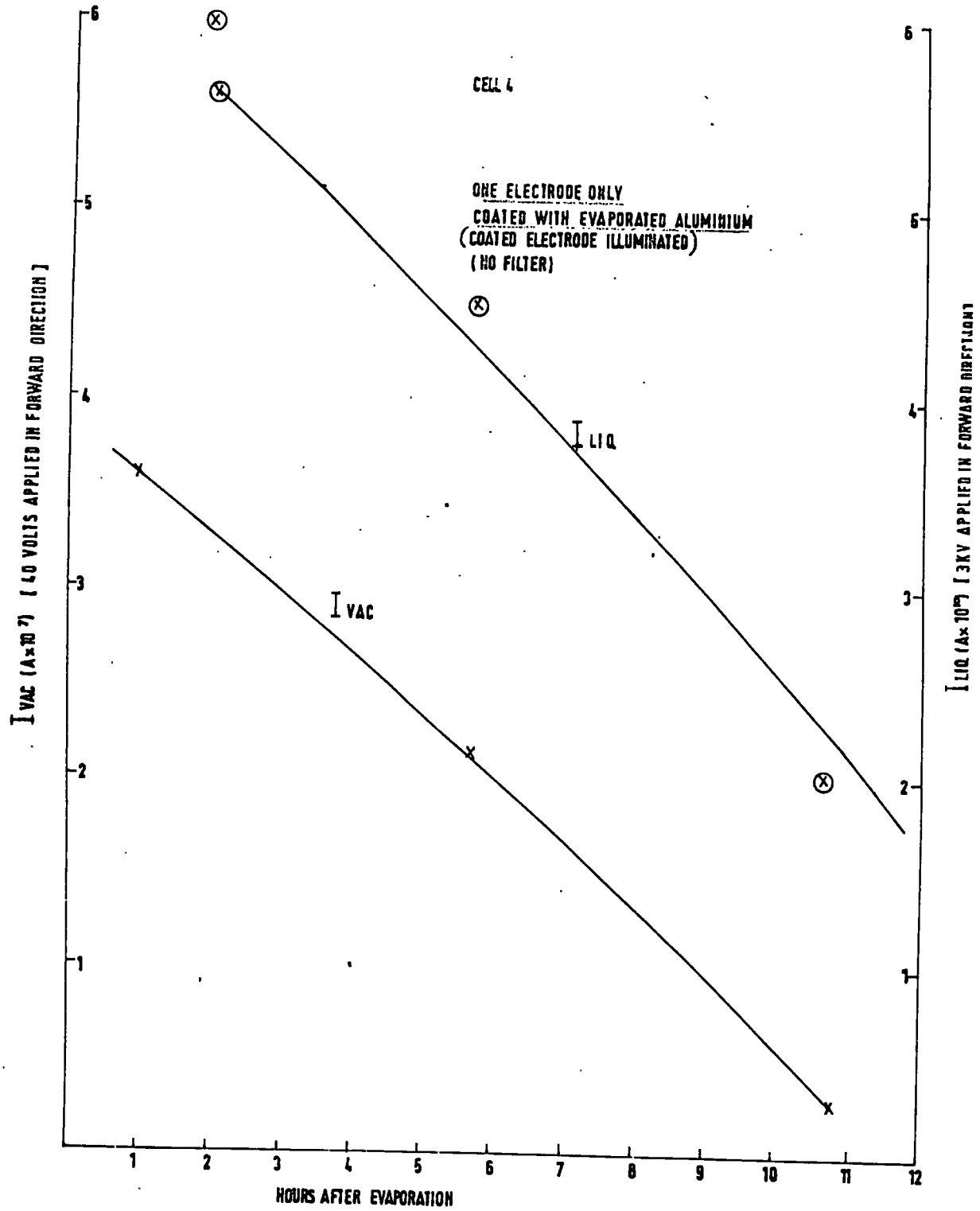
CELL 4
ONE ELECTRODE ONLY
COATED WITH EVAPORATED ALUMINIUM
(COATED ELECTRODE ILLUMINATED)
(NO FILTER)
I LIQ
I VAC
I VAC (A×10⁻⁷) (40 VOLTS APPLIED IN FORWARD DIRECTION)
I LIQ (A×10⁻⁹) (3KV APPLIED IN FORWARD DIRECTION)
HOURS AFTER EVAPORATION
1
2
3
4
5
6
7
8
9
10
11
12

Fig. 6.37

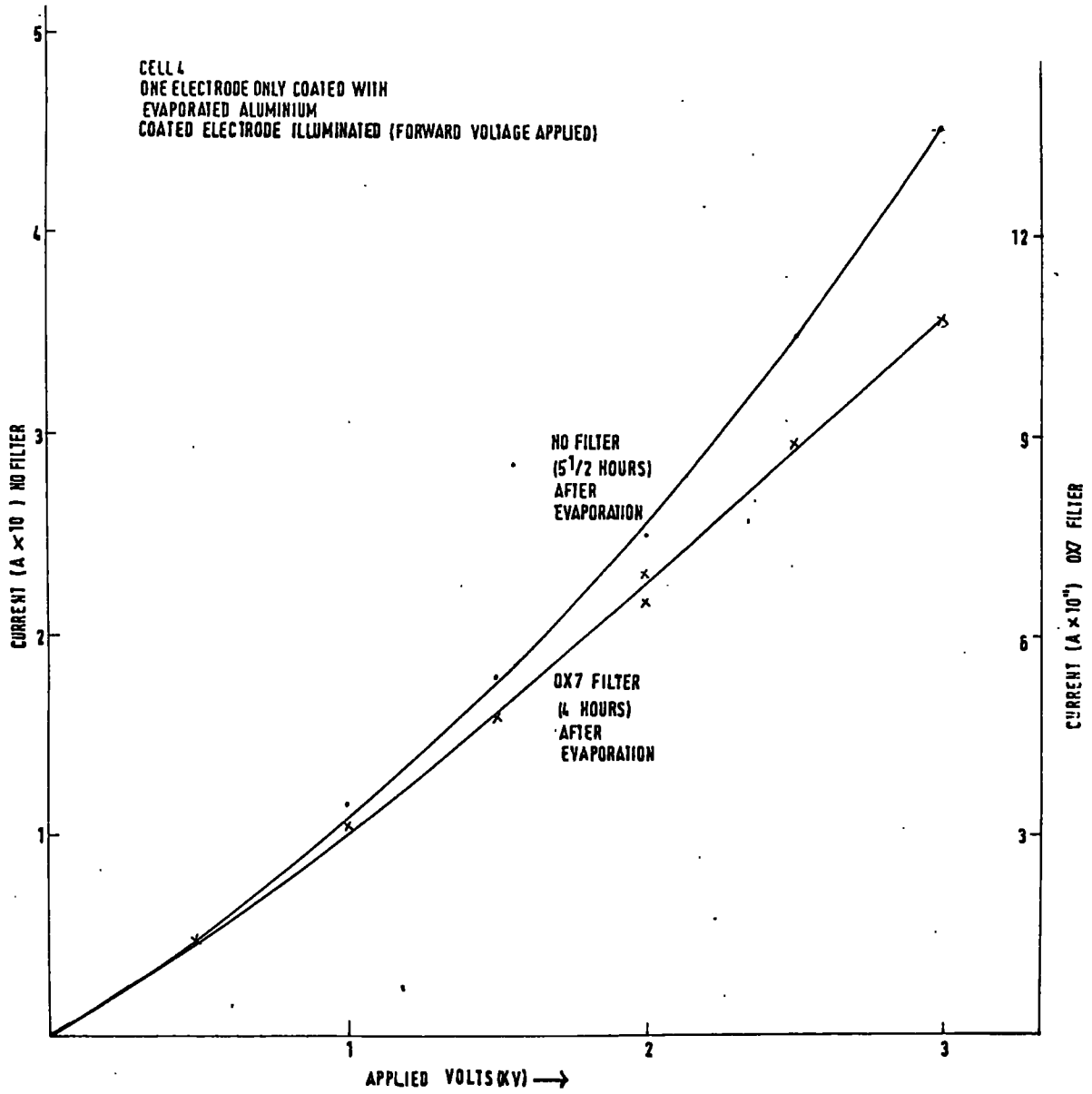
CELL 4
ONE ELECTRODE ONLY COATED WITH
EVAPORATED ALUMINIUM
COATED ELECTRODE ILLUMINATED (FORWARD VOLTAGE APPLIED)
NO FILTER
(5 1/2 HOURS)
AFTER
EVAPORATION
0X7 FILTER
(4 HOURS)
AFTER
EVAPORATION
CURRENT (A ×10) NO FILTER
CURRENT (A ×10⁻⁹) 0X7 FILTER
APPLIED VOLTS (KV) ⟶
1
2
3
4
5
6
9
12

Fig. 6.38

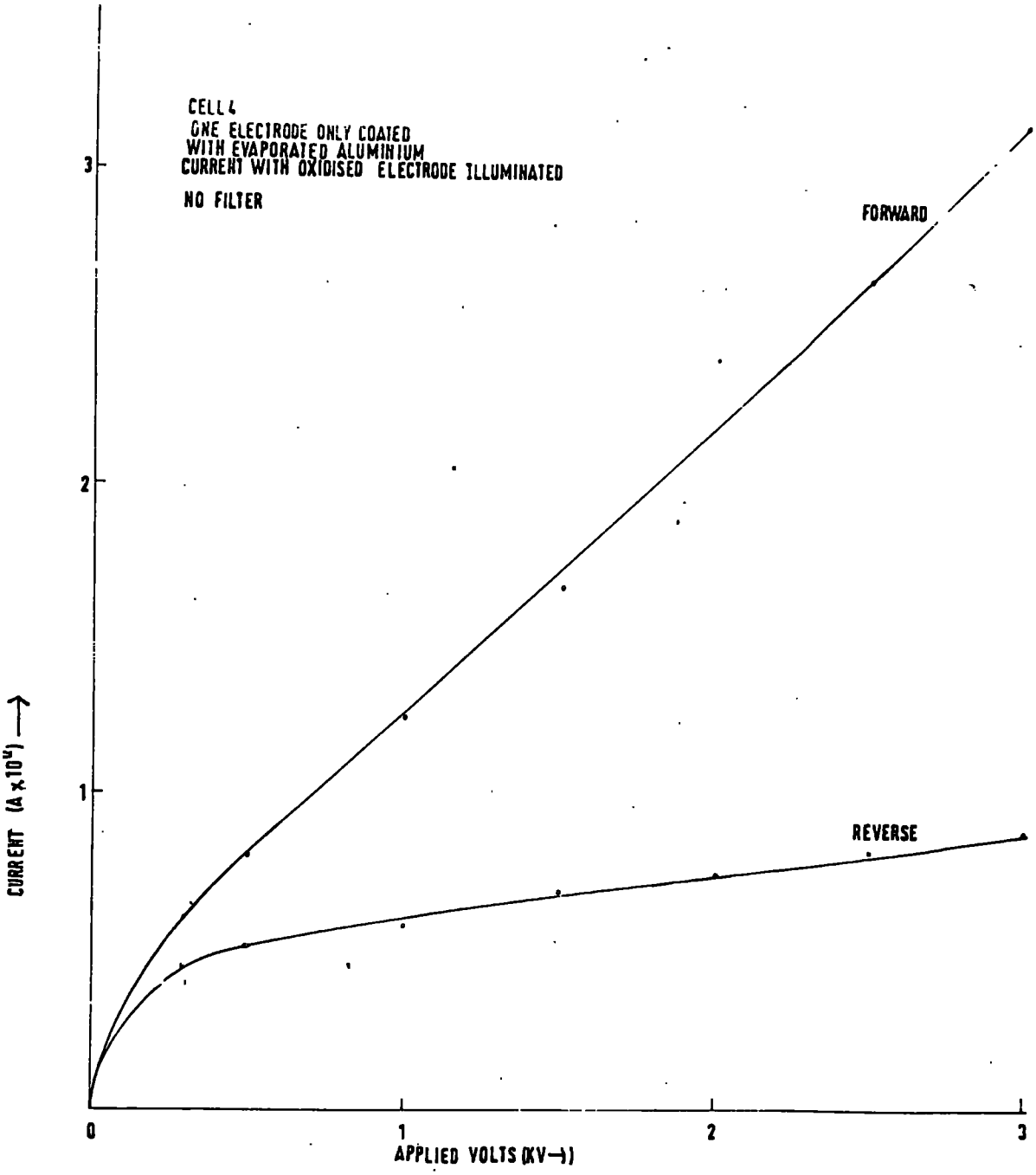
CELL 4
ONE ELECTRODE ONLY COATED
WITH EVAPORATED ALUMINIUM
CURRENT WITH OXIDISED ELECTRODE ILLUMINATED
NO FILTER
FORWARD
REVERSE
CURRENT (A x 10⁻⁶) ⟶
APPLIED VOLTS (KV⟶)
0
1
2
3

mercury vapour lamps were positioned so that either electrode could be obliquely irradiated.

After completing the evaporation and filling the cell with H.D.P. n-hexane, some measurements were made of the forward/reverse ratio of the photocurrents. The forward current for (OX7)-filtered irradiation of the coated electrode (3KV. applied) was, initially, $\sim 2 \times 10^{-10}$A., but in the reverse direction the photocurrent was $< 10^{-14}$A. This ratio ($\sim 10^4$:1), and the large forward current, indicated the absence of significant injection from the anode and showed that the negative carriers were being efficiently discharged at the oxidised surface.

A series of 'spot' measurements were made at increasing times from the evaporation to compare the photocurrents in the liquid with the photoemission (in vacuo) from the coated surface (see Figs. 6.35 and 6.36). Fig. 6.37 shows the 'injection' type $\frac{I}{V}$ curves resulting from OX7- and unfiltered irradiation of the coated electrode. The measurements in Fig. 6.38 were obtained, about 3 hours after the evaporation, by the unfiltered irradiation of the oxidised electrode. This diagram shows that the (rather high) 'bulk' photocurrents and the currents due to injection were additive (a feature already observed, see Fig. 6.9). Switching both lamps on at the same time also produced currents which were additive.

The photoemission (in vacuo) on direct irradiation of the oxidised electrode did not change throughout the experiment, being 6×10^{-12}A. (OX7) and 2×10^{-9}A. (no filter).

The results indicate that the discharge of photoinjected carriers is insensitive to the state of oxidation of the anode surface. In addition, it appears that the generation of charges in the bulk liquid is independent of the injection of charges from the negative electrode. Some correlation has been found between the photoinjection of negative charges into the liquid and the vacuum photoemission.

6.15. Photocurrents in air-saturated hexane.

One of the main features of the photoinjection, from evaporated metal layers into degassed hexane, was its decay as the surfaces oxidised. It was hoped (by the use of gassy hexane) to observe similar, but more rapid changes; in which case electrode activity would be incontrovertible.

Photoinjection by 'activated' metal surfaces into air-saturated hexane has been reported by Gzowski and Terlecki[55]. Their technique was to use an external vacuum coating unit to deposit layers of aluminium on the electrodes. The cell was then assembled and, with the hexane introduced, measurements were begun. It appears (from their account), that the assembly of the cell took about two hours; the active surface being exposed to air (or air-saturated hexane) for this length of time.

Cell 5, which was assembled before the deposition of the layers was considered to have two advantages over Gzowski's arrangement; (i) Neither the electrode surfaces nor any part of the cell needed

to be handled. (ii) Measurements could be started within 2 minutes of the evaporation of the metal layer, with only 10 seconds exposure to air before the introduction of the liquid (the time taken to remove the cell from the evaporator).

In view of the absence of 'bulk' photocurrents in the air-saturated liquid, it was considered 'safe' to stimulate the evaporated layers with unfiltered radiation, provided; (a) That the period of exposure was not prolonged and (b) That a fresh sample of liquid was used for each test. Discrepancies between samples were avoided by the use of highly purified n-hexane.

Quite large photocurrents were injected from evaporated aluminium electrodes, but there was a rapid decay of activity. Some measurements of the photocurrents (the cathode being continuously irradiated) were made for three values of applied voltage (see Fig. 6.39), each curve corresponding to a fresh evaporation. The $\frac{I}{V}$ curves were very similar to those obtained with the same type of electrode in degassed hexane, e.g. Fig. 6.40 (these curves have been 'corrected' to allow for the decay of the photocurrents in the time, $\sim$ 5 mins, taken to make the measurements). The forward/reverse ratio of the photocurrents (with respect to the irradiated electrode) was generally about 20:1 for the first two hours after evaporation. However, this ratio dropped to only 2:1 after 24 hours; the shape of the current-voltage curves indicating the presence of 'bulk' photo-conduction. It must also be pointed out that after this time the

Fig. 6.39

DECAY OF CURRENT UNFILTERED U/V
AIR SATURATED N-HEXANE
EVAPORATED ALUMINIUM ELECTRODES
a) 3KV. APPLIED VOLTAGE
b) 1·5KV " "
c) 500V. " "

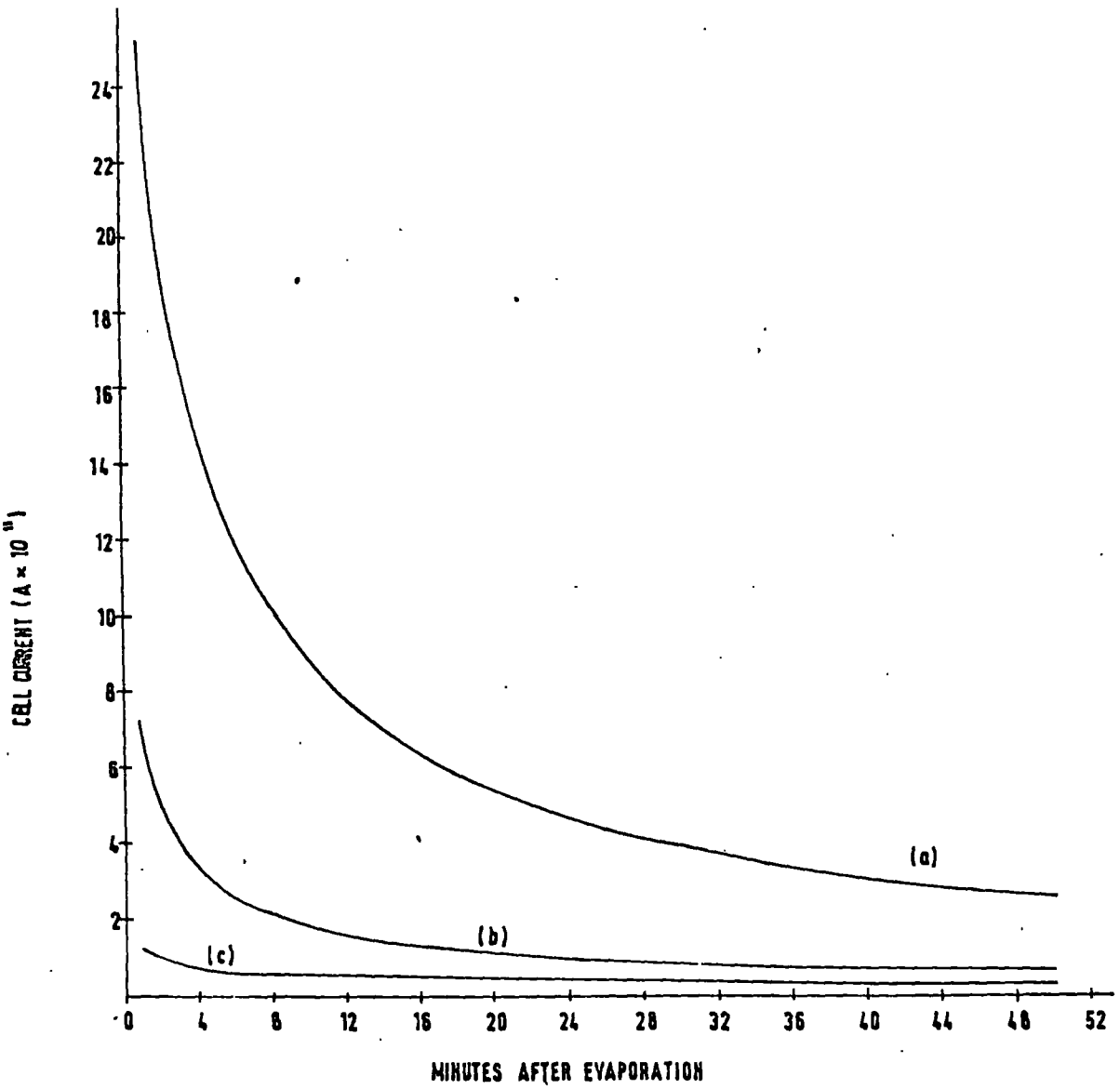

Fig. 6.40

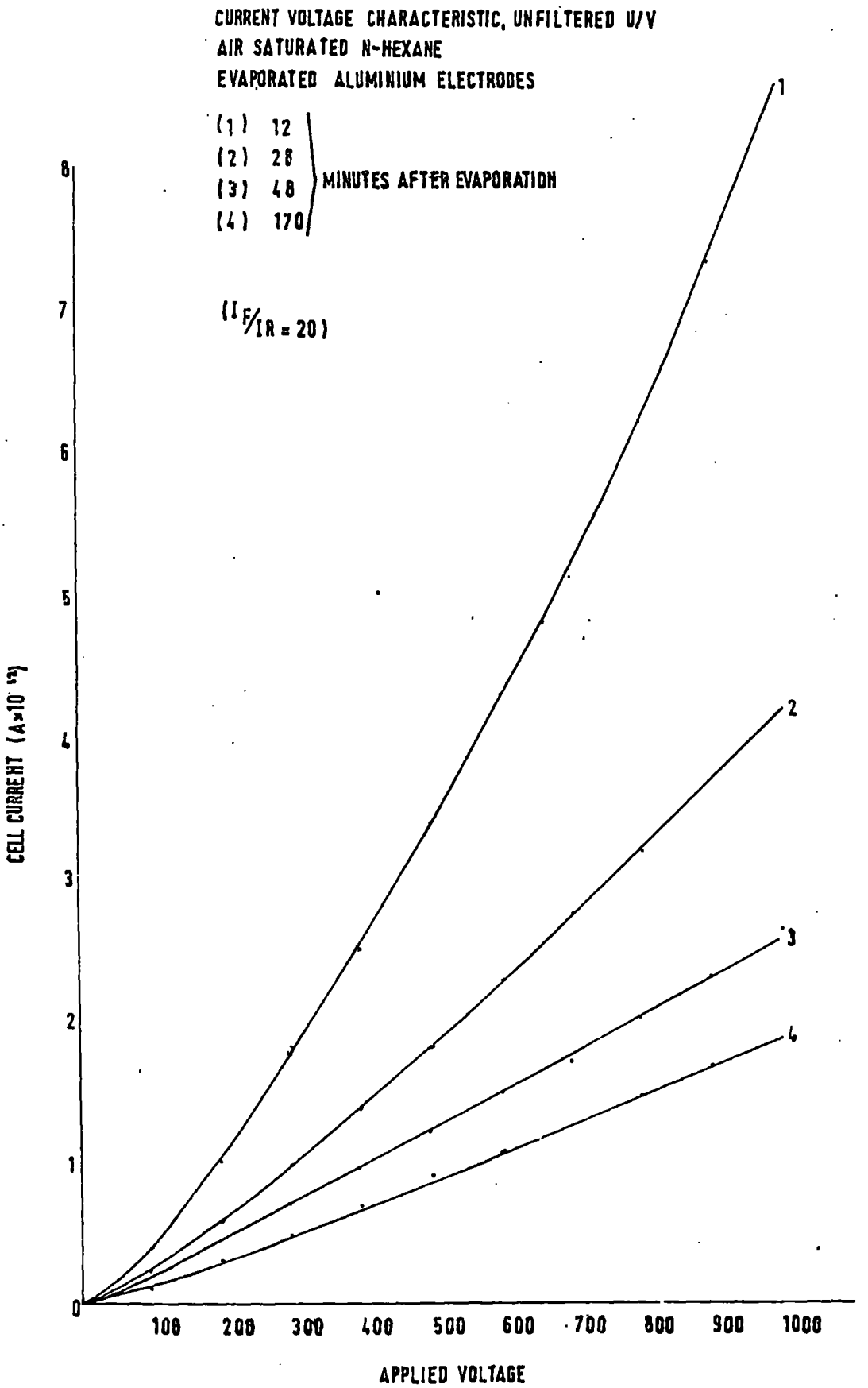
CURRENT VOLTAGE CHARACTERISTIC, UNFILTERED U/V
AIR SATURATED N-HEXANE
EVAPORATED ALUMINIUM ELECTRODES
(1) 12
(2) 28
(3) 48
(4) 170
MINUTES AFTER EVAPORATION
(IF/IR = 20)
CELL CURRENT (A×10 ¹³)
APPLIED VOLTAGE
0
1
2
3
4
5
6
7
8
100
200
300
400
500
600
700
800
900
1000
1
2
3
4

Fig. 6.41

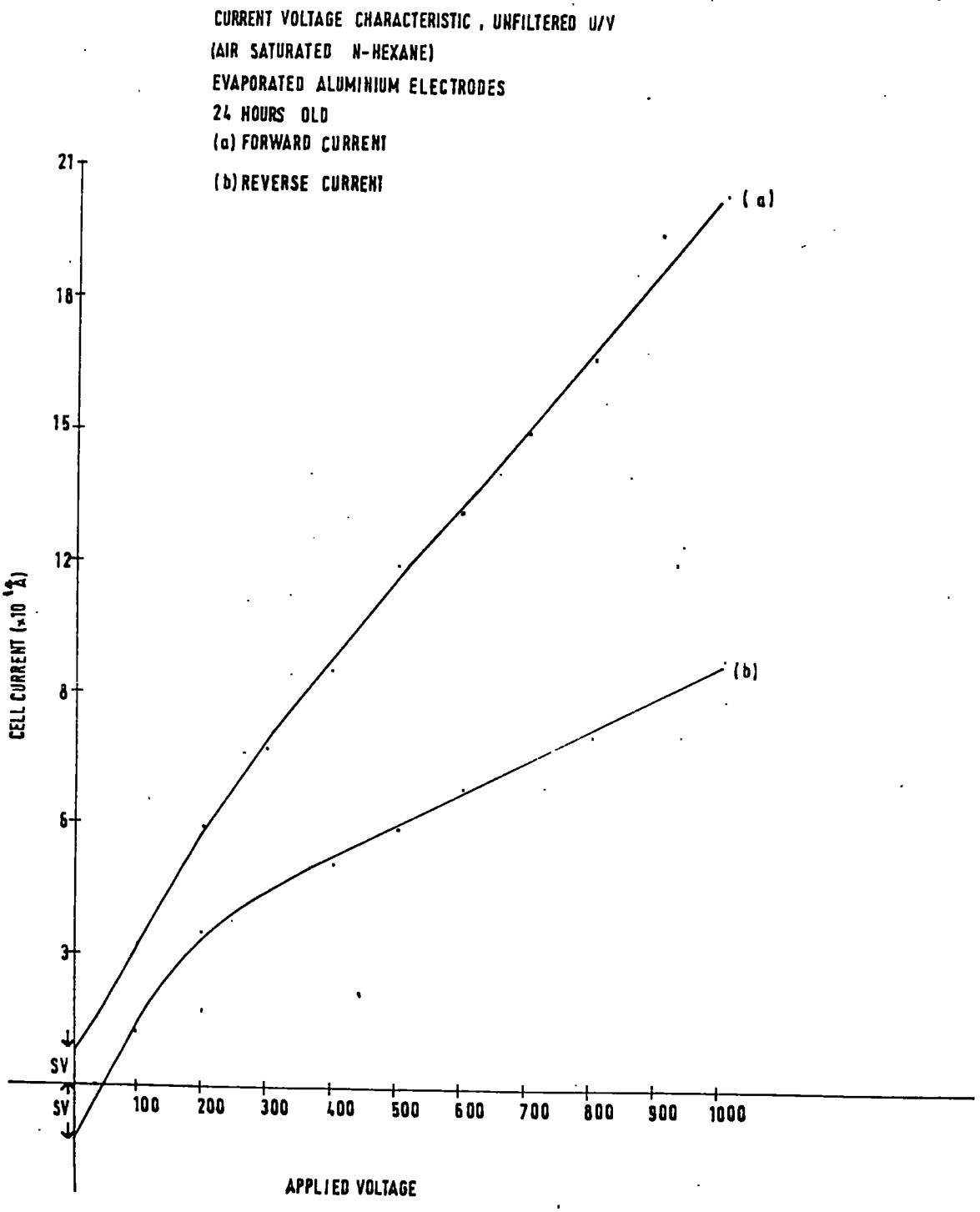
CURRENT VOLTAGE CHARACTERISTIC , UNFILTERED U/V
(AIR SATURATED N-HEXANE)
EVAPORATED ALUMINIUM ELECTRODES
24 HOURS OLD
(a) FORWARD CURRENT
(b) REVERSE CURRENT
CELL CURRENT (×10 ¹⁴A)
21
18
15
12
8
6
3
SV
SV
100
200
300
400
500
600
700
800
900
1000
APPLIED VOLTAGE
(a)
(b)

Fig. 6.42

DECAY OF CELL CURRENT UNFILTERED U/V
AIR SATURATED N-HEXANE
EVAPORATED MAGNESIUM ELECTRODES
a) 3KV • APPLIED VOLTAGE
b) 1·5KV. " "
c) 500 V. " "

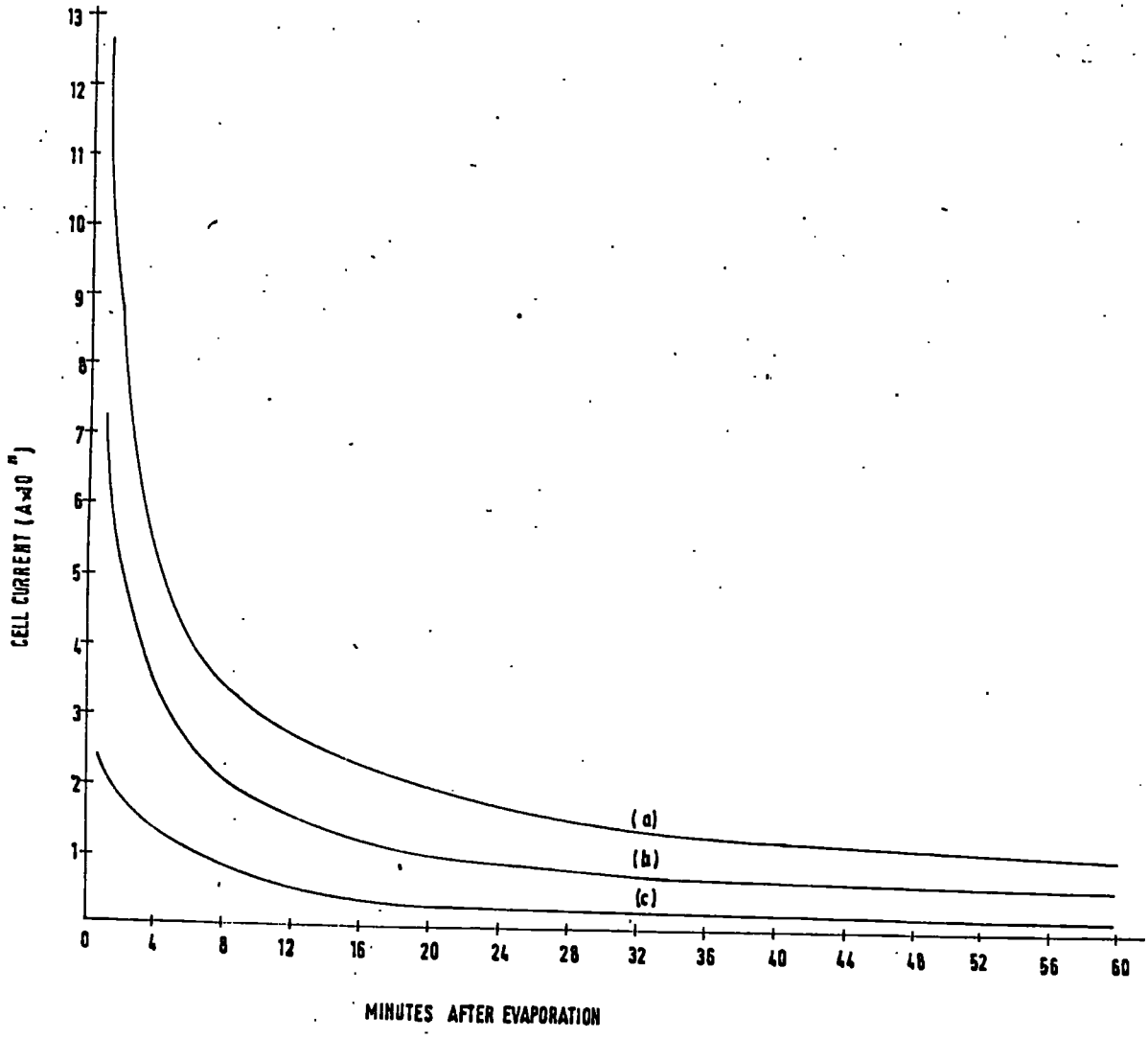

Fig. 6.43

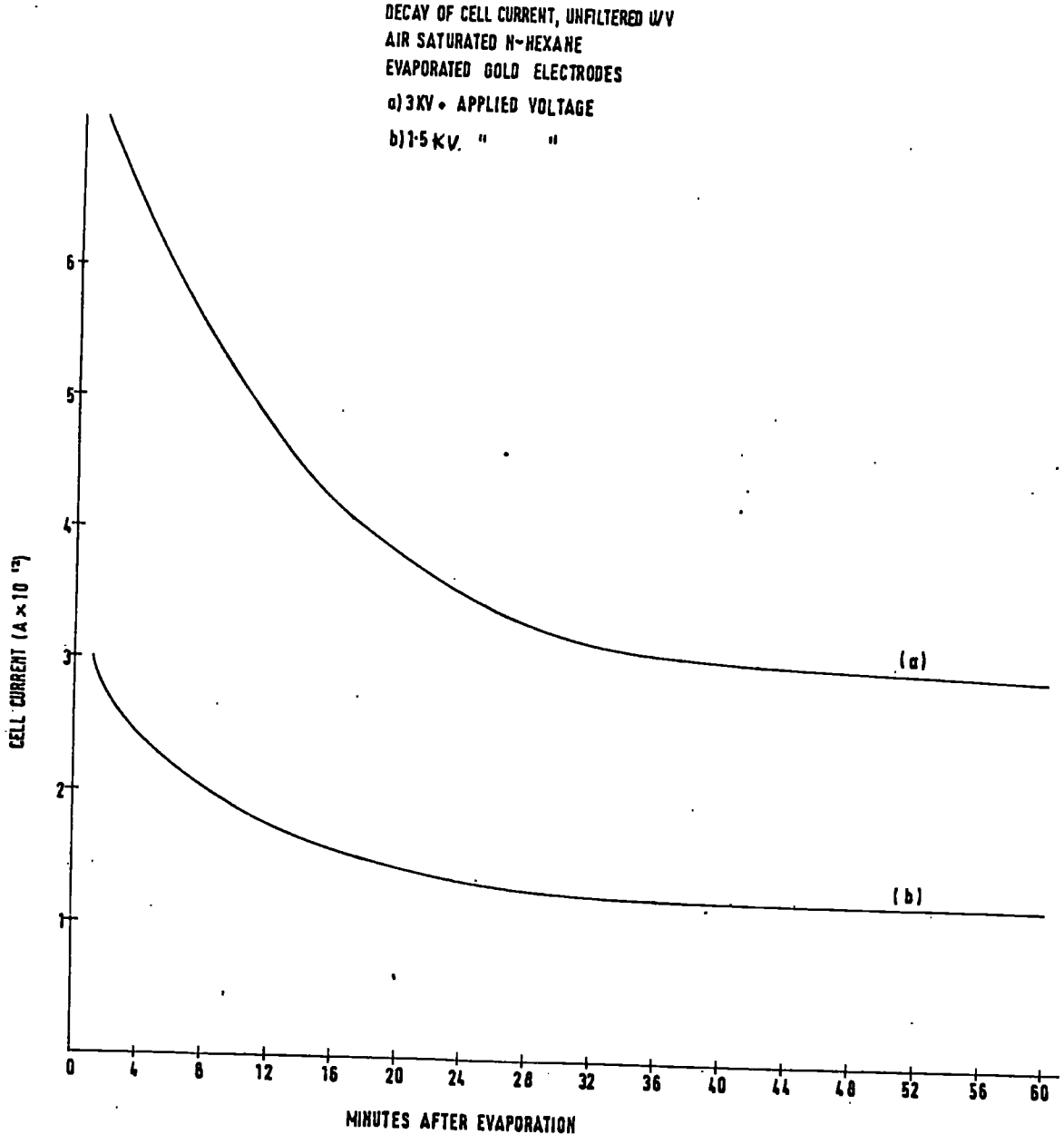
DECAY OF CELL CURRENT, UNFILTERED UV
AIR SATURATED N-HEXANE
EVAPORATED GOLD ELECTRODES
a) 3 KV • APPLIED VOLTAGE
b) 1·5 KV. " "
CELL CURRENT (A × 10 ⁻¹³)
6
5
4
3
2
1
(a)
(b)
0
4
8
12
16
20
24
28
32
36
40
44
48
52
56
60
MINUTES AFTER EVAPORATION

Fig. 6.44(a)

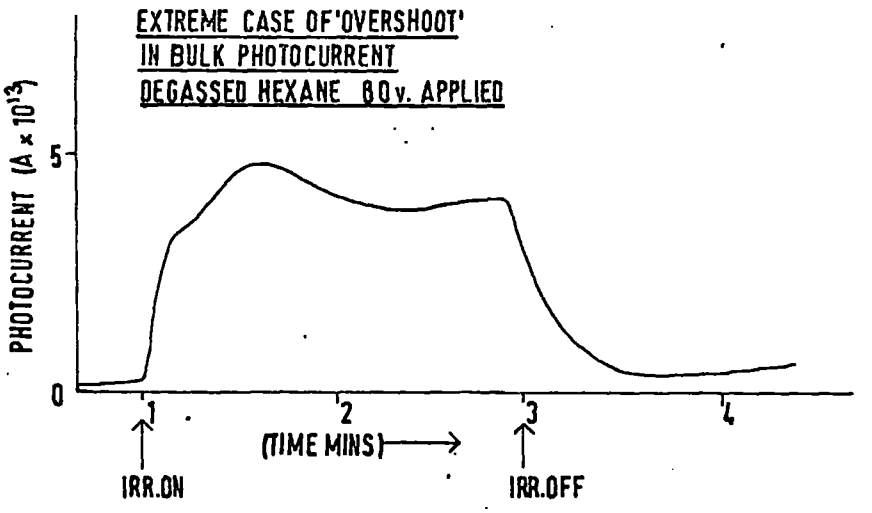

Fig. 6.44(b)

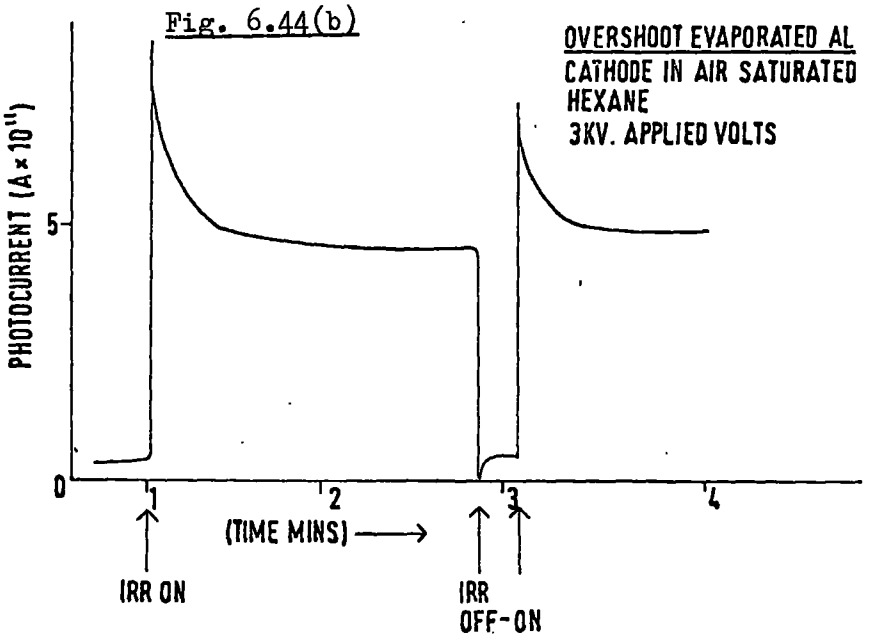

electrode activity had decayed by three orders of magnitude (see Fig. 6.41).

Similar measurements were made after evaporating magnesium or gold over the electrodes (Figs. 6.42, 6.43). Magnesium was found to decay (in activity) rather less rapidly than Al., but the photo-injected currents were also lower. Gold was very inactive, and (as expected), was relatively stable. Al. and Mg., but not Au., were also sensitive to OX7-filtered radiation.

There was some suspicion, at this stage, that part of the decay in the photocurrents was due to the sudden application of voltage to the electrodes. However, apart from a disturbance, lasting perhaps 2 minutes, the photocurrents followed the original decay curve if the voltage was pulsed or if the cell was emptied and the liquid sample quickly replaced.

There was also an 'overshoot' when the radiation was interrupted. The extent of this overshoot increased with time that had elapsed in the dark, (see Fig. 6.44,b) and there was a systematic decrease as the electrode activity decayed. A comparable observation has been reported by Gzowski, Fig. 2.4b). It was noticed that overshoot did not occur for evaporated gold electrodes. Because of these transients the decay of electrode activity was probably exaggerated for the first few minutes of measurement (Figs. 6.40-6.42).

6.16. Photochemical reactions.

Dissolved air suppresses 'bulk' photoconduction (Sec. 6.1), but increases the ultraviolet absorption of purified n-hexane (Sec. 4.6).

Both these processes, and other electrical properties of gassy hexane, are associated with oxygen[10] as the active component of the air. Prolonged exposure to unfiltered radiation increases the photoconduction of the degassed liquid (see Secs. 6.5, 6.10), thus indicating some sort of photochemical reaction. Two mechanisms may be visualised (i) the formation of impurities which are more easily ionised than hexane or (ii) the destruction of an impurity (probably oxygen) which quenches the photoconduction of the hexane itself. Accordingly, a search for the products of photochemical reactions in air-saturated and degassed hexane was made. The methods of detection and analysis (V.P.C. and u.v. spectrophotometry) were the same as described in Chapter IV.

The (unfiltered) irradiation of air-saturated n-hexane, with the mercury vapour lamp, substantially increased the ultraviolet absorption of the liquid (see Fig. 6.45). The absorption spectrum is seen to be rather featureless; the broad peak between 2500Å and 3000Å is characteristic of a wide range of paraffinic aldehydes and ketones.

In spite of a new, rather acidic, smell to the irradiated liquid, the new compounds were unexpectedly difficult to detect by V.P.C. Particular care was taken to detect possible fragmentation products (e.g. lower homologues of the paraffin series) and isomers, but it was concluded that these had not been formed in significant quantities.

By increasing the temperature of the chromatograph column (and hence reducing the retention times) it was subsequently found that

EFFECT OF UNFILTERED IRRADIATION ON GASSY HEXANE

Fig. 6.45

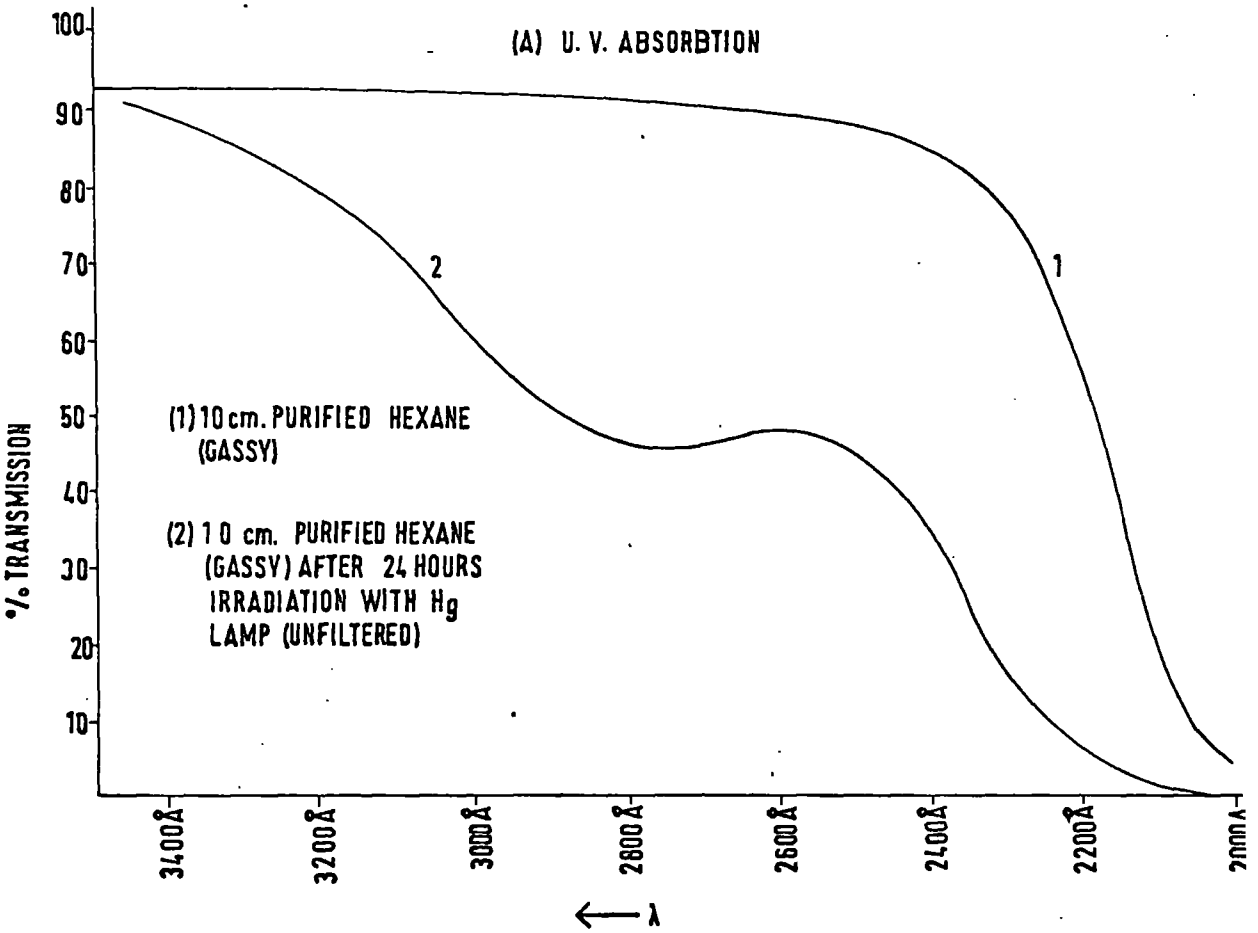

Fig. 6.46

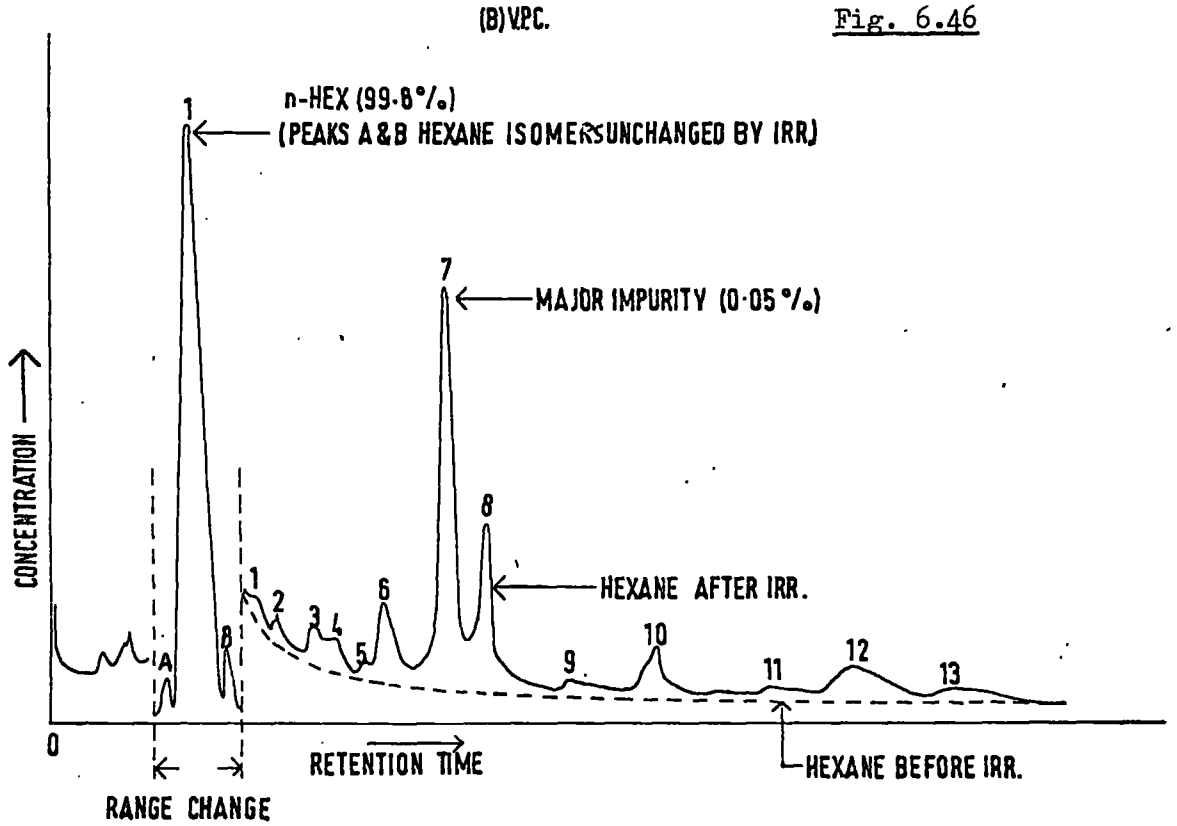

the products were considerably less volatile than the hexane (see Fig. 6.46). Some 12 new peaks were detected, but an attempt to identify them (by the comparison of the retention times of likely compounds) was not successful. The (heavier) impurities were concentrated by evaporating off most of the hexane. Infra-red analysis showed that this (waxy) deposit contained aldehydes, ketones (and possibly acids) although, once again, the exact compounds could not be distinguished.

There were no signs of any changes in the liquid after (OX7)-filtered irradiation, even after days of continuous exposure.

Samples of highly degassed hexane were subjected to similar treatment and analysis. Neither the u.v. absorption nor subsequent analysis by V.P.C. showed any sign of change. It was concluded that any reactions were probably between the hexane and the (very small quantities of) oxygen remaining in the liquid.

A routine search was made for chemical changes in the liquid after the electrical measurements. There appeared to be no new impurities, but it must be pointed out that the optical absorption was disturbed by the introduction of air in transferring the liquid to a spectrophotometer cell. Two (rather dubious) peaks (corresponding to butane and pentane)were found in the V.P.C. of one sample, but these were sometimes present in the liquid taken from the bottle.

The interaction of silica, Pyrex, and evaporated aluminium with degassed hexane vapour (before and after ultraviolet irradiation)

was investigated with the aid of a mass spectrometer. The multiplicity of hexane fragments (produced by the 11eV. electron beam) confused the analysis, and so a small quantity of deuterium was mixed with the hexane for a second test. Thus, the (most likely)[106] 'place exchange' processes at the surfaces could be monitored by the increase in mass of the ion fragments. No reaction of any sort was detected by this means, and it was concluded that (to hexane vapour at least) these surfaces were not chemically or photo-chemically very active.

Summary of Observations

Currents can be induced in liquid hexane by;

(i) The photoionisation of the bulk liquid

(ii) The photoinjection of negative charges from the cathode.

Depending on the experimental conditions (e.g. Sec. 6.8), the photocurrents may be predominantly due to (i) or (ii). Either mechanism can proceed independently of the other (Sec. 6.5), so that 'bulk' and 'injection' photocurrents can be considered separately.

Bulk Photoconduction

Currents originating from the photoionisation of the bulk liquid have been found to;

(i) Be independent of the polarity of the applied field (Sec. 6.1.2)

(ii) Exhibit a tendency towards 'saturation' as the applied field is increased beyond a few hundred volts $cm.^{-1}$ (e.g. Fig. 6.1)

(iii) Result from the irradiation of the degassed liquid with wavelengths shorter than $\sim 2400\text{Å}$, i.e. in the region of the u.v. absorption edge of the purified liquid (Secs. 6.8 and 4.6).

(iv) Increase in magnitude after exposing the degassed liquid to long periods of unfiltered radiation (Sec. 6.7).

(v) Be inhibited by dissolved air (Secs. 6.1 and 6.5).

(vi) Be insensitive to the state of oxidation of the electrode surfaces (e.g. Sec. 6.7).

(vii) Involve peculiar transients on pulsing the radiation (e.g. Fig. 6.44a).

Photoinjected Currents

Negative charges can be injected into liquid hexane from immersed photocathodes of Al., Mg., or Au. The photosensitivity of Al. or Mg. is substantially increased, compared to their polished surfaces, if the photocathode is prepared by vacuum evaporation. The activity of such layers (like the photoemission in vacuo, e.g. Fig. 6.35) decreases with time after deposition, presumably because of re-oxidation. This decay can, however, be retarded by maintaining the surfaces in vacuo for subsequent photostimulation in the highly degassed liquid.

The rate of photoinjection into the liquid (degassed or air-saturated) has been found to;

(i) Increase faster than the applied field, the I/V curves exhibiting an upward curvature (e.g. Fig. 6.17). Photo-injected currents for 'forward' polarity of the applied field are much greater than for 'reverse', i.e. the injection process has rectifying properties (e.g. Fig. 6.34).

(ii) Depend on the nature of the cathode surface as well as the spectral composition of the incident radiation (e.g. Table 6(iii)). Radiation of longer wavelengths than are absorbed by the purified liquid is effective in photo-stimulating the cathode if the work function remains low enough.

(iii) Increase with the intensity of the radiation, so that the photoinjected currents at the higher field strengths are nearly proportional to the radiation intensity (e.g. Sec. 6.13).

(iv) Be insensitive to the state of oxidation of the anode surface (Sec. 6.14).

(v) Exhibit a short-term (reversible) decay in the air-saturated liquid, but not in degassed hexane (Fig. 6.44b).

These properties, and other details (e.g. the significance of the photochemical reactions), will be discussed in the next Chapter.

CHAPTER VII

DISCUSSION

Some care has been taken to indicate those results which show most clearly the points under discussion. Whole sections of the thesis are referred to when details are abstracted from them. Section 7.1 deals with the 'bulk' photocurrents, and 7.2 with the currents due to photoinjection.

7.1.1. The current-voltage curves for 'bulk' photoconduction

It is evident (Figs. 6.1, 6.3 etc.) that the photocurrents were tending towards 'saturation' at fields much lower than predicted by the Onsager theory (Sec. 3.1). It is assumed that the charges were subject (primarily) to volume recombination, and so the analysis of the conduction at low fields is treated accordingly.

Unfortunately, the (oblique) configuration of irradiation used for most of the measurements complicates an exact analysis. In the circumstances, two limiting (and idealised) geometries of ionisation are considered;

(1) Where the radiation is directed along a line parallel to the electrodes (uniform distribution of ions).

(2) Where the radiation enters normal to the electrodes (as in Cell 2). (An exponential distribution of ions from one electrode to the other, due to the absorption of the radiation).

The currents, assuming volume recombination, have been calculated elsewhere for both these configurations[62,107].

The ionisation in cell 1 (Sec. 6.1) is assumed to be nearly uniform. In this case the rate of generation of charges 's' per unit volume is balanced (for zero voltage applied) by the loss due to recombination. If the recombination coefficient is 'α', then;

$$s - \alpha pn = 0 \qquad \text{---- (1)}$$

and because of the symmetry of ionisation;

$$n = p = s/\alpha^{\frac{1}{2}} \qquad \text{---- (2)}$$

For low applied fields (U/L), the rate of removal of charges at the electrodes is small compared to their neutralisation through recombination. Thus, the values of 'n' and 'p' (the concentration of 'free' ions) is essentially the same as for zero voltage. The current density 'J' is given by;[62]

$$J = \frac{eU}{L}\left(\frac{s}{\alpha}\right)^{\frac{1}{2}}\left[\mu_n + \mu_p\right] \qquad \text{---- (3)}$$

The slope 'm_o' of the current-voltage curve for electrodes of Area 'A', is;

$$m_o = \frac{e\not{V}A}{L}\left(\frac{s}{\alpha}\right)^{\frac{1}{2}}\left[\mu_n + \mu_p\right] \qquad \text{---- (4)}$$

For higher field strengths the rate of neutralisation at the electrodes increases to make volume recombination unimportant. The current 'saturates' at a level I_o, which is given (ideally) by the rate of generation of 'free' ion-pairs in the volume of liquid between the electrodes;

$$I_o = e\ sLA \qquad \text{---} \quad (5)$$

Eliminating s in (4) from (5) and squaring, we obtain;

$$\frac{m_o}{I_o}^2 = \frac{e\ A}{\alpha L^3} \left[\mu_n + \mu_p \right]^2 \qquad \text{---} \quad (6)$$

I_o is identified as the extrapolation to zero volts of the 'saturation' current-voltage characteristic (Fig. 2.2). A value might be estimated from the measurements with pulsed u.v.. Unfortunately these measurements were complicated by peculiar 'overshoots' as well as the time constant of the Vibron. For n-hexane the value of α is (calculated[60] to be) $\sim 2 \times 10^{-9}$ cc. ion^{-1}sec^{-1}. From Fig. 6.1, $I_o \sim 3 \times 10^{-12}$A. and $m_o \sim 2{\cdot}5 \times 10^{-14}$A.V.$^{-1}$, substitution of α, m_o and I_o in equation (6) results in;

$$\mu_p + \mu_n \sim 1{\cdot}2 \times 10^{-3} \text{ cm.}^2 \text{ V}^{-1}\text{sec}^{-1}$$

so that if $\mu_p \simeq \mu_n$

$$\mu \sim 6 \times 10^{-4} \text{ cm.}^2 \text{ V}^{-1}\text{sec}^{-1}$$

which is in fair agreement (considering some of the approximations made) with the accepted value. For this value of μ, the density of ions

(at zero field) would have been $\sim 10^9$ cm.$^{-3}$.

In the 'saturation' region, the steady-state lifetime of the free ions (in the absence of an applied field) must be longer than their average transit time between the electrodes.[60] The transit time is approximately;

$$T = \frac{2L^2}{(\mu_p + \mu_n)\, U}.$$

The average lifetime τ of the free ions (with zero field) is

$$\tau = \frac{1}{\alpha n} = \frac{1}{(\alpha s)^{\frac{1}{2}}}$$

Saturation is obtained when $\tau > T$, i.e. when

$$U \gg LE_s = \frac{2\, L^2\, (\alpha s)^{\frac{1}{2}}}{(\mu_p + \mu_n)} \qquad \text{(7)}$$

α is given for ions (Langevin formula[119]) as

$$\alpha = 4\pi r\, (D_p + D_n) \qquad \text{(8)}$$

where D_p and D_n are the diffusion coefficients of the positive and negative ions respectively; 'r' is the effective collision radius of the pair of ions, given by Onsager's criterion (Sec. 3.1);

$$r = \frac{e^2}{\varepsilon (kT)}. \qquad \text{(9)}$$

Since $\frac{D}{\mu} = \frac{KT}{e}$, (8) becomes (after substitution for r from (9));

$$\alpha = 4\pi \frac{e}{\varepsilon} (\mu_p + \mu_n) \qquad \text{(10)}$$

Substituting (10) and (5) into (7) and squaring

$$U_s^2 > \frac{16\pi I_o L^3}{A\varepsilon(\mu_p + \mu_n)} \qquad \text{(11)}$$

This equation shows that the voltage required for saturation against volume recombination increases as the square root of the saturation current. For $(\mu_p + \mu_n) \sim 1.2 \times 10^{-3}$ cm.^{2}V^{-1}sec., $I_o \sim 3 \times 10^{-12}$A., and L = 1 cm., saturation is obtained for;

$$U > 400 \text{ V.}$$

This value agrees well with the trend of Fig. 6.1.

The exponential fall in the intensity of ionisation across the cell for configuration (2) modifies equations (3) and (5) to;

$$J = \frac{2eU}{L}\left(\frac{s}{\alpha}\right)^{\frac{1}{2}} (\mu_n \mu_p)^{\frac{1}{2}} \qquad \text{(12)}$$

$$I_m = e\, s_o\, d\, A \qquad \text{(13)}$$

where 's' is the intensity of ionisation at $x = 0$, (at the 'window' electrode). The extinction depth 'd' replaces L since $s(x) = s_o \exp(-x/d)$. Saturation is obtained for;

$$U^2 > \frac{(s\alpha)\, d^2}{\mu_n \mu_p}$$

A comparison of the photocurrents for configurations (1) and (2) should allow μ_n and μ_p to be distinguished. However, the experiments

with cell 2 were concerned with photoinjection rather than 'bulk' photoconduction; the measurements are not detailed enough for an analysis to be made.

Summary

At low voltages, the current is carried by 'free' ions which are subject to volume recombination. The conduction should depend on $s^{\frac{1}{2}}$, where s is the intensity of the radiation. At higher voltages most of the ions are discharged at the electrodes so that the 'saturation' current I_o becomes proportional to s. There is a regime, between $^{U}s/_{L} < 8KV.cm^{-1} = E_s$, in which volume and initial recombination compete in importance (depending on the concentration of 'free' ions). For $^{U}/_{L} > E_s$ the neutralisation of the ion-pairs by initial recombination is the limiting process. Charge generation in the latter circumstances may be considered to be field-assisted. The current should then increase slowly, but linearly, with the voltage and be proportional to the intensity of irradiation (Sec. 3.1).

(The measurements did not extend as far as E_s).

7.1.2. Photoionisation of liquid hexane.

The radiation must be absorbed for photoionisation to occur. The u.v. absorption of liquid hexane is very sensitive to dissolved impurities (Fig. 4.6), and it would seem likely that these impurities would be photoionised in preference to the hexane itself. However, the following observations lead to a different conclusion;

1. The threshold wavelength for photoconduction (even in unpurified samples) is in the region of the u.v. absorption edge of the pure and degassed liquid. (Sec. 6.1 etc.).
2. Photoconduction was, in each sample, inhibited by dissolved air. (Sec. 6.1 etc.).
3. There is a bathochromic shift in the absorption edge of purified n-hexane when saturated with air. (Fig. 4.9).
4. Photochemical reactions in hexane involve oxygen. (Sec. 6.16).
5. The photoconductivity increased after exposing degassed samples to long periods of unfiltered radiation. (Fig. 6.9).

It is likely that;

A. The threshold wavelength for photoconduction was not changed by long periods of unfiltered radiation. (Judging from the parallelism of the curves for different filters in Fig. 6.9).
B. The u.v. absorption of dissolved air corresponds to the excitation of hexane/oxygen charge-transfer complexes. (Sec. 3.2).

It must be concluded (from (2) and (4)) that photochemical reactions involving oxygen, take place in preference to photoionisation. From (A) and (5) it is likely that the increase in photoconductivity was due to the removal of molecular oxygen (by photochemical reactions) rather than to the formation of more easily ionisable impurities. Hence, from (3) and (B) the absorption edge of the purified and degassed liquid is due to the hexane and not remaining impurities; and from (1) that photoconduction results from the absorption of radiation by the hexane itself.

Eller's[47] measurements (Sec. 2.5) agree with the latter conclusion. He found no photoconduction in benzene (the major impurity in some of the present samples) and, more significantly, that the threshold for photoconduction in a series of n-paraffins kept in step with their u.v. absorption edges.

Volmer[46] found a threshold of ~ 2250Å for the photoconduction of anthracene in hexane. Porter and Windsor[85] have shown, however, that u.v. irradiation of similar solutions removes oxygen but does not affect the concentration of the anthracene. The latter observation indicates that, even in anthracene solutions, the hexane photochemically reacts with the oxygen.

More recently, Morant[52] has found a threshold of ~ 3000Å in degassed hexane. He noted that this corresponds to the threshold for photoemission (in vacuo) from the electrodes. It is likely (in view of the ohmic behaviour of the photocurrents near this threshold, which is a characteristic of photoinjection rather than photoionisation) that the threshold for the liquid was at rather shorter wavelengths. It is seen (Fig. 2.3(a)) that for unfiltered radiation the photocurrents 'saturated' with low applied voltages, i.e. were more in keeping with 'bulk' photoconduction.

Very pure, highly degassed, n-hexane exhibits a u.v. absorption edge which begins at ~ 2200Å. The reason for this absorption is not known at present. Radiation ($\lambda >$ 1849Å) from a mercury vapour lamp is not sufficiently energetic even to excite an isolated hexane molecule. It is necessary to look for a mechanism other than direct

ionisation of the hexane ($I_q \sim 10{\cdot}2eV.$) to explain the photoconduction.

It is (very tentatively) proposed that photons may be absorbed by pairs of hexane molecules in the liquid. Thus, if M_1 and M_2 are two such (adjacent) molecules, the reaction may be envisaged as;

$$(M_1, M_2)_{liq} \xrightarrow{h\nu} M_1^+ M_2^- \rightleftharpoons M_1^- M_2^+ \qquad \text{(1)}$$

The structure on the R.H.S. of (1) is described as a resonant change transfer complex[78] (which, for n-hexane, may be termed the Π^* excitation)must contain equal contributions from structures of type $M_1^+ M_2^-$ and $M_1^- M_2^+$; and there will be no <u>overall</u> charge displacement associated with the transition (hence the distinction between charge-transfer and charge-resonant[78] systems). For identical molecules the ionic structures $M_1^+ M_2^-$ and $M_1^- M_2^+$ will occur with equal weight in the eigenfunctions. (The theory of the H_2 molecule exemplifies this principle[108]). For large organic molecules, containing a number of substructures, it is likely that non-identical sections of two molecules will overlap; the process is then more adequately described by wave functions analagous to (1), (2) and (3) in Sec. 3.2.

Mulliken's formula for the characteristic absorption of charge-transfer complexes is;

$$h\nu_{C.T.} = I_q - C - E_A$$

For a charge-resonant structure, the electron affinity term 'E_A' is set to zero. C remains the coulomb attraction energy of the separated charges.

The transition to the Π^* state may be regarded as a partial ionisation. The energy required for this excitation will be

$$h\nu = I_G - C \qquad \text{(2)}$$

The liquid is observed to start absorbing at ~ 2200Å; so that $h\nu \sim \frac{I_G}{2}$. From a consideration of the symmetry of (1), the maximum value of $C = C_{max} = \frac{I_G}{2}$. Thus the u.v. absorption of n-hexane (if not complicated by impurities) would be expected to start at 2400Å and to become increasingly intense at shorter wavelengths (as more molecules come within a suitable configuration for this type of excitation).

Now, the <u>single</u> molecules of hexane are excited by radiation of ~ 1750Å. It is clear that for decreasing wavelengths both charge-resonant and monomolecular absorption processes may occur. It is not possible to estimate the relative probabilities of the two mechanisms without a detailed knowledge of the radial distribution function. However, a simplification is possible for liquid n-hexane if the cybotactic groupings[109] are considered. X-ray diffraction methods indicate an intermolecular separation of 4.65Å between these (parallel) molecules[110]. Applying this value to the separation of the charges in the Π^* state, the coulomb energy C in (2) works out to be ~ 3.2eV. Thus, radiation of $\lambda > 1800$Å is, with reasonable certainty, sufficiently energetic to cause excitation to the charge-resonant structure.

It is now necessary to show how the excitation might separate into free charges. So far, the dielectric constant of the liquid has not been involved. (The dielectric constant ε_∞ was taken to be unity in the calculation of C for the charge resonant system. It is considered that energy due to the polarisation of the medium will not be available during the short time for excitation). However, if the resonant aspect of the Π^* excitation is lost in some way, for example if the molecules separate by thermal motion, then the charges may remain long enough to polarise their surroundings. The delayed action of polarisation should assist electrons to escape from the field of the positive ions.[111] Considering energies;

The energy of the Π^* configuration is $h\upsilon \sim \frac{I_q}{2}$, which is approximately equal to the coulomb energy C_o of the charges in free space. The polarisation of the liquid can be expected to reduce the coulomb energy to $\frac{C_o}{\varepsilon_s}$, where ε_s is the static (D.C.) dielectric constant.

The energy difference is[112];

$$P_E = C_o\left(1 - \frac{1}{\varepsilon_s}\right)$$

If P_E is available (e.g. as K.E. to the charges), the excess energy required to produce two 'free' charges from the Π^* excitation is;

$$E_T = \frac{C_o}{\varepsilon_s} - P_E \sim I_q\left(\frac{1}{\varepsilon_s} - \frac{1}{2}\right)$$

For hexane, $\varepsilon_s = 1{\cdot}89$ and $I_q = 10{\cdot}2$eV, and so;

$$E_T \sim 0{\cdot}3\text{eV}$$

E_T may be supplied thermally (as in the Onsager theory) so that;

$$N_F \propto N_o \exp(-E_T/kT)$$

where N_F is the rate of production of 'escaped' ion-pairs, and N_o the density of Π^* excitations. The value of $E_T/2$ (the excess energy for dissociation of each ion) is $\sim$ 0·15eV., which is remarkably close to the accepted 'activation energy'.[113]

The charge-transfer excitation with oxygen (because of the electron affinity of the latter) will take place at rather lower energies. It follows that dissolved O_2 in hexane will not only absorb radiation of longer wavelengths, but also that the reactions;

(1) $\Pi^* + O_2 \rightarrow M_1O_2^* + M_2$

(where $M_1O_2^*$ is the oxygen/hexane complex)

(2) $M_1O_2^* \rightarrow$ oxidation products

will proceed in preference to ionisation. Since the energy of each hexane molecule in the Π^* configuration will be $\frac{I_{\varphi}}{4} \sim$ 2·5eV., which is almost exactly the C-C bond energy (Sec. 3.2), it would appear that the molecules would have the choice of 'storing' the energy in the C-C group orbital or decompressing into radicals. (Transfer of energy along the length of hydrocarbon chains by the C-C linkages is a well-known phenomenon[81].)

It is clear that further experimentation is required (especially with hexane isomers) to positively identify the u.v. absorption with the threshold for photoionisation of hexane. Theoretical calculations (of some complexity) may then be justified to define the Π^* (or similar) state, and to clarify the dissociation process.

7.2.1. Photoinjected Currents - general.

It has been confirmed that negative charges can be injected into (both highly degassed and air-saturated) liquid hexane from photocathodes of aluminium, magnesium or gold. The photosensitivity of Al. or Mg. is substantially increased, with respect to their oxidised surfaces, if the photocathode is prepared by vacuum evaporation. (cf. Sec. 3.4). The activity of such layers decreases with time after deposition (presumably because of re-oxidation). The decay can, however, be retarded by maintaining the surfaces in vacuo for subsequent immersion in highly degassed hexane; useful photocurrents can then be obtained for periods of a week or more after deposition. Similar cathodes decay much more rapidly (in a matter of hours) on immersion in air-saturated liquid.

The behaviour (rectifying action, spectral response, and decay of activity) of the photocathodes in hexane closely resembled that for the photoemission in vacuo (e.g. Table 6(iii)). The conduction appears to be predominantly emission limited (i.e. nearly proportional to the light intensity), and it is likely that photoinjection is a useful technique for measuring the mobility of negative charges in

liquid paraffins. It is considered that electrons are ejected from the metal into the liquid (as for photoemission in vacuo), but that the subsequent conduction is controlled by collisions with the molecules adjacent to the cathode surface (Sec. 7.2.2).

The present work can be taken as additional proof that Gzowski and Terlecki[55] obtained photoinjected currents in air-saturated paraffins, and that their mobility measurements[33] refer to the injected (negative) carriers. It is likely that Swan[54] (unknowingly) measured 'bulk' photoconduction at low applied fields, but that the currents were predominantly due to injection as the field was increased ($> 500V.\ cm^{-1} \rightarrow 40KV.\ cm^{-1}$). Both Swan[54] and Gzowski[55] reported short-term 'fatigue' of aluminium photocathodes; similar (reversible) decays were observed in the present work (with aluminium or magnesium photocathodes) in air-saturated hexane. The latter phenomenon was not noticeable when measurements were made with highly degassed hexane.

Morant's measurements (except possibly with radiation near the threshold for photoconduction ~ 3000Å) relate to the 'bulk' photoconduction in highly degassed hexane.[52]

The precautions taken by LeBlanc,[15] to purify the liquid and to avoid the use of radiation of wavelengths shorter than ~ 2400Å, are taken to indicate the observation of 'injected' as opposed to 'bulk' photocurrents (although the effects of reversing the polarity of the applied field are, unfortunately, not stated in his publications). The mobility of the charge carriers ($\sim 10^{-3} cm^2 V^{-1} sec.^{-1}$) and the activation energy ($\sim 0{\cdot}1eV.$), as found by LeBlanc,[15] have since been

verified by Chong and Inuishi.[57] However, these workers did not consider the possible consequences of bulk liquid motion. It remains to be seen if future work (in particular by Bloor;[59] which includes a comparison of the mobilities in highly degassed and air-saturated hexane) leads to the above (rather high) mobility value.

Photoinjected currents in the present work were, typically, of the order of 10^{-10}A. for the (maximum) applied field of 3KV.cm^{-1}. The space-charge limited current for this field applied to cell 4, and, assuming no bulk liquid motion, would be;

$$I_{SCL} = 2 \times 10^{-9}\text{A.}$$

(Taking LeBlanc's value for μ.)

The maximum current obtained in the present work (for the '1st' evaporation and with unfiltered radiation in Fig. 6.28) was $\sim 5{\cdot}5 \times 10^{-10}$A. at $\sim$ 3KV.cm^{-1}. This current was reproduced, after the electrode activity had decayed, by depositing a fresh layer of aluminium on the photocathode ('3rd evaporation'). It is unlikely that exactly similar layers were consecutively deposited by the evaporation technique (as is indicated by the differences in the decay of current with time for the '1st', '2nd', and '3rd' evaporations). The conclusion is that;

(i) The higher current densities approached the condition of space-charge limitation.

(ii) That the conduction may be predominantly space-charge-limited for lower voltages, (since the 'ordinary' S.C.L. current falls with the square of the applied voltage, Sec. 3·3).

Fig. 6.17 (for example) shows that currents of $\sim 8 \times 10^{-11}$A. were

measured for 500V. applied to the same cell. The 'ordinary' SCL current formula (for $\mu = 1{\cdot}4 \times 10^{-3} cm^2 V^{-1} sec^{-1}$) results in only 6×10^{-11}A. Contradictions of this sort are, however, explanable by any of the following phenomena;

(1) An increase in the effective value of u because of bulk liquid motion[10].

(2) The effects of convection currents (resulting from the heating of the liquid and(or cathode surface by the radiation).

(3) The release of 'trapped' electrons as a consequence of the infra-red radiation entering the liquid.

The contributions of (1) and (2) are not easily calculable, although they are considered to be important. The process indicated in (3) is very interesting and (in hindsight) experiments to estimate its applicability would have been relatively straightforward. However, there is no reason to doubt that space charges can cause the 'upward curvature' of the current-voltage characteristics at low voltages.

The currents measured by Gzowski[55] were $\sim 10^{-13}$A. (at $3KV.cm^{-1}$) in air-saturated hexane. Even if the lower mobility of the carriers in air-saturated hexane[33] is taken into account, the above current is far less than for space-charge-limitation. Similarly, Swan[54] found currents of $\sim 10^{-12}$A. in degassed hexane at a similar field strength (see Fig. 2·3). It is considered significant that both workers report that;

(a) The current-voltage characteristics maintain their (slight upward curvature for fields far in excess of 3KV.cm^{-1} (the maximum applied in the present work).

(b) The magnitude of the photocurrent depended on the field strength, but not the electrode spacing.

(c) The photocurrent (at a given field) was proportional to the intensity of irradiation, and that the current depended on the conditions at the cathode surface.

For low current densities (e.g. Figs. 6.33 and 6.34) the present work is substantially in agreement with the above. (The electrode spacing was not varied, for technical reasons). Such currents may be regarded as emission limited; Section 7.2.2 considers a possible (but simplified) model for the conduction.

7.2.2 The photoinjection process.

The measured current-voltage curves follow the same general pattern (e.g. Fig. 6.34). At low applied voltages (U), the current is small, but increases faster than U. Depending on the magnitude of the current, the 'upward curvature' becomes less pronounced at the higher voltages; so that 'I_A' (the observed current) becomes more or less proportional to U. It is found that the exact shape of the current-voltage curve depends on the nature of the cathode surface (e.g. Fig. 6.35), on the intensity of irradiation (e.g. Fig. 6.34), on the range of wavelengths contained in the radiation (e.g. Fig. 6.21) and, of course, on the polarity of the applied

TABLE 7.1. Data abstracted from Table 6(iii)

FILTER	RATIO I_{VAC}/I_{LIQ} (i)	RATIO I_{VAC}/I_{LIQ} (ii)	RATIO I_{VAC}/I_{LIQ} (iii)	RATIO $I_{LIQ(i)}/I_{LIQ(ii)}$	$I_{VAC(i)}/I_{VAC(ii)}$
NONE	620	490	450	2	2·6
OW1	460	440	400	2·3	2·5
OX7	450	340	420	2·3	2·9
OX1	130	200	270	2·4	1·6
OX9A	130	200	160	2·3	1·4
OX1A	120	200	170	2·5	1·5
OB8	65	55	80	2·3	2·7
OB10	62	65	76	2·5	2·5
OV1	71	64	55	2·4	2·7
OB2	83	57	65	2·2	3·1
ON16	70	63	40	2·2	2·3
ON11A	86	53	60	2·1	3·4

voltage. The photocurrent in the liquid depends on (and, for wavelengths near the threshold, is roughly proportional to) the 'saturated' photoemission in vacuo (Table 7.1).

It is proposed that photoelectrons emerge from the interior of the cathode and enter the liquid with kinetic energies of a few eV. Some of these electrons are scattered back into the cathode after only a few collisions with the hexane molecules; others travel further into the liquid, with correspondingly greater numbers of collisions. It is anticipated that the electrons lose kinetic energy by exciting 'dormant' modes of vibrational energy[120] in the hexane molecules, and that the rate of energy loss[121] is sufficient to reduce the kinetic energy of most electrons to less than their 'image' potential with the cathode surface.[122] These electrons rapidly return to the electrode surface. [Such 'cathodic recombination' is regarded as analagous, in one dimension, to the Onsager theory of the 'initial' recombination of ion-pairs.].

However, the velocity with which electrons leave the cathode surface will be much higher than the (drift) velocity with which they return, especially if 'trapping' occurs in the liquid. Consequently, there will be an accumulation of electrons in the liquid adjacent to the cathode until the 'reverse' current is comparable to the rate of emission. The problem reduces to a calculation of this rate of recombination.

The actual recombination process is not considered to be important if the rate of injection is such that the accumulated

electrons may participate in an approximation to S.C.L. current. However, for reduced intensities of irradiation the field due to space charges can probably be neglected in comparison with the 'image' field, and the conduction is emission limited [See Sec. 3.3]. The latter regime is considered first.

The potential, ϕ, traversed by non-interacting charges leaving the cathode is taken to be the usual image + applied field (Schottky) barrier. (This type of barrier is usually associated with the process of field-assisted thermionic emission,[123] but is also applicable to photoemission[124]).

$$\phi = W_a - \frac{e}{4\varepsilon x} - E_A x$$

Where 'W_a' is the zero-field work function, 'x' is the distance of the (negative) charge 'e' from the cathode surface, E_A is the applied field in the direction of the anode.

ϕ is a maximum when

$$x = x_m = \tfrac{1}{2}\left(\frac{e}{\varepsilon E_A}\right)^{\frac{1}{2}} \qquad \text{(1)}$$

A 'thermalised' charge has kinetic energy kT, and can be considered 'free' from the image attraction (to diffuse at random) when;

$$\frac{e^2}{4\varepsilon x} < kT$$

So that, for $E_A = 0$, the 'critical distance' x_{co} is given by;

$$x_{co} = \frac{e^2}{4\varepsilon(kT)} \simeq 135\text{Å} \qquad \text{(2)}$$

The field at x_{co} is $4(\frac{kT}{e})^2 \frac{\epsilon}{e} = E_{co}$ (in the direction of the cathode).

For hexane at room temperature E_{co} is $\sim$ 32KV.cm^{-1} (see Sec. 3.1). The maximum applied field in the range of measurements was $\sim$ 3KV.cm^{-1}, so that $E_A \ll E_{co}$. Consequently; x_{co}, for our purposes, is nearly independent of E_A; and $x_m > x_{co}$.

The plane $x = x_{co}$ is regarded as a 'critical boundary' (cf. Sec. 3.1 for Onsager's 'critical radius'). Electrons at distances greater than x_{co} from the cathode can be considered to be 'free' to diffuse. Since the position of this boundary is fixed (which, as has been indicated, holds for $E \ll E_{co}$) the rate of 'injection' of 'free' electrons can be taken as independent of E_A. Furthermore, the plane $x = x_m$ (for E_A = 3KV.cm^{-1}) is $\sim$ 450Å from the cathode; even the most energetic electrons are likely to be thermalised at distances much less than this, and the drift will be predominantly towards the cathode. The conduction may now be estimated by considering the rate of recombination of the 'free' electrons with the cathode, i.e. the drift towards the cathode at $x = x_{co}$ (cf. Langevin's equation, Sec. 7.1.1).

Suppose that the rate of injection through $x = x_{co}$ constitutes a current I_s. If the (steady state) anode current is I_A, then the accumulation of charges (N per unit volume) at $x = x_{co}$ must be such that[125];

$$I_s = N\,Aer + I_A \qquad \text{(3)}$$

where 'r' is a velocity expressing the rate at which electrons disappear at the cathode (area 'A'). This velocity is given by

$$r = \mu (E_{co} - E_o) \qquad \text{(4)}$$

where E_o replaces E_A, to include the effects of space charges (see Sec. 3.3). If the concentration N is large enough to supply the anode current by diffusion alone, then $E_o \leq 0$ (because of the concentration gradient in the positive x-direction) and the current is space-charge limited. However, if I_A increases so that $E_o \longrightarrow E_A$ then there must be a minimum concentration N_o at $x = x_{co}$ to balance I_A with I_s. The (reverse) field at $x = x_{co}$ by a thermalised (negative)charge density N_o is given by;[126]

$$E = \left\{\frac{2N_o kT}{\varepsilon}\right\}^{\frac{1}{2}} \qquad \text{(5)}$$

so that

$$E_o = E_A - E_R \qquad \text{(6)}$$

Substitution of (4) and (6) into (3) with the proviso that

$E_{co} \gg E_A - \left(\frac{2N_o kT}{\varepsilon}\right)^{\frac{1}{2}}$, leads to;

$$I_s = N_o Ae\mu \left[E_{co} - E_A + E_R\right] + I_A = \text{const (or nearly so).}$$

with $I_s \simeq N_o Ae\mu E_{co}$ (cf. Sec. 7.1.1).

The observed current I_A becomes;

$$I_A = N_o Ae\mu (E_A - E_R) = \frac{I_s}{E_{co}} \left[\frac{U - U^*}{L}\right] \qquad \text{(7)}$$

where U^* is identified as the intercept on the voltage axis of the 'linear' part of the current-voltage characteristic (e.g. Fig. 6.34). Equation (7) indicates that I_A will be proportional to the light

intensity (through N_o) as long as $E_A \gg E_R$. Both I_s and N_o will be (indirectly) related to the vacuum photoemission of electrons (they might be calculated with the use of a range-energy relationship for superthermal electrons in hexane). U* will increase with the square of I_s and will depend on the geometry of the cell (if I_s is small, then the current-voltage curves will be linear for low applied voltages). The upward curvature of the current-voltage relationship is not predicted by the above derivation, but it is anticipated that bulk liquid motion (and the residual effects of space-charges) can cause the required (slight) non-linearity. The current will not 'saturate' for $E_A > E_{co}$ but will approach a different gradient in an expression similar to Onsager's for 'initial' recombination, since x_m will be nearer the cathode than x_{co}. [I have not been able to calculate the latter equation, nor a satisfactory expression for I_s; both these would require a knowledge of the energy distribution of electrons emerging from the cathode, the effects of scattering and, of course, the range-energy relationship for hexane.]

Curve (3) in Fig. 6.34 cuts the voltage axis at (approximately) 150V. The density N_o, derived from equation (5), corresponds to $\sim 2 \times 10^7$ carriers cm^{-3}. The insertion of this value in equation (7) results in $\mu \sim 10^{-3} cm^2.V^{-1}.sec^{-1}$.(which is in agreement with LeBlanc's figure[15]).

It is not profitable to elaborate the analysis of the results, since the experiments (and the test cells) were designed for

versatility rather than accuracy. Precision measurements of the mobility (with similar photocathodes, and degassed hexane) will shortly be published by Bloor,[59] together with further technical developments.

CONCLUSION

The purpose of this research, to distinguish between the conduction due to cathodic photoinjection and the volume photo-ionisation in liquid hexane, has been accomplished. In particular, photoinjection has been shown to proceed in the absence of significant 'bulk' photoconduction provided that; (a) suitably 'activated' photocathodes are used, (b) radiation of wavelengths absorbed by the hexane are avoided at all times. The rate of photoinjection, into highly degassed hexane, may be controlled so that the conduction can be (approximately) space-charge-limited or emission-limited. In either of the latter circumstances it should be possible to make accurate measurements of the mobility of the injected charges. Simple calculations in this Thesis indicate that the charges enter the liquid as 'bare' electrons, become thermalised, and then behave like high-mobility negative ions. There is, however, a good deal of work to be done in elucidating the (complicated) processes at the cathode surface; there might be some scope in applying the theory of 'initial recombination' in gases,[63] of metal-semiconductor contacts,[42] or of photoinjection into molecular solids.[127]

Future measurements might include the use of (1) intermediate to high field strengths, (2) homologues of hexane, (3) superimposed liquid motion. It might also be possible to employ the methods (E.S.R., N.M.R., and infra-red analysis) which have been successfully employed to investigate the 'solvated' electron in metal solutions.

APPENDIX I

AUTOXIDATION OF HEXANE

Air-saturated hexane is known[69] to become contaminated after storage (even in coloured bottles) for any length of time. The formation of impurities may influence the electrical properties, and so a brief account of this decomposition (which is initiated by the oxygen in the air) is included for consideration in future investigations.

The C-H bonds of hexane are susceptible to attack by molecular oxygen, the initial products being of the type R-O-O-H (hydroperoxide) or R-O-O-R' (peroxide). This reaction does not involve inflammation or temperatures above 100°C. The reactions are initiated by ultraviolet radiation,[116] radical sources (e.g. metals) and by the hydroperoxide products themselves[114]. This last feature makes autoxidation autocatalytic, and involves an 'induction period' after which the reaction proceeds more rapidly. Inhibition by radical scavengers (common additives to transformer oil) indicates a radical mechanism for the reactions[115]. Products of autoxidation are complex because of side reactions.

[For example, n-hexane contained 47% of 2,5 dimethyl-tetrahydrofuran and 30% 2ethyl - 4 methyloxetan on gaseous oxidation[86].]

Oxidation in the liquid phase has not been a popular topic of research because of the difficulty in supplying enough oxygen for the reaction to proceed very far, but the products are (i) free radicals,

alcohols, aldehydes, ketones, etc.[116]

The process proceeds as follows;[114]

$$\text{Initiator} + \text{R-H} \longrightarrow \text{R}^{\bullet} + \text{R}^{\prime}\bullet \quad \text{(Initiation)}$$

$$\text{R}\bullet + \text{O}_2 \longrightarrow \text{ROO}\bullet$$

$$\text{ROO}\bullet + \text{R-H} \longrightarrow \text{ROOH} + \text{R}\bullet \quad \text{(propagation)}$$

$$\text{ROO}\bullet + \text{R}\bullet \longrightarrow \text{ROOR}$$

$$\text{R}\bullet + \text{R}^{\prime} \longrightarrow \text{R-R}^{\prime} \quad \text{(termination, non radical products)}$$

$$2\text{ROO}\bullet \longrightarrow \text{ROOR} + \text{O}_2$$

Some decomposition of the hydroperoxide may be expected (especially above 100°C) i.e.

$$\left.\begin{array}{l} \text{ROOH} \longrightarrow \text{RO}\bullet + .\text{OH} \\ 2\text{ROOH} \longrightarrow \text{RO}. + \text{H}_2\text{O} + \text{ROO}\bullet \end{array}\right)$$

The process of interest here, is the action of metal surfaces (M) in catalysis of the hydroperoxide to form radicals

e.g. (1) Addition of an electron

$$\text{ROOH} + \text{M}^{n+} \longrightarrow \text{RO}\bullet + \text{OH}^{-} + \text{M}^{(n+1)+} \qquad -(1)$$

(2) Removal of an electron

$$\text{ROOH} + \text{M}^{(n+1)+} \longrightarrow \text{ROO}\bullet + \text{H}^{+} + \text{M}^{n+} \qquad -(2)$$

The sum of reactions (1) and (2) is equivalent to thermal decomposition; the role of the metal surface is genuinely catalytic.

Peroxides are very polar. It is considered that they may be a source of ions (O^-, O_2^-, H^+, OH^-) if a high enough field is applied to the liquid. They may also decompose on absorbing u/v radiation (i.e. may be responsible for the u/v absorption edge). On metal surfaces reactions (1) and (2) may predominate (depending on the conditions).

APPENDIX II

THE PURIFICATION OF HEXANE WITH SILICA GEL

The following facts, concerned with the adsorption processes at silica gel surfaces, have been found in the literature. They are included here for their possible application to future work.

The surface of the gel is critical to the method, and (depending on the conditions) may be;[117]

(1) Completely hydrated.

(2) Covered with a layer of hydroxyl groups, but with some adsorbed water as well.

(3) Free from all adsorbed water, but retaining the characteristic hydroxyl groups of the gel.

If the gel is exposed to moist air at room temperature, capillary condensation produces a surface as in (1). If the hydrated gel is subjected to prolonged evacuation at ordinary temperatures (not above 150°C) a dense coating of hydroxyl groups remains on the surface (condition (2)). Evacuation at above 200°C produces a strongly dehydrated surface retaining no adsorbed water (condition (3)). Heating the gel above 350°C destroys the crystal structure.

The presence of a hydroxyl coating on the surface of the gel results in the strong adsorption[118] of molecules which are capable of forming hydrogen bonds with the hydroxyl groups (i.e. water, alcohols, etc.). There is also (more importantly) a sharp increase in the

adsorption of molecules which are non-polar as a whole, but with a very non-uniform electron distribution. With favourable orientation of the quadrupole moment (parallel to the hydroxyl axis) the latter molecules are adsorbed in preference to molecules of similar dimensions having the same (or even higher) polarisability but smaller quadrupole moment. This quadrupole-dipole interaction energy is available for unsaturated but not for saturated hydrocarbons, e.g. the adsorption energy for benzene (10.4 K.cal.mole^{-1}) is much higher than for hexane (8.8 K.cal.mole^{-1}). The removal of dipoles from the surface of the gel (dehydration) results in a fall of the adsorption energy of unsaturated, but not saturated compounds. Thus, the heats of adsorption of benzene and hexane will become almost identical (8.6 K.cal.mole^{-1}), and there will be practically no separation of these compounds.

It is seen that the hydrated gel* is the most suitable for the purification of hexane. Suitably hydrated gel is produced by;

(i) Removing capillary moisture with a stream of dry, inert, gas (preferably heating to not more than 150^{o}C).

(ii) A short evacuation (to remove occluded air and water vapour).

The entire purification process should be conducted in an inert gas atmosphere (to avoid the formation of peroxide in the hexane, see Appendix I).

*More recently, silica gel with trimethylsilyl surface groupings has been shown to be considerably more efficient than the ordinary

(hydrated) gel.[118] Unfortunately, such 'modified' gel is rather difficult to prepare, and (as yet) is not commercially available.

REFERENCES

1. A. Rogozinski, Phys. Rev. 60, 148, (1941).
2. A.A. Zaky, H. Tropper and H. House, Brit J. Appl. Phys. 14, 651, (1963).
3. E. Kahan, Ph.D. Thesis, Durham, (1964).
4. T.J. Lewis, 'Progress in Dielectrics Vol. 1' p. 99 et seq., Heywood and Co. Ltd. (London), (1959).
5. A.H. Sharbaugh and P.K. Watson, 'Progress in Dielectrics Vol. 4', p. 201 et seq., Heywood and Co. (London), (1962).
6. D.W. Swan, Brit. J. Appl. Phys. 13, 208, (1962).
7. M.J. Morant, Conf. of Phys. Soc. Durham. Brit. J. Appl. Phys. 14, 469, (1964).
8. I. Adamczewski, Brit. J. Appl. Phys. 16, 759, 1965.
9. A.M. Sletten, Nature 183, 311, (1959).
10. A.M. Sletten and T.J. Lewis, Brit, J. Appl. Phys. 14, 883, (1963).
11. H. House, Proc. Phys. Soc. (London) B70, 913, (1957).
12. W.B. Green, J. Appl Phys. 27, 921, (1956).
13. H. Tropper, J. Electrochem. Soc. 108, (1959).
14. D.W. Swan and T.J. Lewis, J. Electrochem. Soc. 107, 180 (1960).
15. O.H. LeBlanc, J. Chem. Phys., 30, 1443 (1959).
16. H. Eyring, J. Chem. Phys. 4, 283, (1936).
17. A. Glasstone 'Textbook of Phys. Chem.' p.898. Macmillan (London), (1956).
18. W.G. Chadband and G.T. Wright, Brit. J. Appl. Phys. 16, 305, (1965).
19. P.E. Secker and T.J. Lewis, Brit. J. Appl. Phys. 16, 1649, (1965).
20. O.M. Stuetzer, J. Appl. Phys. 31, 136, (1960).
21. V. Essex and P.E. Secker, Brit. J. Appl. Phys. series 2, vol. 1, 63, (1968).

22. S.A. Rice and J. Jortner, 'Progress in Dielectrics Vol. 6', p. 185 et seq., Heywood and Co. (London), 1965.

23. E.O. Forster, J. Chem Phys.,37, 1021, (1962).

24. F. Gutmann and A. Netshey, J. Chem. Phys.,36, 2355, (1962).

25. A.F. Ioffe and A.R. Regel, Progr. Semiconductors 4, 237, (1960).

26. A.I. Gubanov, 'Quantum Electron Theory of Amorphous Conductors', Publ. Consultants Bureau, New York, (1965).

27. W.L. McCubbin, Trans Farad. Soc., 59, 769, (1963).

28. R.A. Keller and H.E. Rast, J. Chem. Phys., 36, 2640, (1962).

29. O.H. LeBlanc, J. Chem. Phys., 37, 916, (1962).

30. D.C. Northrop and O. Simpson, Proc. Roy. Soc. A234, 124, (1956).

31. G. Jaffe, Ann. Phys. Lpz., 42, 331, (1913).

32. J. Terlecki, PhD. Thesis (1961).

33. O. Gzowski, Nature, Lond. 194, 173, (1962)

34. O. Gzowski, Z. Phys. Chem. 221, 288, (1962).

35. J.M. Geist and M.R. Cannon, Ind. Eng. Chem. (Anal. Ed.), 18, no. 11, 611, (1946).

36. H. Ullmaier, Z. Phys. 178, 44, (1964).

37. D. Blanc and J. Mathieu, J. Phys. Radium, 21, 675, (1962).

38. A. Hummel and A.O. Allen, Disc. Farad, Soc. 36, 95, (1963).

39. A. Hummel, A.O. Allen, F.H. Watson, J. Chem. Phys., 44, 9, 3431, (1966).

40. D.H. Wilkinson, 'Ionisation Chambers and Counters', C.U.P., (1950).

41. H.A. Dewhurst, J. Am. Chem. Soc., 83, 1050, (1961).

42. M.J. Morant, J. Electrochem. Soc., 107, no. 8, 671, (1960).

43. E. Spenke, 'Electronic Semiconductors' (McGraw-Hill) p. 74 (1958).

44. E. Gray, PhD, Thesis, London (1967).

45. A. Byk and H. Borck, Verh. d. Deutch Phys. Ges.,12, 621, (1910).

46. M. Volmer, Ann. d. Phys., 40, 775, (1913).

47. W.H. Eller, J. Opt. Soc. America, 20, 71, (1930).

48. G. Jaffe, Ann. Phys. Lpz., 42, 303, (1913).

49. R.W. Dornte, J. Appl. Phys. 10, 514, (1939).

50. R.W. Dornte, Ind. Eng. Chem., 32, 1529, (1940).

51.) R.H. Fowler and L. Nordheim, Proc. Roy. Soc. (London),A119, 173, (1928).

52. M.J. Morant, Nature (London), 190, 904, (1961).

53. M.J. Morant, Conf. Phys, Soc. (Durham 1963), paper 5.2.

54. D.W. Swan, Nature (London), 190, 904, (1961).

55. O. Gzowski and J. Terlecki, Acta Phys. Aust., 337, (1961).

56. O.H. LeBlanc, J. Chem. Phys., 30, no. 6, 1443, (1959).

57. P. Chong, T. Sugimoto and Y. Inuishi, J. Phys, Soc. Japan, 15, 1137, (1960).

58. J. Terlecki, Nature (London), 194, 172, 1962

59. A. Bloor, Private communication (PhD. Thesis to be published, Durham University).

60. G.R. Freeman, J. Chem. Phys., 39, 1580,(1963).

61. L.B. Loeb, 'Electrical Discharges in Gases', Chap. 2, 2nd Ed. J. Wiley, (1947).

62. Z. Croitoru, 'Progress in Dielectrics, Vol. 6', 105, Heywood and Co. (London), (1965).

63. L. Onsager, Phys. Rev. 54, 554, (1938)

64. G.R. Freeman, J. Chem. Phys., 39, 978, (1963).

65. A. Hummel and A.O. Allen, J. Chem. Phys., 46, 1602, (1967).

66. G.C. Hall and J.E. Lennard-Jones, Disc. Farad. Soc., 10, 22, (1951).

67. G.C. Hall, (Trans. Farad Soc., 49, 113, (1953).
(" " " 50, 319, 773, (1954).

68. J.W. Raymonda and W.T. Simpson, J. Chem. Phys. 47, 430, (1967).

69. W.J. Potts, J. Chem. Phys., 20, 809, (1952).

70. R.G. Snyder, J. Chem. Phys. 47, 1316, (1967).

71. G.H. Beaver and E.A. Johnson, 'Molecular Spectroscopics', Heywood and Co., (1961).

72. E.J. Bowen, 'Chemical Aspects of Light', Chap. 2, O.U.P., (1949).

73. Evans, J. Chem. Phys., 23, 1436, (1954).

74. Orgel and Mulliken, J. Amer. Chem. Soc., 79, 4839, (1957).

75. Mulliken, J. Phys. Chem., 56, 801, (1952).

76. F. Gutmann and L.E. Lyons, Org. Semiconductors', Table 8.5, John Wiley, New York, (1967).

77. S.F. Mason, Quart. Rev. Chem. Soc. 15, 353, (1961).

78. J.N. Murrell, Quart. Rev. Chem. Soc. 15, 191, (1961).

79. (A.U. Munck and J.F. Scott, Nature (London), 177, 587, (1956).
(
(cf. U.P. Oppenheim and A. Goldman, J. Chem, Phys., 46, 3493, (1967).

80. A. Glasstone, 'Textbook of Physical Chemistry', Chap. 7, MacMillan (London), (1956).

81. J.G. Calvert and J.W. Pitts, 'Photochemistry', John Wiley, (1966).

82. J.L. Magee and A.H. Samuel, J. Chem. Phys., 20, 760, (1952).

83. F. Gutmann and L.E. Lyons, 'Org. Semiconductors' Table 5.1, John Wiley, New York, (1967).

84. J.P. Simons, Quart. Rev. Chem. Soc., 13, 8, (1959).

85. G. Porter and M.W. Windsor, Disc. Farad. Soc., 17, 178, (1954).

86. A. Fish, Quart. Rev. Chem. Soc., 13, 8, (1959).

87. J.J. and G.P. Thomson, 'Conduction of Electricity through Gases', Chap. 4, C.U.P., (1928).

88. J.A. Ramsey, Journ, Australian Inst. of Metals., 10, no. 4, 323, (1965).

89. F.R. Brotzen, Phys. Stat. Sol., 22, 9, 1967.

90. R.M. Noyes, J. Amer. Chem. Soc., 82, 1868, (1960).

91. J.A. Ramsey and G.F.J. Garlick, Brit. J. Appl. Phys., 15, 1353, (1964).

92. R.N. Bloomer, Brit. J. Appl. Phys., 8, 321, (1957).

93. L. Grunberg and K.H.R. Wright, Proc. Roy. Soc., A, 232, 403, (1955).

94. R.J. Cashman and W.S. Huxford, Phys. Rev., 48, 734, (1935).

95. Gaviola and Strong, Phys. Rev., 48, 734, (1935).

96. W. Edlinger and H. Muller, Anz. Öst. Akad. Wiss, 91, 89, (1954).

97. L. Grunberg, Brit. K. Appl. Phys., 9, 85, (1958).

98. (Grimley and Trapnell, Proc. Roy. Soc. A, 234, 405, (1956).
(Grimley 'Chemistry of the Solid State', ed. Garner, Butterworths, (1957).

99. Hughes and DuBridge, 'Photoelectric Phenomena' p. 78, McGraw-Hill, (1932).

100. Pickup and Trapnell, J. Chem. Phys., 25, 182, (1956).

101. R.P. Madden, 'Physics of Thin Films I', p. 167, Academic Press, (1963).

102. H.L. Caswell, 'Physics of Thin Films I' p. 5, Academic Press, (1963).

103. E. Kahan and M.J. Morant, Brit. J. Appl. Phys., 16, 943, (1965).

104. R.L. Augustine, 'Catalytic Hydrogenation', p. 147, Edward Arnold (Publ.), (1965).

105. Cairns and Samson, (J. Opt. Soc. Amer., 57, 433, (1968).
(Rev. Sci. Instr., 36, 19, (1965).

106. Private communication, Dr. R. Moyes, Chem. Dept., Hull.

107. O. Simpson, Symp. on Electrical Cond in Organic Solids (1960), p.27, Interscience, London.

108. L. Pauling, Nature of the Chemical bond, Chap. 2, Cornell Univ. Press, New York, 1940.

109. J. Frenkel, 'Kinetic Theory of Liquids', Chapter V, section 10, Clarendon Press (Oxford) (1940)

110. Stewart, Phys. Rev. 31, 174, (1928).

111. R. Schiller, J. Chem. Phys., 43, 2766 (1964).

112. R.W. Gurney, Ions in solution, p.3, Dover Publ. (New York) 1962.

113. E.O. Forster, J. Chem Phys., 40, 86, (1964).

114. C.J.M. Stirling, 'Radicals in Organic Chemistry' Chapter 5, Oldbourne Press (London) 1965.

115. H. Basseches and D.A. Mclean, Ind. Eng. Chem., 47, 1782, (1955).

116. G.H. Twigg, Chem. and Ind., (1962).

117. A.V. Kiselev, 'The Structure and Properties of Porous Materials', p.175, publ. F. Stone (London) 1958).

118. A.V. Kiselev, Quart. Rev. Chem. Soc., 15, 99, (1961).

119. P. Langevin, Compt. Rend., 146, 1011, (1908).

120. J.G.Aston and S.V.R. Mastrangelo, 'Physical Chemistry of the hydrocarbons, Vol II, Chapter 3 (and references therein). Academic Press, New York, (1953).

121. A. Hummel, A.O. Allen and F.H.Watson, J. Chem. Phys., 44, 3435, (1966).

122. (H. Fröhlich, Proc. Roy. Soc. A160, 230, (1937).
(H. Fröhlich and R.L. Platzmann, Phys. Rev., 92, 1152, (1953).

123. A.J. Dekker, 'Solid State Physics', Sec. 9.8, Macmillan and Co. (London), 1958.

124. E. Guth and C.J. Mullin, Phys. Rev. 59, 867, (1941).

125. Sir J.J. Thomson, 'Conduction of Electricity through Gases Vol. I.' Sec. 134, Cambridge University Press, (1928).

126. J. Frenkel, 'Kinetic Theory of Liquids', Chapter VI, Sec. 6, Clarendon Press (Oxford).

127. H.P. Kallmann and M. Pope, J. Chem. Phys., 36, 2482, (1962).